UiT The Arctic University of Norway

Faculty of Health Sciences
Department of Pharmacy

Horizontal transfer, selection and maintenance of antibiotic resistance determinants

Julia Kloos
A dissertation for the degree of Philosophiae Doctor - March 2021

Horizontal transfer, selection and maintenance of antibiotic resistance determinants

Julia Kloos

A dissertation for the degree of Philosophiae Doctor
March 2021

Microbial Pharmacology and Population Biology Research Group
Department of Pharmacy
Faculty of Health Sciences
UiT The Arctic University of Norway

Acknowledgements

The presented work was carried out in the Microbial Pharmacology and Population Biology Research Group at the Department of Pharmacy (IFA), UiT The Arctic University of Norway.

I am grateful to former and current colleagues and students at IFA that made me feel welcome ever since I started working here and made these last years so enjoyable. I would like to thank the Norwegian PhD School of Pharmacy and the National Graduate School in Infection Biology and Antimicrobials for providing travel grants and organizing meetings, which allowed me to explore the microbial world internationally.

Most of all, I am deeply grateful to my main supervisor Pål Johnsen, for being full of enthusiasm, great ideas and good humor. I admire the way you share your profound knowledge and scientific experience with your students and colleagues and are available for questions, discussions and new results at any time. Your guidance and trust were always encouraging and invaluable to me - thank you!
My co-supervisor Klaus Harms taught me many tips and tricks in microbiological laboratory methods since the first day I arrived at IFA, which encouraged me to consider a PhD in microbiology. Thank you, Klaus, for pondering with me on the many molecular puzzles that bacteria provide, patiently and enduringly. Thank you Ørjan for bringing smelly, interesting bugs to our lab, for your structured thinking, and fast and thorough feedback based on your great expertise in clinical microbiology.

Finishing this PhD was only possible with the good colleagues I had. Thank you all for making MicroPop the diverse, lively and supportive research group that it is. To Ane, Elizabeth, Nicole, Conny and Iren: thank you for sharing both joy and frustration about lab life with me, and for all the trust and support. You are great scientific role models and friends to me. Thank you João, a.k.a. 'team piggy' co-responsible and 'husband', for allowing all the questions and discussions, and for being such a reliable companion.

Dear Theresa, thank you for being my constant source of encouragement and inspiration. Our trips across northern Norway, exploring mountains on long tracks, mean a lot to me. Thank you Anke and Marita, for keeping our friendship alive over long distance and many years and being curious about my Tromsø-life and work. Thank you, Tony, for so much joy and support ☺.

Danke and meine Familie ♡

Tromsø, March 2021 Julia Kloos

Table of contents

List of papers

Paper I

Podnecky, N.L., Fredheim, E.G.A., Kloos, J., Sørum, V., Primicerio, R., Roberts, A.P., Rozen, D.E., Samuelsen, Ø., Johnsen, P.J.

Conserved collateral antibiotic susceptibility networks in diverse clinical strains of *Escherichia coli*.

Nature Communications, 2018. https://doi.org/10.1038/s41467-018-06143-y

Paper II

Kloos, J., Johnsen, P.J., Harms, K.

Tn*1*-transposition in the course of natural transformation enables horizontal antibiotic resistance spread in *Acinetobacter baylyi.*

Microbiology, 2020. https://doi.org/10.1099/mic.0.001003

Paper III

Kloos, J.*, Gama, J.A.*, Hegstad, J., Samuelsen, Ø., Johnsen, P.J.

Piggybacking on niche-adaptation improves the maintenance of multidrug resistance plasmids.

accepted manuscript Molecular Biology and Evolution, 2021

https://doi.org/10.1093/molbev/msab091

* These authors contributed equally to this work.

Abbreviations

ArcAB	Aerobic Respiration Control
AST	Antimicrobial Susceptibility Testing
BMD	Broth Microdilution
CCR	Carbon Catabolite Repression
CR	Collateral Resistance
CS	Collateral Sensitivity
DHFR	Dihydrofolate Reductase
DR	Direct Repeat
dsDNA	double-stranded DNA
ESBL	Extended Spectrum Beta-Lactamase
EUCAST	European Committee on Antimicrobial Susceptibility Testing
G-/G+	Gram-negative/Gram-positive
HGT	Horizontal Gene Transfer
IC90	Inhibitory Concentration 90%
ICE	Integrative Conjugative Element
IR	Inverted Repeat
IS	Insertion Sequence
MDR	Multidrug Resistance
MGE	Mobile Genetic Element
MIC	Minimal Inhibitory Concentration
MPC	Mutant Prevention Concentration
MSC	Minimal Selective Concentration
MSW	Mutant Selection Window
NDM	New-Delhi Metallo-β-lactamase
PBP	Penicillin-Binding Protein
ssDNA	single-stranded DNA
ST	Sequence Type
TSD	Target Site Duplication
UPEC	Uropathogenic *E. coli*
UTI	Urinary Tract Infection
VIM	Verona-Integron Metallo-β-lactamase
WGS	Whole Genome Sequencing

Summary

The rapid emergence of antibiotic resistance in bacterial pathogens represents a substantial clinical and financial burden to our society. The development of antibiotics is generally unprofitable and challenged by the need for innovative and evolution-robust drugs. It is thus insufficient to rely on the discovery of new therapeutic agents, but important to understand the selection, spread and maintenance of bacterial antibiotic resistance in order to counteract its emergence. The work presented in this thesis focused on mechanisms and evolutionary dynamics underlying these factors.

Collateral sensitivity, when bacterial resistance to one antibiotic potentiates the effect of other antibiotics, may be exploited in infection treatment to limit resistance evolution. We assessed collateral susceptibility changes in ten diverse isolates of single-drug resistant uropathogenic *Escherichia coli* towards 16 antibiotics and found conserved changes especially in ciprofloxacin resistant mutants. Collateral responses changed also another parameter important for resistance selection, the mutant prevention concentration, accordingly. We reveal that knowledge of the mechanism as well as the fitness cost of resistance supports the predictability of bacterial collateral responses in antibiotic resistant mutants (**paper I**).

Horizontal gene transfer between bacterial pathogens contributes to the rapid spread of antibiotic resistance, and natural transformation is one of the major routes for bacterial horizontal gene acquisition. We demonstrate, that natural transformation of *Acinetobacter baylyi* by the resistance-encoding, replicative transposon Tn*1* occurred through its transposition from incoming donor DNA into the chromosome. In this process, host and transposon proteins were essential. We present a model of transposition-mediated natural transformation from a circular, double-stranded intermediate molecule of cytoplasmic donor DNA (**paper II**).

Antibiotic resistance plasmids play a major role in the dissemination of multidrug resistance between bacteria and are increasingly recognized to establish stable associations with clinical bacterial hosts. We show that the biological burden of carrying a clinical resistance plasmid in an *E. coli* uropathogen is reduced after adaptation of this host to the laboratory environment through mutations in its CCR and ArcAB regulatory systems. We identify that transcriptional downregulation of plasmid genes explains the reduced plasmid cost mechanistically. Thus, we reveal that simple niche-adaptation presents a novel solution to the 'plasmid paradox' by improving the permissiveness of bacteria towards resistance plasmids (**paper III**).

Introduction

Evolution of antibiotic resistance

Bacteria have been and will always be with us[1] and our dependence on effective treatment options for human infections with disease causing bacteria is immense. Paul Ehrlich introduced the term *chemiotherapy* to describe the use of chemically synthesized drugs in the treatment of microbial infections. The identification of compounds with antisyphilitic and antistreptococcal activity, Salvarsan (1909) and the sulfonamide Prontosil (1932), respectively, lead to their worldwide distribution and further development[2]. A major scientific breakthrough of the 20th century was the discovery of penicillin, a natural product of the *Penicillium* mold with activity against *Staphylococcus aureus*, by Sir Alexander Fleming in 1928[3]. Soon after however, a penicillin-destroying enzyme was identified in *Escherichia coli*[4], and Fleming highlighted in his Nobel prize lecture that bacterial resistance evolution could eventually render these 'magic' drugs inefficient[5].

Today, infections with multidrug-resistant (MDR) bacteria endanger basic and modern medicine globally since adequate therapeutic options are limited[6]. Estimates based on European surveillance data from the year 2015 indicate that resistant bacteria caused more than 670 000 infections, and around 5% of patients died consequently[7]. This creates a health burden which is, measured in disability-adjusted life years, comparable to the combined effect of influenza, tuberculosis and HIV/AIDS in Europe[7]. Members of the Gram-negative (G-) *Acinetobacter* spp. and *Enterobacterales*[8] represent priority MDR pathogens[9,10] and are the focus of the presented thesis. For the latter, the problem of antibiotic resistance is worsened by the successful association of epidemic MDR plasmids[11] with high-risk clones, exemplified by *E. coli* sequence type (ST)131 and *Klebsiella pneumoniae* ST258[12]. Worldwide in 2014, these two bacterial species were the estimated cause of 50 million infections that required hospital treatment with last resort antibiotics (carbapenems), while 3.1 million infections were even resistant to these drugs[13].

In this thesis, the term 'antibiotics' comprises substances of microbial origin as well as synthetic drugs that are used in the treatment of bacterial infections. Their overuse and misuse in animal and human health significantly drives the selection for inherent or acquired bacterial antibiotic resistance[14]. To date, the enormous number of bacterial genetic resistance determinants[15] and mechanisms[16] compromise the effect of all routinely used antibiotics. It is even suggested that resistance evolves faster to newly introduced antibiotics[17]. In order to avoid this development for future antibiotics, we require improved understanding of the multiple factors that contribute to bacterial antibiotic resistance evolution (**Figure 1**) and how they interplay with each other.

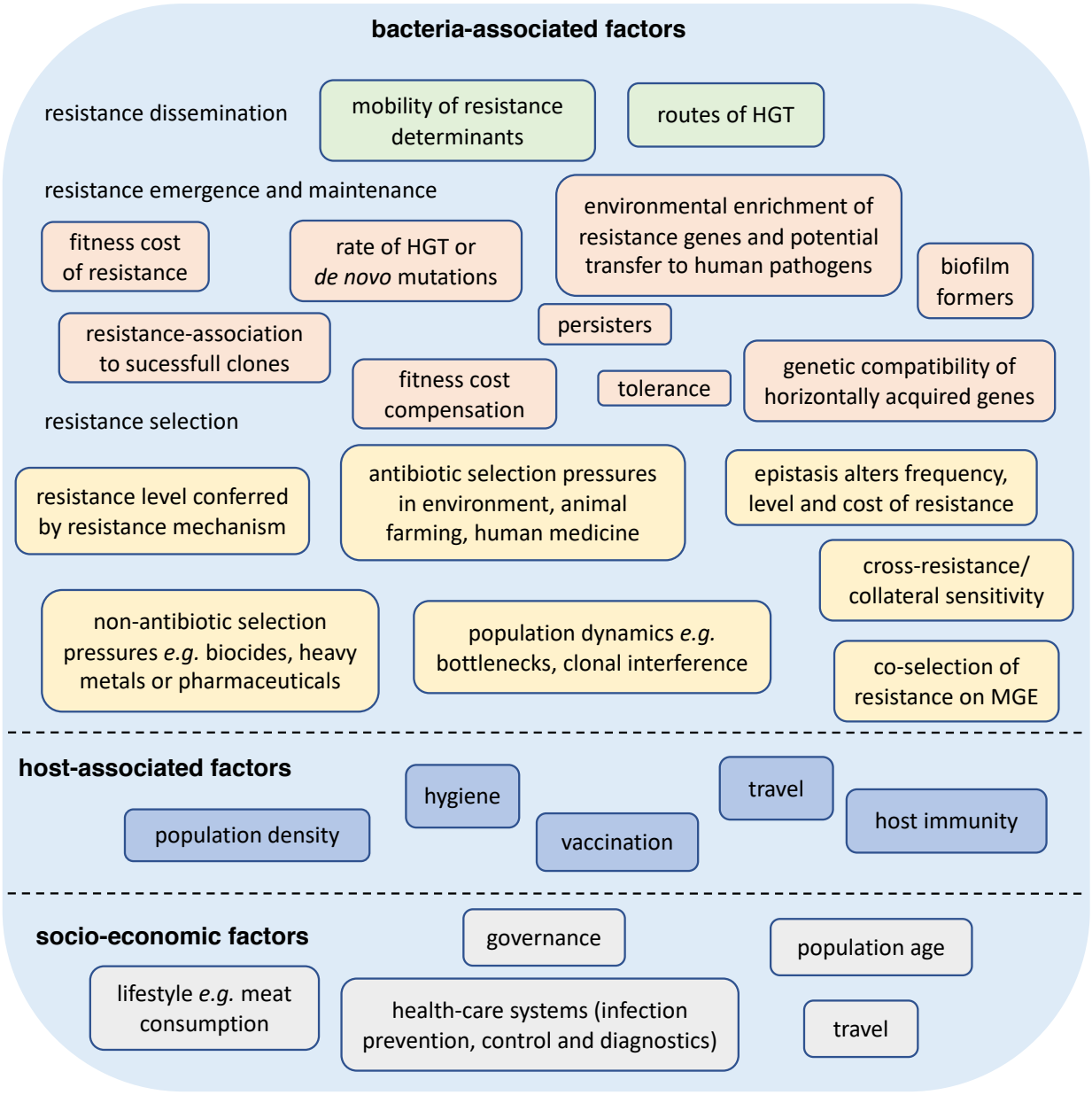

Figure 1: Factors that influence antibiotic resistance evolution in bacteria. The figure is based on references[14,18-20]. HGT = horizontal gene transfer; MGE = mobile genetic element.

Discovery and classification of antibiotics

Traditionally, antibiotics are small, organic molecules and categorized according to their chemical class. The sulfonamides were the first chemically synthesized drugs with antibacterial activity and have been used since 1935[21]. The discovery that microbes, mainly *Streptomyces* spp. in the order actinomycetes, produce antibiotics[22] led to the identification of the major chemical classes of antibiotics that are currently in clinical use. Throughout the 1940's and 1950's, the β-lactams, aminoglycosides, tetracyclines, macrolides, glycopeptides, ansamycins and polymyxins were isolated from bacteria[15,23]. Nitrofurantoin, quinolones, nitroimidazoles and trimethoprim are examples of

chemically synthesized antibiotics that were developed in the 1950's and 60's[15]. Essentially all major chemical drug classes were discovered by the 1960's, and only five additional ones, all active against Gram-positive (G+) bacteria, have reached approval for human use since then. These include the oxazolidinones (2000, linezolid), lipopetides (2003, daptomycin), pleuromutilins (2007, retapamulin), the macrolacton Fidaxomicin (2011) and the diarylquinolone Bedaquiline (2012)[24]. More recently, Teixobactin (2015, depsipeptide) and Malacidin A (2018, malacidins) were discovered using *in situ* cultivation or culture-independent approaches, respectively[25,26]. Both represent novel antibiotic classes with activity against G+ bacteria, while new chemical classes for G- infections are alarmingly scarce[6]. The recently launched agents avibactam and vaborbactam represent first-in-class chemical scaffolds that are used in combination with β-lactam antibiotics. They inhibit some but not all resistance determinants (β-lactamases; see β-lactam resistance) present in G- bacteria and are thus adding only limited clinical benefit over existing treatment options[6]. It is estimated that 11 new antibiotics will be approved between 2019 and 2024, of which the majority will only be chemical modifications of already existing drug classes[6].

Antibiotics can further be classified as bacteriostatic (*e.g.* trimethoprim) or bactericidal (*e.g.* quinolones, β-lactams, nitrofurantoin), which specifies if their effect inhibits bacterial growth or kills bacteria, respectively. Their activity against a broad (*e.g.* tetracyclines, β-lactams, fluoroquinolones) or narrow spectrum (*e.g.* polymyxins) of bacterial species further classifies antibiotics. Finally, antibiotics are categorized according to their dose-dependent (*e.g.* quinolones, aminoglycosides) or time-dependent (*e.g.* β-lactams, macrolides) antibacterial effect.

Molecular target sites of antibiotics

Antibiotics inhibit growth or induce death in bacterial cells by selectively acting on biochemical pathways that are essential for bacterial physiology and metabolism. Examples for the major molecular target sites of antibiotics in bacteria are presented below, with a special focus on the clinically relevant drugs used in **paper I** (**Figure 2**).

β-lactams represent the oldest but still most important class of antibiotics. They target the **bacterial cell wall** by blockage of enzymes that are bound to the cytoplasmic membrane and involved in **peptidoglycan** synthesis of G- and G+ bacteria[27]. These so-called penicillin-binding proteins (PBPs) exhibit transpeptidase and transglucosylase function and perform polymerization, reconstruction and degradation of the bacterial cell wall during active cell growth. Penicillins (*e.g.* amoxicillin, mecillinam, temocillin), cephalosporins (*e.g.* ceftazidime) and carbapenems (*e.g.* ertapenem) covalently bind to and inhibit these bacterial enzymes. The antibiotic fosfomycin inhibits the synthesis of bacterial cell wall precursor molecules by binding to the cytoplasmic enzyme MurA[28].

Protein synthesis (translation) in G+ and G- bacteria is affected by a variety of antibiotic classes, such as macrolides (*e.g.* azithromycin), aminoglycosides (*e.g.* gentamicin), tetracyclines (*e.g.* tetracycline, tigecycline) or amphenicols (*e.g.* chloramphenicol). These drugs bind either to the ribosomal RNA or to ribosomal polypeptide-structures of the large (50S) or small (30S) sub-unit of bacterial ribosomes. Their binding interferes with the initiation, elongation or termination of protein synthesis and results in truncated and misfolded proteins[29]. **DNA transcription** to messenger RNA is blocked by binding of rifamycin drugs (*e.g.* rifampicin) to the β-subunit of bacterial RNA polymerase, which is encoded by *rpoB*[29]. Ciprofloxacin is an example of a fluoroquinolone antibiotic. In G- bacteria, quinolone antibiotics bind primarily to the GyrA subunit of the topoisomerase II tetramer $GyrA_2GyrB_2$ (bacterial gyrase), while the ParC subunit of the topoisomerase IV tetramer $ParC_2ParE_2$ is a preferred target for antibiotic binding in G+ bacteria[30]. Both enzymes are involved in the cleavage and re-ligation of DNA**,** which facilitates the molecule's relaxed and negatively super-coiled topology, and chromosome separation, during and after **DNA replication**[30]. The DNA-enzyme-fluoroquinolone complex stalls bacterial DNA synthesis by blocking replication fork movement. High drug concentrations introduce double-strand breaks and cause chromosome fragmentation[30]. Sulfonamides and trimethoprim are antifolate antibiotics that inhibit the pathway for *de novo* **synthesis of folate**, which is for example required in bacterial nucleic acid synthesis. Sulfonamides such as sulfamethoxazole bind to the enzyme dihydropteroate synthase (DHPS) in competition with the enzyme's bacterial substrate para-aminobenzoic acid. Trimethoprim targets folic acid synthesis in a later step than sulfonamides and binds to bacterial dihydrofolate reductase (DHFR) in competition with dihydrofolic acid[31]. The **outer membrane** of G- bacteria is the target site of polymyxins such as colistin. These peptide antibiotics interact with the lipopolysaccharide structure on the bacterial outer membrane and subsequently disrupt both, the outer and inner membranes[23]. Nitrofurantoin is a prodrug that requires intracellular bioactivation by type I nitroreductase enzymes[32,33]. The reactive intermediates of the drug are thought to have **multiple target sites** in G+ and G- bacteria and cause for example DNA and ribosome damage[34].

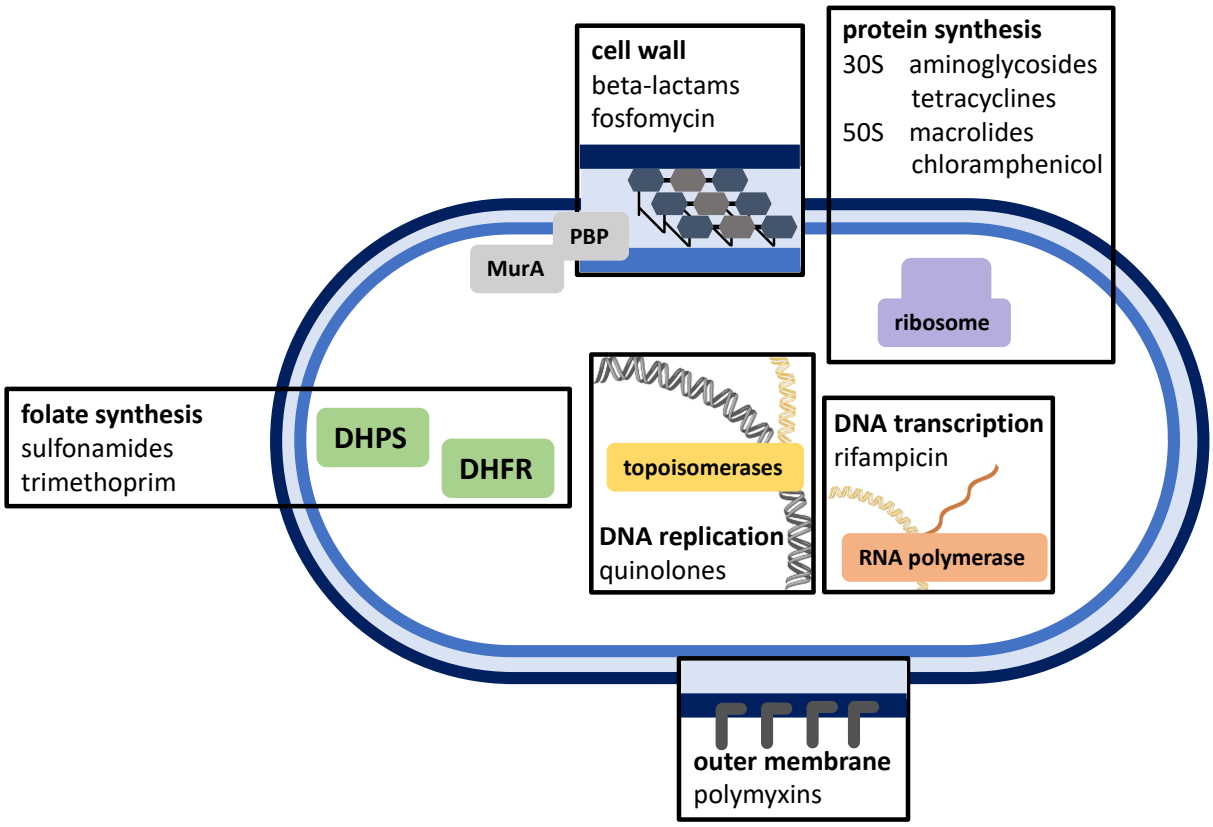

Figure 2: Illustration of the major molecular target sites of antibiotics in bacteria.

Development of antibiotic resistance

Antibiotic resistance develops either from *de novo* mutational changes in the bacterial genome or through horizontal gene transfer (HGT; see Horizontal gene transfer). The relative importance of these two modes of resistance acquisition depends on the bacterial species as well as the antibiotic class. In *M. tuberculosis* for example, MDR towards the key therapeutic agents evolves through the acquisition of chromosomal resistance mutations, while HGT is assumed to play a limited role in this pathogen[35]. However, in the majority of healthcare-associated pathogens, resistance develops through both mutations and HGT. Ciprofloxacin resistance in *E. coli*, for example, evolves primarily through chromosomal mutations but plasmid-associated *qnr*, *aac(6')-Ib-cr* and *qep* quinolone resistance genes also reduce susceptibility to this drug[15,36]. Resistance to colistin was until 2015 believed to be only chromosome-encoded, however, transferable *mcr* genes were identified to confer resistance to this important last-line antibiotic, especially in *E. coli* and *K. pneumoniae* isolates[23]. In *Enterobacterales*, resistance to β-lactams is driven by the horizontal spread of drug-destroying enzymes (see β-lactam resistance), and in *Acinetobacter* spp., resistance development is facilitated by the genus's participation in several horizontal gene acquisition pathways[37]. While chromosomal

resistance mutations are transmitted vertically through bacterial binary fission, HGT facilitates the spread of resistance determinants both between related and unrelated bacterial pathogens[38,39].

Resistance evolved also as a natural bacterial trait and independent from the human use of antibiotics[40,41]. This so-called intrinsic or inherent resistance allows bacteria to withstand antibiotics that are present in their environmental niche or from their own production but renders them also resistant towards therapeutically used antibiotics[16,41]. Species-specific functional or structural characteristics contribute to intrinsically decreased bacterial antibiotic susceptibility[42]. The combination of intrinsic resistance at clinically relevant levels and resistance acquisition by mutations or HGT in important nosocomial pathogens such as *P. aeruginosa*, *Acinetobacter* spp. and enterococci minimizes treatment options tremendously[10,43].

In clinical settings, an infection is considered resistant when appropriate dosing and administration of antibiotics are not effective in the eradication of bacteria and/or the patient's curation. To evaluate the likelihood of treatment failure or success, clinical breakpoints were implemented (see below). Microbiologically, resistance is defined as the presence of molecular mechanisms that let bacteria survive the exposure to antibiotics[15,16] (see Bacterial resistance mechanisms towards antibiotics).

Determining antibiotic susceptibility and clinical breakpoints

Bacterial susceptibility towards an antibiotic is measured as the *in vitro* growth-preventing effect of the drug on the organism. The lowest concentration of an antibiotic that inhibits the visible growth of bacteria is defined as the minimal inhibitory concentration (MIC) (**Figure 3**), and the MIC of resistant bacteria is increased compared to the MIC of wildtype bacteria. To determine MIC values, antimicrobial susceptibility testing (AST) is performed and involves phenotypic methods such as broth microdilution (BMD) or diffusion gradient strip tests. These methods yield the MIC for a specific bacteria-antibiotic combination. BMD is the 'gold standard' technique for the vast majority of species-antibiotic combinations, and other methods of AST should be calibrated against BMD (ISO 20776-1:2019)[44,45]. The European Committee on Antimicrobial Susceptibility Testing (EUCAST) provides guidance in the interpretation of AST to facilitate the standardized surveillance of antibiotic resistance[46].

To assist clinicians in the interpretation of susceptibility testing, the concept of clinical breakpoints is internationally applied and regularly revised for clinically relevant species-drug combinations[45,47]. These represent MIC 'cutoff' values and are used to categorize bacterial isolates and predict treatment outcome. Isolates with MIC values below the clinical breakpoint fall into either of the two *susceptible* categories, where the likelihood of therapeutic success is high under a standard drug dosing regimen (S) or when drug exposure is increased (I). However, an MIC value at or above the clinical breakpoint

represents the *resistant* category (R), where the likelihood of therapeutic failure is high[46]. Clinical breakpoints are based on pharmacokinetic/pharmacodynamic data of the tested species-drug combination as well as information about the resistance mechanism[44]. Additionally, knowledge of the epidemiological cut-off value, which is the highest MIC value measured for a wildtype population of a bacterial species, is addressed[44]. MICs above the EUCAST clinical breakpoint was the inclusion criteria for resistant *E. coli* mutants generated in **paper I.**

Mutant selection window

From a pharmacokinetic perspective it was traditionally assumed, that antibiotic resistance is selected for between the MICs of the susceptible and the resistant members of the population. The latter antibiotic concentration is termed the mutation prevention concentration (MPC) and the antibiotic concentration range between MIC and MPC represents the so-called mutant selection window (MSW)[48] (**Figure 3**).

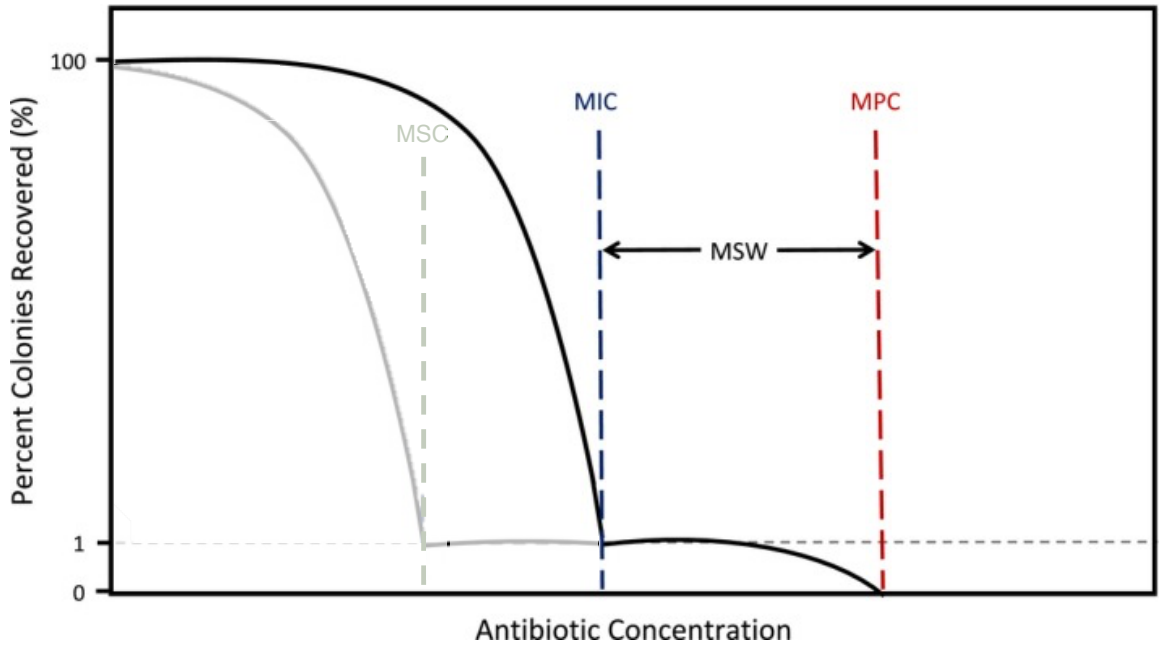

Figure 3: Schematic of the traditional mutant selection window. The growth of wildtype bacteria (until MIC) and resistant mutants (until MPC) is illustrated (black line) in increasing antibiotic concentrations. At the MIC, growth has declined by 99%. At the MPC, even bacteria with an acquired resistance mutation do not survive antibiotic exposure. The minimal selective concentration (= MSC) is indicated as shaded lines. Reprinted and adapted under the Creative Commons Attribution 4.0 International License from[49].

However, it was later demonstrated that resistant bacteria, pre-existing or *de novo* generated, are selected for even at antibiotic selection pressures far below the MIC. *In vitro*, Gullberg and colleagues showed that antibiotic concentrations at more than 100-fold reduced wildtype MICs still provided a growth advantage to *E. coli* with chromosomal resistance[50] or with an MDR plasmid[51]. Their findings suggested that the MSW expands to an even lower concentration than the MIC, which they designated the minimal selective concentration (MSC)[50]. Thus, research on the selection dynamics at MSC and MPC elucidates the impact of antibiotic concentration gradients in the treated human body, and also in the environment, on the evolution of resistance[52].

Bacterial resistance mechanisms towards antibiotics

Different biochemical mechanisms lead to resistance in bacteria. They may affect the antibiotic agent itself, which can be enzymatically inactivated, degraded or modified. Furthermore, the antibiotic molecular target can be structurally altered, overproduced or circumvented by alternative cellular pathways. Finally, reduced drug uptake or increased drug efflux impacts the effective antibiotic concentration in the cell[16,53] (**Figure 4**, from left to right). As a consequence, the pharmacodynamic interaction between the drug and the bacterial target is decreased or becomes irrelevant and the bacteria is less affected by the antibiotic.

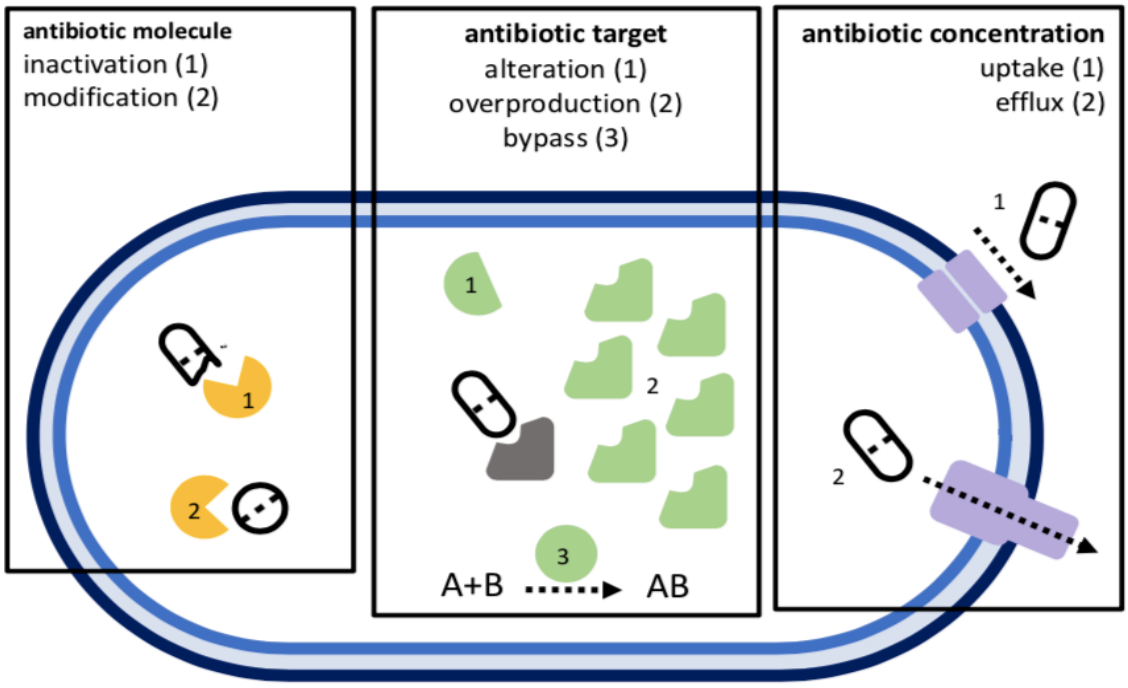

Figure 4: Illustration of the major antibiotic resistance mechanisms in bacteria. Bacterial enzymes that act on the drug are indicated in yellow, molecular target sites of the antibiotic are indicated in green, and bacterial cell wall/cell membrane proteins are indicated in purple.

The examples for resistance mechanisms given below are based on specific drugs and mechanisms focused on in this thesis. They evolved through *de novo* mutations in *E. coli* (**paper I**), or by horizontal transfer of plasmids into *E. coli* (**paper III**).

Ciprofloxacin resistance

E. coli acquires ciprofloxacin resistance most frequently by *de novo* mutations in the **drug target** genes *gyrA* (bacterial DNA gyrase) and *parC* (topoisomerase IV) affecting codons that are located in the so-called quinolone resistance determining region (abbreviated as QRDR)[54]. In clinical isolates, increasing resistance develops by several mutational paths in a multistep process[55-57] and is generally initiated by a *gyrA*-located mutation (S83L)[58]. Clinical resistance (MIC >0.5 µg/mL) is not achieved by acquisition of a single mutation[56,57,59] and triple drug target mutants in *gyrA* (S83L, D87N) and *parC* (S80I) are the predominant genotypes in clinical *E. coli*. This is likely due to the isolates' selectively beneficial resistance level (up to 16 µg/mL) and growth rate (relatively unchanged)[56,58]. Although *gyrB* and *parE* drug target mutations are observed in *E. coli* clinical isolates[57,58,60], their role in ciprofloxacin resistance evolution is less characterized. Higher-level resistance (>32 µg/mL) results from the acquisition of four to six putative resistance mutations, most often combining drug target alterations and **increased ciprofloxacin efflux**[58,61]. Mutations in the transcriptional repressor genes *marR*, *acrR* and *soxR* lead to upregulation of the major efflux pump in *E. coli*, AcrAB-TolC[61-63], while mutations in the RNA polymerase β-subunit gene *rpoB* increase the expression of the MdtK efflux pump[59] (**paper I**). Growth reduction of *E. coli* efflux-mutants inhibits their early selection during clinical ciprofloxacin resistance evolution[56]. Finally, mutations in transcriptional regulator genes *marA* and *envZ* and the consequent decrease in expression of the outer membrane porin OmpF cause resistance by **reduced ciprofloxacin uptake**[64,65] (**paper I**).

Mecillinam resistance

In *E. coli*, the described mutational target for mecillinam resistance is very large. *In vitro*, *E. coli* resistance levels above the clinical breakpoint (MIC >8 µg/mL) were achieved through single mutations in altogether 38 target genes, which affected different cellular functions and occurred at high frequencies[66,67]. In the patient however, resistance arises only at low and stable frequencies[68] and the diversity of mutational targets observed *in vitro* is not reflected in resistant clinical isolates[66]. This is possibly due to the slow growth that reduces their survival in the rapidly flushing urinary tract, as observed in experimentally obtained resistant mutants[66]. In clinical *E. coli* isolates, high-level resistance (MIC = 32 µg/mL) was due to loss-of-function mutations in *cysB*, which encodes a transcription regulator for the biosynthesis of the amino acid cysteine[66]. A decline in cellular cysteine

caused an oxidative stress response and subsequent increase in the expression of PBP1B, LpoB (activator of PBP1B) and FtsZ (cell division protein), which represents a **bypass mechanism** leading to mecillinam resistance[67]. A recent Tn-seq approach identified that the induction of the stringent response or the Rcs envelope stress response through elevated ppGpp levels could be linked to more than 100 genes in mecillinam resistant *E. coli*[69] (*relA*, *aspS*, *tusB* or *aceE*, *aceF*, respectively), some of which were also target for resistance mutations in clinical isolates (**paper I**). Finally, mutations in the cellular **drug target** PBP2 (*mrdA*) or its functional partner RodA (*mrdB*) inhibit peptidoglycan synthesis and lead to mecillinam resistance[70].

Nitrofurantoin resistance

E. coli evolves mutational resistance to nitrofurantoin through highly reproducible trajectories *in vitro*[71]. Since the biologically active toxic intermediates are formed by enzymatic reduction[32,33], the primary targets for nitrofurantoin resistance mutations, both in resistant clinical isolates and in experimentally generated mutants, are the genes *nfsA* and *nfsB* of the type I nitroreductase[72] (**paper I**). Clinical resistance levels (MIC >64 µg/mL) are reached by the acquisition of multiple mutations, although *in vitro*, this resistance-level was occasionally observed for single-mutants in *nfsA* as well[72] (**paper I**). The stepwise acquisition of two putatively inactivating nitroreductase-mutations, first in *nfsA* and then in *nfsB*, increased resistance in *E. coli* mutants to high levels (MIC >128 µg/ml)[72]. *In vitro*, nitroreductase mutations are frequently selected in combination with loss-of-function mutations in the gene *mprA* (encoding EmrR) of an EmrAB-TolC efflux pump repressor[71] (**paper I**), which promotes *E. coli* nitrofurantoin resistance by increased **drug efflux**[73].

Trimethoprim resistance

The great majority of trimethoprim resistance mutations in *E. coli* are related to one single locus, the *folA* gene encoding the **drug target** enzyme DHFR. DHFR is the primary cellular drug target, and in experimentally evolved *E. coli*, DHFR-associated mutations are either found in the substrate-binding region of the enzyme or in the promoter region of *folA*[74,75] (**paper I**). Mutational alterations in active site residues of DHFR decreases the binding affinity of trimethoprim, while binding of the natural substrate dihydrofolic acid is unaffected[76]. Mutations in the *folA* promoter region caused a more than 100-fold enzyme **overproduction** in a clinical *E. coli* isolate, which decreased the impact of drug-bound DHFR[77]. It can be assumed that *folA*-amplification during *in vitro* drug adaptation resulted in DHFR overproduction and resistance above clinical breakpoint[74] (**paper I**). A single drug-target mutation leads to resistance just above clinical breakpoint (MIC >4 µg/mL) (**paper I**), however, high-level resistance requires the stepwise acquisition of mutations in the DHFR-promoter and drug

binding-site, as demonstrated for resistant clinical isolates[77] and experimentally generated mutants[74,75] (**paper I**).

β-lactam resistance

Enzymatic inactivation of β-lactam antibiotics was first described in 1940 for penicillin[4]. Today, it represents the predominant resistance mechanism against this drug class in G- bacteria and is commonly acquired by HGT mechanisms (see Horizontal gene transfer). The responsible enzymes are encoded by *bla*-genes, universally termed β-lactamases, and close to 3000 variants were identified until 2018[78]. β-lactamases are present in the bacterial periplasm and active at the peptidoglycan layer. Collectively, they have the ability to inactivate all known β-lactam antibiotics by hydrolytic cleavage of the drug's characteristic β-lactam ring[78].

As shown in **Figure 5** (left), β-lactamases are categorized on different levels. Structural and biochemical differences separate serine β-lactamases (SBL) from metallo-β-lactamases (MBL). SBLs form intermediate acyl-enzymes with β-lactam antibiotics using an active site serine and successively perform fast drug-hydrolysis[79], whereas MBLs interact with β-lactams via Zn^{2+}-dependent recognition before hydrolyzing the drug[80]. Furthermore, β-lactamases are classified based on amino acid sequence relatedness[81] (**Figure 5**, left, class) or characteristics regarding their substrate specificity or inhibitor sensitivity (Bush subgrouping)[82].

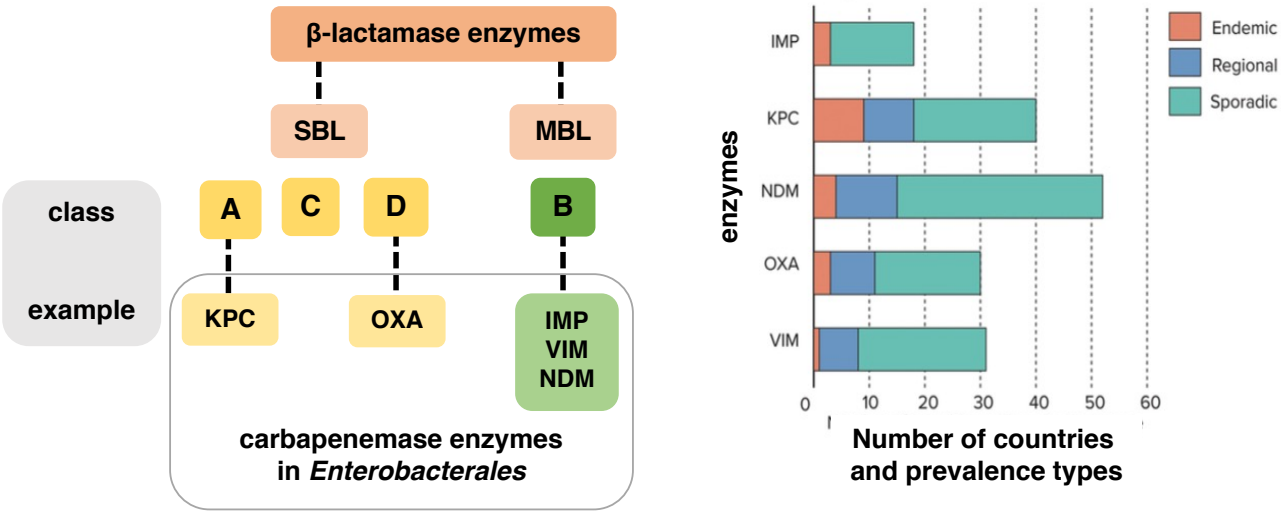

Figure 5: Simplified categorization scheme for β-lactamase enzymes. Biochemical characteristics divide β-lactamases according to their active site serine (= SBL) or metal-dependence (= MBL). Further categorization follows Ambler molecular classes (A, B, C and D). Clinically important carbapenemases in *Enterobacterales* are highlighted (grey circle). **The global spread** of major carbapenemases in *Enterobacterales* is indicated by the number of countries per enzyme. Reprinted and adapted with permission from[83].

In the context of this thesis, the MBLs Verona-Integron-encoded (VIM-type) and New-Delhi MBL (NDM-type) are highlighted here. The plasmids employed in **paper III** harbor variants thereof, namely VIM-1 in pG06-VIM-1 and NDM-1 in pK71-77-1-NDM (see Multidrug resistance plasmids). They represent so-called carbapenemases which have the capacity to inactivate all β-lactam antibiotics except monobactams[83]. Among the targeted drugs, carbapenems are valuable, synthetic, last-line antibiotics for the treatment of MDR infections, especially by extended-spectrum-β-lactamases (ESBL)-producing *Enterobacterales.* Compared to other β-lactamases, carbapenemases emerged rather late[78], for example VIM-1 in 1997[84] and NDM-1 in 2009[85]. Nevertheless, they are the primary cause of carbapenem-resistant G- bacteria today and among *Enterobacterales*. Carbapenemase-producing *K. pneumoniae* as well as *E. coli* from the family *Enterobacteriaceae* are clinically predominant and frequently associated with horizontally transferrable carbapenem resistance[86-88]. Besides VIM and NDM-type, widely distributed carbapenemases in *Enterobacterales* are the SBLs *K. pneumoniae* carbapenemase (KPC-type) and oxacillinases of the OXA-48 subgroup (OXA-type), as well as the IMP-type MBL (imipenemase)[83] (**Figure 5**, left). Although VIM-1 is not the most common VIM-type variant worldwide, it is endemic both in *K. pneumoniae* and *E. coli* in Greece[83]. NDM-type carbapenemases are the geographically most widespread MBL in *Enterobacterales* and its endemicity is currently reported for Bangladesh, India, Pakistan and China[83] (**Figure 5**, right).

Horizontal gene transfer

Sequence analyses of biological samples from different environmental or clinical sources such as plants, soil, wastewater, gut microbiome of human and animals, hospital surfaces or plumbing systems frequently confirm that resistance genes are abundant[89,90]. Pathogenic bacteria can acquire these resistance determinants by HGT[39,89], of which transduction, conjugation and natural transformation represent the three canonical mechanisms[91].

Transduction is mediated by bacteriophages, which accidentally exchange genetic material between donor and recipient bacteria during their own propagation between hosts[92]. During transduction, the randomly packed genomic donor DNA in the phages' head is protected from degradation over a long time and over long distances. Phage-host recognition may be limited to closely related bacteria; however, some phages have evolved a broader host-range[93]. Sequence analysis frequently reveals that antibiotic resistance genes can be associated with phages in hospital environments[39] and *in vitro* transduction transferred resistance plasmids up to 30 kb between clinical isolates of *S. aureus*[94].

Conjugation is the directed transfer of genetic material from a donor to a recipient cell that are in close proximity[92] and is mediated either by integrative conjugative elements (ICEs) or by extra-chromosomal DNA elements called plasmids (see Plasmids). Plasmids either encode the conjugative machinery for DNA transport between donor and recipient cell on *tra*-genes or encode mobility (*mob*) genes that make them mobilizable through simultaneous transport with a conjugative plasmid[95]. HGT by conjugation is the primary mechanism by which antibiotic resistance genes are disseminated between bacterial pathogens[39], especially *Enterobacterales*[86], and facilitates plasmid-associated outbreaks of MDR[96,97]. Plasmid instability and the metabolic costs related to the conjugation process and to plasmid maintenance represent limitations to conjugative gene transfer (see **Fitness cost of plasmid carriage**). **Natural transformation** was central in the experiments for **paper II.** The requirements for successful gene acquisition in the naturally competent G- bacterium *A. baylyi* are thus described in more detail below.

Recent studies reveal **additional routes** for the horizontal transmission of genetic material, for example by DNA-containing membrane vesicles released from bacterial cells[98], through cell-to-cell connecting nanotubes[99] or by phage-like gene transfer agents[89]. The relevance of these newer mechanisms in the spread of antibiotic resistance between bacterial pathogens, however, requires further confirmation and examination. Intra- and interspecies transfer of resistance-encoding plasmids by *A. baylyi* outer membrane vesicles occurred at low frequencies (10^{-6} and 10^{-8}; respectively)[100], and nanotube-mediated transfer of plasmid-DNA among *Bacillus subtilis* cells[99] may be a result of the recipients' ability for DNA uptake by natural transformation[101].

Natural transformation

Natural transformation is the process by which bacterial cells take up, integrate and express free DNA from the extracellular environment[91]. This 'transformation principle' was first described in 1928 by Frederick Griffith. He observed that avirulent *Streptococcus pneumoniae* cells became virulent when he injected them together with heat-inactivated cells of virulent *S. pneumoniae* into mice, which could later be explained by DNA transfer[102]. Our current understanding of natural transformation developed especially through more than 50 years of research in model organisms such as *S. pneumoniae*, *B. subtilis, Neisseria gonorrhoeae* and *A. baylyi*[103], however experimental evidence for natural transformability of more than 80 species, with similar proportions of G+ and G-, exists[104]. These mainly represent environmental species[104,105], but also important hospital-associated, pathogenic species[9,104], and some experimental evidence for the potential to undergo natural transformation was also obtained in clinical isolates[39,106,107].

Competence and DNA uptake during natural transformation

Since natural transformation is not facilitated by infecting agents such as phages or plasmids, the recipient's competence to bind and actively transfer donor DNA into the cytoplasm is required[108]. Competence is a physiological state encoded by the recipient, and the 'competence regulon' includes a conserved set of genes that is common to almost all naturally transformable species[104]. In *A. baylyi*, the proteins of the DNA-uptake machinery are encoded by the *com* and *pil* genes, and *drpA*[109]. These proteins make up the DNA-uptake pilus and membrane-associated uptake pores and facilitate binding and translocation of double-stranded DNA (dsDNA) through the periplasmic space and peptidoglycan layer[109]. They further mediate transport of single-stranded DNA (ssDNA) into the bacterial cytoplasm and finally, initiate recombination of the foreign DNA with the bacterial genome[109] (**Figure 6**). Competence genes are constitutively expressed in some species, for example *A. baylyi, Helicobacter pylori* and *N. gonorrhoeae*, while other species require certain conditions and signals (growth phase, cell density, chemicals, stress conditions like nutrient starvation, antibiotic treatment, DNA damage) to regulate a transient state of competence[103]. Moreover, the DNA-uptake apparatus of *N. gonorrhoeae* or *Haemophilus influenzae* only binds DNA that contains a specific nucleotide sequence, while other bacteria such as *B. subtilis* or *A. baylyi* take up DNA from any source[105,110].

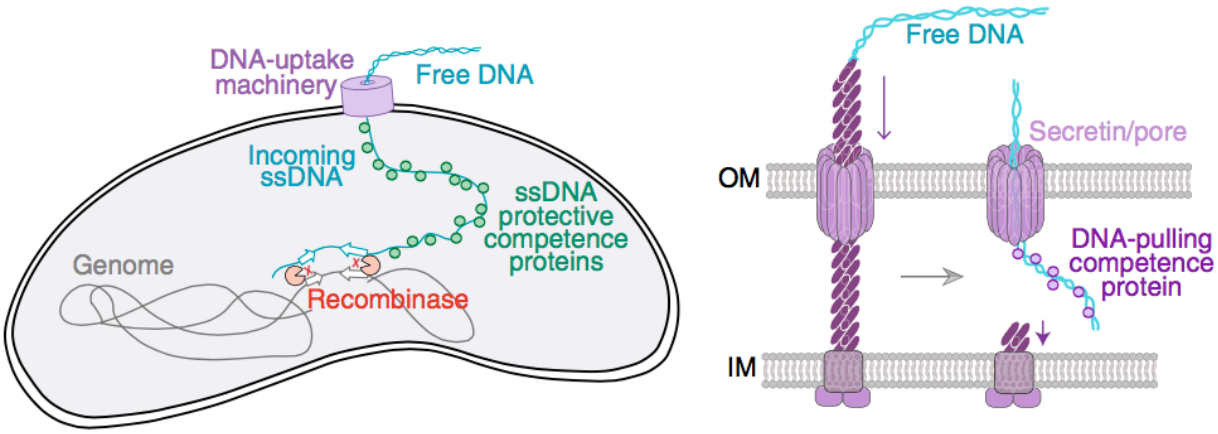

Figure 6: Illustration of natural transformation in competent G- bacteria. The DNA-uptake machinery of a competent recipient bacterium can bind dsDNA (blue) from the environment and translocate it into the cell. The single-strand DNA-binding protein SSB and DNA processing protein DprA (both in green) protect incoming, linear ssDNA from enzymatic degradation by exonucleases, and DprA loads the recombinase (= RecA)[111]. RecA initiates homology search within the recipient's chromosome, which eventually leads to integration of the transforming ssDNA by recombination. **DNA-translocation** of bound dsDNA (blue) to the cytoplasmic membrane in G- bacteria is achieved by retraction of the DNA-uptake pilus (type IV pilus, dark purple), opening of the secretin pore ComQ (light purple) in the outer membrane (OM), and binding of the periplasmic, DNA-pulling competence protein ComEA. Finally, dsDNA is degraded to ssDNA, which crosses the inner membrane (IM) through the ComA membrane channel (not shown here) and reaches the cytoplasm. Reprinted with permission from[103] with protein names according to the model of DNA uptake in *A. baylyi*[109].

DNA uptake during natural transformation requires free and naked DNA in the environment. Prokaryotic DNA is abundant in the environment through the lysis of dead bacterial cells, the disruption of live cells or active excretion of DNA by, for example, *Acinetobacter, Pseudomonas, Bacillus* and *Streptococcus* spp.[105]. Compared to DNA that is transferred during conjugation and transduction, this extracellular DNA is not protected by a membrane (pore) or virus capsule, which can cause biochemical, chemical and/or physical modification, and fragmentation of the DNA spontaneously or by nucleases. However, DNA of different sources (plant, bacteria) was demonstrated to persist in environments such as soil, water, saliva or blood to varying degrees and may eventually transform bacteria[91,105,112].

DNA recombination during natural transformation

To ensure further inheritance, the incoming ssDNA has to be integrated within the recipient genome during natural transformation[91]. Depending on the type of donor DNA and its sequence similarity to the recipient chromosome, different recombination mechanisms are possible after DNA uptake in *A. baylyi*. Plasmids can establish extra-chromosomally and replicate autonomously[110] (see Plasmids). Homologous recombination is mediated by the RecA recombinase and occurs between donor and

recipient DNA segments with at least 20 nucleotides sequence homology[105]. The integration of acquired DNA by RecA-dependent mechanisms during natural transformation is reduced if proteins of the RecBCD/RecFOR DNA repair pathways, which generate RecA-loaded 3'-DNA ends, are absent[113]. Interestingly, a RecA-independent mechanism of DNA integration was described for short, homologous fragments of 20 to 80 nucleotides[114]. The recombination frequency for foreign DNA decreases with the degree of sequence dissimilarity between donor and recipient DNA but can be facilitated even if only limited or no sequence similarity is present (homology-facilitated illegitimate recombination (HFIR)[115] and double-illegitimate recombination (DIR or HFDIR)[116]. In *A. baylyi*, recombination during natural transformation can occur at frequencies from 10^{-3} for homologous chromosomal donor DNA and integration of a selectable resistance marker gene, or 10^{-12} for short fragments of fully heterologous DNA (*B. subtilis*) (short-patch double-illegitimate recombination, SPIDR)[117]. Finally, an important finding was that integron-associated resistance from unrelated species can be chromosomally acquired by *A. baylyi* through the site-specific recombination functions of transposons or insertion sequence (IS) elements during natural transformation[118]. However, the frequency of natural transformation events in nature or hospital settings and their relevance for clinical antibiotic resistance evolution is poorly understood[39].

Mobile genetic elements

Mobile genetic elements (MGEs) move between and within DNA molecules. They are abundant in bacterial genomes and encode functions for their own mobility and adaptive traits such as antibiotic or heavy metal resistance, virulence or pathogenicity factors, or metabolic functions[95]. Conjugative plasmids, ICEs or bacteriophages represent MGEs that move between bacterial cells by HGT mechanisms (see **Horizontal gene transfer**), while transposons and IS elements encode site-specific recombination functions to move intracellularly[95] (see Transposable elements). Integrons and gene cassettes are resistance-encoding genetic elements that are mobilizable through their association to MGEs such as plasmids and transposons. Due to interactions between transposable and conjugative genetic elements, HGT can essentially mobilize any chromosomal gene, which has great impact on bacterial niche-adaption by acquisition of new ecological functions. The relevant MGEs for this thesis are plasmids (**paper III**) and transposons (**paper II**) and are described in more detail below.

Plasmids

Plasmids are extra-chromosomal, double-stranded and generally circular DNA molecules that naturally exist in bacteria. They represent the best characterized and most promiscuous vectors of horizontal resistance spread. The so-called plasmid backbone comprises functions for plasmid replication and inheritance or for their horizontal infectious transfer by conjugation (see **Horizontal gene transfer**). A more variable plasmid region harbors accessory genes that promote host adaptation to, for example, antibiotics[119].

Plasmids replicate semi-autonomously within the host cell by theta, rolling-circle or strand-displacement mode of replication[120]. Theta-type replication is described for small and large plasmids and most often used by plasmids in *Enterobacterales*. Here, leading and lagging strands are replicated simultaneously from the plasmid's origin of replication (*ori*). In rolling circle replication, first identified for small plasmids in G+ bacteria, leading and lagging DNA strands are synthesized in two separated cycles, from the double-stranded origin (*dso*) and the single-stranded origin (*sso*), respectively[120]. Importantly, plasmid replication usually sequesters host enzymes like helicases, primases and polymerases, which reflects the parasitic character of plasmids within a bacterial host[120]. A plasmid therefore contains sites that both plasmid and host-encoded proteins may interact with. For example, replication at the *ori* can be initiated by plasmid-encoded Rep proteins, or independent of that, by host polymerases after the binding of a plasmid-encoded RNA II primer[120], which is for example the case for ColE1-like MDR plasmids in *Enterobacterales*[86].

The dependence on host-functions for plasmid replication affects the host-range and horizontal spread of plasmids, because elements that have similar requirements for their replication and partitioning are

unstable if they coexist in the same cell. Such plasmids are members of the same 'incompatibility group'. Current methods identify plasmid-incompatibility (Inc)-types for example by *in vitro* PCR-based replicon-typing, which targets conserved regions specific to plasmid replication[121], or *in silico* from sequencing data[122]. In *Enterobacterales*, contemporary resistance plasmids represent Inc-types that were common already before antibiotic introduction[123]. *Enterobacterales* species comprise close to 30 plasmid Inc-types of varying host ranges, and IncF, IncI, IncA/C and IncH are frequently found resistance encoding plasmid types[86]. IncQ plasmids, for which RSF1010 is a widely used reference, replicate by a strand-displacement type and encode their own initiation, helicase and primase proteins, which makes them less dependent on host-factors and broadens their host-range beyond *Enterobacterales*[120].

In addition to replication, several plasmid-encoded factors determine the stable vertical inheritance of these genetic elements. For example, **multimer resolution systems** (*mrs*) facilitate plasmid separation into monomers by site-specific recombination after plasmid-replication[119]. The subsequent segregation of plasmid molecules into each daughter cells is enabled by a high plasmid copy-number and random diffusion, or by **partitioning systems** (*par*) that facilitate the active assembly of plasmid molecules at either cell pole[119]. Plasmid-encoded addiction systems function as **post-segregational killing systems** (*psk*) and as such ensure survival of plasmid-containing cells while plasmid-free cells are eradicated. This can take place by endonuclease attack through restriction-modification systems, or by a stable toxin factor in toxin-antitoxin systems[119]. The majority of resistance plasmids in *Enterobacterales* are present in only a few copies per cell[86] and their stability in bacterial populations depends on the above-mentioned mechanisms. However, further plasmid-host dynamics affect plasmid persistence and are described below (see Fitness cost of plasmid carriage).

Multidrug resistance plasmids

Since plasmids accumulate and physically link resistance determinants encoded by other MGEs, for example transposons or integrons, they contribute greatly to the horizontal spread of resistance. The majority of resistance plasmid types that are described in *Enterobacterales* is conjugative and/or exhibit a broad host range, while some are at least mobilizable[86,95]. Carriage of MGEs and also conjugative functions leads to larger plasmids, and the described resistance plasmids in *Enterobacterales* range in size from 45 kb to above 200 kb[86]. Plasmid-associated resistance determinants are described for all major antibiotic classes[15] and more than 75% of plasmids in *Enterobacterales* can be associated to resistance gene carriage[124]. A phylogenetic analysis estimates that genes encoding an OXA-type β-lactamase moved onto plasmids already more than 100 million years ago[125], however, the introduction of antibiotics in medical use reinforced the selection for

resistance genes in existing plasmids of human pathogens[123]. A recent study found up to seven plasmids in human intestinal *Enterobacteriaceae* samples, and plasmid-associated resistance genes, including ESBLs, lead to a MDR phenotype[126]. Carbapenemase genes are frequently mobilized through their association to plasmids and other MGEs[11], as exemplified here for the enzymes carried by the plasmids of **paper III**, pG06-VIM-1 and pK71-77-1-NDM (**Figure 7**). The *bla*$_{\text{VIM-1}}$-gene cassette is commonly incorporated into the variable region of a plasmid-located class I integron[88], and associated to rarely detected, but broad host-range plasmid-types such as IncR (pG06-VIM-1) or IncW[86]. IncR plasmid sequences are also reported as part of multi-replicon plasmids for example with the promiscuous IncA/C or IncF plasmids, which facilitates their horizontal mobility as they are otherwise immobile[11,127]. *Bla*$_{\text{NDM-1}}$ is linked to plasmid-located IS*26* and a complete or truncated ISAba125[88,128], and commonly associated to IncA/C-type plasmids, although many other replicon types also carry this carbapenemase-variant[11,87].

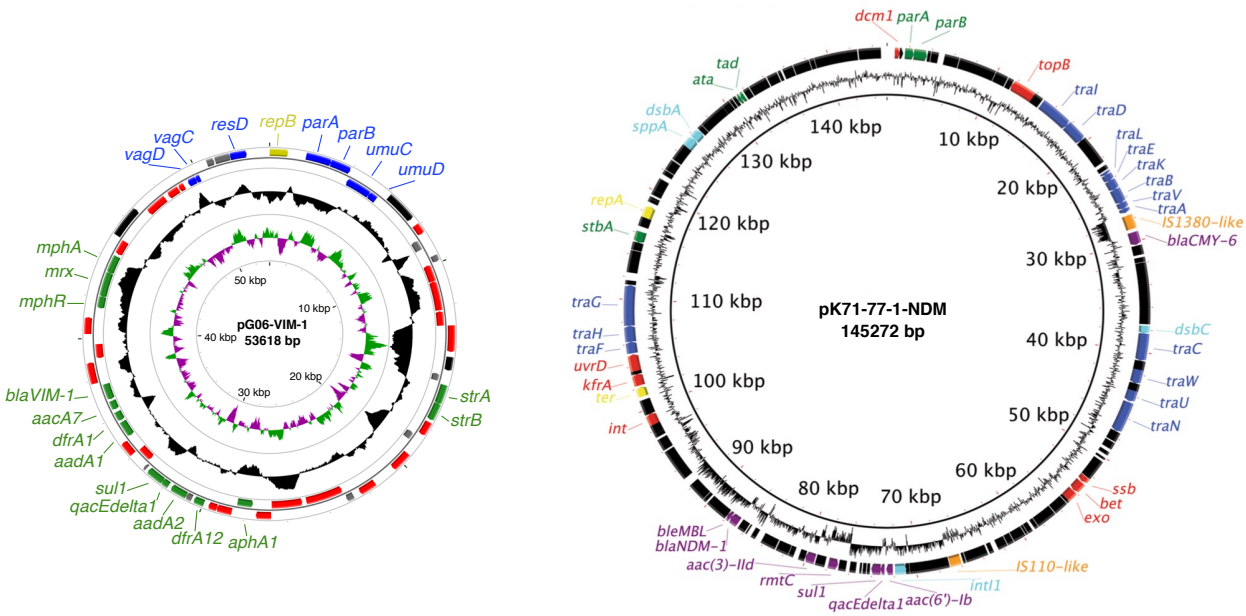

Figure 7: Examples for carbapenemase-encoding MDR plasmids of clinical origin. The maps illustrate the plasmids used in **paper III**. **Plasmid pG06-VIM-1** (GenBank KU665641) originates from a *K. pneumoniae* wound infection isolate[129]. It belongs to the IncR-group, for which *repB* encodes the replication initiation protein. A carbapenemase is encoded by *bla*$_{\text{VIM-1}}$ and additionally, the plasmid carries aminoglycoside (*aadA1, aadA2, aacA7, aphA1*), macrolide (*mphA, mphR, mrx*), sulfonamide (*sul1*) trimethoprim (*dfrA1, dfrA12*) and antiseptic (*qacEΔ1*) resistance genes (all in green), a toxin-antitoxin system (*vagCD*), a recombinase for multimer resolution (*resD*), and genes *parAB* involved in partitioning of the plasmid (blue)[130]. Mobile elements are indicated in red. Genes *bla*$_{\text{VIM-1}}$, *aacA7*, *dfrA1*, *aadA1* are associated to a class 1 integron[127], and gene *aphA1* is part of transposon Tn*4352*[131]. Reprinted and adapted with permission from[130]. **Plasmid pK71-77-1-NDM** (GenBank CP040884) was isolated from uropathogenic *E. coli*[132]. It is a IncC type 1 plasmid (also designated IncA/C$_2$) and replication initiation is encoded by *repA* (yellow). The plasmid encodes resistance to β-lactams (*bla*$_{\text{NDM-1}}$ and *bla*$_{\text{CMY-6}}$), aminoglycosides (*aac(6')-Ib*, *aac(3)-II*, *rmtC*), sulfonamide (*sul1*) and bleomycin (*ble*$_{\text{MBL}}$) (purple). Genes for conjugative transfer (*tra*) are blue and mobile elements are indicated in orange. Reprinted under the Creative Commons Attribution 4.0 International License from[128].

Transposable elements

Transposable elements are distinct DNA segments that are associated to the bacterial chromosome or to plasmids and able to move between genomic locations by transposition[133]. Transposition involves the cleaving and rejoining of DNA strands, as well as the formation of double- or single-stranded DNA-intermediates[134]. This autonomous movement of genetic segments was first suggested in 1950 by Barbara McClintock[135]. Her observation was, that DNA-translocation in the chromosomal loci encoding maize kernel pigmentation resulted in gene activation or inactivation and correlated with a varying color pattern of the kernels. Eventually, she received the Nobel prize for her discovery of MGE in 1983[136]. In bacteria, transposition of resistance determinants was first described in the early 1970's, and the designation 'transposons' was then introduced for bacterial DNA segments with the potential to move by transposition[137]. Today we know that transposons are ubiquitous in bacteria and Tn numbers are assigned to more than 600 unique bacterial transposons[138]. In their entirety, bacterial transposons carry resistance determinants against all major classes of antibiotics[138], and their site-specific recombination functions were shown to promote the spread of antibiotic resistance by transposition between different plasmids[97], or between a chromosomal and plasmid location[126,139] in clinical strains.

The best-characterized examples of autonomously moving transposable elements are **IS** elements[140] and transposons[138]. IS elements can be as small as 700-900 bp, as is the case for example for the ubiquitous IS*6*-family including IS*26*, and they typically only contain the minimal transposition module consisting of a transposase gene (*tnp*) and two terminal inverted repeats (IRs) to which the transposase binds for transposition initiation[95,140] (**Figure 8**, top). **Unit transposons** are distinct from IS elements in that they carry so-called passenger genes, which encode for example antibiotic, antiseptic or heavy metal resistance, virulence, or catabolic processes, in addition to the transposition module[95]. Their size can be up to 86 kb, but the average is around 12 kb[138]. Further, any genomic segment can be moved by transposition if it is flanked by two related IS-elements and is than called a **composite transposon**[95]. Autonomous transposable elements such as **conjugative transposons** (= ICE) encode genes for their intercellular transfer in addition to excision and insertion functions, or carry genes for DNA processing during conjugation such as in **mobilizable transposons**[133].

Intracellular transposition can also move otherwise immobile resistance elements onto horizontally transferable genetic units. For example, genetic elements called **integrons** do not encode transposition functions. Instead, they efficiently capture antibiotic resistance functions encoded by gene cassettes; the integron-integrase (*intI*) performs DNA insertion by site-specific recombination between the integron *attI* site and the gene cassette *attC* site, or DNA excision by recombination between two *attC* sites of gene cassettes. Despite their own immobility, integrons expressing

resistance gene cassettes are important elements in resistance evolution and their translocation to new sites is mediated by the transposable elements they are associated with[141]. Below I will focus on the large and widespread Tn*3*-family of unit transposons of which two members, Tn*1* and Tn*4401*, were employed in the work for **paper II.**

Tn*3*-family transposons

Examples for well-described representatives of Tn*3*-family transposons are Tn*1* (**Figure 8**, middle), Tn*2* and Tn*3*, which are the earliest identified bacterial resistance transposons[142]. Furthermore Tn*4401*[143] (**Figure 8**, bottom) and the integron-carrying Tn*21*, which also carries a mercury resistance operon[144], are well-known. More Tn*3*-family transposons that harbor integrons with associated gene cassettes are for example Tn*1696* and Tn*1331*[95]. Tn*3*-family transposons in clinical isolates are often plasmid-associated, and those described in G- bacteria carry for example β-lactam (Tn*2* [bla_{TEM}]), carbapenem (Tn*4401* [bla_{KPC}]), colistin (Tn*6452* [*mcr*]), aminoglycoside (Tn*5393* [*strA*, *strB*]) and tetracycline (Tn*1721* [*tetA*]) resistance genes. In G+ bacteria, Tn*1546* is a Tn*3*-family representative that mobilizes vancomycin resistance (*vanA*)[95].

Tn*3*-family transposons: structure

Transposons exhibit different structural compositions, transposase types, transposition mechanisms (replicative/non-replicative) and target site preferences. Structural characteristics for Tn*3*-family elements are the *tnpA* and *tnpR* genes which encode the transposase and resolvase proteins[145], respectively, as well as the *res* site and two 38-bp IRs, which together facilitate a replicative transposition mechanism (**Figure 8**, middle and bottom)[146]. The TnpA proteins of the Tn*3*-family are called DDE-transposases due to a conserved motif of three amino acids in their catalytic site (aspartic acid/aspartic acid/glutamic acid, or short DDE), but are also known as RNase H-like enzymes[147]. TnpR represents an S- or Y-recombinase with an active site serine or tyrosine, respectively, and is involved in the resolution step of the transposition pathway (see below)[147]. For members of subgroups to this transposon family *tnpA* and *tnpR* may be organized differently with respect to the *res* site (Tn*21*-subfamily) or show little sequence similarity with the same genes in Tn*3*-like elements (Tn*4401* and its variants[143]), however, their flanking IRs are related to IRs of other Tn*3*-family transposons[148].

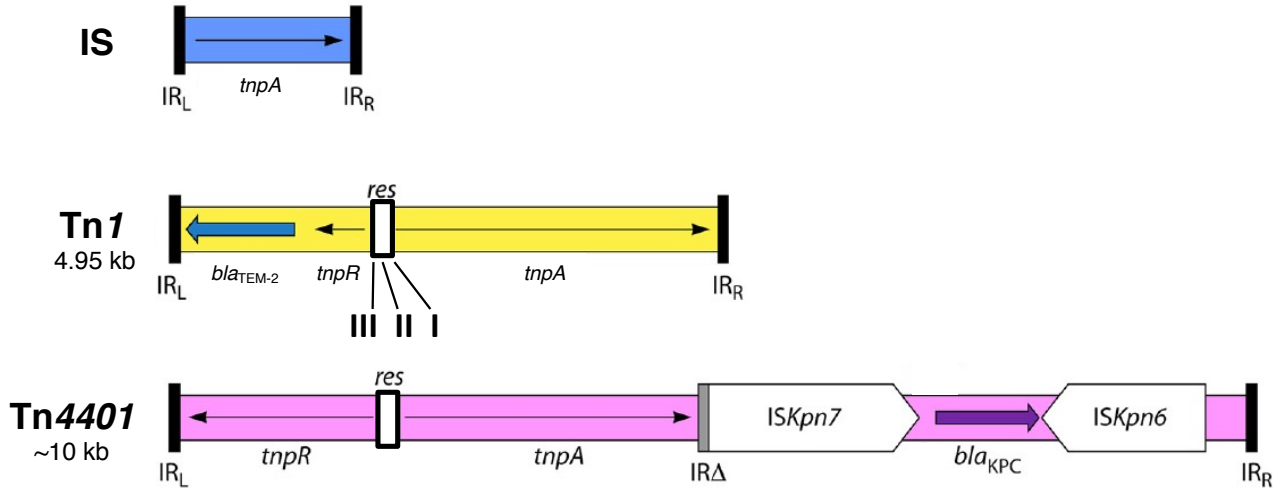

Figure 8: The genetic composition of a typical IS element, and two thesis-relevant transposons.
IS elements are simple, short transposable elements and only contain a minimal transposition module consisting of a transposase gene (*tnpA*), and the left and right IRs (IR_L and IR_R; vertical black bars). The transposase gene usually covers the entire element. **Tn*1*** is a Tn*3*-family transposon and carries a broad-spectrum β-lactam resistance gene (bla_{TEM-2}) in addition to the transposition module. This is comprised of *tnpA* and *tnpR*, which are transcribed in opposite directions, and the two 38-bp IRs, which contain an external transposase cleavage site, and an internal transposase recognition and binding site (domain A and B, respectively; not shown). The resolvase TnpR is a site-specific serine recombinase but acts also as repressor for *tnpR* and *tnpA*[145]. The 120-bp *res* site separates these two genes and contains three sub sites (I, II and III), which are binding sites for the resolvase during replicative transposition[147], and promoters for *tnpA* and *tnpR*. **Tn*4401*** is a Tn*3*-like transposon and is bracketed by two 39-bp long IRs. The transposon harbors IS*Kpn7* and IS*Kpn6* up- and downstream of a bla_{KPC-2} carbapenemase gene, respectively. It is suggested that the interrupted IR (IRΔ) has evolved from IS*Kpn7* insertion into the ancestral IR_R, and a downstream 'replacement' IR_R now delimits Tn*4401*[143]. Reprinted and modified with permission from[95].

Tn*3*-family transposons: transposition mechanism

Tn*3*-family transposons move by a 'copy-in' mechanism, and much of our knowledge about the biochemistry of this transposition pathway is based on studies using bacteriophage Mu as a model. This replicative transposition mechanism involves the formation of a double-stranded, circular DNA co-integrate, for which the Tn*3*-family transposase does not require sequence similarity between the transposon and the target site. After resolution of this structure, one copy of the transposon is inserted into the target molecule, while the donor molecule also contains the elements[147] (**Figure 9**). In a first step, the transposase recognizes and binds the IRs, and catalyzes the cleavage of DNA single-strands at the outermost 3′ ends of the transposon by hydrolysis. The transposase binds the transposon ends and transfers them to the target DNA. This nucleoprotein complex is also referred to as the 'transpososome'[134]. In the so-called strand-transfer reaction, Tn*3*-family transposases typically introduce a 5-bp single-strand gap into the target DNA which creates free 5'-ends that are joined with the transposon's 3′-OH groups[147]. This generates a branched molecule, called a Shapiro-intermediate, which contains two structures that resemble replication forks as a consequence of the staggered target

DNA cleavage[149]. Further steps involve the repair of the gaps between target and transposon DNA and synthesis of the complementary strands of the transposon by host replication functions[147] (**Figure 9**, left). If the donor and target molecules were circular, the result is a circular, double-stranded co-integrate structure in which the target and the donor DNA are connected through directly repeated copies of the transposon, of which each has one newly synthesized strand[147]. In this co-integrate, 5-bp long target site duplications (TSDs) are present where transposon DNA was joined to target DNA (**Figure 9**, middle). These TSDs are direct repeats and a characteristic result of a transposition event. They reflect the preferred target site sequence of the transposase protein, the 'consensus sequence', which is generally AT-rich and 5-bp long for Tn*3*-family transposases[150,151] (**Figure 9**, right). However, transposon insertion is probably not only determined by the sole presence of the consensus sequence but may abide also other characteristics of the target DNA[152] (**paper II**). It is suggested that replication processes or DNA repair events at the target site provide a signal for transposition[147].

In most characterized Tn3-family transposons, resolution of the cointegrate is mediated by a TnpR serine resolvase, which performs site-specific recombination between the two transposon *res*-sites. Once the *res* recombination sites (subsite I in each element) are aligned in parallel, TnpR can bind and introduce double-strand breaks, perform DNA strand-exchange through rotation of the DNA-protein complex within subsite I, and rejoin DNA[147]. The donor and target molecules are now separated and contain one copy of the transposon each.

In vitro, Tn*3*-transposition between plasmid replicons can occur at frequencies of $10^{-2}/10^{-3}$ [153], and for Tn*4401* at frequencies of $10^{-3}/10^{-4}$ [154]. Although cointegrate resolution occurs independent from host recombination functions, RecA-mediated homologous recombination between the directly repeated transposons can resolve co-integrates in the absence of TnpR, although less efficiently[155]. New Tn*3*-based transposons evolve by a sequence of homology- and resolvase-mediated recombination events between related and unrelated elements as it is suggested for Tn*2*-like transposons[142], or by the recruitment of 'replacement' IRs as described for Tn*4401* evolution[143] (**Figure 9**, bottom).

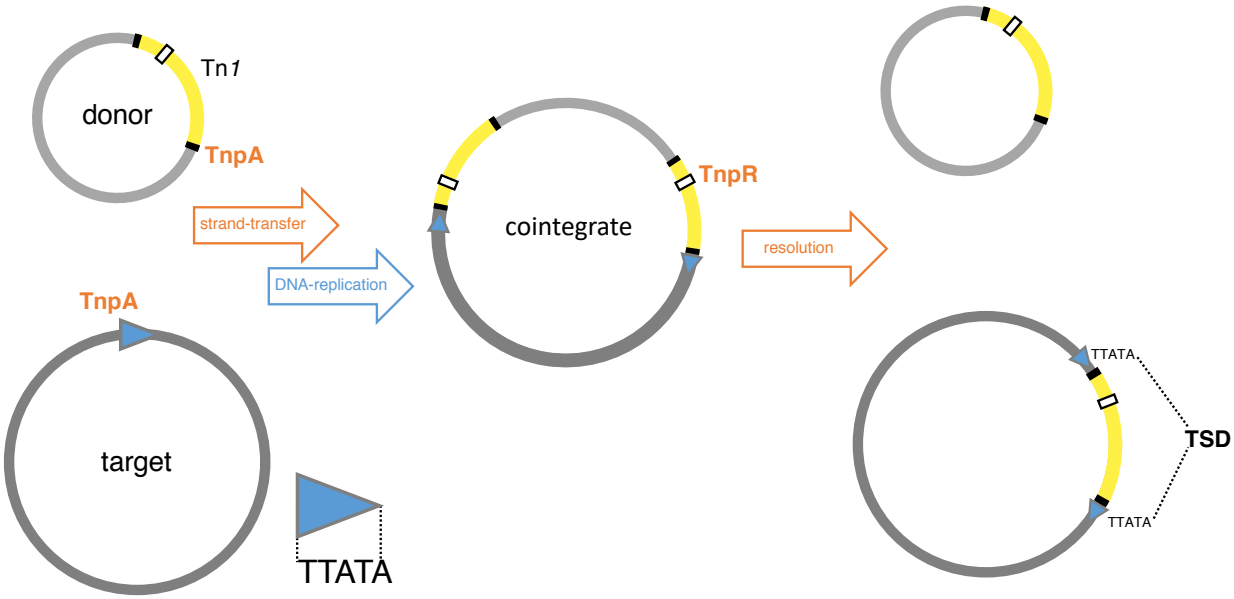

Figure 9: Schematic of the transposition mechanism used by Tn*3*-family transposons.
Replicative transposition by the copy-in mechanism is a two-step process and requires transposon- and host-encoded functions (indicated in orange and blue, respectively). The transposase (TnpA) cleaves DNA single-strands at the transposon's IRs (black) and joins them with DNA ends at the target site (blue triangle with 5-bp target sequence) during the so-called "strand-transfer" reaction. Single-strand gaps between target and transposon DNA, and also the complementary transposon-strand, are filled up by cellular DNA replication functions. This generates a double-stranded, circular co-integrate molecule called Shapiro-intermediate, which contains two copies of the transposon. During resolution, the resolvase (TnpR) performs site-specific recombination at the transposon's *res*-sites (white box), which leads to the separation of donor and target molecule. Characteristic TSDs are present at either end of the newly inserted transposon in the target molecule.

Bacterial fitness and cost of antibiotic resistance

The biological fitness of bacteria is, at the broadest level, defined as their ability to survive and divide in a particular environment. Traditionally, growth rate and competitiveness are measured *in vitro* or *in vivo* to estimate the fitness of one bacterial genotype relative to another when both strains are growing under the same conditions. For example, the maximum exponential growth rate r of strain A and strain B is measured, and the relative fitness w is calculated as the ratio of absolute growth rates ($w = r_A/r_B$). The assessment of competitiveness is the 'gold standard' of fitness estimation[156]. Here, a 1:1 volumetric mixture of strains A and B is inoculated and the population density (N) of each competitor is determined at the start (i) and the end (f) of an experimental cycle. The respective net population growth is calculated as $m_{A/B} = \ln (N_{A/B(f)}/N_{A/B(i)})$ (m = Malthusian parameter), and the relative competitive fitness as $w = M_A/M_B$[157]. The relative fitness w can be increased (>1), equal (1) or reduced (<1). As a consequence of fitness differences between two bacterial populations, their frequencies will change over time, and the less fit population will decrease due to negative selection.

The selective benefit of resistance acquisition in bacteria is futile once antibiotics are removed and the fitness of resistant relative to susceptible strains represents a key criterion for the persistence of resistance in bacterial populations[20]. The effect of newly acquired resistance on fitness has been studied *in vitro* for many antibiotics and types of resistance mutations[158] (**paper I**), for resistance plasmids (**paper III** and below), resistance encoding integrons[159] and transposons[160,161], and also *in vivo*[56,160,162]. The general observation is that resistance acquisition reduces bacterial fitness in antibiotic-free conditions[163]. The predictability of this so-called 'fitness cost' for a particular combination of resistance determinant and host genetic background is however limited since both factors impact the cost[128,130,164-166] (**paper I and III**), in addition to the bacterial environmental context[167]. A recent meta-analysis shows, however, that costs associated to resistance mutations are generally greater than the costs imposed by horizontally acquired resistance determinants[168]. This is explained by the acquired type of resistance mechanism. *De novo* resistance mutations in the antibiotic target site cause perturbation of essential cellular functions like cell wall synthesis, DNA replication or protein synthesis by changing the proteins involved in these processes (PBPs, DNA gyrase and topoisomerase, RNA polymerase, ribosomes)[169]. Different from that, horizontally acquired resistance determinants mainly encode proteins for enzymatic drug modification (*e.g.* aminoglycoside-modifying enzymes) or degradation (*e.g.* β-lactamases), or for proteins involved in drug influx or efflux, and these alterations interfere less with cellular processes[15]. For horizontally acquired resistance, fitness costs are however also created by other factors than the resistance mechanism (see Fitness cost of plasmid carriage; reviewed in[170,171]).

The cost of resistance usually leads to a decline in resistant versus susceptible bacteria in absence of antibiotics. The greater the fitness cost is, the faster resistance should theoretically decrease in bacterial populations[172]. However, several studies revealed that newly acquired resistance by mutations[173] (**paper I**) or HGT events[128,130,160,161] (**paper III**) can impose a low or no fitness cost, and most worryingly, some examples for resistance determinants that confer a fitness benefit to their bacterial host also exist for mutations[56,165] and plasmids[161]. Another important observation is that resistance-associated fitness costs can be reduced or ameliorated over evolutionary time, while resistance is maintained (see Solutions to the plasmid paradox). The evolution of no or low-cost resistant bacteria decreases the likelihood that they are outcompeted by drug-sensitive strains even when selective pressures are removed and stabilizes antibiotic resistance in bacterial populations. To contextualize the work of **paper III**, I will hereafter focus on the fitness costs associated to horizontal plasmid acquisition in bacteria and the proposed mechanisms that reduce this cost.

Fitness cost of plasmid carriage

There is not one straight forward mechanism that can be attributed to the cost of recently acquired plasmids (reviewed in[171]). Instead, several genetic and molecular conflicts arise from plasmid-host interactions, as indicated in **Figure 10** and described below.

All major HGT mechanisms, conjugation, transformation and transduction, facilitate the acquisition of plasmids, which involves the entry of ssDNA into the recipient bacterium. RecA-binding to this ssDNA triggers the cell's SOS response, and as a consequence of DNA repair induction and slower bacterial cell division, fitness is temporarily reduced[171] (**Figure 10**-2). Furthermore, specific fitness costs are associated with plasmid transfer by conjugation and presumably due to several factors such as the expression of plasmid-encoded ATPases and the conjugational transfer machinery (T4SS)[174], as well as the transient overexpression of plasmid-encoded genes upon plasmid arrival in the recipient cell[171]. Likewise, infection of plasmid-carrying cells by so-called 'male-specific' phages via the conjugation apparatus reduces fitness inevitably (**Figure 10**-1). Once a plasmid is established in the cell, recombinase expression of plasmid-associated MGEs such as transposons can mobilize these elements into the host chromosome and cause detrimental effects on bacterial fitness if the element's insertion interrupts genes that code for relevant host proteins or regulators[171] (**Figure 10**-3). Although plasmid acquisition implies replication of some additional DNA, the requirement for extra nucleotides does generally not restrain bacterial fitness[168]. However, the expression of plasmid replication proteins was associated with induction of the bacterial SOS response and to plasmid costs, possibly through sequestration or inhibition of host replication or repair proteins. This was demonstrated for example for the interaction of RepA-expression from plasmid pSC101 and the host

primase DnaG in *E. coli*[175], interaction of the replication protein gene *rep* of pNUK73 and *P. aeruginosa* helicases and proteinases[176] and was also suggested for TrfA1, an IncP-1b replication protein, and the *Shewanella oneidensis* helicase DnaB[177] (**Figure 10**-4). It appears however, that the greatest metabolic burden of plasmid carriage results from the sequestration or occupation of cellular components such as RNA polymerases and ribosomes, tRNAs, amino acids, which causes inefficient and inaccurate transcription and translation, respectively. In line with this, costly plasmid acquisition was associated to an increased, global transcriptional demand on the host cell, involving genes associated with translation or SOS response[176,178] (**Figure 10**-5). The resulting lack or alteration/misfolding of essential host proteins disturbs downstream bacterial physiology or is lethal to the cell. Moreover, the more horizontally acquired proteins interact with established host protein networks, for example the cellular replication network, the more they impact a host's fitness[176] (**Figure 10**-6). Finally, interference of plasmids with other horizontally transferred MGEs can produce fitness costs, which was demonstrated for plasmid pNUK73 in *P. aeruginosa* and the expression of proteins associated to a horizontally acquired transposon and phage[176] (**Figure 10**-7).

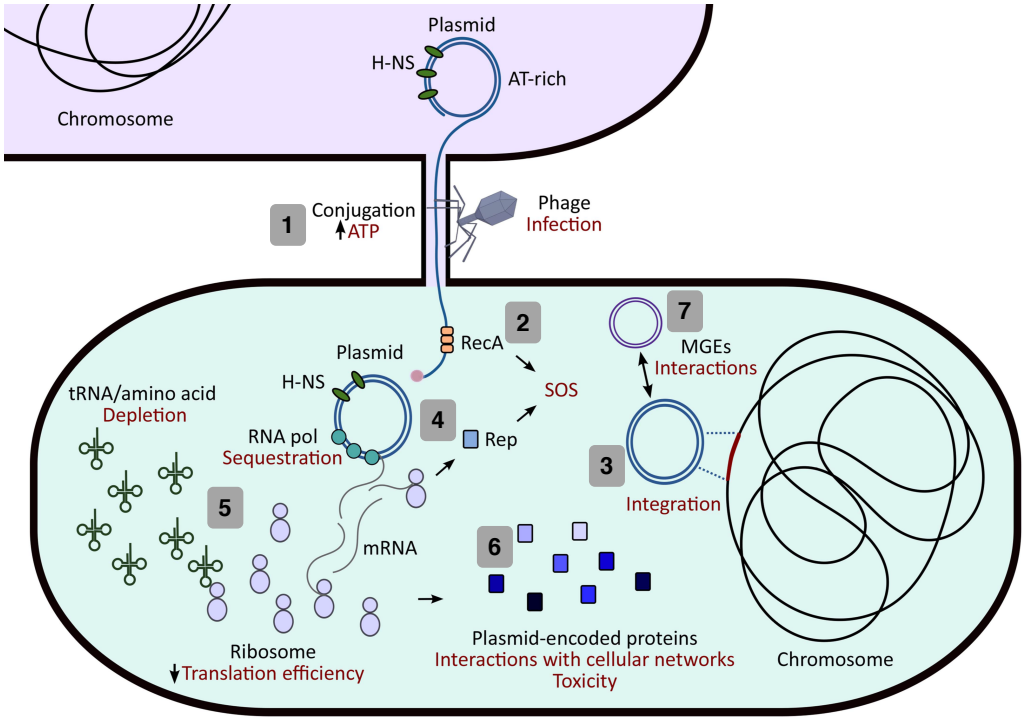

Figure 10: Illustration of plasmid-host interactions. Different stages of plasmid acquisition and maintenance by a bacterial host may cause fitness costs: 1) plasmid transfer by conjugation, 2) entry of ssDNA during HGT, 3) recombinational interaction between plasmid and chromosome, 4) plasmid replication, 5) plasmid-gene expression (transcription, translation), 6) plasmid- and host-protein interaction, 7) plasmid interactions with other MGEs. Reprinted and adapted with permission from[171].

The size of a plasmid does generally not correlate with the fitness burden it creates[168,179]. Both large and small resistance-encoding plasmids can be either rather costly or not so costly (**Table 1**). However, clinical resistance plasmids generally show low or no fitness burden in a clinically isolated host (see **Table 1**-a), while model plasmids or artificial plasmids largely impose a significant cost in laboratory strains (see **Table 1**-b). Larger resistance plasmids also carry more resistance genes[180]. However, it is the presence of particular resistance genes or an increasing number of antibiotics that the element confers resistance to that are responsible for higher fitness costs rather than the plasmid size, as demonstrated experimentally for *bla*$_{\text{CTX-M-15}}$ and *tetA/R* in *E. coli*[180], or in a meta-analysis[168], respectively. For resistance plasmids in *E. coli* it was further shown *in vitro* that the number or the type of plasmid replicons that a host carries is not a good indicator for fitness costs, and this may be because known resistance plasmid replicons vary in their resistance gene content, which is a better predictor of fitness cost[181]. Furthermore, fitness costs vary between different plasmid-host combinations and depend both on the genetic background as well as the acquired plasmid that is tested[128,130,161].

Solutions to the plasmid paradox

Undoubtedly, plasmids facilitate rapid bacterial adaptation to selective environments. However, their accessory traits are not generally essential for bacteria, and host fitness costs in plasmid-unselective conditions or their segregational loss during vertical inheritance should cause a decline in the frequency of plasmid-bearing cells relative to plasmid-free cells. However, studies of different plasmid-host combinations show that conjugative as well as non-conjugative plasmids persist in bacterial populations over several hundred generations of plasmid-unselective cultivation[128,130,161,182] (**paper III**). This so-called 'plasmid paradox' has been the focus of theoretical models[183,184] and experimental evolution studies (reviewed in [185,186]), which describe at least five non-exclusive mechanisms for the maintenance of plasmids over evolutionary time scales. Solutions to the plasmid paradox comprise mechanisms of plasmid-host adaptation that impact plasmid stability, mobility and cost, which originate from genetic changes in the plasmid, the host, or both. The key mechanisms are related to:

- improved segregational plasmid stability: evolution of a model plasmid in *E. coli* showed that stability was increased in the absence of plasmid-selection through a small duplication involving the plasmid's *ori* region. This reduced the interference between plasmid replication and the transcription of a plasmid-associated accessory gene in proximity to the *ori* and improved plasmid stability[187]. Alternatively, plasmids can acquire addiction systems to improve their stability, which was

demonstrated for a conjugation-deficient as well as a conjugative plasmid and a transposon-associated toxin-antitoxin system in *Pseudomonas moraviensis*[188] or *S. oneidensis*[189], respectively. Similarly, the insertion of transposon-associated resolvases into plasmids positively affected the resolution of plasmid multimers and thus plasmid segregation[188]. Finally, an increase in plasmid copy number can facilitate plasmid stability by counteracting ineffective plasmid partitioning[177,190].

- selection for plasmid-associated traits: *in vitro*, sporadic exposure to plasmid-selective agents promotes the maintenance of extremely costly plasmids in bacteria[191,192]. However, mathematical models postulate that constant selection for plasmid-associated beneficial traits will not maintain the element extra-chromosomally, but select for backgrounds that captured the selective trait chromosomally[184]. This was also demonstrated *in vitro* and facilitated through the association of beneficial plasmid genes to transposons. Surprisingly, transposition to the chromosome of *Pseudomonas* spp. occurred in plasmid selective as well as unselective conditions and decreased plasmid frequency[178,193].

-high conjugation rates: theory suggests that the loss of plasmid-bearing cells through segregation or fitness costs can be offset by high rates of conjugational plasmid transfer[183]. *In vitro*, this was shown for some very efficient plasmid donors[194], but sufficiently high conjugation rates are not commonly observed *in vitro*[186]. In addition, conjugational plasmids could be maintained by infection of bacteria that are not under negative selection, for example other strains or species that are present in the specific ecological niche[184]. However, the costs associated to horizontal plasmid spread by conjugation reduce vertical plasmid inheritance[195] and conjugation may thus not represent the major evolutionary trajectory for plasmid maintenance[174,196]. Especially since analysis of GenBank plasmid sequences shows that only around 50% of these plasmids are conjugative[197]. Yet, plasmids seem to be maintained by other HGT mechanisms or by plasmid-host dynamics described here, and also benefit from the simultaneous spread with conjugative plasmids if they are mobilizable.

- compensation of fitness costs: the evolutionary selection for reduced plasmid costs is very likely key to plasmid persistence, however the so far described underlying mechanisms are rather diverse. This is different from mutational resistance, for which *in vitro* and *in vivo* (mice and humans) studies frequently demonstrate that cost compensation primarily occurs through the re-establishment of the cellular function that got impaired by the resistance mechanisms[198]. Compensatory mutations can arise in the same gene as the resistance mutation, or externally, and restore for example the translation

elongation rate at the ribosomes of aminoglycoside resistant *E. coli*[199], or the RNA polymerase transcription efficiency in rifampicin resistant *E. coli*[200], thus reducing fitness costs.

Plasmid cost compensation was first described in the late 80's by Bouma and Lenski, who found that, after 500 generations of host-plasmid adaption, pACYC184-carriage was even beneficial[201]. More recent reports on the genetic changes and mechanisms behind this so-called compensatory evolution find that host adaptation occurs more frequent than changes in the plasmid but appears also in both loci simultaneously (**Table 1**). Importantly, compensatory mutations arise specifically in plasmid-carrying lineages where they improve fitness, but not in plasmid-free cells, where they might even reduce fitness[178,201]. Plasmid-host adaptation was observed after experimental evolution with[177,188,190,201] and without[161,196,202] (**paper III**) antibiotic selection pressure.

At least four studies demonstrated that mutations in plasmid or host replication proteins improved bacterial fitness by reducing the detrimental interference between the replication machineries, and by prevention of the SOS response[176,177,190,203]. Mechanistically, this was achieved by mutations in the plasmid's replication initiation protein TrfA1[189,190], which decreased the protein's affinity to the DNA helicase DnaB of *S. oneidensis* and *Pseudomonas putida*[177]. Likewise, the loss of chromosomal UvrD-like helicase or kinase functions of *P. aeruginosa* PAO1 reduced the expression of a plasmid's replication protein, and thus fitness costs[176]. In *Pseudomonas sp*. H2, mutations affecting chromosomal helicase functions (Xpd/Rad3 or UvrD-like) were even shown to provide RP4-carrying strains with a fitness benefit compared to isogenic plasmid-free strains[203]. Further, the deletion of plasmid-associated resistance genes[204], genes for conjugational transfer[196], or both[174] alleviated the plasmid cost. Such events are facilitated if costly genes are flanked by MGEs[174,204]. *In vitro*, the cost of conjugative plasmids was also decreased by host-adaptive changes that reduced transfer rates[196], which could also theoretically be correlated to cost reduction[195]. Finally, compensatory mutations that altered the transcriptional demand of plasmid-carriers ameliorated plasmid costs. This was for example achieved by mutational inactivation of the global regulators GacA/S in *Pseudomonas fluorescens*[178] or inactivation of chromosomal helicase/kinase functions in *P. aeruginosa*[191], which resumed transcription profiles of the compensated strains to that of plasmid-free strains.

Table 1: Fitness costs of newly acquired plasmids in various hosts and the effect of compensatory evolution.

Host	Plasmid	Fitness effect[c]	Effect of adaptation (which part[d])
E. coli[128] (23 isolates)	pK71-77-1-NDM (~145 kb) [(a)] (*bla*$_{NDM-1}$)	majority no cost, 3% to 27% cost	not studied
E. coli MG1655[187]	pCON (~3 kb) [(b)]	no cost	not studied
E. coli[130] (2 isolates)	pG12-KPC-2 (~111 kb) [(a)] (*bla*$_{KPC-2}$)	2 and 4% cost	not studied
K. pneumoniae[205]	pKpQIL (~114 kb) [(a)] (*bla*$_{KPC-3}$)	no cost	not studied
K. pneumoniae and *E. coli*[96]	pUUH239.2 (~220 kb) [(a)] (*bla*$_{CTX-M-15/TEM-1/OXA-1}$)	no and 4% cost	not studied
E. coli[206]	seven plasmids (>100 kb) [(a)] (*bla*$_{CTX-M-14/15/27}$)	no cost	not studied
Enterobacteriaceae[207] (29 isolates)	p3R-IncX3 (~46 kb) [(a)] (*bla*$_{NDM-5}$)	majority no cost	not studied
E. coli MG1655[208]	R1 (~100 kb) [(b)]	32% cost	cost amelioration or fitness benefit (**p**+**c**)
E. coli B[201,209]	pACYC184 (~4 kb) [(b)]	5-10% cost	fitness benefit (**c**)
E. coli K12[196]	RP4 (~60 kb) [(b)] R1 (~100 kb) [(b)]	21% cost, 6% cost	cost reduction (**p**+**c**)
K. pneumoniae and *E. coli*[174]	pKP33, (~73 kb) (*bla*$_{CTX-M-15/TEM-1/OXA-1}$) [(a)]	6% to 12.5% cost	cost amelioration (**p**)
P. aeruginosa PAO1[191]	pNUK73 (~5 kb) [(b)]	21% cost	cost amelioration (**c**)
P. fluorescens SBW25[178]	pQBR103 (~425 kb) [(b)]	27% cost	cost amelioration (**c**)
E. coli **paper III** (1 isolate)	pK71-77-1-NDM (~145 kb) [(a)] pG06-VIM-1 (~53 kb) [(a)] (*bla*$_{NDM-1}$ and *bla*$_{VIM-1}$)	5% cost	cost amelioration (**c**)
Pseudomonas sp. H2[203]	RP4 (~60 kb) [(b)]	7% cost	fitness benefit (**c**)
Enterococcus faecium[161] (6 isolates)	six vanA-plasmids [(a)] (between 80 and 200 kb)	25% cost, no cost, or 10% benefit	fitness benefit (**p**+**c**)

a: clinical plasmid/host; b: model plasmid/lab host; c: fitness assessed by growth rate measurements or competition experiments; d: **p** = plasmid, **c** = chromosome.

In conclusion, plasmid persistence in bacterial populations is impacted by several factors, and the long-term maintenance of plasmids is likely due to a combination of the above-described evolutionary dynamics. Interestingly, plasmid-host evolution frequently results in trade-offs, such that compensation increases fitness and improves the vertical inheritance of plasmids but at the same time reduces their horizontal spread[174,196] or constrains the plasmid's host-range by specialization of plasmid-host pairs[190]. However, in addition to cost compensation, plasmid-host adaptation also improved the permissiveness of adapted *Pseudomonas* hosts to various naive plasmids[203]. So far, our knowledge on plasmid-host adaptation is largely based on studies in controlled laboratory environments using laboratory-based model systems. This situation warrants research towards understanding the evolutionary trajectories that stabilize plasmid-associated resistance in plasmid-host pairs of clinical origin as in Porse *et al.*[174] or **paper III**, where we find that growth adaptation of patient-derived *E. coli* isolates to the experimental conditions pleiotropically alleviates the cost of clinical MDR plasmids. The cost compensating adaptation occurred independent of plasmid-carriage and thus represents a novel solution to the 'plasmid paradox'.

Reversibility of resistance

Since the use of antibiotics selects resistant and removes susceptible clones in bacterial populations, a reduction in drug consumption should also decrease the frequency of resistance. The major driving force for the loss of resistance in such unselective conditions is the fitness burden that resistance determinants usually impose on bacteria, and resistant bacteria theoretically emerge less the greater the fitness cost is[172]. Most antibiotics are prescribed on the community-level[210]. However, interventions to reduce antibiotic use in the community did not result in an adequate decline in resistance[211,212], showed persisting resistance even after 12 years[20], or worse, significantly increased the prevalence of plasmid-associated resistance due to a fitness benefit of resistant strains over susceptible ones[213]. These observations can be explained by several biological and evolutionary processes that stabilize resistance determinants in bacterial populations[20,214], for which examples are listed here:

- if bacteria re-acquire resistance at high enough rates by mutations or HGT events
- if resistance is co-selected with physically linked beneficial traits, for example antibiotic or heavy metal resistance genes or virulence factors (*e.g.* on MGE; see Mobile genetic elements)
- if resistance is genetically associated with highly transmissible, clinically widespread clones[12]
- if resistance is associated with plasmid-stability functions (see Plasmids)
- if the selective disadvantage of resistance is weak or absent due to low or no cost of resistance, and/or compensatory evolution (see Bacterial fitness and cost of antibiotic resistance)
- if antibiotic selection pressures are sustained either because the overall volume of drug use is unchanged or sporadic exposure to antibiotics, even at very low concentrations, occurs[50,51]

It becomes apparent that, even if antibiotics are removed, straightforward reversal of resistance is difficult or even impossible due to the interplay of the many factors mentioned above. Unfortunately, the development of innovative antibiotics, for example from a novel drug class, with a novel drug target or binding site or with a novel mode of action, is stagnating[6]. In the light of this antibiotic void, research increasingly focuses on optimizing the use of available drugs and minimizing resistance evolution. To provide the background for the work done in **paper I,** I describe an evolution-informed approach for infection treatment using drug combinations below.

Evolution-informed treatment strategies

Typically, drug combinations are used in the treatment of chronic or severe infections with the rationale to clear the infection more efficiently through a broadened and stronger antibiotic effect, and to delay the emergence of *de novo* resistance[215]. Treatment efficacy is ideally enhanced by interactions between the combined drugs that change the bacterial physiology and increase the killing or growth inhibitory effect beyond what is expected based on the individual drug effects (synergism[215]). More recently, selection inversion strategies were described in the context of combination therapy[216]. Those rely on the spontaneous evolution of resistance before the benefit of combining antibiotics is conveyed. For example, resistance acquisition can relax a suppressive drug-interaction or induce synergistic drug-interactions and thus increase antibiotic potency upon evolution of single-drug resistant mutants[216]. Moreover, resistance evolution can lead to a biological phenomenon called collateral sensitivity (CS)[217]. CS is the opposite of cross resistance (CR = resistance to one drug confers also resistance to other antibiotics) and confers resistant mutants with increased susceptibility to certain antibiotics. Therefore, the phenomenon is also called negative cross-resistance[218] or hypersensitivity[219]. Research into the design of CS-informed treatment strategies has gained considerable interest during the last decade with the aim of limiting resistance development by selecting against resistant mutants.

Collateral sensitivity: concept

CS in bacteria was first described in 1952, when Szybalski and Bryson reported that "a strain made resistant to one antibiotic [became] considerably more sensitive to another"[217]. The usefulness of this sensitivity-tradeoff in bacterial infection treatment was however only put under scrutiny in 2013, when Sommer *et al*. introduced the idea of 'collateral sensitivity cycling'[220]. In this context and considering the use of two drugs, resistance evolution during treatment with drug A could be counteracted by switching to drug B if the genotype resistant to A collaterally increased its susceptibility to B (**Figure 11**). Such an evolutionary tradeoff inverts the usual selection dynamics and resistant mutants are not selected anymore. If CS to A and B evolves reciprocally, the drugs can be switched periodically upon *de novo* resistance emergence. At every switch, the resistant subpopulation is preferentially eliminated compared to the sensitive wildtype and hence the population susceptibility returns to wildtype levels. Then, the infection can be cleared by the combined effect of drug treatment and host immune system. CS could be exploited using one drug at a time *i.e.* sequentially/cycled[218,220], or by co-administration of drugs[219,221,222]. Single-drug therapy, however, reduces the overall drug load and thus exhibits less adverse effects as well as it decreases the likelihood to select for resistance to both drugs.

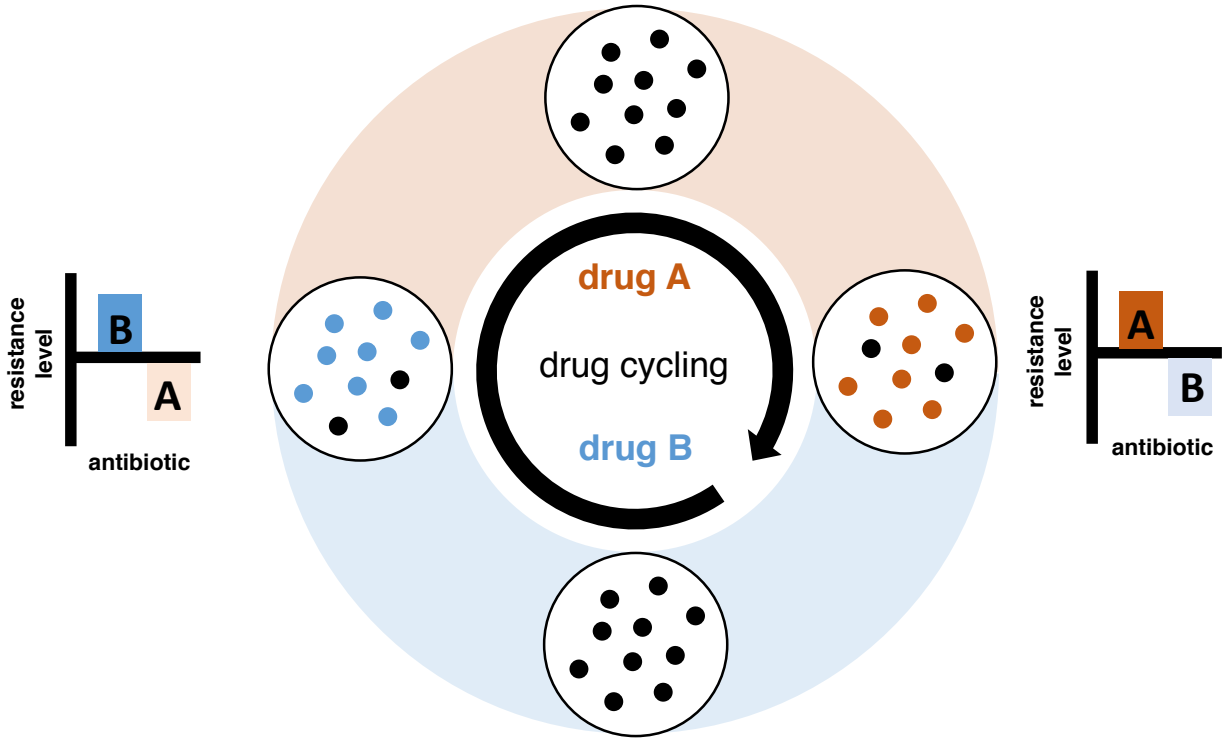

Figure 11: Example of a cycling protocol using a drug pair (A and B) for which resistance evolution in bacteria (orange and blue dots) results in reciprocal CS, meaning that resistance to one drug reinforces increased susceptibility to the other drug and vice versa (indicated as graphs). Thus, antibiotics can be used to select against the resistant subpopulation.

Collateral sensitivity: findings, limitations and predictors

To identify collateral responses in bacteria, the first systematic *in vitro* studies measured susceptibility changes in laboratory-evolved, single-drug resistant *E. coli* mutants towards large panels of antibiotics[219,220]. Those first screens found that in *E. coli*, CS evolved reciprocally between aminoglycoside, polymyxin and tetracycline drugs classes[220]. By today, a variety of clinically relevant G+ and G- pathogens such as *S. aureus* or *Staphylococcus epidermidis*[49,218,222,223], *E. faecalis*[224], *Burkholderia multivorans*[225], *Salmonella enterica*[164], *P. aeruginosa*[226], and other clinical relevant organisms[227] have been investigated for CS/CR, most of the studies using single laboratory model strains. Importantly, the more recent reports employed larger sample sets of clinical isolates of *E. coli* (**paper I**), *P. aeruginosa*[228] or *S. aureus*[222] to study CS/CR responses.

CS/CR effects are typically assessed by measuring the antibiotic concentration that is required to inhibit growth of a resistant strain as well as its susceptible wildtype strain, and calculation of the relative fold changes of susceptibility, which are visualized in heat maps and in networks of collateral responses[219,220] (**paper I**). Hitherto it was demonstrated, that both CS and CR are common phenomena in single-drug resistant bacteria, that CR is more prevalent than CS, and that CS changes

are often as small as 2 to 4-fold[219,220,227] (**paper I)**. Even for such small magnitudes, the selective consequences associated to CS could be demonstrated by different approaches: *in vitro* dose-response experiments confirmed that the growth of resistant mutants with CS towards a certain antibiotic is inhibited at lower drug concentrations than the wildtype[219,220] (**paper I**). Aminoglycoside-resistant *E. coli* exhibited CS towards a particularly large number of antibiotics, also from different drug classes, which lead to the selective growth inhibition of such mutants in dose-response experiments[219,220]. Compared to single antibiotic exposure, the combined[221,223] or sequential[218] use of drugs to which CS evolved, slowed down resistance evolution of *E. coli*[221] and *S. aureus*[218,223], which was experimentally demonstrated by the lower resistance levels developed during drug exposure compared to a wildtype. Time-kill experiments in *E. coli* demonstrated that a resistant mutant is eliminated faster than the wildtype by the drug towards which CS was observed[220]. The latter was shown for antibiotics from different drug classes to which the respective resistant mutant exhibited reciprocal CS, for example gentamicin and cefuroxime[220]. Furthermore, reciprocal CS effects between antibiotics of the same drug class (β-lactams) slowed down *E. coli*[229] or methicillin-resistant *S. aureus*[222] resistance evolution *in vitro* and in a mouse model. Finally, *in vitro* cycling of two bactericidal antibiotics with reciprocal CS repeatedly eradicated the resistant subpopulation from a mixed *E. coli* wildtype/resistant population[220].

So far, few *in vitro* studies investigated in which way collateral effects on growth inhibition of resistant mutants also alter the MPC (see Mutant selection window) to secondary drugs. In resistant *E. coli*, the MPC was shifted towards lower or higher antibiotic concentrations according to the sign of the collateral susceptibility change[220] (**paper I**). CS towards erythromycin in different single-drug resistant *S. epidermidis* mutants frequently narrowed the concentration range in which first-step mutants emerged (MSW)[49]. Importantly, the same study found that CS network patterns based on growth inhibition and MPC were similar[49].

Our knowledge on the relevance of collateral effects emerging from horizontal resistance acquisition is still limited, but was investigated for the plasmid-associated genes $bla_{\text{CTX-M-15}}$[229] and bla_{OXA48}[230], or MDR plasmids[231] in *E. coli*. Evolution of resistance to ceftazidime and mecillinam by mutations in bla_{OXA48} and $bla_{\text{CTX-M-15}}$, respectively, resulted in CS towards other β-lactams, including carbapenems[230] or cefotaxime[229], respectively. Furthermore, reciprocal CS between mecillinam-resistant and cefotaxime-resistant $bla_{\text{CTX-M-15}}$-variants limited resistance evolution *in vitro* and in mice during combination treatment with these drugs[229]. Such CS phenotypes exemplify how collateral responses upon resistance evolution would allow the use of previously ineffective drugs for strains that harbor these widely disseminated MDR determinants. *E. coli* acquisition of MDR

plasmids resulted in small but, in some cases, significant CS for aminoglycosides, macrolides or polymyxins[231].

Despite the frequent evolution of CS in single-drug resistant bacteria, several factors affect the successful use of CS-informed treatment in medical practice. It was demonstrated that CS responses evolve repeatedly in independent populations exposed to a specific drug, however the responses varied with the diversity of mutational paths towards resistance *in vitro*[164,226] and in a mathematical model[232]. When investigated across different species, even the same resistance mutation led to different CS responses[164]. Also, genetic interaction with *de novo* resistance mutations in the resistant strain during treatment[233] or the acquisition of compensatory mutations over evolutionary time (Sørum *et al*., unpublished data) interfere with the stability of collateral networks and how efficient bacteria can be eradicated through CS tradeoffs. Importantly, we identified that the resistance mechanism, especially efflux mutations, as well as the relative fitness of resistant mutants provide some degree of predictability for collateral responses across diverse uropathogenic *E. coli* isolates (**paper I**).

Collateral sensitivity: mechanisms

Albeit the number of studies that investigate the frequency of CS is growing, the mechanisms of this phenomenon are still poorly understood. CS is likely achieved by an enhanced antibiotic-target interaction and growth inhibition, which represents, on a molecular level, an inversion of resistance mechanisms[234]. Firstly, CS can be caused by an increased net uptake of drug molecules into the cell, or by their reduced efflux. For the latter, Lazar *et al.* were the first to describe a CS mechanism in *E. coli*. Mutations in *trkH, cyoB/C, ispA, nuo* or *hemA* resulted in aminoglycoside resistance due to a decreased inner membrane potential and reduced active uptake of these drugs[219]. Simultaneously, antibiotics that are substrate for proton motif force-dependent efflux pumps such as AcrAB-TolC accumulated intracellularly, leading to CS[219]. Secondly, increased chemical activation of nitrofurantoin was linked to CS. Mutations in *spoT*, *lon*, *or hemL* in mecillinam- and tigecycline-resistant *E. coli* upregulated expression of the nitroreductases NfsA and NfsB, and the increased formation of the toxic intermediate led to CS towards nitrofurantoin[234]. Thirdly, CS could be caused by an increased toxicity of the drug, for example by activation of the SOS response. This effect was described for a tigecycline-resistant *lon* mutant of *E. coli* with CS towards nitrofurantoin[234]. Lastly, an enhanced drug binding at the target can promote CS. This can be caused by allosteric changes of the target structure[222], or as suggested for mecillinam-resistant $bla_{\text{CTX-M-15}}$-variants, by reduced affinity of the mutated enzyme to another antibiotic, in this case cefotaxime, which is free to bind to the target[229].

Objectives

This PhD thesis aimed to increase our understanding of the selection, spread and maintenance of bacterial antibiotic resistance. We investigated:

1. a strategy of selection inversion in drug resistant populations (**paper I**)
2. a mechanism that facilitates the horizontal spread of antibiotic resistance (**paper II**)
3. the maintenance of plasmid-mediated antibiotic resistance (**paper III**).

The specific objectives were:

Paper I

- to determine collateral sensitivity networks for relevant antibiotics across a diverse set of single-drug resistant (ciprofloxacin, mecillinam, nitrofurantoin, trimethoprim), clinical isolates of uropathogenic *E. coli*;
- to analyze the generality and evaluate predictors of the identified collateral responses.

Paper II

- to determine the frequency of Tn*1*-transposition during natural transformation of *A. baylyi*;
- to identify host and element functions that are required for transposition.

Paper III

- to determine the fitness of uropathogenic *E. coli* isolates that carry carbapenemase-encoding resistance plasmids ($bla_{\text{VIM-1}}$ or $bla_{\text{NDM-1}}$) before and after experimental evolution;
- to identify genomic targets of plasmid-host adaptation;
- to investigate mechanisms that contribute to plasmid maintenance.

Materials and Methods

Bacterial species

Escherichia coli and the ECOSENS collection

Escherichia comprises motile, facultative anaerobic, G- rods of the family *Enterobacteriaceae*. The first isolate of the genus was obtained from the gut of an infant in 1885[235]. The species *Escherichia coli* is a symbiotic inhabitant of the mammalian gut and predominantly found in the small intestine[236]. Increasingly, environmental samples of *Escherichia* can be genetically distinguished[237,238]. For more than 100 years, descendant strains of *E. coli* K-12 and B[239] have been exploited as malleable model organisms for molecular, biotechnological and genetic studies[240]. For example, fundamental findings in *E. coli* are related to sexual recombination in bacteria, such as the discovery of bacterial gene transfer by conjugation[241] and transduction[242], and the description of today's plasmids[243,244]. The amount of research done on *E. coli* is also exemplified by over 22 000 *E. coli* genomes that are deposited online to date[245]. The first fully assembled genome was available in 1997 (*E. coli* strain MG1655)[246], followed by increasingly accurate sequences[247], which facilitated the construction of an *E. coli* single-gene knock-out collection for the study of gene essentiality[248]. Experimental evolution studies using *E. coli* cover different aspects of microbial adaptation processes, for example the adaptation to different growth conditions[249,250], fitness dynamics of adaptation[157,161] (**paper III**) or the evolution of antibiotic resistance[50,219,221,251] (**paper I**). An immense effort and scientific commitment are put into the continuation and analysis of the long-term experimental evolution of *E. coli* by Lenski and co-workers, which is already exceeding 76 000 bacterial generations[252].

Apart from being a persistent or transient commensal, pathogenic *E. coli* frequently cause diarrhea, urinary tract infections (UTIs) and even serious bloodstream infections or meningitis[253,254]. From the human gut as a common reservoir, **i**ntestinal and **ex**tra-intestinal sites can be colonized by **p**athogenic ***E. coli***, which are abbreviated as **IPEC** or **ExPEC**, respectively[255]. *E. coli*'s etiological potential is further categorized into pathotypes based on disease symptoms, virulence determinants and phylogeny, for example **u**ro**p**athogenic ***E. coli*** (abbreviated as **UPEC**) or **e**ntero**h**emorrhagic ***E. coli*** (abbreviated as **EHEC**)[255]. Additional subdivision based on surface antigen -O, -H, and -K (serotype), multi-locus sequence typing, and biochemical properties (biotype) is important to understand the epidemiology of *E. coli* pathogens[255,256]. A combination of core and accessory genome analysis is suggested to more accurately distinguish *E. coli* pathogens from commensals[255,257], and also *E. coli* pathotypes from one another[258].

UTIs are most often caused by UPEC[254]. In two multicenter studies including 16 European countries and Canada the prevalence of UPEC ranged between 74%-77% of all tested organisms associated to

community-acquired uncomplicated UTI in women (ECOSENS Project I[259] and II[68]). UPEC present an enhanced metabolic flexibility to survive in the rather hostile microenvironment of the bladder and kidney, which is nutritionally poor and nitrogen-rich[260]. Via the fecal-periurethral route UPEC infect the bladder (cystitis), however, the infection can also involve the kidneys (pyelonephritis) and from there enter the bloodstream through tissue invasion[253]. UPEC belong to diverse STs and mainly to phylogroups B2, A and D[261,262]. The *E. coli* strains used in this thesis originate from the ECOSENS studies I[259] (**paper I**) and II[68] (**paper I and paper III**), respectively, and were isolated in Greece, Portugal, Sweden, and the UK. These 11 UPEC isolates were pan-susceptible according to disc diffusion tests, belonged to diverse STs as determined by multi-locus sequence typing and were plasmid-free according to results from pulse-field-gel electrophoresis and PCR-based replicon typing[261]. Our own bioinformatic analysis revealed a different ST than previously described for two isolates, the presence of plasmids for three of the employed isolates and an acquired resistance element or mutational resistance determinants in four strains (**paper I**).

Acinetobacter and strain *A. baylyi* ADP1

The first organism that represents the current *Acinetobacter* classification was isolated in 1911 from soil[263]. This genetically diverse genus comprises more than 60 species that belong to the family *Moraxellaceae*[264,265]. Its members are G-, non-motile, non-spore forming and strictly aerobically growing coccobacilli *i.e.* they may form rod-shaped cells during exponential growth that become coccoid when entering stationary phase[266]. *Acinetobacter* spp. can be isolated in high abundance from soil and aquatic environments[267], or activated sludge[268]. Also food samples (vegetables, dairy products, meat and fish) and the human flora, especially skin, represent a natural habitat[269,270]. However, members of the '*Acinetobacter baumannii* complex' (*A. baumannii, A. pittii, A. nosocomialis*) are only rarely found in environmental habitats but instead represent the frequent cause of MDR hospital infections, for example UTI, wound infections, ventilator-associated pneumonia and bloodstream infections[271-273].

In **paper II**, a spontaneous rifampicin-resistant mutant of *A. baylyi* strain ADP1 was used[268,274]. Taylor and Juni first isolated the organism from soil in 1960[275], and its high competence for the uptake of exogenous DNA by bacterial natural transformation was soon after demonstrated[276]. Genome analysis of diverse *Acinetobacter* spp. suggests that most members of the genus can undergo natural transformation under conditions that induce the expression of competence genes[37]. Interspecies transformability was confirmed for clinical isolates of *A. baumannii* and also other *Acinetobacter* spp.[106,107,277-280]. *A. baylyi* is closely related to *A. baumannii*[37] and shares around 80% identity in core

genes with clinical isolates of this species[281,282]. It is gaining more attention as a potential pathogen due to its, still sporadic, clinical occurrence in immune-compromised patients[283,284].

A. baylyi ADP1 is a widely used model organism to study the adaptive potential of bacterial natural transformation[113,285,286]. This is due to its competence for DNA uptake at high frequencies[110,274,287] from all kinds of sources[110], even eukaryotic[114], and easy handling in the lab, which results from its minimal nutritional requirements and a short generation time[288]. The transformation capabilities of ADP1 are thoroughly investigated; frequencies as high as 10^{-3} can be measured for homology-facilitated transformation with chromosomal donor DNA and 10^{-4} for plasmid transformation, respectively[110]. In liquid culture, ADP1 develops maximum competence for DNA uptake once the availability of nutrients is increased, for example directly after dilution of an overnight culture into fresh medium[110]. Competence only drops when the strain enters stationary phase[289]. Transformation is facilitated by the addition of DNA into a growing culture, and ADP1 binds and takes up extracellular, dsDNA indiscriminate of origin (*e.g.* not species-specific[287]), topology (linear or circular DNA[110]) or nucleotide sequence (heterologous or homologous DNA[110]). DNA-uptake sequences are not described for *Acinetobacter* spp., and ssDNA transformation of ADP1 can occur but is inefficient[110,114]. The ADP1 genome does not include plasmids[281] and is unusually small but represents the average genome size of the *Acinetobacter* genus[37] (3.6 and 3.8 Mbp, respectively). A single-gene knock-out collection of ADP1 has been constructed[290], and further genetic manipulation of ADP1 was used to study various metabolic pathways and molecular mechanisms that contribute to genome plasticity in bacteria, thereby exploiting its nutritional versatility and natural transformability[285,291].

No drugs for bad bugs

Both of the above-described bacterial genera include species that present a particular threat in the global emergence of resistant pathogens[292]. *A. baumanni* and *E. coli* are classified as so-called ESCAPE organisms[293] (originally ESKAPE[294]) together with *E. faecium*, *S. aureus*, *Clostridium difficile*, *P. aeruginosa* and other *Enterobacterales* such as *K. pneumoniae*, for which current treatment options are increasingly insufficient due to MDR infections. More specifically, ESBL-producing or carbapenem-resistant *Enterobacterales* including *E. coli*, and carbapenem-resistant *A. baumannii*, represent pathogens for which research and drug development efforts are of critical priority according to the World Health Organization[9].

Although the rate of carbapenem-resistant *E. coli* blood isolates in most European regions is reported to be below 2% in 2019, a rising trend can be observed[10]. For example, colonisations and infections with carbapenem-resistant isolates of *Enterobacterales* in Norway increased 10 times from 2008 to 2018 (54 patients)[295]. During this time, selection for carbapenem resistance rose with the clinical use

of these drugs in infections with third generation cephalosporin-resistant *E. coli,* which increased significantly across Europe[10,296] (**Figure 12**, top).

Many *Acinetobacter* spp., including the clinically predominant *A. baumannii,* are intrinsically resistant to a wide range of antibiotics[43]. Incidence of clinical *Acinetobacter* isolates resistant to carbapenems (mainly due to carbapenemases), aminoglycosides (mostly through aminoglycoside-modifying enzymes) and fluoroquinolones (efflux pump-related) is especially high in some Baltic, Southern and South-eastern European countries, and evolves through a combination of mutational, and importantly, horizontal resistance acquisition[10] (**Figure 12**, bottom).

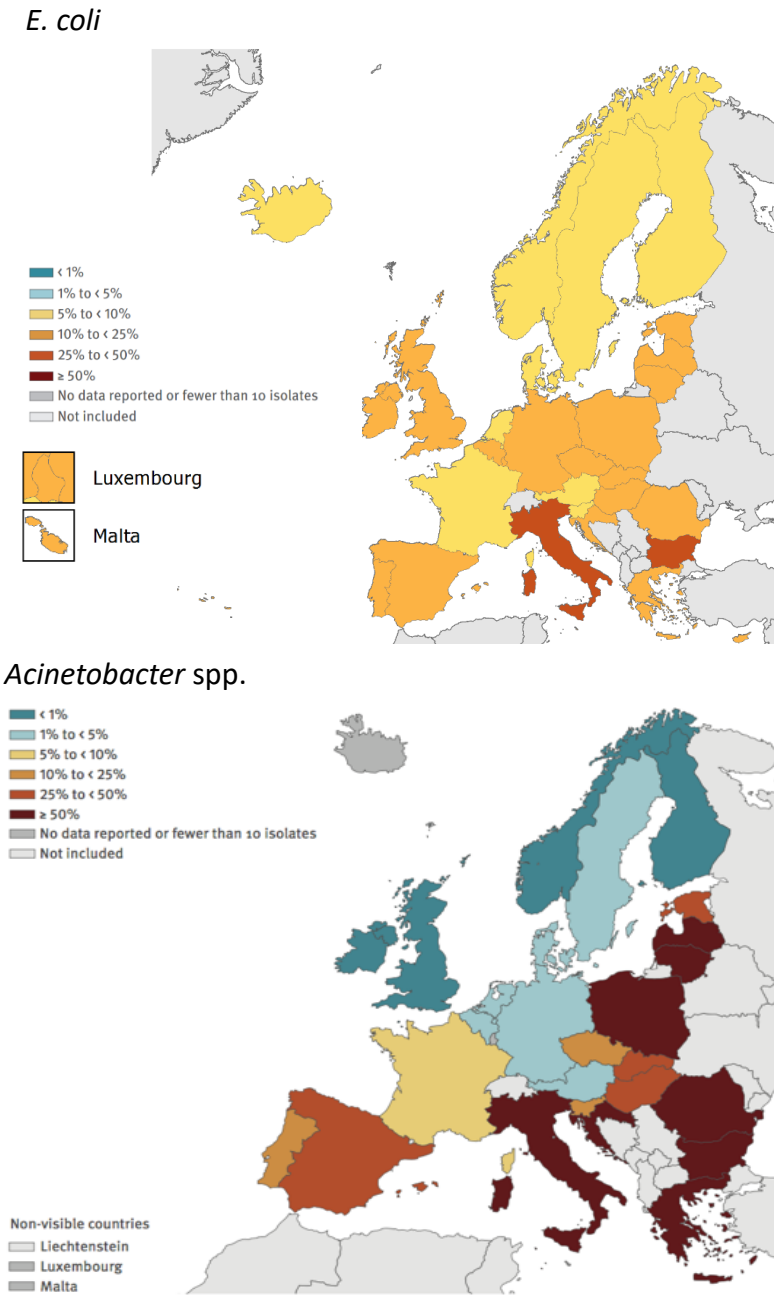

Figure 12: National percentages for blood isolates of third generation cephalosporin-resistant ***E. coli*** (2019) and ***Acinetobacter* spp.** resistant to fluroquinolones, aminoglycosides and carbapenems (2018). Reprinted from[10,297]

Methodological approaches

Further experimental details can be found in the respective **papers I-III**.

Collateral sensitivity networks in *E. coli* UTI isolates (paper I)

As previous studies tested collateral responses against a larger panel of antibiotics only in laboratory strains (*E. coli* MG1655[220,221], *E. coli* BW25113[219]), we employed ten *E. coli* isolates from patients diagnosed with uncomplicated UTI (ECOSENS I[259] and II[68]). Importantly, the strains were phenotypically pan-susceptible to antibiotics and thus collateral effects could be determined for individual antibiotic resistance mutations. To account for the impact of strain diversity on collateral networks, we chose to work with different STs, as determined in[261]. The antibiotics to which primary resistance was evolved in these strains (ciprofloxacin, nitrofurantoin, mecillinam, trimethoprim) were chosen due to their clinical relevance in the treatment of uncomplicated UTI in women according to national (Norway)[298] and international (Europe and USA)[299] guidelines. Nitrofurantoin, trimethoprim (-sulfamethoxazole) and (piv)mecillinam represent drugs which are recommended in the first-line, empiric therapy of uncomplicated UTIs caused by common uropathogens due to their good clinical and microbiological efficacy. Other β-lactams and also fluoroquinolones, such as ciprofloxacin, should only be considered as alternative treatment options for complicated UTI[298,299].

To obtain resistant *E. coli* mutants at or above the respective clinical breakpoint according to EUCAST[45] (version 7.1), we used a static, stepwise selection regime on solid media containing ciprofloxacin, nitrofurantoin, mecillinam or trimethoprim in two-fold increasing concentrations. This method is comparable to the gradient plate technique employed in the pioneering studies investigating bacterial CR/CS[217,220]. In several selection rounds, increasing lethal concentrations of antibiotics are used to select for increasingly resistant mutants. At each replating event on higher concentrations, strong selection pressure for resistance acquisition, and bottlenecks, are applied. The cultivation steps were kept at a minimum throughout this selection procedure to avoid acquisition of adaptive mutations to the laboratory environment. To confirm resistance of the 40 mutants phenotypically, we performed AST by the gradient strip method to obtain the MIC. Next, we assessed collateral effects in our mutants by BMD, monitoring bacterial growth in an antibiotic gradient and measuring optical density (OD_{600}), determination of the 90% inhibitory concentration therefrom (IC_{90}; strongly correlates to inhibition levels IC_{50} or IC_{95} and thus approximates the MIC[221]), and generation of heat maps and CS/CR networks, as previously described[220]. The BMD method represents the gold standard in AST and improved overall sensitivity and precision. Compared to strip tests, where changes in susceptibilities are estimated from visual determination of growth inhibition and with a sensitivity of 2-fold, BMD allowed high-throughput screening of susceptibility changes by automated

endpoint absorbance measurements, and an increase in resolution to 1.5-fold. We assayed CR/CS responses towards 16 different antibiotics, including bacteriostatic and bactericidal drugs with diverse modes of action to which our wildtype strains were phenotypically susceptible. Furthermore, the selected agents represented frequently or conservatively used (for example the last-line drug colistin), clinically relevant antibiotics, older antibiotics (for example temocillin and fosfomycin), and drugs that are not licensed in all European countries (fosfomycin). Conserved collateral effects (when CR/CS to a specific antibiotic was prevalent in ≥50% of mutants) where further characterized by generating dose-response growth inhibition curves and MPC measurements for representative resistant mutant-wildtype pairs, as was also done previously[220].

Similar to Lazar *et al.*[219], we investigated the genetic mechanism of resistance by whole genome sequencing (WGS). Short-read next generation, paired-end sequencing was performed by Illumina technology, which is currently the most accurate sequencing technique. A reference genome was assembled for each wildtype strain. By using WGS, read alignment, BLAST search, and intensive literature study, we identified putative resistance mutations. WGS was especially useful for mecillinam mutants, since resistance to this drug reportedly can be achieved by mutations in at least 38 different genes[66]. The concentration at which first-step resistant mutants are prevented to arise, the MPC, was determined similar to Imamovic *et al.*[220]. Two-fold increments in antibiotic concentrations were employed since the endpoint determination by distinction of growth/no growth turned out problematic using 1.5-fold changes. This was likely due to the required large amount of inoculum (approximately 10^{10} cells[48]) causing an uneven growth inhibition.

To determine the relative fitness (w) of resistant mutants, we measured the maximum exponential growth rate (r), which is a commonly used fitness parameter and reflects a strain's ability to reproduce. Growth rate measurements were performed on all 40 mutants and their respective wildtypes and determined by following changes in the optical density (OD_{600}) of individually growing strains in liquid culture. Although this measure captures growth dynamics just during exponential phase and only fitness differences >5% are detected, it represents a quick and easy method to approximate fitness without the need for a selective marker gene[156]. Multivariate statistical analysis was performed by redundancy analysis to quantify how much strain background, presence of efflux-related mutations and relative fitness explains the observed variation in collateral responses.

Horizontal spread of resistance-transposons by natural transformation (paper II)

The horizontal dissemination of resistance by transposition-mediated natural transformation was first demonstrated in *A. baylyi* strain ADP1 by Domingues *et al.*[118]. To further investigate this finding, we employed the same recipient strain since it is highly competent for natural transformation, which

facilitated the detection and quantification of the expected rare recombination events, and easy genetic manipulation of recipient strains. Standard *in vitro* assays for bacterial natural transformation can be performed either in liquid culture or by applying the transformation mix on a filter (detailed protocols in[300]). Since the frequency of transposition was reported to be low[118], we performed our transformation assays in liquid culture, as described previously[301], where the detection limit can be decreased simply by upscaling of the assay volume.

Domingues *et al.*[118] reported the transposition of Tn*21*, a well-described element of the Tn*3*-family of replicative transposons. Relating to this finding, our donor DNA contained Tn*1*, an element of the same transposon-family which also moves by a copy-and-paste transposition mechanism[147]. Tn*1* encodes a β-lactamase ($bla_{\text{TEM-2}}$)[302] and its sequence is highly identical to Tn*2* and Tn*3*[142]. All three elements express resistance to ampicillin and additional β-lactam antibiotics and are of clinical relevance especially in G- species[95]. Tn*1* has a small size (4.9 kb), which simplified cloning procedures. To increase the amount of intracellular transposon copies per net amount of incoming DNA during natural transformation, we constructed a plasmid-vector containing Tn*1*. This narrow-host range plasmid carried an origin of replication (p15A) that is only functional within *Enterobacteriaceae*, so stable plasmid replication in ADP1 was not expected. Donor DNA and recipient genome did not contain sequence similarities that would promote homology-facilitated recombination events.

The efficiency of natural transformation increases with the amount of donor DNA added, following a saturation kinetic[110]. Due to the low frequency of reported transposition events[118], near-saturating amounts of extracellular donor DNA were added to the assay to ensure DNA uptake by the majority of cultured cells. Both circular plasmid DNA as well as linear donor DNA were employed in transformation assays to investigate whether the transient expression of transposon genes in the bacterial cytoplasm depended on the possibility for plasmid establishment. Linear donor DNA was amplified by PCR from plasmid templates, or by restriction enzyme digestion of the plasmid. However, the complete elimination of circular template DNA could only be achieved by enzymatic restriction of donor DNA and additional agarose gel purification of previously restricted DNA.

Transposition results in characteristic TSDs[147]. We verified transposition events phenotypically by selection of ampicillin-resistant candidate clones and transposon-specific PCR. To confirm transposition events genetically, genomic DNA was isolated from Tn*1*-containing isolates and Sanger sequencing was performed using outward facing primers with respect to the Tn*1* sequence. This allowed the identification of transposon insertion-site within the ADP1 chromosome.

The requirement for host- and/or transposon-functions for transposition in the course of natural transformation was not investigated before, and we used ADP1 mutant recipients or modified donor DNA to study the role of specific enzymes on transposition-mediated natural transformation.

Evolution of plasmid-mediated antibiotic resistance (paper III)

With respect to the clinical problem of plasmid-driven resistance, there is a lack of studies employing clinically relevant plasmid-bacteria combinations to investigate compensatory evolution[303]. Here, two plasmid-host combinations were constructed from clinical plasmids that confer carbapenem resistance, pG06-VIM-1[129,130] and pK71-77-1-NDM[128,304], and a clinical UPEC isolate (ST537)[259,261]. The plasmids varied in their size, Inc-type, resistance profile and potential for horizontal mobilization. Experimental evolution is a common method to study adaptation in bacteria[157,305]. *In vitro* evolution studies are most often performed using a serial transfer regime on growing liquid cultures, which rapidly increases the number of bacterial generations reached[306]. Transfer bottlenecks of 1/100 maintain enough genetic diversity for natural selection to act towards the enrichment of the fittest mutants. The use of standard laboratory growth media was the most practical starting point to investigate the so far unknown evolutionary dynamics of clinical plasmid-host pairs, whereas artificial or even human urine represent a more complex environment that could affect growth dynamics in unexpected ways. We froze down mixed populations after 300 generations as bacterial growth adaptation is highest immediately after transfer to a new medium[157].

Researchers in the field of plasmid-host dynamics are urged to combine 'omic' technologies, for example genomics and transcriptomics (and more) to determine the outcome of plasmid-host experimental evolution[303]. We performed WGS on our evolved populations and on purified ancestral and evolved clones using short-read, paired-end Illumina sequencing. For sequence comparison, a closed reference genome of the ancestral host was generated by hybrid-assembly of long- (PacBio) and short-read sequencing data. Closed plasmid sequences were available from previous studies[128,130]. A high coverage in the evolved populations (average >1000) allowed the identification and comparison of single-nucleotide changes and small indels arising above 1% frequency on the chromosome and the plasmids. The breseq pipeline allowed the analysis of short-read DNA re-sequencing data from the heterogenic population data, and also the clonal data, relative to the reference[307]. Although the use of short-read data limited the analysis of structural variations in our study, some conclusions on rearrangement, deletion or insertion of larger genomic regions could be inferred from read coverage plots generated using breseq.

To measure the fitness effect of plasmid carriage in ancestral and evolved backgrounds, we determined the relative fitness w of representative clones, either from the growth rate (r) or, to gain

resolution, by measuring the 'head-to-head' competitiveness of two genotypes. The latter captures a more comprehensive picture of fitness since growth dynamics across the lag, log and stationary phase are considered. The competitors, plasmid-free and plasmid-containing isogenic strains, are mixed 1:1 in liquid culture and in certain time intervals, viable bacteria are determined[156]. This method requires a selectable marker gene, for example a resistance gene, which was present on the plasmid. We employed serial transfer competition experiments over an extended period of time and calculated a selection coefficient from the relative frequencies of the competitors, as previously described[161,308]. Small differences in fitness (1%) can be detected by this method[169]. Smaller differences (0.1%) could be revealed by high throughput competition experiments using flow cytometry and fluorescence tagged strains (fluorescence-activated cell sorting)[191]. This would require genetic modification of the strains, and the fact that clinical isolates are commonly difficult to manipulate represented an obstacle to this approach.

Since gene expression is a major determinant for the cost of plasmids, transcriptomic analyses are used to identify the cellular processes that cause and compensate plasmid fitness costs through changed expression levels[176,178]. For the analysis of bacterial transcription profiles in ancestral and evolved strains, we performed Illumina-based RNA-Seq. SARTools (DESeq2-based) was used for genome-wide differential gene expression (DGE) analysis[309]. As established tools for functional pathway analysis and visualization of DGE results rely on lab strain annotations, those were not suitable for our clinical isolates. We used the PANTHER classification system to assign protein families based on our own sequence data[310].

To investigate the role of the individual proteins that were targeted by mutations in plasmid cost compensation, we employed single-gene deletion strains in competition assays using knock-out strains of the Keio collection[248] to circumvent molecular work in our clinical strains. We employed ELISA (enzyme-linked immunosorbent assay) to determine the effect of a *cpdA* mutation on intracellular cAMP levels in an evolved strain biochemically.

Summary of Results

Paper I: Conserved collateral antibiotic susceptibility networks in diverse clinical strains of *Escherichia coli*.

Collateral sensitivity-informed treatment aims at reducing the emergence of resistance in bacterial populations during antibiotic therapy.

Resistance mutations affecting drug target (ciprofloxacin, trimethoprim), drug activation (nitrofurantoin), drug efflux (ciprofloxacin, nitrofurantoin, mecillinam) and diverse cellular targets (mecillinam) were identified by WGS in clinical *E. coli* isolates with generated single-drug resistance. IC_{90} measurements revealed the most conserved and also strongest collateral responses in ciprofloxacin-resistant mutants, including CS towards gentamicin, fosfomycin, ertapenem and colistin, and CR towards temocillin, chloramphenicol, ceftazidime, mecillinam and trimethoprim. The collateral susceptibility changes in this resistance group were linked to efflux-related resistance mechanisms. Reciprocal CS responses were not identified across the different resistance groups. On average, resistance acquisition reduced relative fitness by 1% (nitrofurantoin), 6% (trimethoprim), 36% (mecillinam) and 47% (ciprofloxacin). Multivariate statistical analysis identified that resistance mechanisms, particularly efflux mutations (33%) and fitness costs (17%) were significant predictors of the observed collateral effects, while the genetic diversity of the strain backgrounds did not influence the observed collateral networks. The MPC changed correspondingly to the identified CR/CS responses in 71% of cases.

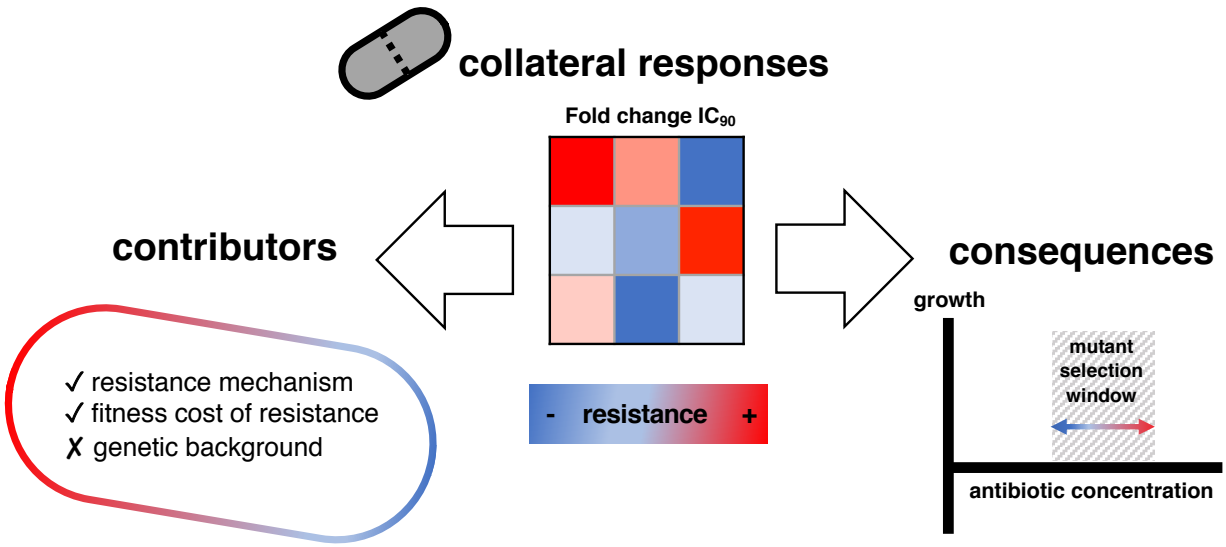

Paper II: Tn*1*-transposition in the course of natural transformation enables horizontal antibiotic resistance spread in *Acinetobacter baylyi.*

Transposition is a DNA-recombination mechanism that facilitates the movement of transposon-associated resistance genes intracellularly, and also horizontally through plasmid conjugation. Natural transformation of *A. baylyi* ADP1 by a non-replicative, pACYC184-based donor DNA substrate carrying Tn*1* (bla_{TEM-2}) resulted in chromosomal transposon-insertion at a frequency of 8×10^{-9}. Transposition was observed in the wildtype ADP1 and an exonuclease deficient ADP1 strain (Δ*recBCD* Δ*sbcCD*). Chromosomal target site duplications were verified for 43 insertion events and represented the typical consensus sequence that is reported for the Tn*3*-family. In 80% of cases, a 170-kb region around the ADP1 replication terminus was the preferred target for Tn*1*-insertions. Transposition was not observed when the Tn*1*-transposase (*tnpA*) or Tn*1*-resolvase (*tnpR*) were deleted from the donor DNA substrate, or when the transposon was present on a linear donor DNA fragment. Natural transformation assays with ADP1 mutant strains (Δ*recO*, Δ*recA,* Δ*dprA* or Δ*recBCD*Δ*sbcCD*) revealed an essential (RecA) or inhibiting (RecBCD) role of host proteins on plasmid transformation. The results were summarized in a model. This suggests that donor DNA circularized in the cytoplasm from rare dimeric plasmid molecules with redundant ends, which facilitated the observed transposition events during natural transformation.

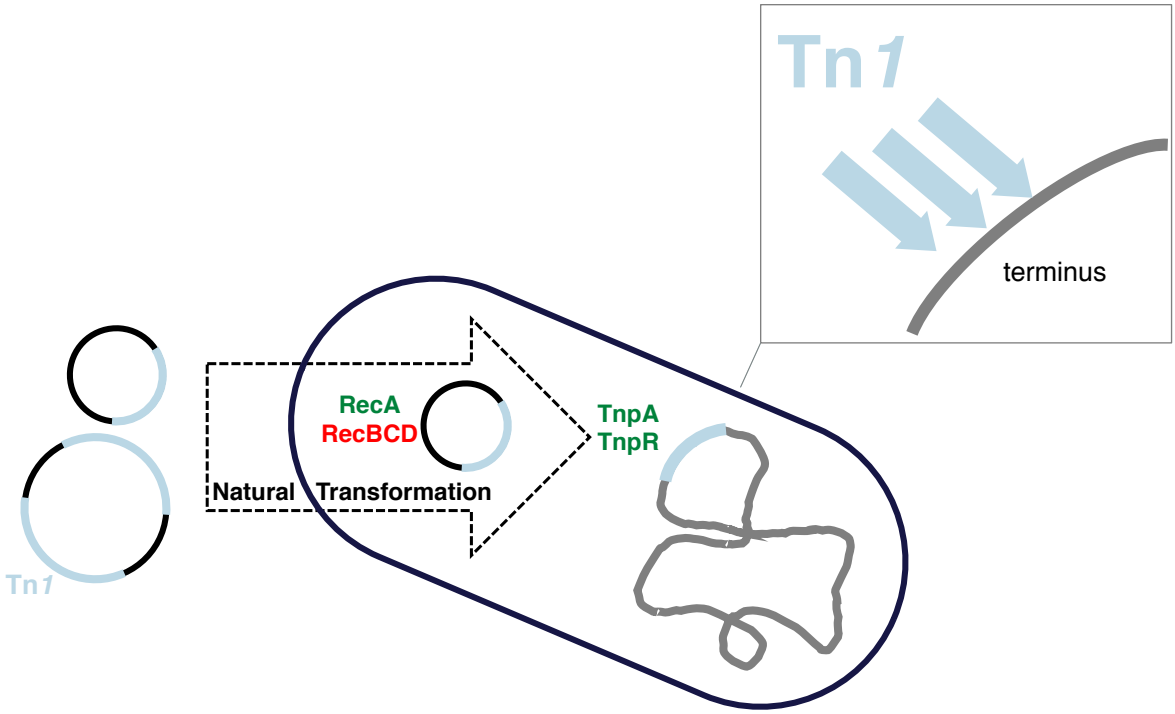

Paper III: Piggybacking on niche-adaptation improves the maintenance of multidrug resistance plasmids.

The evolution of stable, low-cost plasmid-host relationships drives the maintenance of resistance in nosocomial pathogens.

The clinical MDR plasmids pG06-VIM-1 (bla_{VIM-1}) from *K. pneumoniae* and pK71-77-1-NDM (bla_{NDM-1}) from *E. coli* displayed a 5.3% and 5.5% cost in a uropathogenic *E. coli* isolate in head-to-head competitions, respectively. WGS of experimentally evolved plasmid-free and plasmid-carrying lineages revealed strong parallel adaptation of the *E. coli* regulatory systems ArcAB and CCR. The targeted genes, *arcA*, *arcB*, *cpdA*, *crp* and *cyaA* presented known targets for bacterial growth adaptation under laboratory conditions. None of the evolved plasmid sequences were altered by point mutations. Growth rate measurements of evolved relative to ancestral strains displayed growth improvement (7-17%) irrespective of pG06-VIM-1 presence. The cost of pG06-VIM-1-carriage was ameliorated to below 1% in head-to-head competitions of adapted backgrounds. CpdA had lost its cAMP-degrading function in adapted backgrounds (*cpdA*.Δ3.bp488-490) with and without pG06-VIM-1, which was indicated by the doubling of intracellular cAMP. The cost of pG06-VIM-1 carriage was either significantly reduced (Δ*cpdA*) or ameliorated to no cost (Δ*crp*) in *E. coli* single-gene deletion mutants. Transcriptome analysis revealed a net downregulation of plasmid gene expression in adapted backgrounds.

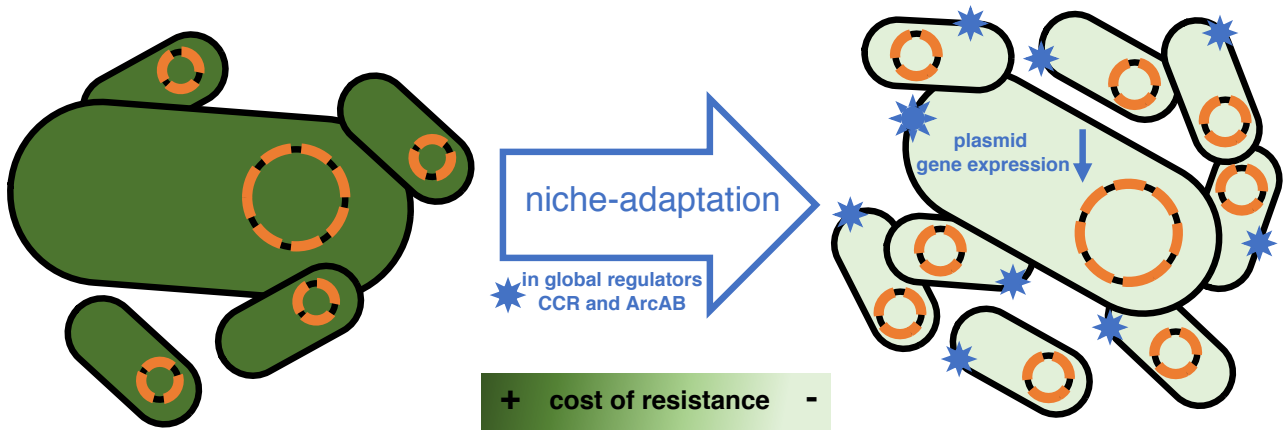

Discussion

This thesis approached the problem of antibiotic resistance by investigating aspects of its selection, spread and maintenance in bacteria (**paper I, II and III**, respectively).

The development of resistance in bacterial pathogens increasingly challenges empiric infection therapy[9,10]. Besides the usual strategies to fight antibiotic resistance such as the reduction in drug consumption or misuse, the search for novel drugs or improved diagnostics, it is also important to consider concepts from evolutionary biology, for example collateral sensitivity[19]. This evolutionary tradeoff makes bacteria that are resistant to one antibiotic more vulnerable to other antibiotics. Hence, CS-informed treatment strategies have the potential to select against rather than for resistance in bacteria[220]. In **paper I**, we described this biological phenomenon in the context of UTI treatment and identified predictors for conserved collateral susceptibility changes across clinical uropathogenic *E. coli* (UPEC) isolates.

Horizontal gene transfer (HGT) facilitates the rapid dissemination of plasmids and associated resistance elements therein, for example transposons[95]. The horizontal spread of transposons relies however not only on their plasmid-location and the possibility to 'hitch a ride' during conjugation. In addition, they have the potential to activate their transposition properties during natural transformation[118]. In **paper II**, we determined the frequency and mechanistic requirements of such events for a replicative transposon in the natural transformation model organism *A. baylyi* and propose a mechanistic model for this route of horizontal transposon spread.

From a bacterial perspective, antibiotic resistance acquisition often confers selective pitfalls. The bacterial host frequently experiences a fitness burden of maintaining resistance plasmids in the absence of antibiotic selection pressures, and the biological cost of resistance is a major determinant for the stability or loss of plasmids in bacterial populations. However, this conflict is resolved by adaptive mechanisms that compensate plasmid fitness costs[171]. In **paper III**, we demonstrate the compensatory evolution of two clinical MDR plasmids in a UPEC isolate and provide a new solution to the question why plasmids persist, the so-called plasmid paradox[185,186].

Collateral susceptibility changes in a clinical context

UTIs caused by UPEC are very common both in the community and hospitals and linked to considerable morbidity and mortality[254]. Over the years 2000 to 2014, a significant increase in ciprofloxacin and trimethoprim resistant UPEC was reported for five European countries (4-16% and 17-31%, respectively), while resistance to mecillinam and nitrofurantoin remained at low levels (2-

4%)[311]. In **paper I**, we employed UPEC isolates to investigate collateral susceptibility changes in a clinical context, rather than in single laboratory strains[219,220].

A finding of clinical relevance in our study was that resistance development towards trimethoprim, nitrofurantoin and mecillinam did not limit the choice of secondary drugs in our strains, since only few collateral responses (trimethoprim, nitrofurantoin) or more frequent cases of CS than CR (mecillinam) were found. Hence, our results encourage continuation of first-line use of these antibiotics as recommended by national and international guidelines[298,299]. Furthermore, our results support the reserved use of ciprofloxacin in the treatment of complicated UTI, as our ciprofloxacin resistant mutants evolved conserved CR responses towards the two UTI drugs trimethoprim and mecillinam, and cases of CR towards chloramphenicol and amoxicillin beyond clinical breakpoints. Both would limit treatment choices for ciprofloxacin-resistant strains.

It should be noted that we did not observe any cases of reciprocal CS-effects, which are a prerequisite for clinical drug cycling approaches as suggested by Imamovic *et al.*[220]. However, our results provided support for the mutant selection window hypothesis[48] and implied, that CR increases the likelihood to select for MDR strains. In this regard, results from a recent investigation of collateral effects on MPCs in *S. epidermidis* confirm our finding[49]. Importantly, the results from our statistical model suggested that specific resistance mechanisms in a given clinical isolate forecast collateral effects. Hence, their rapid identification could inform clinical CS-based treatment.

Predictors for conserved collateral responses

The main research question asked in **paper I** was whether conserved collateral susceptibility changes occur across different UPEC strains. We found that this was particularly the case in ciprofloxacin-resistant mutants and this finding agreed with frequent collateral responses in ciprofloxacin-resistant mutants of a clinical *P. aeruginosa* strain[228]. In that study, CS towards several aminoglycosides was common, and similarly, CS towards gentamicin was observed in all our ciprofloxacin-resistant mutants.

Our data demonstrates for the first time, that strain diversity does not contribute to collateral changes as much as resistance mechanism and/or relative fitness of the resistant strains, which we identified as main predictors for the observed collateral responses. However, the identified costly mutations in our ciprofloxacin- and mecillinam-resistant mutants (**paper I**) are less commonly acquired *in vivo*[56,66] and thus highly conditional. In contrast to our finding, a recent study modelled susceptibility and fitness changes that were experimentally derived from *S. pneumoniae* resistant mutants, together with antibiotic pharmacodynamics, and found that fitness has no predictive value for collateral responses in this species[312]. Furthermore, it is well-established that compensatory evolution can ameliorate the

fitness cost associated to resistance mutations[198]. Especially the costly efflux-related resistance in ciprofloxacin-resistant mutants (**paper I)** imposes selective pressures towards evolutionary adaptation, and our research group recently demonstrated that fitness cost compensation returned drug-efflux to wildtype levels and weakened collateral responses in *E. coli* (Sørum *et al*., unpublished data).

Although the results of **paper I** cannot be generalized beyond *E. coli*, they revealed important aspects of collateral responses in clinical isolates. It will be important to separate the contribution of distinct resistance mechanisms and genetic background on susceptibility changes in future studies and assess collateral networks for a variety of resistance mechanisms across large isolate collections using the isogenic wildtype for comparison. Confounding factors could for example be epistatic interactions between resistance mutations and preexisting mutations in the genome[164] or inherent resistance mechanisms[227]. Furthermore, fitness as well as resistance levels of resistant mutations are context-dependent[167,313], and thus collateral responses may vary in different growth media.

Knowledge-gaps in CS-based treatment strategies

The clinical implementation of CS-informed antibiotic therapy depends strongly on the predictable evolution of collateral responses across different bacterial strains and species. However, it was shown that for some antibiotics, several (mutational) evolutionary paths towards resistance are possible and depending on the order of mutation acquisition, different collateral responses evolved within the same species[226]. More recent CS/CR studies also demonstrated divergent outcomes of *de novo* resistance evolution towards the same drug across different pathogen species *in vitro*[227] and in theoretical models of stepwise resistance evolution[164]. In *P. aeruginosa*, the order of drug use affected the efficient killing of resistant strains or the evolution of CS phenotypes differently[233]. Thus, even though collateral responses in bacteria appear pervasive and our results suggest possible predictability, the existing literature confirms various complicating factors which require further investigation before this useful trade-off can be exploited in medical practice.

Furthermore, the major bulk of studies on collateral responses was generated in single-drug resistant mutants, although resistance in clinical settings is mainly driven by horizontal plasmid acquisition[11,86]. Three reports have so far demonstrated that clinical MDR plasmids[231] or plasmid-associated resistance genes[229,230] contributed to relevant collateral susceptibility changes in *E. coli*. It is however not clear if collateral phenotypes associated with plasmids are due to particular resistance genes alone or if other plasmid-specific traits play a role. Different collateral responses may be caused by horizontally acquired resistance towards the employed primary drugs in **paper I**, especially in the case of trimethoprim, where resistance is mainly mediated by plasmids[15,31], and frequently co-

selected with mobile ciprofloxacin resistance genes[68]. However, ciprofloxacin[36] and nitrofuratoin[314] resistance above the clinical breakpoint is largely only achieved in the presence of additional chromosomal resistance mutations. Similarly, it is likely that mecillinam resistance in UPEC cannot be attributed substantially to horizontal gene transfer, since the drug is relatively stable against plasmid-mediated β-lactamases including ESBLs and some carbapenemases[315].

Evolution of better plasmid hosts in a clinical context

Plasmid-mediated resistance is the main driver of multidrug resistance (MDR) in isolates of *Enterobacterales*[11,86], however, plasmid persistence in absence of antibiotic selection pressures represents an enigma[183,185]. In **paper III**, we approached the lack of studies that mimic plasmid acquisition events as they occur in nosocomial pathogens[303] and we expand the so far limited molecular data on co-evolution dynamics between clinical plasmids and their G- hosts[174]. We found that the carbapenemase-encoding plasmids pG06-VIM-1 and pK71-77-1-NDM moderately reduced fitness of our UPEC strain by around 5%, which was consistent with existing literature in that clinical plasmid-host combinations are less costly[205,316]. The main research question asked in **paper III** was, if and how such low costs could be minimized during plasmid-host co-evolution by compensatory adaptation, as opposed to the amelioration of large costs previously observed in laboratory-plasmid combinations[178,191]. We found that general adaptation of our UPEC strain to the laboratory environment, and not plasmid-specific compensatory evolution, improved its permissiveness towards the here employed, unrelated, non-conjugative and conjugative plasmids. Importantly, niche-adaptation ameliorated plasmid-associated fitness burdens and may represent a more commonly distributed way of plasmid pre-adaptation in bacteria than so far anticipated, with the potential to promote long-term maintenance of plasmids in their clinical hosts. Hence, our observations added a new rationale to the already described mechanisms of plasmid persistence in bacterial populations.

Pleiotropic effect of niche-adaptation on plasmid maintenance

In **paper III**, we examined the genetic basis underlying plasmid-mediated fitness costs and their compensation, which were so far mainly investigated in laboratory strains and plasmids[171]. Our WGS analysis revealed that two *E. coli* regulatory systems (CCR and ArcAB) were target for mutational niche-adaptation across all evolved replicate lineages, while the plasmids were largely unchanged. The improved growth of adapted strains independent of pG06-VIM-1 presence confirmed that CCR and ArcAB mutations were associated with *E. coli* adaptation to the *in vitro* conditions, as previously reported[249,317,318]. The results of **paper III** agreed with existing reports in laboratory plasmid-host pairs in that plasmid-associated fitness costs were frequently mitigated by adaptation of the bacterial

host to the plasmid[178,203,209,319]. Likewise, global regulators (*e.g. gacA/S*[178]) were previously identified as mutational targets for the compensation of costly plasmids. Different to existing reports, we demonstrated that the effect on plasmid costs was the consequence of UPEC adaptation to the experimental conditions, and not to the plasmid. Previously, population genomic analysis of the high-risk clone *E. coli* ST131 showed that alterations in gene regulatory regions can be associated to the acquisition and maintenance of MDR plasmids[320]. Importantly, the results of **paper III** provided *in vitro* evidence that links bacterial niche-adaptation and plasmid persistence as it happens that hosts adapt to their environment by regulatory changes[249,317,318]. Further research is warranted to understand if such pleiotropic effects improve the ability of pathogens to maintain MDR plasmids also across other growth media (*e.g.* urine), plasmid types and kinds of environmental adaptation.

Transcriptional changes that relieve plasmid burden

Gene expression processes have been advocated to be the major causes of fitness burdens associated to plasmid acquisition[171]. This was supported and exemplified in two studies where plasmid acquisition led to 13% (749 genes[176]) and 17% (1006 genes[178]) changes in chromosomal gene expression. In contrast, our findings revealed that acquisition of a clinical plasmid resulted in less dramatic chromosomal gene expression changes (max. 0.4% = 16 genes; **paper III**) and thus agreed with recent reports of low fitness and also transcriptional burdens from MDR plasmid uptake in clinical hosts[316]. *In vitro*, compensatory mutations in global regulators mitigated the translational burden in *P. fluorescens* plasmid-carriers[178], and similarly we found that the majority of chromosomal genes with altered expression upon plasmid acquisition in adapted clones were associated to translation (Clone 2+VIM; **paper III**). As expected from the nature of CCR and ArcAB related mutations, niche-adapted backgrounds showed frequent transcriptional changes to chromosomal genes (21-34% of genes), which did not appear plasmid-specific.

Two recent transcriptomic studies provided evidence for an association between plasmid gene expression and plasmid cost, which was supported by highly expressed plasmid genes compared to chromosomal genes[166], and particularly high expression of plasmid-associated antibiotic resistance genes[166,180]. We hypothesized that the observed regulatory mutations would impact plasmid gene expression in a beneficial way, as compensatory evolution relieved bacterial hosts also from the transcriptional demand generated by plasmid genes[176,178]. We found that 14-28% of plasmid genes altered their expression in niche-adapted backgrounds, which resulted in a net decrease of pG06-VIM-1-associated transcriptional burden. This effect was consistent with a 17% downregulation of plasmid gene expression in *P. fluorescens* due to compensatory mutations in global regulators[178]. Three pG06-VIM-1-located antibiotic resistance genes (*strB, aadA2, sul1*; **paper III**) were

downregulated in adapted backgrounds, however, the low total number of altered genes per clone complicated the systematic analysis of affected biological processes. Since not one single pG06-VIM-1 gene changed expression beyond the 2-fold threshold and the remaining affected plasmid genes varied between the two investigated adapted clones, we were careful to conclude on the specific cause of fitness cost more precisely. Taken together, the results of **paper III** demonstrated that niche-adaptive mutations ameliorated plasmid costs by reducing the transcription-associated burden of pG06-VIM-1 in our UPEC strain. The findings advanced our understanding of plasmid-mediated resistance and the emergence of successful relationships between plasmids and their bacterial host. More studies should examine the transcriptional perturbations caused by MDR plasmids in their clinical hosts to increase our knowledge on the biological pathways that are impacted by plasmid-host conflicts and thus represent targets for compensatory evolution. Ideally, such investigations also examine how transcriptional changes transfer into proteomic and metabolomic alterations.

Multiple evolutionary strategies towards plasmid persistence

In two cases, mobile elements associated with the large, conjugative pK71-77-1-NDM may have been responsible for the removal of costly plasmid traits (**paper III)**, corresponding to the previously reported loss of plasmid-encoded conjugation machinery[174,196] and/or resistance genes[174]. The relative growth rates for the pK71-77-1-NDM-co-evolved replicate clones were significantly improved by 14-23%, with exception of the strain in which the ~8.8 kb deletion in pK71-77-1-NDM occurred (unchanged) (unpublished results **paper III**). Future studies could investigate the consequences of pK71-77-1-NDM-deletions as well as CCR/ArcAB mutations on competitive fitness, plasmid conjugation and plasmid stability in pK71-77-1-NDM-hosts. While deletion of the observed costly regions likely promotes plasmid maintenance over short terms by improving host fitness and thus vertical inheritance[174,195], it limits the potential for horizontal plasmid spread or host adaptation to a selective niche by conjugation. Alternatively, increased conjugational transfer can promote plasmid persistence in a population, and we found that native pK71-77-1-NDM transferred at a higher frequency from adapted backgrounds. The results of **paper III** were thus in agreement with existing literature in that long-term plasmid persistence is facilitated by a combination of different evolutionary processes that impact plasmid cost compensation, plasmid mobility, plasmid maintenance functions as well as episodes of positive selection for plasmid traits[191]. In addition, transduction and natural transformation may have a greater potential to contribute in plasmid dissemination than anticipated so far, as suggested previously[197].

Resistance spread by transposition during natural transformation

The relevance of natural transformation events in clinical settings is poorly understood, although the ability to acquire novel genetic information by this HGT mechanisms is prevalent in G+ as well as G- species including highly important nosocomial pathogens[39]. In **paper II**, we showed that the *bla*$_{TEM-2}$-encoding transposon Tn*1* can spread horizontally by replicative transposition during natural transformation. This was hence the second study that evidenced the potential of (replicative) transposons to participate in the horizontal, nonclonal spread of their associated resistance traits beyond plasmid conjugation, but during natural transformation of competent species, as proposed by Domingues *et al.*[118]. As the species-specific requirements for competence development are still largely unexplored[104], we probably underestimate the contribution of natural transformation in general, and the specific mechanism described here, in antibiotic resistance evolution. It would be interesting to test the capacity for Tn*1*-mediated natural transformation in clinically relevant species. Isolates of *A. baumannii* could be possible recipients. *In vitro* studies increasingly demonstrate the specie's ability to undergo natural transformation, and different experimental conditions are identified that promote competence induction[106,107,277-280].

A mechanistic model of transposon-mediated natural transformation

Transposition during natural transformation uncouples transposon spread from the host-range properties of conjugative elements and recombines genetic material independent from the relatedness between donor and recipient bacterium[118]. In **paper II,** we were the first to examine the molecular requirements for this mechanism of transposon mobilization in more detail. Taken together, we showed that transposition in our model system depended on the stabilization of incoming vector-DNA through intramolecular circularization, followed by transposon gene expression. More specifically, our results indicated that the Tn*1*-encoded proteins TnpA and TnpR rather than *A. baylyi* recombinases (transposases and ISs[321]) or RecA-mediated homologous recombination[155] facilitated replicative transposition into the chromosome of *A. baylyi* via formation of typical, circular co-integrate structures and their resolution, as described for this transposon-family[147]. We concluded that the absence of TnpR halted Tn*1*-transposition at the step of co-integrate resolution. This implied that stable, circular co-integrates were formed once *tnpA* was expressed from reconstituted donor DNA vector, which appeared more efficient when the *tnpA* repressor, TnpR[322], was deleted. This model was consistent with the occurrence of transient plasmid transformants of *A. baylyi* when naturally transformed with donor DNA vector. It is however not clear why lack of TnpA abolished not only the formation of transposants or co-integrate transformants, but also that of transient plasmid transformants. Finally, the requirement for a transient circular cytoplasmic intermediate, and not a

linear as previously suggested[118], was further supported by the lack of colony growth with linear Tn*1*-vector as donor DNA. DNA that enters the bacterial cytoplasm in the course of natural transformation is however linear and single-stranded[108], but double-stranded plasmid DNA reassembles efficiently when dimeric plasmid strands are present intracellularly[323]. The genomic integration of transforming DNA by recombination with the chromosome[113,324,325] or plasmid reconstitution[326] is impacted by cytoplasmic proteins that act on DNA single-strands (RecA, DprA, RecO) or degrade DNA double-strands (RecBCD). We inferred the role of these host factors in the circularization of cytoplasmic Tn*1*-vector DNA from plasmid transformation frequencies in *A. baylyi* deletion mutants. We found that RecA-mediated homology search and DprA-mediated loading of RecA on ssDNA are processes that facilitated plasmid transformation to a greater degree than RecO-mediated hybridization of complementary ssDNA strands did. According to our model, a dimeric ssDNA strand with overlapping ends, and a complementary strand-fragment, are minimum requirements for plasmid reconstitution with involvement of the above-mentioned enzymes. Lack of RecBCD increased plasmid transformation efficiencies, which implied that plasmid circularization in *A. baylyi* involved RecBCD-sensitive linear dsDNA intermediates. Building up on our results, also larger fragments of transforming chromosomal DNA could circularize at repeat regions or be protected from RecBCD degradation by Chi sequences[327], and facilitate transient transposon-gene expression in the course of natural transformation. Generally, one should keep in mind that chromosomally inserted resistance may confer lower resistance levels than plasmid-associated genes[126,328], and selection pressures for transposition events may have to be adjusted.

Dynamics of transposition events

Transposon-insertion can disrupt genes that are essential for viability, and have further metabolic effects for example on host fitness[170]. In **paper II**, Tn*1*-transposition did not occur into essential genes of *A. baylyi* but revealed a clear preference for the replication terminus. Interestingly, this resembled the pattern of Tn*917*-transposition into the chromosome of the G+ species *E. faecalis*[329] and *B. subtilis*[152] from a temperature-sensitive plasmid. It was demonstrated, that the activity of proteins that mediate DNA replication fork termination or chromosome separation attracted Tn*917*-transposition into the *B. subtilis* terminus[152]. Unexpectedly, lack of the XerC-recombinase, which resolves chromosome dimers in *A. baylyi*, abolished transformant growth (**paper II**). In conclusion, we cannot exclude that local DNA repair or replication dynamics represent mechanistic requirements of Tn*1*-transposition that underlie the observed transposon insertion in proximity to the *A. baylyi* terminus, since host replication factors are required during replicative transposition[147]. This

hypothesis is further supported by the lack of correlation between the prevalence of consensus sequence in the recipient chromosome and Tn*1*-insertion around the terminus (**paper II**).

The fitness of *A. baylyi* transposants was not investigated in **paper II**. In previous reports, transposon acquisition had variable outcomes, including beneficial[160], neutral or negative[118,161] effects of different elements. The different transposants obtained in **paper II** could be used in the future to compare fitness-consequences of Tn*1*-acquisition into the terminus region versus other chromosomal loci, and it remains to be tested whether transposition from our Tn*1*-vector is attracted to the terminus of other naturally competent bacterial species.

Potential of transposon spread by transposition during natural transformation

Although we confirm that transposition-mediated natural transformation contributes to the horizontal transfer of resistance at lower frequencies than other HGT mechanisms (10^{-9} **paper II;** < 10^{-8} [118]), it has the potential to facilitate MDR dissemination across species borders. Subsequently, transposon-associated resistance can spread more efficiently between related species. This can for example occur by the intermolecular movement of the chromosome-located transposon to a plasmid and between plasmids, which represents a relevant mean of transposon-associated MDR spread in hospital settings[97,126,330]. Furthermore, once chromosomally acquired, transposons can promote the spread of their embedded resistance determinants via homologous recombination-mediated natural transformation. The latter possibility is exemplified by the 1,000-times increased (now 10^{-4} to 10^{-5}) intraspecies transfer of a Tn*21*-embedded integron during natural transformation with donor DNA from an *A. baylyi* Tn*21*-transposant *in vitro*[118].

A possible effect of altered transposon activity on the frequency of transposition during natural transformation could be investigated based on reports of transposition 'triggers' such as nutritional starvation in *E. coli*[331] or antibiotic-induced SOS-response and its consequences on integrase activity[332]. It would be interesting to use our Tn*1*-vector and test the potential for transposition-mediated natural transformation in a plasmid-carrying strain as recipient, since it was previously observed that Tn*3*-transposition between plasmid replicons occurred more frequent than between plasmid and chromosome[333].

Conclusion

The presented thesis examined the dynamics of bacterial antibiotic resistance evolution by chromosomal (**paper I**) as well as mobile resistance determinants (**paper II, III**).

In **paper I**, the evolution of conserved collateral responses across resistant mutants of diverse *E. coli* isolates was demonstrated for the first time. Collateral changes were primarily driven by efflux-mutations, and resistance mechanism may hence be a useful predictor of bacterial collateral responses during evolution-informed treatment. Furthermore, transposons mobilized antibiotic resistance during natural transformation of *A. baylyi* (**paper II**). Future research can build up on our model of transposition-mediated natural transformation to explore molecular requirements and insertion dynamics of other transposons in different bacterial hosts. Finally, *E. coli* accidentally became a better plasmid-host by adapting to a new environmental niche **(paper III)**. This finding advanced plasmid paradox research in clinical pathogens and represented a novel explanation for the persistence of plasmids in bacterial populations.

References

1. Sender, R., Fuchs, S. & Milo, R. Revised Estimates for the Number of Human and Bacteria Cells in the Body. *PLoS Biol* **14**, e1002533 (2016).
2. Wright, P. M., Seiple, I. B. & Myers, A. G. The evolving role of chemical synthesis in antibacterial drug discovery. *Angew Chem Int Ed Engl* **53**, 8840-8869 (2014).
3. Fleming, A. On the Antibacterial Action of Cultures of a Penicillium, with Special Reference to their Use in the Isolation of *B. influenzæ*. *Br J Exp Pathol* **10**, 226-236 (1929).
4. Abraham, E. P. & Chain, E. An Enzyme from Bacteria able to Destroy Penicillin. *Nature* **146**, 837-837 (1940).
5. Sir Alexander Fleming – Nobel Lecture 1945. *NobelPrize.org. Nobel Media AB 2021*, Available from https://www.nobelprize.org/prizes/medicine/1945/fleming/speech/ (Wed. 17 Mar 2021).
6. 2019 Antibacterial agents in clinical development: an analysis of the antibacterial clinical development pipeline. *Geneva: World Health Organization* (2019).
7. Cassini, A. *et al.* Attributable deaths and disability-adjusted life-years caused by infections with antibiotic-resistant bacteria in the EU and the European Economic Area in 2015: a population-level modelling analysis. *Lancet Infect Dis* **19**, 56-66 (2019).
8. Adeolu, M., Alnajar, S., Naushad, S. & R, S. G. Genome-based phylogeny and taxonomy of the '*Enterobacteriales*': proposal for *Enterobacterales* ord. nov. divided into the families *Enterobacteriaceae*, *Erwiniaceae* fam. nov., *Pectobacteriaceae* fam. nov., *Yersiniaceae* fam. nov., *Hafniaceae* fam. nov., *Morganellaceae* fam. nov., and *Budviciaceae* fam. nov. *International journal of systematic and evolutionary microbiology* **66**, 5575-5599 (2016).
9. Organization, W. H. Global Priority List of Antibiotic-Resistant Bacteria to Guide Research, Discovery, and Development of New Antibiotics. *WHO Press*, p. 1-7 (2017).
10. Antimicrobial resistance in the EU/EEA (EARS-Net) *Annual Epidemiological Report for 2019* (2019).
11. Carattoli, A. Plasmids and the spread of resistance. *Int J Med Microbiol* **303**, 298-304 (2013).
12. Mathers, A. J., Peirano, G. & Pitout, J. D. The role of epidemic resistance plasmids and international high-risk clones in the spread of multidrug-resistant *Enterobacteriaceae*. *Clinical microbiology reviews* **28**, 565-591 (2015).
13. Temkin, E. *et al.* Estimating the number of infections caused by antibiotic-resistant *Escherichia coli* and *Klebsiella pneumoniae* in 2014: a modelling study. *Lancet Glob Health* **6**, e969-e979 (2018).
14. Holmes, A. H. *et al.* Understanding the mechanisms and drivers of antimicrobial resistance. *Lancet* **387**, 176-187 (2016).
15. van Hoek, A. H. *et al.* Acquired antibiotic resistance genes: an overview. *Frontiers in microbiology* **2**, 203 (2011).
16. Blair, J. M., Webber, M. A., Baylay, A. J., Ogbolu, D. O. & Piddock, L. J. Molecular mechanisms of antibiotic resistance. *Nature reviews. Microbiology* **13**, 42-51 (2015).
17. Witzany, C., Bonhoeffer, S. & Rolff, J. Is antimicrobial resistance evolution accelerating? *PLoS pathogens* **16**, e1008905 (2020).
18. Hughes, D. & Andersson, D. I. Evolutionary Trajectories to Antibiotic Resistance. *Annual review of microbiology* **71**, 579-596 (2017).
19. Andersson, D. I. *et al.* Antibiotic resistance: turning evolutionary principles into clinical reality. *FEMS microbiology reviews* **44**, 171-188 (2020).
20. Johnsen, P. J. *et al.* Factors affecting the reversal of antimicrobial-drug resistance. *Lancet Infect Dis* **9**, 357-364 (2009).
21. Domagk, G. Ein Beitrag zur Chemotherapie der bakteriellen Infektionen. *Dtsch. Med. Wochenschr.* **61 (7)**, 250-253 (1935).

22. Waksman, S. A., Schatz, A. & Reynolds, D. M. Production of antibiotic substances by actinomycetes. *Ann N Y Acad Sci* **1213**, 112-124 (2010).
23. Andrade, F. F., Silva, D., Rodrigues, A. & Pina-Vaz, C. Colistin Update on Its Mechanism of Action and Resistance, Present and Future Challenges. *Microorganisms* **8** (2020).
24. Butler, M. S. & Paterson, D. L. Antibiotics in the clinical pipeline in October 2019. *J Antibiot (Tokyo)* **73**, 329-364 (2020).
25. Ling, L. L. *et al.* A new antibiotic kills pathogens without detectable resistance. *Nature* **517**, 455-459 (2015).
26. Hover, B. M. *et al.* Culture-independent discovery of the malacidins as calcium-dependent antibiotics with activity against multidrug-resistant Gram-positive pathogens. *Nat Microbiol* **3**, 415-422 (2018).
27. Egan, A. J., Biboy, J., van't Veer, I., Breukink, E. & Vollmer, W. Activities and regulation of peptidoglycan synthases. *Philos Trans R Soc Lond B Biol Sci* **370** (2015).
28. Dijkmans, A. C. *et al.* Fosfomycin: Pharmacological, Clinical and Future Perspectives. *Antibiotics* **6** (2017).
29. Kohanski, M. A., Dwyer, D. J. & Collins, J. J. How antibiotics kill bacteria: from targets to networks. *Nature reviews. Microbiology* **8**, 423-435 (2010).
30. Drlica, K., Malik, M., Kerns, R. J. & Zhao, X. Quinolone-mediated bacterial death. *Antimicrobial agents and chemotherapy* **52**, 385-392 (2008).
31. Huovinen, P. Resistance to trimethoprim-sulfamethoxazole. *Clinical Infectious Diseases* **32**, 1608-1614 (2001).
32. Asnis, R. E. The reduction of Furacin by cell-free extracts of Furacin-resistant and parent-susceptible strains of *Escherichia coli*. *Arch Biochem Biophys* **66**, 208-216 (1957).
33. McCalla, D. R., Kaiser, C. & Green, M. H. Genetics of nitrofurazone resistance in *Escherichia coli*. *Journal of bacteriology* **133**, 10-16 (1978).
34. Jenkins, S. T. & Bennett, P. M. Effect of mutations in deoxyribonucleic acid repair pathways on the sensitivity of *Escherichia coli* K-12 strains to nitrofurantoin. *Journal of bacteriology* **125**, 1214-1216 (1976).
35. Davies, J. & Davies, D. Origins and evolution of antibiotic resistance. *Microbiol Mol Biol Rev* **74**, 417-433 (2010).
36. Redgrave, L. S., Sutton, S. B., Webber, M. A. & Piddock, L. J. Fluoroquinolone resistance: mechanisms, impact on bacteria, and role in evolutionary success. *Trends in microbiology* **22**, 438-445 (2014).
37. Touchon, M. *et al.* The genomic diversification of the whole *Acinetobacter* genus: origins, mechanisms, and consequences. *Genome Biol Evol* **6**, 2866-2882 (2014).
38. Juhas, M. Horizontal gene transfer in human pathogens. *Crit Rev Microbiol* **41**, 101-108 (2015).
39. Lerminiaux, N. A. & Cameron, A. D. S. Horizontal transfer of antibiotic resistance genes in clinical environments. *Can J Microbiol* **65**, 34-44 (2019).
40. D'Costa, V. M. *et al.* Antibiotic resistance is ancient. *Nature* **477**, 457-461 (2011).
41. D'Costa, V. M., McGrann, K. M., Hughes, D. W. & Wright, G. D. Sampling the antibiotic resistome. *Science* **311**, 374-377 (2006).
42. Cox, G. & Wright, G. D. Intrinsic antibiotic resistance: mechanisms, origins, challenges and solutions. *Int J Med Microbiol* **303**, 287-292 (2013).
43. The European Committee on Antimicrobial Susceptibility Testing - EUCAST. Intrinsic resistance and unusual phenotypes version 3.2. Available from http://www.eucast.org/expert_rules_and_intrinsic_resistance/ (2019).
44. Kahlmeter, G. The 2014 Garrod Lecture: EUCAST - are we heading towards international agreement? *J Antimicrob Chemother* **70**, 2427-2439 (2015).

45. The European Committee on Antimicrobial Susceptibility Testing - EUCAST. Breakpoint tables for interpretation of MICs and zone diameters, version 10.0. Available from https://www.eucast.org/clinical_breakpoints/ (2020).
46. The European Committee on Antimicrobial Susceptibility Testing (EUCAST). https://www.eucast.org.
47. Clinical and Laboratory Standards Institute (CLSI). https://www.fda.gov/drugs/development-resources/antibacterial-susceptibility-test-interpretive-criteria.
48. Drlica, K. & Zhao, X. Mutant selection window hypothesis updated. *Clinical Infectious Diseases* **44**, 681-688 (2007).
49. Lozano-Huntelman, N. A. *et al.* Evolution of antibiotic cross-resistance and collateral sensitivity in *Staphylococcus epidermidis* using the mutant prevention concentration and the mutant selection window. *Evol Appl* **13**, 808-823 (2020).
50. Gullberg, E. *et al.* Selection of resistant bacteria at very low antibiotic concentrations. *PLoS pathogens* **7**, e1002158 (2011).
51. Gullberg, E., Albrecht, L. M., Karlsson, C., Sandegren, L. & Andersson, D. I. Selection of a multidrug resistance plasmid by sublethal levels of antibiotics and heavy metals. *mBio* **5**, e01918-01914 (2014).
52. Andersson, D. I. & Hughes, D. Microbiological effects of sublethal levels of antibiotics. *Nature reviews. Microbiology* **12**, 465-478 (2014).
53. Walsh, C. Molecular mechanisms that confer antibacterial drug resistance. *Nature* **406**, 775-781 (2000).
54. Yoshida, H., Bogaki, M., Nakamura, M. & Nakamura, S. Quinolone resistance-determining region in the DNA gyrase *gyrA* gene of *Escherichia coli*. *Antimicrobial agents and chemotherapy* **34**, 1271-1272 (1990).
55. Heisig, P. & Tschorny, R. Characterization of fluoroquinolone-resistant mutants of *Escherichia coli* selected in vitro. *Antimicrobial agents and chemotherapy* **38**, 1284-1291 (1994).
56. Marcusson, L. L., Frimodt-Moller, N. & Hughes, D. Interplay in the selection of fluoroquinolone resistance and bacterial fitness. *PLoS pathogens* **5**, e1000541 (2009).
57. Komp Lindgren, P., Karlsson, A. & Hughes, D. Mutation rate and evolution of fluoroquinolone resistance in *Escherichia coli* isolates from patients with urinary tract infections. *Antimicrobial agents and chemotherapy* **47**, 3222-3232 (2003).
58. Huseby, D. L. *et al.* Mutation Supply and Relative Fitness Shape the Genotypes of Ciprofloxacin-Resistant *Escherichia coli*. *Mol Biol Evol* **34**, 1029-1039 (2017).
59. Pietsch, F. *et al.* Ciprofloxacin selects for RNA polymerase mutations with pleiotropic antibiotic resistance effects. *J Antimicrob Chemother* **72**, 75-84 (2017).
60. Yoshida, H., Bogaki, M., Nakamura, M., Yamanaka, L. M. & Nakamura, S. Quinolone resistance-determining region in the DNA gyrase *gyrB* gene of *Escherichia coli*. *Antimicrobial agents and chemotherapy* **35**, 1647-1650 (1991).
61. Wang, H., Dzink-Fox, J. L., Chen, M. & Levy, S. B. Genetic characterization of highly fluoroquinolone-resistant clinical *Escherichia coli* strains from China: role of *acrR* mutations. *Antimicrobial agents and chemotherapy* **45**, 1515-1521 (2001).
62. Duval, V. & Lister, I. M. MarA, SoxS and Rob of *Escherichia coli* - Global regulators of multidrug resistance, virulence and stress response. *Int J Biotechnol Wellness Ind* **2**, 101-124 (2013).
63. Oethinger, M., Podglajen, I., Kern, W. V. & Levy, S. B. Overexpression of the marA or soxS regulatory gene in clinical topoisomerase mutants of *Escherichia coli*. *Antimicrobial agents and chemotherapy* **42**, 2089-2094 (1998).
64. Cohen, S. P., McMurry, L. M. & Levy, S. B. marA locus causes decreased expression of OmpF porin in multiple-antibiotic-resistant (Mar) mutants of *Escherichia coli*. *Journal of bacteriology* **170**, 5416-5422 (1988).

65. Forst, S., Delgado, J. & Inouye, M. Phosphorylation of OmpR by the osmosensor EnvZ modulates expression of the ompF and ompC genes in *Escherichia coli*. *Proc Natl Acad Sci U S A* **86**, 6052-6056 (1989).
66. Thulin, E., Sundqvist, M. & Andersson, D. I. Amdinocillin (Mecillinam) resistance mutations in clinical isolates and laboratory-selected mutants of *Escherichia coli*. *Antimicrobial agents and chemotherapy* **59**, 1718-1727 (2015).
67. Thulin, E. & Andersson, D. I. Upregulation of PBP1B and LpoB in cysB Mutants Confers Mecillinam (Amdinocillin) Resistance in *Escherichia coli*. *Antimicrobial agents and chemotherapy* **63**, e00612-00619 (2019).
68. Kahlmeter, G. & Poulsen, H. O. Antimicrobial susceptibility of *Escherichia coli* from community-acquired urinary tract infections in Europe: the ECO.SENS study revisited. *Int J Antimicrob Agents* **39**, 45-51 (2012).
69. Lai, G. C., Cho, H. & Bernhardt, T. G. The mecillinam resistome reveals a role for peptidoglycan endopeptidases in stimulating cell wall synthesis in *Escherichia coli*. *PLoS Genet* **13**, e1006934 (2017).
70. Thulin, E. *Mechanisms and Dynamics of Mecillinam Resistance in Escherichia coli* ISBN 978-91-513-0090-0 thesis, Acta Universitatis Upsaliensis, Uppsala (2017).
71. Chevereau, G. *et al.* Quantifying the Determinants of Evolutionary Dynamics Leading to Drug Resistance. *PLoS Biol* **13**, e1002299 (2015).
72. Sandegren, L., Lindqvist, A., Kahlmeter, G. & Andersson, D. I. Nitrofurantoin resistance mechanism and fitness cost in *Escherichia coli*. *J Antimicrob Chemother* **62**, 495-503 (2008).
73. Puertolas-Balint, F., Warsi, O., Linkevicius, M., Tang, P. C. & Andersson, D. I. Mutations that increase expression of the EmrAB-TolC efflux pump confer increased resistance to nitroxoline in *Escherichia coli*. *J Antimicrob Chemother* **75**, 300-308 (2020).
74. Toprak, E. *et al.* Evolutionary paths to antibiotic resistance under dynamically sustained drug selection. *Nat Genet* **44**, 101-105 (2011).
75. Baym, M. *et al.* Spatiotemporal microbial evolution on antibiotic landscapes. *Science* **353**, 1147-1151 (2016).
76. Watson, M., Liu, J. W. & Ollis, D. Directed evolution of trimethoprim resistance in *Escherichia coli*. *FEBS J* **274**, 2661-2671 (2007).
77. Flensburg, J. & Sköld, O. Massive overproduction of dihydrofolate reductase in bacteria as a response to the use of trimethoprim. *Eur J Biochem* **162**, 473-476 (1987).
78. Bush, K. Past and Present Perspectives on beta-Lactamases. *Antimicrobial agents and chemotherapy* **62** (2018).
79. Knott-Hunziker, V., Waley, S. G., Orlek, B. S. & Sammes, P. G. Penicillinase active sites: Labelling of serine-44 in β-lactamase I by 6β-bromopenicillanic acid. *FEBS Letters* **99**, 59-61 (1979).
80. King, D. T., Worrall, L. J., Gruninger, R. & Strynadka, N. C. New Delhi metallo-beta-lactamase: structural insights into beta-lactam recognition and inhibition. *J Am Chem Soc* **134**, 11362-11365 (2012).
81. Ambler, R. P. The structure of beta-lactamases. *Philos. Trans. R. Soc. Lond.* **289**, pp. 321-331 (1980).
82. Bush, K. & Jacoby, G. A. Updated functional classification of beta-lactamases. *Antimicrobial agents and chemotherapy* **54**, 969-976 (2010).
83. Logan, L. K. & Weinstein, R. A. The Epidemiology of Carbapenem-Resistant *Enterobacteriaceae*: The Impact and Evolution of a Global Menace. *J Infect Dis* **215**, S28-S36 (2017).
84. Lauretti, L. *et al.* Cloning and characterization of bla_{VIM}, a new integron-borne metallo-beta-lactamase gene from a *Pseudomonas aeruginosa* clinical isolate. *Antimicrobial agents and chemotherapy* **43**, 1584-1590 (1999).

85. Yong, D. *et al.* Characterization of a new metallo-beta-lactamase gene, *bla*$_{NDM-1}$, and a novel erythromycin esterase gene carried on a unique genetic structure in *Klebsiella pneumoniae* sequence type 14 from India. *Antimicrobial agents and chemotherapy* **53**, 5046-5054 (2009).
86. Rozwandowicz, M. *et al.* Plasmids carrying antimicrobial resistance genes in *Enterobacteriaceae*. *J Antimicrob Chemother* **73**, 1121-1137 (2018).
87. Wu, W. *et al.* NDM Metallo-β-Lactamases and Their Bacterial Producers in Health Care Settings. *Clinical microbiology reviews* **32**, e00115-00118 (2019).
88. Tzouvelekis, L. S., Markogiannakis, A., Psichogiou, M., Tassios, P. T. & Daikos, G. L. Carbapenemases in *Klebsiella pneumoniae* and other *Enterobacteriaceae*: an evolving crisis of global dimensions. *Clinical microbiology reviews* **25**, 682-707 (2012).
89. von Wintersdorff, C. J. *et al.* Dissemination of Antimicrobial Resistance in Microbial Ecosystems through Horizontal Gene Transfer. *Frontiers in microbiology* **7**, 173 (2016).
90. Weingarten, R. A. *et al.* Genomic Analysis of Hospital Plumbing Reveals Diverse Reservoir of Bacterial Plasmids Conferring Carbapenem Resistance. *mBio* **9**, e02011-02017 (2018).
91. Thomas, C. M. & Nielsen, K. M. Mechanisms of, and barriers to, horizontal gene transfer between bacteria. *Nature reviews. Microbiology* **3**, 711-721 (2005).
92. Frost, L. S., Leplae, R., Summers, A. O. & Toussaint, A. Mobile genetic elements: the agents of open source evolution. *Nature reviews. Microbiology* **3**, 722-732 (2005).
93. Mazaheri Nezhad Fard, R., Barton, M. D. & Heuzenroeder, M. W. Bacteriophage-mediated transduction of antibiotic resistance in enterococci. *Letters in applied microbiology* **52**, 559-564 (2011).
94. Varga, M. *et al.* Efficient transfer of antibiotic resistance plasmids by transduction within methicillin-resistant *Staphylococcus aureus* USA300 clone. *FEMS Microbiol Lett* **332**, 146-152 (2012).
95. Partridge, S. R., Kwong, S. M., Firth, N. & Jensen, S. O. Mobile Genetic Elements Associated with Antimicrobial Resistance. *Clinical microbiology reviews* **31**, e00088-00017 (2018).
96. Sandegren, L., Linkevicius, M., Lytsy, B., Melhus, A. & Andersson, D. I. Transfer of an *Escherichia coli* ST131 multiresistance cassette has created a *Klebsiella pneumoniae*-specific plasmid associated with a major nosocomial outbreak. *J Antimicrob Chemother* **67**, 74-83 (2012).
97. Sheppard, A. E. *et al.* Nested Russian Doll-Like Genetic Mobility Drives Rapid Dissemination of the Carbapenem Resistance Gene *bla*$_{KPC}$. *Antimicrobial agents and chemotherapy* **60**, 3767-3778 (2016).
98. Domingues, S. & Nielsen, K. M. Membrane vesicles and horizontal gene transfer in prokaryotes. *Current opinion in microbiology* **38**, 16-21 (2017).
99. Dubey, G. P. *et al.* Architecture and Characteristics of Bacterial Nanotubes. *Dev Cell* **36**, 453-461 (2016).
100. Fulsundar, S. *et al.* Gene transfer potential of outer membrane vesicles of *Acinetobacter baylyi* and effects of stress on vesiculation. *Applied and environmental microbiology* **80**, 3469-3483 (2014).
101. Pospisil, J. *et al.* Bacterial nanotubes as a manifestation of cell death. *Nat Commun* **11**, 4963 (2020).
102. Griffith, F. The Significance of Pneumococcal Types. *The Journal of hygiene* **27**, 113-159 (1928).
103. Blokesch, M. Natural competence for transformation. *Current Biology* **26**, R1126-R1130 (2016).
104. Johnston, C., Martin, B., Fichant, G., Polard, P. & Claverys, J. P. Bacterial transformation: distribution, shared mechanisms and divergent control. *Nature reviews. Microbiology* **12**, 181-196 (2014).
105. Lorenz, M. G. & Wackernagel, W. Bacterial gene transfer by natural genetic transformation in the environment. *Microbiological reviews* **58**, 563-602 (1994).

106. Domingues, S. *et al.* Competence for Natural Transformation Is Common among Clinical Strains of Resistant *Acinetobacter* spp. *Microorganisms* **7** (2019).
107. Hu, Y., He, L., Tao, X., Meng, F. & Zhang, J. High DNA Uptake Capacity of International Clone II *Acinetobacter baumannii* Detected by a Novel Planktonic Natural Transformation Assay. *Frontiers in microbiology* **10**, 2165 (2019).
108. Dubnau, D. & Blokesch, M. Mechanisms of DNA Uptake by Naturally Competent Bacteria. *Annual review of genetics* **53**, 217-237 (2019).
109. Averhoff, B. & Graf, I. in *Acinetobacter Molecular Biology* (edited by Ulrike Gerischer), Ch. The Natural Transformation System of Acinetobacter baylyi ADP1: A Unique DNA Transport Machinery, 119 (Caister Academic Press, U.K, 2008).
110. Palmen, R., Vosman, B., Buijsman, P., Breek, C. K. & Hellingwerf, K. J. Physiological characterization of natural transformation in *Acinetobacter calcoaceticus*. *Journal of general microbiology* **139**, 295-305 (1993).
111. Mortier-Barriere, I. *et al.* A key presynaptic role in transformation for a widespread bacterial protein: DprA conveys incoming ssDNA to RecA. *Cell* **130**, 824-836 (2007).
112. Nielsen, K. M., Johnsen, P. J., Bensasson, D. & Daffonchio, D. Release and persistence of extracellular DNA in the environment. *Environmental biosafety research* **6**, 37-53 (2007).
113. Hulter, N. *et al.* Costs and benefits of natural transformation in *Acinetobacter baylyi*. *BMC Microbiol* **17**, 34 (2017).
114. Overballe-Petersen, S. *et al.* Bacterial natural transformation by highly fragmented and damaged DNA. *Proc Natl Acad Sci U S A* **110**, 19860-19865 (2013).
115. de Vries, J. & Wackernagel, W. Integration of foreign DNA during natural transformation of *Acinetobacter* sp. by homology-facilitated illegitimate recombination. *Proc Natl Acad Sci U S A* **99**, 2094-2099 (2002).
116. Hulter, N. & Wackernagel, W. Double illegitimate recombination events integrate DNA segments through two different mechanisms during natural transformation of *Acinetobacter baylyi. Molecular microbiology* **67**, 984-995 (2008).
117. Harms, K. *et al.* Substitutions of short heterologous DNA segments of intragenomic or extragenomic origins produce clustered genomic polymorphisms. *Proc Natl Acad Sci U S A* **113**, 15066-15071 (2016).
118. Domingues, S. *et al.* Natural transformation facilitates transfer of transposons, integrons and gene cassettes between bacterial species. *PLoS pathogens* **8**, e1002837 (2012).
119. Norman, A., Hansen, L. H. & Sorensen, S. J. Conjugative plasmids: vessels of the communal gene pool. *Philos Trans R Soc Lond B Biol Sci* **364**, 2275-2289 (2009).
120. del Solar, G., Giraldo, R., Ruiz-Echevarria, M. J., Espinosa, M. & Diaz-Orejas, R. Replication and control of circular bacterial plasmids. *Microbiol Mol Biol Rev* **62**, 434-464 (1998).
121. Carattoli, A. *et al.* Identification of plasmids by PCR-based replicon typing. *Journal of microbiological methods* **63**, 219-228 (2005).
122. Carattoli, A. *et al.* In silico detection and typing of plasmids using PlasmidFinder and plasmid multilocus sequence typing. *Antimicrobial agents and chemotherapy* **58**, 3895-3903 (2014).
123. Datta, N. & Hughes, V. M. Plasmids of the Same Inc Groups in *Enterobacteria* before and after the Medical Use of Antibiotics. *Nature* **306**, 616-617 (1983).
124. Shintani, M., Sanchez, Z. K. & Kimbara, K. Genomics of microbial plasmids: classification and identification based on replication and transfer systems and host taxonomy. *Frontiers in microbiology* **6**, 242 (2015).
125. Barlow, M. & Hall, B. G. Phylogenetic analysis shows that the OXA beta-lactamase genes have been on plasmids for millions of years. *J Mol Evol* **55**, 314-321 (2002).
126. Brolund, A. *et al.* Dynamics of Resistance Plasmids in Extended-Spectrum-beta-Lactamase-Producing *Enterobacteriaceae* during Postinfection Colonization. *Antimicrobial agents and chemotherapy* **63**, e02201-02218 (2019).

127. Drieux, L. *et al.* Complete nucleotide sequence of the large conjugative pTC2 multireplicon plasmid encoding the VIM-1 metallo-beta-lactamase. *J Antimicrob Chemother* **68**, 97-100 (2013).
128. Gama, J. A., Kloos, J., Johnsen, P. J. & Samuelsen, O. Host dependent maintenance of a *bla*$_{NDM-1}$-encoding plasmid in clinical *Escherichia coli* isolates. *Sci Rep* **10**, 9332 (2020).
129. Samuelsen, O. *et al.* Molecular characterization of VIM-producing *Klebsiella pneumoniae* from Scandinavia reveals genetic relatedness with international clonal complexes encoding transferable multidrug resistance. *Clin Microbiol Infect* **17**, 1811-1816 (2011).
130. Di Luca, M. C. *et al.* Low biological cost of carbapenemase-encoding plasmids following transfer from *Klebsiella pneumoniae* to *Escherichia coli*. *J Antimicrob Chemother* **72**, 85-89 (2017).
131. Papagiannitsis, C. C., Miriagou, V., Giakkoupi, P., Tzouvelekis, L. S. & Vatopoulos, A. C. Characterization of pKP1780, a novel IncR plasmid from the emerging *Klebsiella pneumoniae* ST147, encoding the VIM-1 metallo-beta-lactamase. *J Antimicrob Chemother* **68**, 2259-2262 (2013).
132. Samuelsen, O. *et al.* Identification of NDM-1-producing *Enterobacteriaceae* in Norway. *J Antimicrob Chemother* **66**, 670-672 (2011).
133. Roberts, A. P. *et al.* Revised nomenclature for transposable genetic elements. *Plasmid* **60**, 167-173 (2008).
134. Hickman, A. B. & Dyda, F. Mechanisms of DNA Transposition. *Microbiol Spectr* **3**, MDNA3-0034-2014 (2015).
135. McClintock, B. The Origins And Behaviour Of Mutable Loci In Maize. *Proc Natl Acad Sci* **36**, 344-355 (1950).
136. Press release. *NobelPrize.org. Nobel Media AB 2021*, Available from https://www.nobelprize.org/prizes/medicine/1983/press-release/ (Thu. 18 Mar 2021).
137. Jacob, A. & Hedges, R. Transposition of Ampicillin Resistance from RP4 to Other Replicons. *Molec. gen. Genet.* **132**, 31-40 (1974).
138. Tansirichaiya, S., Rahman, M. A. & Roberts, A. P. The Transposon Registry. *Mob DNA* **10**, 40 (2019).
139. Martinez, T., Vazquez, G. J., Aquino, E. E., Martinez, I. & Robledo, I. E. IS*Ecp1*-mediated transposition of *bla*$_{KPC}$ into the chromosome of a clinical isolate of *Acinetobacter baumannii* from Puerto Rico. *J Med Microbiol* **63**, 1644-1648 (2014).
140. Siguier, P., Perochon, J., Lestrade, L., Mahillon, J. & Chandler, M. ISfinder: the reference centre for bacterial insertion sequences. *Nucleic acids research* **34**, D32-36 (2006).
141. Gillings, M. R. Integrons: past, present, and future. *Microbiol Mol Biol Rev* **78**, 257-277 (2014).
142. Partridge, S. R. & Hall, R. M. Evolution of transposons containing *bla*$_{TEM}$ genes. *Antimicrobial agents and chemotherapy* **49**, 1267-1268 (2005).
143. Naas, T. *et al.* Genetic structures at the origin of acquisition of the beta-lactamase *bla*$_{KPC}$ gene. *Antimicrobial agents and chemotherapy* **52**, 1257-1263 (2008).
144. Liebert, C. A., Hall, R. M. & Summers, A. O. Transposon Tn*21*, flagship of the floating genome. *Microbiol Mol Biol Rev* **63**, 507-522 (1999).
145. Gill, R. E., Heffron, F. & Falkow, S. Identification of the protein encoded by the transposable element Tn*3* which is required for its transposition. *Nature* **282**, 797-801 (1979).
146. Kostriken, R., Morita, C. & Heffron, F. Transposon Tn*3* encodes a site-specific recombination system: identification of essential sequences, genes, and actual site of recombination. *Proc Natl Acad Sci U S A* **78**, 4041-4045 (1981).
147. Nicolas, E. *et al.* The Tn*3*-family of Replicative Transposons. *Microbiol Spectr* **3**, MDNA3-0060-2014 (2015).
148. Partridge, S. R. Analysis of antibiotic resistance regions in Gram-negative bacteria. *FEMS microbiology reviews* **35**, 820-855 (2011).

149. Shapiro, J. A. Molecular model for the transposition and replication of bacteriophage Mu and other transposable elements. *Proc Natl Acad Sci U S A* **76**, 1933-1937 (1979).
150. Seringhaus, M., Kumar, A., Hartigan, J., Snyder, M. & Gerstein, M. Genomic analysis of insertion behavior and target specificity of mini-Tn*7* and Tn*3* transposons in *Saccharomyces cerevisiae*. *Nucleic acids research* **34**, e57 (2006).
151. Davies, C. J. & Hutchison, C. A., 3rd. Insertion site specificity of the transposon Tn*3*. *Nucleic acids research* **23**, 507-514 (1995).
152. Garsin, D. A., Urbach, J., Huguet-Tapia, J. C., Peters, J. E. & Ausubel, F. M. Construction of an *Enterococcus faecalis* Tn*917*-mediated-gene-disruption library offers insight into Tn*917* insertion patterns. *Journal of bacteriology* **186**, 7280-7289 (2004).
153. Arthur, A., Nimmo, E., Hettle, S. & Sherratt, D. Transposition and Transposition Immunity of Transposon Tn*3* Derivatives Having Different Ends. *Embo Journal* **3**, 1723-1729 (1984).
154. Cuzon, G., Naas, T. & Nordmann, P. Functional characterization of Tn*4401*, a Tn*3*-based transposon involved in bla_{KPC} gene mobilization. *Antimicrobial agents and chemotherapy* **55**, 5370-5373 (2011).
155. Arthur, A. & Sherratt, D. Dissection of the transposition process: a transposon-encoded site-specific recombination system. *Mol Gen Genet* **175**, 267-274 (1979).
156. DelaFuente, J., Rodriguez-Beltran, J. & San Millan, A. Methods to Study Fitness and Compensatory Adaptation in Plasmid-Carrying Bacteria. *Methods Mol Biol* **2075**, 371-382 (2020).
157. Lenski, R. E., Rose, M. R., Simpson, S. C. & Tadler, S. C. Long-Term Experimental Evolution in *Escherichia coli*. I. Adaptation and Divergence During 2,000 Generations. *The American Naturalist* **138**, 1315-1341 (1991).
158. Melnyk, A. H., Wong, A. & Kassen, R. The fitness costs of antibiotic resistance mutations. *Evol Appl* **8**, 273-283 (2015).
159. Starikova, I. *et al.* A Trade-off between the Fitness Cost of Functional Integrases and Long-term Stability of Integrons. *PLoS pathogens* **8**, e1003043 (2012).
160. Enne, V. I. *et al.* Assessment of the fitness impacts on *Escherichia coli* of acquisition of antibiotic resistance genes encoded by different types of genetic element. *J Antimicrob Chemother* **56**, 544-551 (2005).
161. Starikova, I. *et al.* Fitness costs of various mobile genetic elements in *Enterococcus faecium* and *Enterococcus faecalis*. *J Antimicrob Chemother* **68**, 2755-2765 (2013).
162. Nagaev, I., Bjorkman, J., Andersson, D. I. & Hughes, D. Biological cost and compensatory evolution in fusidic acid-resistant *Staphylococcus aureus*. *Molecular microbiology* **40**, 433-439 (2001).
163. Bjorkman, J. & Andersson, D. I. The cost of antibiotic resistance from a bacterial perspective. *Drug Resist Updat* **3**, 237-245 (2000).
164. Apjok, G. *et al.* Limited Evolutionary Conservation of the Phenotypic Effects of Antibiotic Resistance Mutations. *Mol Biol Evol* **36**, 1601-1611 (2019).
165. Vogwill, T., Kojadinovic, M. & MacLean, R. C. Epistasis between antibiotic resistance mutations and genetic background shape the fitness effect of resistance across species of *Pseudomonas*. *Proc Biol Sci* **283** (2016).
166. San Millan, A. *et al.* Integrative analysis of fitness and metabolic effects of plasmids in *Pseudomonas aeruginosa* PAO1. *ISME J* **12**, 3014-3024 (2018).
167. Hubbard, A. T. M., Jafari, N. V., Feasey, N., Rohn, J. L. & Roberts, A. P. Effect of Environment on the Evolutionary Trajectories and Growth Characteristics of Antibiotic-Resistant *Escherichia coli* Mutants. *Frontiers in microbiology* **10**, 2001 (2019).
168. Vogwill, T. & MacLean, R. C. The genetic basis of the fitness costs of antimicrobial resistance: a meta-analysis approach. *Evol Appl* **8**, 284-295 (2015).
169. Andersson, D. I. & Levin, B. R. The biological cost of antibiotic resistance. *Current opinion in microbiology* **2**, 489-493 (1999).

170. Baltrus, D. A. Exploring the costs of horizontal gene transfer. *Trends Ecol Evol* **28**, 489-495 (2013).
171. San Millan, A. & MacLean, R. C. Fitness Costs of Plasmids: a Limit to Plasmid Transmission. *Microbiol Spectr* **5** (2017).
172. Levin, B. R. *et al.* The population genetics of antibiotic resistance. *Clinical Infectious Diseases* **24** S9-16 (1997).
173. Sander, P. *et al.* Fitness cost of chromosomal drug resistance-conferring mutations. *Antimicrobial agents and chemotherapy* **46**, 1204-1211 (2002).
174. Porse, A., Schonning, K., Munck, C. & Sommer, M. O. Survival and Evolution of a Large Multidrug Resistance Plasmid in New Clinical Bacterial Hosts. *Mol Biol Evol* **33**, 2860-2873 (2016).
175. Ingmer, H., Miller, C. & Cohen, S. N. The RepA protein of plasmid pSC101 controls *Escherichia coli* cell division through the SOS response. *Molecular microbiology* **42**, 519-526 (2001).
176. San Millan, A., Toll-Riera, M., Qi, Q. & MacLean, R. C. Interactions between horizontally acquired genes create a fitness cost in *Pseudomonas aeruginosa*. *Nat Commun* **6**, 6845 (2015).
177. Yano, H. *et al.* Evolved plasmid-host interactions reduce plasmid interference cost. *Molecular microbiology* **101**, 743-756 (2016).
178. Harrison, E., Guymer, D., Spiers, A. J., Paterson, S. & Brockhurst, M. A. Parallel compensatory evolution stabilizes plasmids across the parasitism-mutualism continuum. *Current Biology* **25**, 2034-2039 (2015).
179. Zund, P. & Lebek, G. Generation Time-Prolonging R-Plasmids: Correlation between Increases in the Generation Time of *Escherichia coli* Caused by R-Plasmids and Their Molecular-Size. *Plasmid* **3**, 65-69 (1980).
180. Rajer, F. *Multi-Resistance Plasmids : Fitness Costs, Dynamics and Evolution* ISBN 978-91-513-0708-4 thesis, Acta Universitatis Upsaliensis, Uppsala (2019).
181. Allen, R. C., Angst, D. C. & Hall, A. R. Resistance Gene Carriage Predicts Growth of Natural and Clinical *Escherichia coli* Isolates in the Absence of Antibiotics. *Applied and environmental microbiology* **85** (2019).
182. Johnsen, P. J., Simonsen, G. S., Olsvik, O., Midtvedt, T. & Sundsfjord, A. Stability, persistence, and evolution of plasmid-encoded VanA glycopeptide resistance in enterococci in the absence of antibiotic selection *in vitro* and in gnotobiotic mice. *Microb Drug Resist* **8**, 161-170 (2002).
183. Stewart, F. M. & Levin, B. R. The Population Biology of Bacterial Plasmids: A PRIORI Conditions for the Existence of Conjugationally Transmitted Factors. *Genetics* **87**, 209-228 (1977).
184. Bergstrom, C. T., Lipsitch, M. & Levin, B. R. Natural selection, infectious transfer and the existence conditions for bacterial plasmids. *Genetics* **155**, 1505-1519 (2000).
185. Harrison, E. & Brockhurst, M. A. Plasmid-mediated horizontal gene transfer is a coevolutionary process. *Trends in microbiology* **20**, 262-267 (2012).
186. Carroll, A. C. & Wong, A. Plasmid persistence: costs, benefits, and the plasmid paradox. *Can J Microbiol* **64**, 293-304 (2018).
187. Wein, T., Hülter, N. F., Mizrahi, I. & Dagan, T. Emergence of plasmid stability under non-selective conditions maintains antibiotic resistance. *Nature Communications* **10**, 2595 (2019).
188. Loftie-Eaton, W. *et al.* Evolutionary Paths That Expand Plasmid Host-Range: Implications for Spread of Antibiotic Resistance. *Mol Biol Evol* **33**, 885-897 (2016).
189. Stalder, T. *et al.* Emerging patterns of plasmid-host coevolution that stabilize antibiotic resistance. *Sci Rep* **7**, 4853 (2017).
190. Sota, M. *et al.* Shifts in the host range of a promiscuous plasmid through parallel evolution of its replication initiation protein. *ISME J* **4**, 1568-1580 (2010).

191. San Millan, A. *et al.* Positive selection and compensatory adaptation interact to stabilize non-transmissible plasmids. *Nat Commun* **5**, 5208 (2014).
192. Stevenson, C., Hall, J. P. J., Brockhurst, M. A. & Harrison, E. Plasmid stability is enhanced by higher-frequency pulses of positive selection. *Proc Biol Sci* **285** (2018).
193. Kottara, A., Hall, J. P. J., Harrison, E. & Brockhurst, M. A. Variable plasmid fitness effects and mobile genetic element dynamics across *Pseudomonas species*. *FEMS Microbiol Ecol* **94** (2018).
194. Dionisio, F., Matic, I., Radman, M., Rodrigues, O. R. & Taddei, F. Plasmids spread very fast in heterogeneous bacterial communities. *Genetics* **162**, 1525-1532 (2002).
195. Turner, P. E., Cooper, V. S. & Lenski, R. E. Tradeoff between horizontal and vertical modes of transmission in bacterial plasmids. *Evolution* **52**, 315-329 (1998).
196. Dahlberg, C. & Chao, L. Amelioration of the cost of conjugative plasmid carriage in *Eschericha coli* K12. *Genetics* **165**, 1641-1649 (2003).
197. Smillie, C., Garcillan-Barcia, M. P., Francia, M. V., Rocha, E. P. & de la Cruz, F. Mobility of plasmids. *Microbiol Mol Biol Rev* **74**, 434-452 (2010).
198. Maisnier-Patin, S. & Andersson, D. I. Adaptation to the deleterious effects of antimicrobial drug resistance mutations by compensatory evolution. *Research in microbiology* **155**, 360-369 (2004).
199. Schrag, S. J., Perrot, V. & Levin, B. R. Adaptation to the fitness costs of antibiotic resistance in *Escherichia coli*. *Proc Biol Sci* **264**, 1287-1291 (1997).
200. Reynolds, M. G. Compensatory evolution in rifampin-resistant *Escherichia coli*. *Genetics* **156**, 1471-1481 (2000).
201. Bouma, J. E. & Lenski, R. E. Evolution of a Bacteria-Plasmid Association. *Nature* **335**, 351-352 (1988).
202. De Gelder, L., Williams, J. J., Ponciano, J. M., Sota, M. & Top, E. M. Adaptive plasmid evolution results in host-range expansion of a broad-host-range plasmid. *Genetics* **178**, 2179-2190 (2008).
203. Loftie-Eaton, W. *et al.* Compensatory mutations improve general permissiveness to antibiotic resistance plasmids. *Nat Ecol Evol* **1**, 1354-1363 (2017).
204. Modi, R. I., Wilke, C. M., Rosenzweig, R. F. & Adams, J. Plasmid macro-evolution: selection of deletions during adaptation in a nutrient-limited environment. *Genetica* **84**, 195-202 (1991).
205. Buckner, M. M. C. *et al.* Clinically Relevant Plasmid-Host Interactions Indicate that Transcriptional and Not Genomic Modifications Ameliorate Fitness Costs of *Klebsiella pneumoniae* Carbapenemase-Carrying Plasmids. *mBio* **9** (2018).
206. Schaufler, K. *et al.* Carriage of Extended-Spectrum Beta-Lactamase-Plasmids Does Not Reduce Fitness but Enhances Virulence in Some Strains of Pandemic *E. coli* Lineages. *Frontiers in microbiology* **7**, 336 (2016).
207. Ma, T. *et al.* Fitness Cost of $bla_{\text{NDM-5}}$-Carrying p3R-IncX3 Plasmids in Wild-Type NDM-Free *Enterobacteriaceae*. *Microorganisms* **8** (2020).
208. Dionisio, F., Conceicao, I. C., Marques, A. C., Fernandes, L. & Gordo, I. The evolution of a conjugative plasmid and its ability to increase bacterial fitness. *Biol Lett* **1**, 250-252 (2005).
209. Lenski, R. E., Simpson, S. C. & Nguyen, T. T. Genetic analysis of a plasmid-encoded, host genotype-specific enhancement of bacterial fitness. *Journal of bacteriology* **176**, 3140-3147 (1994).
210. European Centre for Disease Prevention and Control (ECDC). Antimicrobial consumption in the EU/EEA 2019. *Annual Epidemiological Report*, Stockholm (2020).
211. Seppala, H. *et al.* The effect of changes in the consumption of macrolide antibiotics on erythromycin resistance in group A streptococci in Finland. Finnish Study Group for Antimicrobial Resistance. *N Engl J Med* **337**, 441-446 (1997).

212. Sundqvist, M. *et al.* Little evidence for reversibility of trimethoprim resistance after a drastic reduction in trimethoprim use. *J Antimicrob Chemother* **65**, 350-360 (2010).
213. Enne, V. I., Bennett, P. M., Livermore, D. M. & Hall, L. M. Enhancement of host fitness by the *sul2*-coding plasmid p9123 in the absence of selective pressure. *J Antimicrob Chemother* **53**, 958-963 (2004).
214. Andersson, D. I. & Hughes, D. Antibiotic resistance and its cost: is it possible to reverse resistance? *Nature reviews. Microbiology* **8**, 260-271 (2010).
215. Tamma, P. D., Cosgrove, S. E. & Maragakis, L. L. Combination therapy for treatment of infections with gram-negative bacteria. *Clinical microbiology reviews* **25**, 450-470 (2012).
216. Baym, M., Stone, L. K. & Kishony, R. Multidrug evolutionary strategies to reverse antibiotic resistance. *Science* **351**, aad3292 (2016).
217. Szybalski, W. & Bryson, V. Genetic studies on microbial cross resistance to toxic agents. I. Cross resistance of *Escherichia coli* to fifteen antibiotics. *Journal of bacteriology* **64**, 489-499 (1952).
218. Kim, S., Lieberman, T. D. & Kishony, R. Alternating antibiotic treatments constrain evolutionary paths to multidrug resistance. *Proc Natl Acad Sci U S A* **111**, 14494-14499 (2014).
219. Lazar, V. *et al.* Bacterial evolution of antibiotic hypersensitivity. *Mol Syst Biol* **9**, 700 (2013).
220. Imamovic, L. & Sommer, M. O. Use of collateral sensitivity networks to design drug cycling protocols that avoid resistance development. *Sci Transl Med* **5**, 204ra132 (2013).
221. Munck, C., Gumpert, H. K., Wallin, A. I., Wang, H. H. & Sommer, M. O. Prediction of resistance development against drug combinations by collateral responses to component drugs. *Sci Transl Med* **6**, 262ra156 (2014).
222. Gonzales, P. R. *et al.* Synergistic, collaterally sensitive beta-lactam combinations suppress resistance in MRSA. *Nat Chem Biol* **11**, 855-861 (2015).
223. Rodriguez de Evgrafov, M., Gumpert, H., Munck, C., Thomsen, T. T. & Sommer, M. O. Collateral Resistance and Sensitivity Modulate Evolution of High-Level Resistance to Drug Combination Treatment in *Staphylococcus aureus*. *Mol Biol Evol* **32**, 1175-1185 (2015).
224. Maltas, J. & Wood, K. B. Pervasive and diverse collateral sensitivity profiles inform optimal strategies to limit antibiotic resistance. *PLoS Biol* **17**, e3000515 (2019).
225. Kavanaugh, L. G., Flanagan, J. N. & Steck, T. R. Reciprocal antibiotic collateral sensitivity in *Burkholderia multivorans*. *Int J Antimicrob Agents* **56**, 105994 (2020).
226. Barbosa, C. *et al.* Alternative Evolutionary Paths to Bacterial Antibiotic Resistance Cause Distinct Collateral Effects. *Mol Biol Evol* **34**, 2229-2244 (2017).
227. Rodriguez de Evgrafov, M. C., Faza, M., Asimakopoulos, K. & Sommer, M. O. A. Systematic Investigation of Resistance Evolution to Common Antibiotics Reveals Conserved Collateral Responses across Common Human Pathogens. *Antimicrobial agents and chemotherapy* **65** (2020).
228. Jansen, G. *et al.* Association between clinical antibiotic resistance and susceptibility of *Pseudomonas* in the cystic fibrosis lung. *Evol Med Public Health* **2016**, 182-194 (2016).
229. Rosenkilde, C. E. H. *et al.* Collateral sensitivity constrains resistance evolution of the CTX-M-15 beta-lactamase. *Nat Commun* **10**, 618 (2019).
230. Frohlich, C. *et al.* OXA-48-Mediated Ceftazidime-Avibactam Resistance Is Associated with Evolutionary Trade-Offs. *mSphere* **4** (2019).
231. Herencias, C. *et al.* Collateral sensitivity associated with antibiotic resistance plasmids. *Elife* **10** (2021).
232. Nichol, D. *et al.* Antibiotic collateral sensitivity is contingent on the repeatability of evolution. *Nat Commun* **10**, 334 (2019).
233. Barbosa, C., Roemhild, R., Rosenstiel, P. & Schulenburg, H. Evolutionary stability of collateral sensitivity to antibiotics in the model pathogen *Pseudomonas aeruginosa*. *Elife* **8** (2019).

234. Roemhild, R., Linkevicius, M. & Andersson, D. I. Molecular mechanisms of collateral sensitivity to the antibiotic nitrofurantoin. *PLoS Biol* **18**, e3000612 (2020).
235. Escherich, T. & Bettelheim, K. S. The Intestinal Bacteria of the Neonate and Breast-Fed Infant. *Reviews of Infectious Diseases* **10**, 1220-1225 (1988).
236. Donaldson, G. P., Lee, S. M. & Mazmanian, S. K. Gut biogeography of the bacterial microbiota. *Nature reviews. Microbiology* **14**, 20-32 (2016).
237. Oh, S., Buddenborg, S., Yoder-Himes, D. R., Tiedje, J. M. & Konstantinidis, K. T. Genomic diversity of *Escherichia* isolates from diverse habitats. *PloS one* **7**, e47005 (2012).
238. Walk, S. T. *et al.* Cryptic lineages of the genus *Escherichia*. *Applied and environmental microbiology* **75**, 6534-6544 (2009).
239. Daegelen, P., Studier, F. W., Lenski, R. E., Cure, S. & Kim, J. F. Tracing ancestors and relatives of *Escherichia coli* B, and the derivation of B strains REL606 and BL21(DE3). *J Mol Biol* **394**, 634-643 (2009).
240. Blount, Z. D. The unexhausted potential of *E. coli*. *Elife* **4** (2015).
241. Lederberg, J. & Tatum, E. L. Gene recombination in *Escherichia coli*. *Nature* **158**, 558 (1946).
242. Morse, M. L., Lederberg, E. M. & Lederberg, J. Transduction in *Escherichia coli* K-12. *Genetics* **41**, 142-156 (1956).
243. Hayes, W. Observations on a transmissible agent determining sexual differentiation in *Bacterium coli*. *Journal of general microbiology* **8**, 72-88 (1953).
244. Lederberg, J. Cell genetics and hereditary symbiosis. *Physiol Rev* **32**, 403-430 (1952).
245. National Center for Biotechnology Information (NCBI). Available from https://www.ncbi.nlm.nih.gov/genome/genomes/167 (accessed 01/2021).
246. Blattner, F. R. *et al.* The complete genome sequence of *Escherichia coli* K-12. *Science* **277**, 1453-1462 (1997).
247. Hayashi, K. *et al.* Highly accurate genome sequences of *Escherichia coli* K-12 strains MG1655 and W3110. *Mol Syst Biol* **2**, 2006 0007 (2006).
248. Baba, T. *et al.* Construction of *Escherichia coli* K-12 in-frame, single-gene knockout mutants: the Keio collection. *Mol Syst Biol* **2**, 2006 0008 (2006).
249. Knoppel, A. *et al.* Genetic Adaptation to Growth Under Laboratory Conditions in *Escherichia coli* and *Salmonella enterica*. *Frontiers in microbiology* **9**, 756 (2018).
250. Puentes-Tellez, P. E., Hansen, M. A., Sorensen, S. J. & van Elsas, J. D. Adaptation and heterogeneity of *Escherichia coli* MC1000 growing in complex environments. *Applied and environmental microbiology* **79**, 1008-1017 (2013).
251. Jahn, L. J., Munck, C., Ellabaan, M. M. H. & Sommer, M. O. A. Adaptive Laboratory Evolution of Antibiotic Resistance Using Different Selection Regimes Lead to Similar Phenotypes and Genotypes. *Frontiers in microbiology* **8**, 816 (2017).
252. Lenski, R. E., Available from http://myxo.css.msu.edu/index.html (accessed 01/2021).
253. Kaper, J. B., Nataro, J. P. & Mobley, H. L. Pathogenic *Escherichia coli*. *Nature reviews. Microbiology* **2**, 123-140 (2004).
254. Wagenlehner, F. M. E. *et al.* Epidemiology, definition and treatment of complicated urinary tract infections. *Nat Rev Urol* **17**, 586-600 (2020).
255. Leimbach, A., Hacker, J. & Dobrindt, U. *E. coli* as an all-rounder: the thin line between commensalism and pathogenicity. *Curr Top Microbiol Immunol* **358**, 3-32 (2013).
256. Manges, A. R. *et al.* Global Extraintestinal Pathogenic *Escherichia coli* (ExPEC) Lineages. *Clinical microbiology reviews* **32** (2019).
257. Crossman, L. C. *et al.* A commensal gone bad: complete genome sequence of the prototypical enterotoxigenic *Escherichia coli* strain H10407. *Journal of bacteriology* **192**, 5822-5831 (2010).
258. Robins-Browne, R. M. *et al.* Are *Escherichia coli* Pathotypes Still Relevant in the Era of Whole-Genome Sequencing? *Front Cell Infect Microbiol* **6**, 141 (2016).

259. Kahlmeter, G. & Eco.Sens. An international survey of the antimicrobial susceptibility of pathogens from uncomplicated urinary tract infections: the ECO.SENS Project. *J Antimicrob Chemother* **51**, 69-76 (2003).
260. Alteri, C. J. & Mobley, H. L. T. Metabolism and Fitness of Urinary Tract Pathogens. *Microbiol Spectr* **3** (2015).
261. Bengtsson, S., Naseer, U., Sundsfjord, A., Kahlmeter, G. & Sundqvist, M. Sequence types and plasmid carriage of uropathogenic *Escherichia coli* devoid of phenotypically detectable resistance. *J Antimicrob Chemother* **67**, 69-73 (2012).
262. Calhau, V., Domingues, S., Ribeiro, G., Mendonca, N. & Da Silva, G. J. Interplay between pathogenicity island carriage, resistance profile and plasmid acquisition in uropathogenic *Escherichia coli*. *J Med Microbiol* **64**, 828-835 (2015).
263. Dijkshoorn, L. & Nemec, A. in *Acinetobacter Molecular Biology* (edited by Ulrike Gerischer), Ch. The Diversity of the Genus *Acinetobacter*, 1 (Caister Academic Press, U.K, 2008).
264. List of Prokaryotic names with Standing in Nomenclature (LPSN). Available from https://lpsn.dsmz.de/species (accessed 01/2021).
265. Rossau, R., Van Landschoot, A., Gillis, M. & De Ley, J. Taxonomy of *Moraxellaceae* fam. nov., a New Bacterial Family To Accommodate the Genera *Moraxella*, *Acinetobacter*, and *Psychrobacter* and Related Organisms. *International Journal of Systematic Bacteriology* **41**, 310-319 (1991).
266. Baumann, P., Doudoroff, M. & Stanier, R. Y. A study of the *Moraxella* Group. II. Oxidative-negative Species (Genus *Acinetobacter*). *Journal of bacteriology* **95**, 1520-1541 (1968).
267. Baumann, P. Isolation of *Acinetobacter* from soil and water. *Journal of bacteriology* **96**, 39-42 (1968).
268. Carr, E. L., Kampfer, P., Patel, B. K., Gurtler, V. & Seviour, R. J. Seven novel species of *Acinetobacter* isolated from activated sludge. *International journal of systematic and evolutionary microbiology* **53**, 953-963 (2003).
269. Seifert, H. *et al.* Distribution of *Acinetobacter* species on human skin: comparison of phenotypic and genotypic identification methods. *Journal of clinical microbiology* **35**, 2819–2825 (1997).
270. Al Atrouni, A., Joly-Guillou, M. L., Hamze, M. & Kempf, M. Reservoirs of Non-baumannii *Acinetobacter* Species. *Frontiers in microbiology* **7**, 49 (2016).
271. Towner, K. J. *Acinetobacter*: an old friend, but a new enemy. *J Hosp Infect* **73**, 355-363 (2009).
272. Nemec, A. *et al.* Genotypic and phenotypic characterization of the *Acinetobacter calcoaceticus-Acinetobacter baumannii* complex with the proposal of *Acinetobacter pittii* sp. nov. (formerly *Acinetobacter* genomic species 3) and *Acinetobacter nosocomialis* sp. nov. (formerly *Acinetobacter* genomic species 13TU). *Research in microbiology* **162**, 393-404 (2011).
273. Antunes, L. C., Visca, P. & Towner, K. J. *Acinetobacter baumannii*: evolution of a global pathogen. *Pathog Dis* **71**, 292-301 (2014).
274. Nielsen, K. *et al.* Natural Transformation and Availability of Transforming DNA to *Acinetobacter calcoaceticus* in Soil Microcosms. *Applied and environmental microbiology* **63**, 1945-1952 (1997).
275. Juni, E. & Heym, G. A. Pathways for Biosynthesis of a Bacterial Capsular Polysaccharide. Iv. Capsule Resynthesis by Decapsulated Resting-Cell Suspensions. *Journal of bacteriology* **87**, 461-467 (1964).
276. Juni, E. & Janik, A. Transformation of *Acinetobacter calco-aceticus* (*Bacterium anitratum*). *Journal of bacteriology* **98**, 281-288 (1969).
277. Ramirez, M. S. *et al.* Naturally competent *Acinetobacter baumannii* clinical isolate as a convenient model for genetic studies. *Journal of clinical microbiology* **48**, 1488-1490 (2010).

278. Godeux, A. S. *et al.* Fluorescence-Based Detection of Natural Transformation in Drug-Resistant *Acinetobacter baumannii*. *Journal of bacteriology* **200** (2018).
279. Wilharm, G., Piesker, J., Laue, M. & Skiebe, E. DNA uptake by the nosocomial pathogen *Acinetobacter baumannii* occurs during movement along wet surfaces. *Journal of bacteriology* **195**, 4146-4153 (2013).
280. Traglia, G. M. *et al.* Interspecies DNA acquisition by a naturally competent *Acinetobacter baumannii* strain. *Int J Antimicrob Agents* **53**, 483-490 (2019).
281. Vallenet, D. *et al.* Comparative analysis of *Acinetobacters*: three genomes for three lifestyles. *PloS one* **3**, e1805 (2008).
282. Adams, M. D. *et al.* Comparative genome sequence analysis of multidrug-resistant *Acinetobacter baumannii*. *Journal of bacteriology* **190**, 8053-8064 (2008).
283. Chen, T. L. *et al. Acinetobacter baylyi* as a pathogen for opportunistic infection. *Journal of clinical microbiology* **46**, 2938-2944 (2008).
284. Zhou, Z. *et al.* Clinical carbapenem-resistant *Acinetobacter baylyi* strain coharboring $bla_{\text{SIM-1}}$ and $bla_{\text{OXA-23}}$ from China. *Antimicrobial agents and chemotherapy* **55**, 5347-5349 (2011).
285. Elliott, K. T. & Neidle, E. L. *Acinetobacter baylyi* ADP1: transforming the choice of model organism. *IUBMB life* **63**, 1075-1080 (2011).
286. Utnes, A. L. *et al.* Growth phase-specific evolutionary benefits of natural transformation in *Acinetobacter baylyi*. *ISME J* **9**, 2221-2231 (2015).
287. Juni, E. Interspecies Transformation of *Acinetobacter*: genetic evidence for a ubiquitous genus. *Journal of bacteriology* **112**, 917-931 (1972).
288. Harms, K. & Wackernagel, W. The RecBCD and SbcCD DNases suppress homology-facilitated illegitimate recombination during natural transformation of *Acinetobacter baylyi*. *Microbiology* **154**, 2437-2445 (2008).
289. Palmen, R., Buijsman, P. & Hellingwerf, K. J. Physiological regulation of competence induction for natural transformation in *Acinetobacter calcoaceticus*. *Archives of microbiology* **162**, 344-351 (1994).
290. de Berardinis, V. *et al.* A complete collection of single-gene deletion mutants of *Acinetobacter baylyi* ADP1. *Mol Syst Biol* **4**, 174 (2008).
291. Metzgar, D. *et al. Acinetobacter* sp. ADP1: an ideal model organism for genetic analysis and genome engineering. *Nucleic acids research* **32**, 5780-5790 (2004).
292. CDC. Antibiotic resistance threats in the United States 2019. *Atlanta, GA: U.S. Department of Health and Human Services, CDC* (2019).
293. Peterson, L. R. Bad Bugs, No Drugs: No ESCAPE Revisited. *Clinical Infectious Diseases* **49**, 992-993 (2009).
294. Rice, L. B. Federal funding for the study of antimicrobial resistance in nosocomial pathogens: no ESKAPE. *J Infect Dis* **197**, 1079-1081 (2008).
295. Usage of Antimicrobial Agents and Occurrence of Antimicrobial Resistance in Norway. *NORM NORM-VET 2018*, Tromsø / Oslo (2019).
296. European Centre for Disease Prevention and Control (ECDC). Antimicrobial resistance surveillance in Europe 2009. *Annual Report of the European Antimicrobial Resistance Surveillance Network (EARS-Net)* Stockholm (2010).
297. European Centre for Disease Prevention and Control (ECDC). Surveillance of antimicrobial resistance in Europe 2018. *Annual report of the European Antimicrobial Resistance Surveillance Network (EARS-Net)*, Stockholm (2019).
298. Norwegian Directorate of Health. Antibiotic use in Norwegian Primary Healthcare. *National Guidelines*, Version 1.3, Available from www.antibiotikaiallmennpraksis.no (2012).
299. Gupta, K. *et al.* International clinical practice guidelines for the treatment of acute uncomplicated cystitis and pyelonephritis in women: A 2010 update by the Infectious Diseases Society of America and the European Society for Microbiology and Infectious Diseases. *Clinical Infectious Diseases* **52**, e103-120 (2011).

300. Ray, J. & Nielsen, K. Experimental methods for assaying natural transformation and inferring horizontal gene transfer. *Methods Enzymol* **395**, 491-520 (2005).
301. Harms, K., Schon, V., Kickstein, E. & Wackernagel, W. The RecJ DNase strongly suppresses genomic integration of short but not long foreign DNA fragments by homology-facilitated illegitimate recombination during transformation of *Acinetobacter baylyi. Molecular microbiology* **64**, 691-702 (2007).
302. Pansegrau, W., Thomas, C. & Stanisich, V. Complete nucleotide sequence of Birmingham IncP alpha plasmids. Compilation and comparative analysis. *J Mol Biol* **239**, 623-663 (1994).
303. San Millan, A. Evolution of Plasmid-Mediated Antibiotic Resistance in the Clinical Context. *Trends in microbiology* **26**, 978-985 (2018).
304. Samuelsen, O. *et al.* Identification of *Enterobacteriaceae* isolates with OXA-48 and coproduction of OXA-181 and NDM-1 in Norway. *J Antimicrob Chemother* **68**, 1682-1685 (2013).
305. McDonald, M. J. Microbial Experimental Evolution - a proving ground for evolutionary theory and a tool for discovery. *EMBO Rep* **20**, e46992 (2019).
306. Lenski, R. E. Phenotypic and Genomic Evolution during a 20,000-Generation Experiment with the Bacterium *Escherichia coli*. *Plant Breeding Reviews*, 225-265 (2003).
307. Deatherage, D. E. & Barrick, J. E. Identification of mutations in laboratory-evolved microbes from next-generation sequencing data using breseq. *Methods Mol Biol* **1151**, 165-188 (2014).
308. Levin, B. R., Perrot, V. & Walker, N. Compensatory mutations, antibiotic resistance and the population genetics of adaptive evolution in bacteria. *Genetics* **154**, 985-997 (2000).
309. Varet, H., Brillet-Gueguen, L., Coppee, J. Y. & Dillies, M. A. SARTools: A DESeq2- and EdgeR-Based R Pipeline for Comprehensive Differential Analysis of RNA-Seq Data. *PloS one* **11**, e0157022 (2016).
310. Mi, H., Muruganujan, A., Ebert, D., Huang, X. & Thomas, P. D. PANTHER version 14: more genomes, a new PANTHER GO-slim and improvements in enrichment analysis tools. *Nucleic acids research* **47**, D419-d426 (2019).
311. Kahlmeter, G., Ahman, J. & Matuschek, E. Antimicrobial Resistance of Escherichia coli Causing Uncomplicated Urinary Tract Infections: A European Update for 2014 and Comparison with 2000 and 2008. *Infect Dis Ther* **4**, 417-423 (2015).
312. Liakopoulos, A., Aulin, L. B. S., Buffoni, M., van Hasselt, J. G. C. & Rozen, D. E. Allele-specific collateral and fitness effects determine the dynamics of fluoroquinolone-resistance evolution. *bioRxiv* **2020.10.19.345058** (2020).
313. Thulin, E., Thulin, M. & Andersson, D. I. Reversion of High-level Mecillinam Resistance to Susceptibility in *Escherichia coli* During Growth in Urine. *EBioMedicine* **23**, 111-118 (2017).
314. Ho, P. L. *et al.* Plasmid-Mediated OqxAB Is an Important Mechanism for Nitrofurantoin Resistance in *Escherichia coli*. *Antimicrobial agents and chemotherapy* **60**, 537-543 (2016).
315. Giske, C. G. Contemporary resistance trends and mechanisms for the old antibiotics colistin, temocillin, fosfomycin, mecillinam and nitrofurantoin. *Clin Microbiol Infect* **21**, 899-905 (2015).
316. Dunn, S. J., Carrilero, L., Brockhurst, M. & McNally, A. Limited and strain-specific transcriptional and growth responses to acquisition of a multidrug resistance plasmid in genetically diverse *Escherichia coli* lineages. *bioRxiv* **2020.10.23.351718** (2020).
317. Phaneuf, P. V., Gosting, D., Palsson, B. O. & Feist, A. M. ALEdb 1.0: a database of mutations from adaptive laboratory evolution experimentation. *Nucleic acids research* **47**, D1164-D1171 (2019).
318. Chib, S. & Seshasayee, A. S. Modulation of *rpoS* fitness by loss of *cpdA* activity during stationary-phase in *Escherichia coli*. *bioRxiv* **460451** (2018).
319. San Millan, A., Heilbron, K. & MacLean, R. C. Positive epistasis between co-infecting plasmids promotes plasmid survival in bacterial populations. *ISME J* **8**, 601-612 (2014).

320. McNally, A. *et al.* Combined Analysis of Variation in Core, Accessory and Regulatory Genome Regions Provides a Super-Resolution View into the Evolution of Bacterial Populations. *PLoS Genet* **12**, e1006280 (2016).
321. Barbe, V., Vallenet, D., Fonknechten, N., Kreimeyer, A. & Oztas, S. Unique features revealed by the genome sequence of *Acinetobacter* sp. ADP1, a versatile and naturally transformation competent bacterium. *Nucleic acids research* **32**, 5766-5779 (2004).
322. Casadaban, M. J., Chou, J. & Cohen, S. N. Overproduction of the Tn*3* Transposition Protein and Its Role in DNA Transposition. *Cell* **28**, 345-354 (1982).
323. Saunders, C. W. & Guild, W. R. Monomer plasmid DNA transforms *Streptococcus pneumoniae*. *Mol Gen Genet* **181**, 57-62 (1981).
324. Berge, M., Mortier-Barriere, I., Martin, B. & Claverys, J. P. Transformation of *Streptococcus pneumoniae* relies on DprA- and RecA-dependent protection of incoming DNA single strands. *Molecular microbiology* **50**, 527-536 (2003).
325. Harms, K. & Wackernagel, W. The RecBCD and SbcCD DNases suppress homology-facilitated illegitimate recombination during natural transformation of *Acinetobacter baylyi*. *Microbiology* **154**, 2437-2445 (2008).
326. Kidane, D. *et al.* Evidence for different pathways during horizontal gene transfer in competent *Bacillus subtilis* cells. *PLoS Genet* **5**, e1000630 (2009).
327. Dillingham, M. & Kowalczykowski, S. RecBCD Enzyme and the Repair of Double-Stranded DNA Breaks. *Microbiol. Mol. Biol.* **72** (2008).
328. San Millan, A., Escudero, J. A., Gifford, D. R., Mazel, D. & MacLean, R. C. Multicopy plasmids potentiate the evolution of antibiotic resistance in bacteria. *Nat Ecol Evol* **1**, 10 (2016).
329. Shi, Q., Huguet-Tapia, J. C. & Peters, J. E. Tn*917* targets the region where DNA replication terminates in *Bacillus subtilis*, highlighting a difference in chromosome processing in the firmicutes. *Journal of bacteriology* **191**, 7623-7627 (2009).
330. Evans, D. R. *et al.* Systematic detection of horizontal gene transfer across genera among multidrug-resistant bacteria in a single hospital. *Elife* **9** (2020).
331. Twiss, E., Coros, A. M., Tavakoli, N. P. & Derbyshire, K. M. Transposition is modulated by a diverse set of host factors in *Escherichia coli* and is stimulated by nutritional stress. *Molecular microbiology* **57**, 1593-1607 (2005).
332. Guerin, E. *et al.* The SOS response controls integron recombination. *Science* **324**, 1034 (2009).
333. Kretschmer, P. J. & Cohen, S. N. Selected translocation of plasmid genes: frequency and regional specificity of translocation of the Tn*3* element. *Journal of bacteriology* **130**, 888-899 (1977).

Paper I

nature COMMUNICATIONS

ARTICLE

DOI: 10.1038/s41467-018-06143-y OPEN

Conserved collateral antibiotic susceptibility networks in diverse clinical strains of *Escherichia coli*

Nicole L. Podnecky[1], Elizabeth G.A. Fredheim[1], Julia Kloos[1], Vidar Sørum[1], Raul Primicerio[1], Adam P. Roberts[2,3], Daniel E. Rozen[4], Ørjan Samuelsen[1,5] & Pål J. Johnsen[1]

There is urgent need to develop novel treatment strategies to reduce antimicrobial resistance. Collateral sensitivity (CS), where resistance to one antimicrobial increases susceptibility to other drugs, might enable selection against resistance during treatment. However, the success of this approach would depend on the conservation of CS networks across genetically diverse bacterial strains. Here, we examine CS conservation across diverse *Escherichia coli* strains isolated from urinary tract infections. We determine collateral susceptibilities of mutants resistant to relevant antimicrobials against 16 antibiotics. Multivariate statistical analyses show that resistance mechanisms, in particular efflux-related mutations, as well as the relative fitness of resistant strains, are principal contributors to collateral responses. Moreover, collateral responses shift the mutant selection window, suggesting that CS-informed therapies may affect evolutionary trajectories of antimicrobial resistance. Our data allow optimism for CS-informed therapy and further suggest that rapid detection of resistance mechanisms is important to accurately predict collateral responses.

[1] Department of Pharmacy, Faculty of Health Sciences, UiT The Arctic University of Norway, 9037 Tromsø, Norway. [2] Department of Parasitology, Liverpool School of Tropical Medicine, Pembroke Place, Liverpool, L3 5QA, UK. [3] Research Centre for Drugs and Diagnostics, Liverpool School of Tropical Medicine, Pembroke Place, Liverpool, L3 5QA, UK. [4] Institute of Biology, Leiden University, Sylviusweg 72, PO Box 9505, 2300 RA Leiden, The Netherlands. [5] Norwegian National Advisory Unit on Detection of Antimicrobial Resistance, Department of Microbiology and Infection Control, University Hospital of North Norway, 9037 Tromsø, Norway. Correspondence and requests for materials should be addressed to N.L.P. (email: nicole.podnecky@uit.no) or to P.J.J. (email: paal.johnsen@uit.no)

The evolution and increasing prevalence of antimicrobial resistance is driven by the consumption and misuse of antimicrobials in human medicine, agriculture, and the environment[1–3]. Historically, the threat of antimicrobial resistance was overcome by using novel antimicrobials with unique drug targets. However, the discovery rate of new antimicrobial agents has dwindled[4–6] and severely lags behind the rate of resistance evolution[7]. While concerted scientific, corporate, and political focus is needed to recover antimicrobial pipelines[8–10], there is an urgent need for alternative strategies that prolong the efficacy of existing antimicrobials and prevent or slow the emergence, spread, and persistence of antimicrobial resistance. Current global efforts to improve antimicrobial stewardship largely focus on reducing overall antimicrobial consumption and increasing awareness of resistance development[9,11–13]. While these efforts will affect the evolution and spread of resistance, mounting evidence suggests that these changes alone will not lead to large-scale reductions in the occurrence of antimicrobial resistance[14–18].

Several recent studies have examined novel treatment strategies using multiple antimicrobials that could reduce the rate of resistance emergence and even reverse pre-existing resistance. These approaches, collectively termed selection inversion strategies, refer to cases where resistance becomes costly in the presence of other antimicrobial agents[19]. Among the most promising of these strategies are those based on a phenomenon first reported in 1952, termed collateral sensitivity (CS), where resistance to one antimicrobial simultaneously increases the susceptibility to another[20]. CS and its inverse, cross-resistance (CR), have been demonstrated for several bacterial species and across different classes of antimicrobials[21–27]. These results have formed the basis of proposed CS-informed antimicrobial strategies that combine drug pairs[22,28] or alter temporal administration, e.g. drug cycling[21,29]. CS-informed strategies would force bacteria to evolve resistance along a predictable trajectory, resulting in CS; this predictability could be exploited to ultimately reverse resistance and prevent the fixation of resistance and multi-drug resistance development at the population level of bacterial communities.

Initial in vitro experiments support using CS-based strategies to re-sensitize resistant strains[21] and reduce rates of resistance development[29]; however, the broader application of this principle depends on predictable bacterial responses during antimicrobial therapy. This predictability must be general for a given drug class and should not vary across strains of the same species. To date, most studies of CS and CR have focused on describing collateral networks[21–23] using resistant mutants derived from single laboratory-adapted strains and limited numbers of clinical isolates. Two studies on *Pseudomonas aeruginosa* have investigated CS in collections of clinical isolates[30,31]. However, these studies lack either baseline controls[30] or sufficient genetic diversity among tested strains[31]. As valuable as earlier work has been, the responses of single strains (laboratory or clinical) may not be representative of CS and CR responses in other strains.

To address this limitation, here we focus on understanding collateral networks in clinical urinary tract isolates of *Escherichia coli* with selected resistance to drugs widely used for the treatment of urinary tract infections: ciprofloxacin, trimethoprim, nitrofurantoin, and mecillinam. We investigate collateral networks to 16 antimicrobials from diverse drug classes in 10 genetically diverse clinical strains (corresponding to 49 laboratory-generated mutants) to assess the factors contributing to collateral responses (both CS and CR). This approach allows us to identify variation in the sign and magnitude of collateral responses and identify mechanisms of CS and CR that are preserved in various genetic backgrounds. Using multivariate statistical modeling, we show that resistance mutations, particularly those affecting efflux pumps, and the relative fitness of resistant isolates are more important determinants of collateral networks than genetic background. Our results support the idea that collateral responses may be predictable.

Results

Collateral responses vary between and across resistance groups. We examined collateral responses to antimicrobial resistance in a panel of 10 genetically diverse (Supplementary Fig. 1a–b) *E. coli* strains isolated from urinary tract infections. For each of these pan-susceptible strains (Supplementary Fig. 1c)[32], a single resistant mutant was generated to each of four individual antimicrobials used to treat urinary tract infections: ciprofloxacin, trimethoprim, nitrofurantoin, and mecillinam. Here we define resistance group as the collection of mutants from the 10 different genetic backgrounds that were selected for resistance to the same antimicrobial. Mutants resistant to mecillinam required only a single selection step, while multiple selection steps were required to select for resistance above clinical breakpoints for the remaining antimicrobials. In total, 40 resistant mutants were generated with resistance levels above clinical breakpoints, as determined by antimicrobial susceptibility testing using both gradient strip diffusion (Supplementary Table 1) and inhibitory concentration 90% (IC_{90})[21] testing (Table 1). The two methods are correlated, but IC_{90} measurements allow for more robust detection of small relative differences in susceptibility[33,34]. Changes in the IC_{90} of resistant mutants from each respective wild-type strain (Supplementary Fig. 2) were compared for 16 antimicrobials (Table 2). Overall, collateral responses were observed in 39% (233/590) of possible instances (Supplementary Table 2); of these 49% (115/233) were associated with only a 1.5-fold change in IC_{90}. Such small changes would not be observed by typical two-fold antimicrobial susceptibility testing methods frequently used in clinical laboratories.

Overall CR was more frequent than CS, 141 versus 92 instances (Supplementary Table 2), and collateral networks varied considerably between resistance groups. We observed 19 cases of conserved collateral responses (Fig. 1a), where CR or CS to a specific antimicrobial was found in ≥50% of the mutants within a resistance group, defined as CR_{50} or CS_{50}, respectively. For each CR_{50} and CS_{50} observation, IC_{90} results were further assessed by generating dose–response curves of representative strain:drug combinations (Supplementary Fig. 3). Inhibition of growth was shown to vary across antimicrobial concentrations between resistant mutants and respective wild-type strains, confirming the changes in antimicrobial susceptibility determined by the IC_{90} assays.

During the selection of resistant mutants, we often observed colonies of varying size for all resistance groups, suggesting changes to bacterial fitness. To test this, we measured the growth rates of mutants relative to the respective wild-type strains (Supplementary Fig. 4). In general, mutants resistant to ciprofloxacin and mecillinam displayed severely reduced growth rates, suggesting high costs of resistance. Relative growth rates varied between 0.34–0.75 with a mean of 0.53 for ciprofloxacin-resistant mutants and between 0.49–0.79 with a mean of 0.64 for mecillinam-resistant mutants. Mutants resistant to nitrofurantoin and trimethoprim displayed lower fitness effects, and several resistant mutants harbored apparent cost-free resistance mutations (Supplementary Fig. 4). Only two of ten nitrofurantoin-resistant mutants and four of ten trimethoprim-resistant mutants displayed an apparent cost of resistance. Relative growth rates varied between 0.93–1.05 and 0.68–1.07 with averages of

Table 1 Description of *Escherichia coli* strains used in the study and average IC_{90} changes following antimicrobial selection

Strain	ST[a]	Origin	CIP[b]		MEC[b]		NIT[b]		TMP[b]	
			WT[c]	[c]CIP[R]	WT[c]	[c]MEC[R]	WT[c]	[c]NIT[R]	WT[c]	[c]TMP[R]
K56-2	73	Greece	0.014	16	0.146	>30	8	>64	0.225	>28
K56-12	104	Portugal	0.016	1.67	0.273	28	7.33	>64	0.563	>32
K56-16[d]	127	Portugal	0.009	3	0.167	18.7	4	>64	0.25	>30
K56-41	73	Greece	0.016	2.33	0.104	13.3	6	>64	0.25	6.67
K56-44[d]	12	Greece	0.013	1.67	0.141	16	6.67	>64	0.375	6
K56-50	100	Greece	0.012	3	0.141	10.7	12	>64	0.172	18
K56-68	95	Sweden	0.014	4	0.141	30	6.67	>64	0.208	18.7
K56-70	537	Sweden	0.007	2.67	0.083	>32	4.67	>64	0.25	14.7
K56-75[e]	69	UK	0.008	1.17	0.063	13	6	>64	0.167	5.33
K56-78	1235	UK	0.015	6	0.141	16	8	>64	0.5	7.33

[a]Multi-locus sequence type (ST)
[b]The average IC_{90} values (μg mL^{-1}) of three or more biological replicates for wild type (WT) and resistant (^{R}) mutants to ciprofloxacin (CIP), mecillinam (MEC), nitrofurantoin (NIT), and trimethoprim (TMP). Individual results above detection limits (MEC = 32 μg mL^{-1}, NIT = 64 μg mL^{-1}, TMP = 32 μg mL^{-1}) were analyzed as those values, yielding final results with uncertainty (>average). EUCAST Clinical Breakpoints v 7.1 for Enterobacteriaceae[63] were: >0.5 μg mL^{-1} CIP, >8 μg mL^{-1} MEC, >64 μg mL^{-1} NIT, and >4 μg mL^{-1} TMP
[c]The strain number names the WT, and designations CIP^R, MEC^R, NIT^R, and TMP^R describe which drug the isolates were selected with, and resistance achieved
[d, e]Strains containing the Col156 or Col(MP18) replicon, respectively

Table 2 List of antimicrobials used in this study

Antimicrobial[a]	Abbreviation	Drug class	Drug target(s)	Solvent
Amoxicillin	AMX	β-lactam (Penicillin)	Cell wall synthesis	Phosphate buffer[b]
Azithromycin	AZT	Macrolide	Protein synthesis (50S)	≥95% Ethanol
Ceftazidime	CAZ	β-lactam (Cephalosporin)	Cell wall synthesis	Water + 10% (w w^{-1}) Na_2CO_3
Chloramphenicol	CHL	Amphenicol	Protein synthesis (50S)	≥95% Ethanol
Ciprofloxacin	CIP	Fluoroquinolone	DNA replication, cell division	0.1 N HCl
Colistin	COL	Polymyxin	Cell wall & cell membrane	Water
Ertapenem	ETP	β-lactam (Carbapenem)	Cell wall synthesis	Water
Fosfomycin	FOS	Phosphonic	Cell wall synthesis (MurA)	Water
Gentamicin	GEN	Aminoglycoside	Protein synthesis (30S)	Water
Mecillinam	MEC	β-lactam (Penicillin)	Cell wall synthesis (PBP2)	Water
Nitrofurantoin	NIT	Nitrofuran	Multiple[c]	Dimethyl sulfoxide
Trimethoprim	TMP	Antifolate	Folate synthesis (FolA)	Dimethyl sulfoxide
Sulfamethoxazole	SMX	Antifolate	Folate synthesis (FolP)	Dimethyl sulfoxide
TMP + SMX (1:19)	SXT	Antifolate	Folate synthesis (FolA + FolP)	Dimethyl sulfoxide
Temocillin	TEM	β-lactam (Penicillin)	Cell wall synthesis	Water
Tetracycline	TET	Tetracycline	Protein synthesis (30S)	Water
Tigecycline	TGC	Tetracycline	Protein synthesis (30S)	Water

[a]When available, final antimicrobial concentration was determined using manufacturer-provided or calculated drug potencies, otherwise potency was assumed to be 100%. Aliquots were stored at −20 or −80 °C in single-use vials. All antimicrobials and chemical solvents were obtained from Sigma-Aldrich (St. Louis, MO, USA) with the exception of ciprofloxacin (Biochemika, now Sigma-Aldrich) and temocillin (Negaban®)
[b]0.1 mol L^{-1}, pH 6.0 phosphate buffer supplemented with 6.5% (v v^{-1}) 1 M NaOH (sodium hydroxide)
[c]Nitrofurantoin is thought to target macromolecules including DNA and ribosomal proteins, affecting multiple cellular processes, including protein, DNA, RNA, and cell wall synthesis

0.99–0.94 for nitrofurantoin- resistant and trimethoprim-resistant mutants, respectively.

Ciprofloxacin resistance linked to conserved collateral responses. Nearly half (108/233, 46%) of the observed collateral responses were in ciprofloxacin-resistant mutants, while the remaining 125 were distributed between the other three resistance groups (Supplementary Table 2). Within the ciprofloxacin-resistant group, the majority of collateral responses were CR (70/108, 65%). Additionally, CS responses in ciprofloxacin-resistant mutants were the most conserved in our dataset, with CS to gentamicin occurring in 8 of 10 strains and CS to fosfomycin in 7 of 10 strains (Fig. 1a). Gentamicin and other aminoglycosides are important for the treatment of a wide range of infections[35], while fosfomycin is primarily used for treatment of uncomplicated urinary tract infections[36,37]. The ciprofloxacin-resistant mutants were also unique in the magnitude of observed changes, with cases of CR close to 30-fold and CS as high as six-fold changes in IC_{90} (Supplementary Fig. 2).

Characterization of antimicrobial-resistant mutants. We hypothesized that CS and CR variation in and between resistance groups could be attributed to different mutations causing resistance in each strain. Using whole genome sequencing, we identified a total of 149 mutations in the resistant mutants (Supplementary Data 1–4). Of these, 88 mutations affect previously described or putative antimicrobial resistance-associated genes, gene-regions, or pathways (Supplementary Data 1–4). The remaining mutations were found in other cellular processes not known to affect antimicrobial susceptibility (e.g. metabolic pathways and virulence factors), such as mutation to the FimE regulator of FimA that was frequently observed in mecillinam-resistant mutants (Supplementary Data 2). Aside from FimE, we did not observe mutations in regions unrelated to resistance

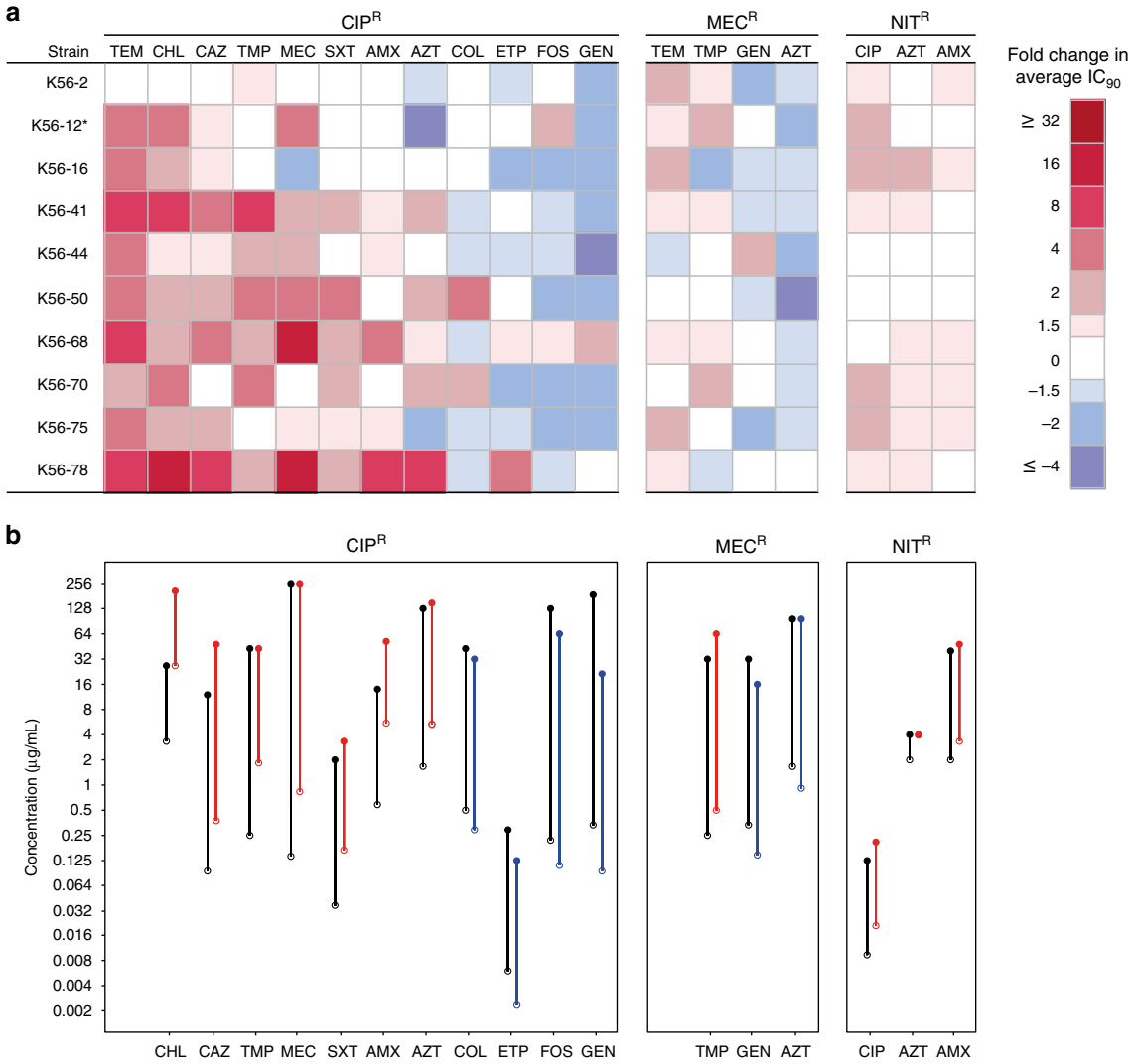

Fig. 1 Conserved collateral responses in antimicrobial resistant mutants. **a** Relative change in antimicrobial susceptibility was determined by comparing average IC_{90} values of resistant mutants to the respective wild-type strain. Collateral responses that were found in ≥50% of the strains are displayed, excluding CR observed in all trimethoprim-resistant mutants to trimethoprim-sulfamethoxazole (see Supplementary Fig. 2). Antimicrobials are ordered by most frequent CR (red; left) to most frequent CS (blue; right) for each group. *The slow growing K56-12 CIP^R was incubated an additional 24 h for IC_{90} determination. **b** The average IC_{90} (open circles) and average mutation prevention concentration (MPC; filled circles) were determined and compared between resistant mutants (colored) with collateral responses, either CS (blue) or CR (red), and their respective wild-type strain (black) in strain:drug combinations representing conserved collateral responses, excluding temocillin. The mutant selection window (vertical lines) was defined as the range between IC_{90} (lower bound) and MPC (upper bound). K56-16 NIT^R had equivalent IC_{90} and MPC values for azithromycin, thus no mutation selection window was reported. Generally, changes in MPC values reflected observed IC_{90} changes, shifting the mutation selection window upwards or downwards accordingly. In 8/10 tested combinations an increase in IC_{90} value (CR) from wild-type to resistant mutant correlated with at least a small increased MPC, with the remaining combinations showing no change in MPC value. Similarly, decreased IC_{90} values (CS) correlated with decreased MPCs (5/7)

across mutants of the same resistance group (parallel evolution), suggesting that such mutations had limited, if any, effect on collateral responses in this study.

For each of the 40 resistant mutants at least one putative resistance mechanism was identified, including mutations to previously described antimicrobial drug targets and promoters of drug targets, drug-modifying (activating) enzymes, regulators of efflux pumps, RNA polymerases and mutations to other metabolic and biochemical processes that may contribute to resistance (Table 3). Briefly, all but one ciprofloxacin-resistant mutant contained mutations in both *gyrA* and efflux regulatory genes and/or gene-regions likely affecting efflux expression (*acrAB* and/or *mdtK*), while one strain had only drug target mutations and displayed the well-described GyrA (S83L) and ParC (G78D) mutation combination (Supplementary Data 1). Both efflux and drug target mutations are frequently found in surveys of clinical isolates[38–41]. Nitrofurantoin-resistant mutants had mutations in one or both nitro-reductases (*nfsA*, *nfsB*) and the majority of strains had additional mutations in *mprA*, which encodes an efflux regulator of EmrAB-TolC pump expression (Supplementary Data 3). Mutants resistant to trimethoprim contained mutations either in *folA* and/or its promoter or genetic amplification of a large region containing *folA* (Supplementary Data 4). The mecillinam-resistant mutants are unique in that they evolved as single step mutants, where a single mutation could confer clinical resistance to mecillinam. Resistance development for the remaining three drugs required several steps, as multiple mutations were required for resistance above clinical breakpoints.

Table 3 The number of antimicrobial resistant mutants with resistance-associated mutations

Resistance mechanism		CIP^R	MEC^R	NIT^R	TMP^R
Drug target	Modification	10[a]			6
	Overproduction				6
Drug activation	Nitroreductase disruption			10	
Drug uptake	Porin mutation	1			
Efflux	AcrAB-TolC	7		1	
	MdtK	9		1	
	MdfA			1	
	EmrAB-TolC			7	
	ABC transport		1		
ppGpp synthesis (stringent response activation)	Stringent response		4		
	tRNA synthesis		4		
	tRNA processing		1		
	Cellular metabolism		3		

[a]All mutants resistant to ciprofloxacin contained one mutation in the *gyrA* gene, except the K56-2 CIP^R mutant that contained two mutations in *gyrA* and a mutation in *parC*

In total, 12 different mutations in genes and/or cellular processes previously linked to mecillinam resistance were identified in this resistance group (Supplementary Data 2)[42].

The ciprofloxacin-resistant group displayed a clear trend where conserved CR responses were strongly linked to mutations in efflux regulatory regions suggesting that *gyrA* drug target mutations had a limited effect on CS and CR. Trimethoprim-resistant mutants also had few collateral responses, likely due to the specific mechanism of resistance affecting a single unique drug target (i.e. overexpression/alteration of FolA). To further investigate the effects of drug target mutations, we assessed the collateral responses of mutants generated following a single selection-step with ciprofloxacin. These first-step mutants contained single, non-synonymous mutations to *gyrA* and no other mutations (e.g. in efflux pumps) linked to ciprofloxacin resistance (Supplementary Data 1). The IC_{90} of these strains was uniformly lower than in ciprofloxacin-resistant strains containing multiple resistance mutations. Few collateral responses were observed in these first-step mutants (Fig. 2), and none were conserved across different strain backgrounds. These results suggest that most collateral responses observed in the ciprofloxacin-resistant mutants are due to the observed efflux mutations.

Efflux and fitness are main contributors to collateral responses. Multivariate statistical approaches were used to investigate the extent to which genetic (strain) background, resistance group, the putative mechanism of resistance (in particular efflux-related mutations), growth rate, and the fitness cost of resistance explain the variation in collateral responses. All factors were investigated individually (Supplementary Fig. 5a–e). Throughout the remaining analyses we focus mainly on efflux-related mutations, rather than resistance group, to explicitly address putative mechanisms of resistance, and relative fitness rather than growth rate.

We estimated several models with individual, or a combination of, factors to assess their effect size and significance given some level of collinearity between fitness and efflux-type (Fig. 3, Supplementary Fig. 5a–r). A model including strain background, relative fitness, and efflux-related mutations as factors explained 62.5% of the total variation in IC_{90} values (Fig. 3a, b, Supplementary Table 3). In this three-factor model there was clear separation of the mutants by resistance group (Fig. 3a). The ciprofloxacin-resistant mutants showed strong CR towards temocillin, chloramphenicol, ceftazidime, and amoxicillin, separating this resistance group from the others along the first ordination axis (Fig. 3a, b). Along the second ordination axis, mecillinam-resistant isolates were distinct, had CR to temocillin, and were more likely to have CS towards drugs, such as azithromycin and chloramphenicol (Fig. 3a, b). Both efflux-type and relative fitness were significant predictors when tested alone and in combination (Supplementary Table 3). The model (Fig. 3a, b) also revealed that strain background had a non-significant ($p = 0.993$) contribution (Supplementary Table 3). Even when modeled alone (Supplementary Fig. 5a), strain background only accounted for 6.5% of the variation and was non-significant (Supplementary Table 3).

We initially hypothesized that genetic background would significantly affect collateral responses. Our initial analysis suggests that it does not. Arguably, the inclusion of IC_{90} data from the drugs to which primary resistance was selected could confound the analysis, despite our efforts to minimize these effects using log-transformed data. We used the same approaches to assess a subset of collateral responses, excluding data for all of the 40 resistant mutants to five antimicrobials containing the drugs used for selection (ciprofloxacin, mecillinam, nitrofurantoin, trimethoprim) and trimethoprim-sulfamethoxazole. Within the subset model, patterns consistent with the full model were observed, but with a lower degree of clustering by resistance group (Fig. 3c). For example, K56-2 CIP^R is now co-localized with the mecillinam-resistant isolates, indicating that this isolate is distinct from other ciprofloxacin-resistant mutants (Fig. 3c), which still showed strong tendencies of CR to temocillin, chloramphenicol, ceftazidime, and amoxicillin (Fig. 3c, d). Despite these changes, efflux-type and fitness were still significant predictors of collateral networks, and strain background remained non-significant (Supplementary Table 3) when modeled alone (Supplementary Fig. 5f) and in two-factor combinations (Supplementary Fig. 5n–o), but had a limited, significant contribution ($p = 0.040$), determined by permutation tests, in the three-factor model (Fig. 3c, d, Supplementary Table 3). However, mutations in efflux-related genes and gene regulators were the strongest predictor of collateral responses tested, explaining over 33% of the variation in the subset. Fitness alone also had significant predictive value, but to a lesser extent (17% variation explained). It is important to note that we observed a correlation between efflux mutations and relative fitness that is likely explained by reduced fitness resulting from the cost of overexpression of efflux pump(s)[39].

To investigate the influence of resistance mechanism on IC_{90} variation at a higher resolution, we modeled each resistance group separately relating the putative resistance mechanism (beyond efflux-type) and fitness separately and in combination (Supplementary Fig. 6a–o). However, potentially due to a lower number of samples within each resistance group that were separated into more detailed classifications of resistance mechanism, these factors had varying degrees of contribution. For mutants resistant to ciprofloxacin (Supplementary Fig. 6a) and trimethoprim (Supplementary Fig. 6j), resistance mechanism was non-significant, but it was a significant factor for those resistant to mecillinam (Supplementary Fig. 6d) and nitrofurantoin (Supplementary Fig. 6g). Fitness was a significant factor only for the mecillinam resistance group (Supplementary Fig. 6e) and similarly, models containing both resistance mechanism and fitness were non-significant for all resistance groups, with the exception of the mecillinam-resistant mutants (Supplementary Fig. 6f).

In the first-step (GyrA) ciprofloxacin mutants, strain background was a significant factor for collateral responses

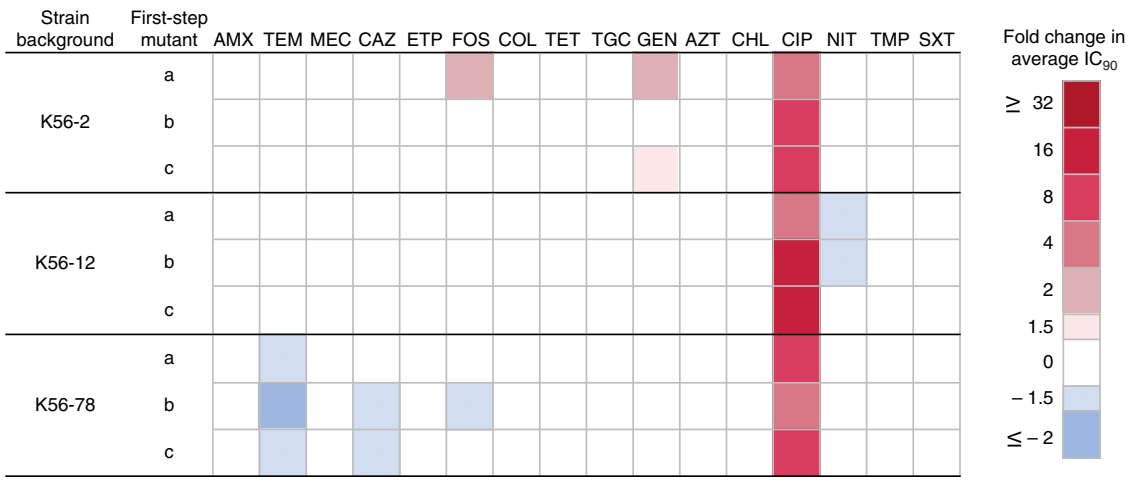

Fig. 2 Collateral effects in *gyrA* mutants with decreased susceptibility to ciprofloxacin. Relative changes in antimicrobial susceptibilities, CS (blue) and CR (red), were determined by comparing average IC_{90} values of nine first-step mutants to their respective wild-type strain. Antimicrobials are ordered by antimicrobial class, as in Supplementary Fig. 2

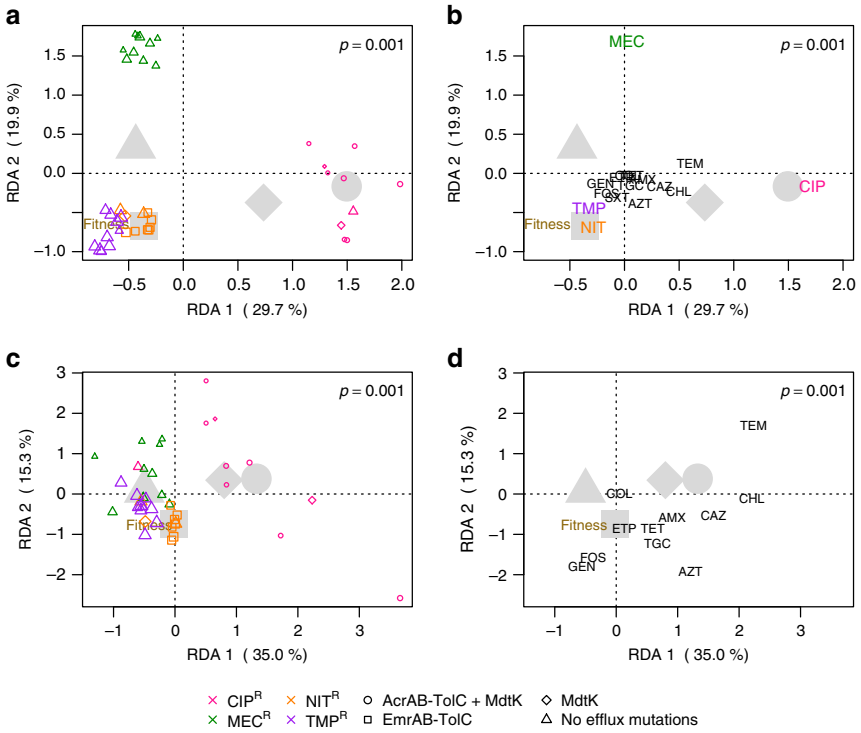

Fig. 3 Results of multivariate statistical modeling. Graphical representations of two redundancy analyses (RDA, triplot) results relating various parameters to the observed changes in IC_{90} between resistant mutants and respective wild-type strains for (**a**, **b**) 16 antimicrobials tested and (**c**, **d**) a subset of these antimicrobials, excluding ciprofloxacin, mecillinam, nitrofurantoin, trimethoprim, and trimethoprim-sulfamethoxazole. Each RDA is broken down into two plots; (**a**, **c**) where weighted averages of resistant mutants are plotted as colored symbols (color indicates resistance group, shape the assigned efflux group, and symbol size proportional to relative fitness, see Supplementary Fig. 4). In (**b**, **d**) antimicrobial drug names indicate the tip of vectors that pass through the origin in the direction of increasing IC_{90} fold change or CR (direction of steepest ascent). Vectors can be used to interpret the change in IC_{90} for the antimicrobials shown. For both statistical models, the first and second RDA axes shown display the majority of explained variation in IC_{90} changes. Large gray symbols show centroids (average effect) for all resistant mutants within a given efflux group (shape). The vector tip of relative fitness (brown) is also shown. **a** The majority of explained variation is driven by primary resistances, where ciprofloxacin (pink)-resistant and mecillinam (green)-resistant mutants cluster distinctly from the other resistance groups, which showed higher relative fitness. **b** Resistant mutants possessing MdtK mutations alone (diamond) or together with AcrAB-TolC mutations (circle) are likely to show CR to chloramphenicol, ceftazidime, temocillin, and azithromycin, but sensitivity to gentamicin, fosfomycin, and trimethoprim. Whereas those without efflux mutations (triangle) are more likely to display low-level CS or no change to most antimicrobials tested. The analysis of the subset RDA (**c**, **d**) shows patterns consistent with the full model, but with less clustering of mutants by resistance group (**c**). The combination of AcrAB-TolC and MdtK efflux mutations displayed the greatest fitness costs, while mutants lacking efflux-related mutations were the most fit (**d**). RDA significance was assessed by permutation tests (1000 permutations), where $p \leq 0.05$ was considered significant. For more comprehensive multivariate models see Supplementary Fig. 5–6

(Supplementary Fig. 6m). However, this was not the case when the original ciprofloxacin-resistant mutants from the same strain backgrounds were added to the analysis (Supplementary Fig. 6n), suggesting again that other factors are more important than strain background. Overall, in comparison to the ciprofloxacin-resistant mutants, collateral responses of first-step mutants were far less frequent and more closely resembled those of the GyrA/ParC mutation-containing K56-2 CIP^R mutant. A final redundancy analysis was performed on all ciprofloxacin-resistant and first-step mutants (Supplementary Fig. 6o), and showed a significant effect of resistance mechanism, supporting that mechanism, efflux in particular, is a major driver of collateral responses.

Collateral responses shift the mutation selection window. The mutant selection window can be defined as the concentration space between the lowest antimicrobial concentration that selects for and enriches resistant mutants[43] and the concentration that prevents the emergence of first-step resistant mutants, the mutation prevention concentration (MPC)[44,45]. In theory, if drug concentrations remain above the MPC during treatment, antimicrobial resistance is less likely to evolve[44,45]. It was recently demonstrated in *E. coli* MG1655 that changes in MPC correlated with collateral responses in resistant mutants[21]. We determined the MPC for 17 strain:drug combinations that exemplified conserved collateral responses (Fig. 1b). The MPC for each resistant mutant and its respective wild-type were compared. In 12/17 (70.6%) the change in MPC was consistent with the sign of collateral responses as determined by IC_{90}. This demonstrates that even small CS/CR changes can affect the mutant selection window, correspondingly shifting it down or up. In 4/17 (23.5%) the MPC displayed no change between the wild-type and mutant. This was observed when testing the MPC for mecillinam, trimethoprim, and azithromycin, though we speculate that increasing the precision of the MPC assay (as was done with IC_{90} testing) might negate these discrepancies. Changes in MPC results with azithromycin were inconsistent with the change in IC_{90} for a ciprofloxacin-resistant mutant and the mutants resistant to mecillinam and nitrofurantoin, which displayed a decreased MPC instead of an expected increase or no change, respectively.

Discussion

Here, we identify conserved collateral responses in antimicrobial susceptibility across genetically diverse clinical *E. coli* strains following antimicrobial resistance development. Our findings are relevant beyond urinary-tract infections because uropathogenic *E. coli* are shown to also stably colonize the bladder and gut[46] and to cause bloodstream infections[47]. Our data show that CS and CR are pervasive in clinical *E. coli* strains, consistent with earlier results based on laboratory-adapted strains of various species[21–23,25,30,48] and a limited number of clinical isolates[21,30]. Resistance to ciprofloxacin resulted in a greater number of collateral responses than resistance to mecillinam, nitrofurantoin, or trimethoprim. This is likely due to mutations to known regulators of the AcrAB-TolC and MdtK efflux pumps. Both have broad substrate specificities to diverse antimicrobials including fluoroquinolones, β-lactams, tetracycline, chloramphenicol, trimethoprim-sulfamethoxazole, and some macrolides for the AcrAB-TolC efflux pump[49,50], and fluoroquinolones, chloramphenicol, trimethoprim, and some β-lactams for the MdtK pump[39,51]. Interestingly, both overexpression of MdtK[51] and RpoB[39] mutations (that were linked to MdtK expression) have been shown to reduce susceptibility to fosfomycin, as was observed in the ciprofloxacin-resistant mutants in this study (Fig. 1a). Overall, CR was much more prevalent than CS, and the magnitude of collateral responses were most often small, consistent with other reports[21–23]. We observed that collateral responses varied substantially by resistance group, but variation was also observed within resistance groups.

Using CS_{50} and CR_{50} thresholds to identify conserved responses, we found that conserved CR was more than twice as common as conserved CS. Whereas many of the conserved collateral responses identified in this study support the findings in previous work using single laboratory-adapted strains, we observed several clinically relevant differences. For example, our finding of conserved CS in ciprofloxacin-resistant mutants to gentamicin was previously reported in *E. coli* K12[22] but not in *E. coli* MG1655[21]. In mutants resistant to ciprofloxacin we also observed conserved CR towards chloramphenicol, as reported in ref. [21], but not in ref. [23]. We identified conserved CR of nitrofurantoin-resistant mutants to amoxicillin, and this was not reported in MG1655[21]. These observations underscore the importance of exploring collateral networks in multiple mutants of different clinical strain backgrounds and with different resistance mechanisms to assess their potential clinical application.

Visual inspection of the data revealed a few clinically relevant examples of CS phenotypes that appeared independent of putative mechanism of resistance. We show that *E. coli* strains resistant to ciprofloxacin display CS towards gentamicin, fosfomycin, ertapenem, and colistin, and these phenotypes were conserved across multiple mechanisms of resistance. These results parallel those of a recent study on *P. aeruginosa* clinical isolates from cystic fibrosis patients, where resistance to ciprofloxacin was associated with CS to gentamicin, fosfomycin, and colistin[31]. Taken together these data support the presence of general, conserved collateral networks that may both affect the population dynamics of antimicrobial resistance during treatment and counter-select for resistance, as recently indicated[31].

We assumed a priori that genetic background, resistance group, resistance mechanism, and the fitness cost of resistance could potentially affect the generality, sign, and magnitude of collateral networks in clinical *E. coli* strains. Despite the fact that some collateral responses are conserved across different strains and mechanisms of resistance, our multivariate statistical approaches show overall that mechanism of resistance is the key predictor of CS and CR variability. This is primarily the case for efflux-related mutations. However, mechanism of resistance also significantly contributed to the observed CS and CR variation in the mecillinam mutants where no efflux mutations were found. The presented data are consistent with earlier reports based on multiple resistant mutants derived from single strains with different resistance mechanisms towards specific antimicrobials[22,23,52]. Our finding that genetic background did not significantly contribute to collateral responses is an important addition to these earlier studies. Finally, we found that the fitness cost of resistance also contributed significantly to the observed variation in CS and CR, despite some collinearity between efflux-related mutations and reduced fitness. Taken together, our data and previous reports indicate that applied use of collateral networks in future treatment strategies may be dependent on rapid identification of specific resistance mechanisms. Moreover, clinical application of CS as a selection inversion strategy warrants further investigations to ideally explore CS in isogenic backgrounds, representing several diverse strains, with permutations of all known antimicrobial resistance-associated traits. Such extensive studies would likely provide valuable information on the mechanisms of CS. Other confounding factors such as mobile genetic elements with heterogeneous resistance determinants should also be investigated as they would likely influence and reduce the predictability of collateral networks.

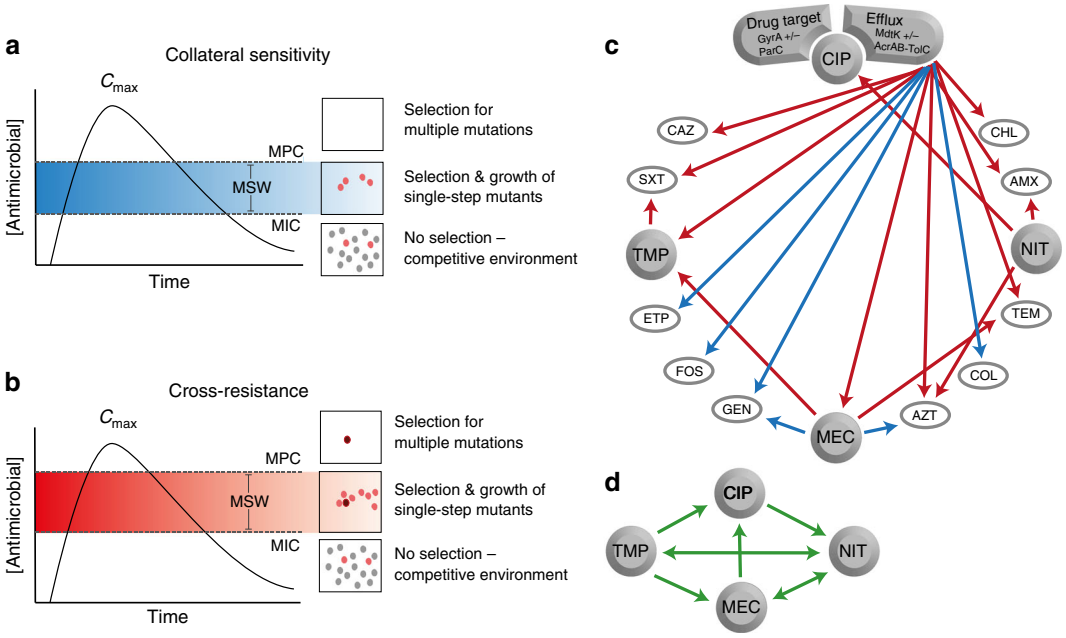

Fig. 4 Presentations of the potential effects and implications of CS and CR. **a** Sequential drug administration informed by CS (blue) could potentially narrow or shift the mutant selection window (MSW) downwards in concentration space whereas (**b**) CR (red) results in a widened or shifted upwards mutant selection window for secondary antimicrobials. This would affect the probability of acquiring second-step mutations leading to high-level resistance. Consequently, CS-informed secondary therapies could reduce selection and thus propagation of first-step mutants resulting in a reduced opportunity for second-step mutations to occur. Dots represent bacteria resistant to a primary antibiotic (gray), spontaneous mutants with reduced susceptibility to a secondary drug (pink), or those with high-level resistance to the secondary drug (dark red). Note that these are hypothetical schematics and in many cases the maximum concentration achieved (C_{max}) may be below the MPC. **c** Arrows indicate conserved collateral responses, where CS (blue) and CR (red) are depicted. The collateral responses in this study are mainly predicted by efflux-related mutations in the ciprofloxacin-resistant mutants. These data suggest potential secondary treatment options that may reduce the rate of resistance evolution (**a**, **b**) following initial treatment failure. **d** Green arrows indicate putative temporal administration of four antimicrobials used for the treatment of urinary-tract infections, as informed by the collateral networks in (**c**)

Selection inversion, as described by ref. [21], depends on the cycling of drug pairs that display reciprocal CS. We did not observe reciprocal CS between any of the four drugs studied here that are widely used for treatment of urinary tract infections. However, we asked if modest reductions and increases in antimicrobial susceptibilities would affect the mutant selection window[44] for the most prevalent CS and CR phenotypes. We subjected conserved CS and CR phenotypes to MPC assays and revealed that even a small 1.5-fold change in IC_{90} could equally alter the MPC, resulting in a shift of the mutant selection window (Fig. 1b). These results suggest that antimicrobial treatment strategies informed by collateral networks could affect the evolutionary trajectories of antimicrobial resistance. Sequential treatment using drug pairs that display CR would, following resistance development, shift the mutant selection window towards higher antimicrobial concentrations, as was previously observed[53], and increase the likelihood for resistance development to subsequent treatment options (Fig. 4a). Conversely, sequential treatment based on drug pairs that display CS can shift the mutant selection window down and reduce the window of opportunity for high-level resistance development (Fig. 4b). This result suggests that the initial choice of antimicrobial may set the stage for later resistance development.

Based on our in vitro findings, trimethoprim and nitrofurantoin are attractive from a clinical perspective, as resistance to these resulted in few collateral responses, preserving the innate sensitivity to available secondary antimicrobials (Fig. 4c, d). However, mecillinam could be even more attractive, as CS largely dominates the observed collateral responses in resistant mutants. Additionally, isolates resistant to mecillinam, especially those evolved in vivo, are associated with high fitness costs[42]. In contrast, exposure to ciprofloxacin was more likely to cause dramatic collateral responses that depend on the mechanism of resistance and could potentially negatively impact future therapeutic options (Fig. 4c). These observations align with antimicrobial treatment recommendations in Norway, where mecillinam, nitrofurantoin, and trimethoprim are recommended for first-line therapy of uncomplicated urinary-tract infections, and ciprofloxacin is reserved for otherwise complicated infections[54]. Similarly, in the United States nitrofurantoin, trimethoprim-sulfamethoxazole, and mecillinam are recommended before fluoroquinolones, such as ciprofloxacin, ofloxacin, and levofloxacin[55].

Our conclusions are not without limitations. First, we acknowledge that including more clinical isolates from different infection foci, more diverse genetic backgrounds including different bacterial species, as well as other selective agents, could change the outcome of our statistical analyses. This would allow increased sensitivity for the assessment of the different factors controlling collateral responses. A more targeted approach to assess the impact of specific resistance mechanisms on CS and CR across genetically diverse clinical strains is lacking in the field. Our analyses suggest that the fitness cost of resistance explains some variability in the collateral networks reported here. We used relative growth rates as a proxy for relative fitness, and our data are consistent with reports demonstrating that growth rates affect susceptibilities to several antimicrobials[56,57]. It is unclear if collateral networks will be perturbed by compensatory evolution, which eliminates the fitness costs of primary resistance[58–60]. Finally, this and previous studies focus on antimicrobial

resistance development to a single drug, and there is a complete lack of data on how multidrug resistance, including resistance genes on mobile genetic elements, will affect collateral networks. We are currently investigating these and other questions that will aid in our understanding of collateral networks and their potential therapeutic application.

Methods

Bacterial strains. We used 10 clinical, urinary-tract infection isolates of *E. coli* from the ECO-SENS collections[61,62] originating from countries across Europe between 2000 and 2008 (Table 1). The isolates were chosen to represent pan-susceptible strains with diverse genetic backgrounds and were reported plasmid-free[32]. Subsequent analysis based on whole-genome sequencing discovered two changes to previously reported sequence types and the presence of plasmid replicons in three strains (Supplementary Table 4). *E. coli* ATCC 25922 was used for reference and quality control purposes. For general growth, bacterial strains were grown in either Miller Difco Luria–Bertani (LB) broth (Becton, Dickinson and Co., Sparks, MD, USA) or on LB agar; LB broth with select agar (Sigma-Aldrich) at 15 g L^{-1} and incubated at 37 °C.

Selection of antimicrobial-resistant mutants. Single antimicrobial-resistant mutants were selected at drug concentrations above the European Committee on Antimicrobial Susceptibility Testing (EUCAST) clinical breakpoints[63] for ciprofloxacin, nitrofurantoin, trimethoprim, and mecillinam (Supplementary Table 1). Briefly, 100 µL of 10× concentrated overnight culture was spread on Mueller Hinton II agar (MHA-SA; Sigma-Aldrich) plates containing ciprofloxacin (Biochemika), nitrofurantoin (Sigma-Aldrich), or trimethoprim (Sigma-Aldrich) with two-fold increasing concentrations of the antimicrobial. After 24–48 h, a mixture of growth from the highest concentration plate with multiple colonies was used to start a new overnight culture at the same antimicrobial concentration. This was repeated until there was growth above the clinical breakpoint[63]. Mecillinam-resistant mutants and first-step ciprofloxacin mutants (*gyrA* mutation-containing) were selected as single-step mutants on LB or MHA-SA agar, respectively. Mutants were confirmed as *E. coli* using matrix-assisted laser desorption ionization time-of-flight (MALDI-TOF) analysis with MALDI BioTyper software (Bruker, MA, USA).

Antimicrobial susceptibility testing. Mutants were initially screened for resistance above EUCAST breakpoints[63] with gradient diffusion strips following manufacturers guidelines (Liofilchem, Italy), on Mueller Hinton II agar (MHA-BD; Becton, Dickinson and Company). Plates with insufficient growth were incubated for an additional 24 h.

To maximize the precision of our susceptibility estimates and in accord with related studies on CS, collateral changes were determined by IC_{90} testing[21] with some modifications. IC_{90} values were determined following 18 h incubation at 700 rpm (3 mm stroke) in Mueller Hinton Broth (MHB, Becton, Dickinson and Co.). Slow-growing strains where positive growth controls did not reach $OD_{600\ nm}$ of 0.3 after 18 h (i.e. K56-12 CIP^R) were interpreted after 42 h incubation. Standard two-fold concentrations and the median values between them were used as a 1.5-fold testing scale. IC_{90} values were the lowest concentration tested that resulted in ≥90% inhibition of growth. Percent inhibition was calculated compared to the positive control (untreated sample) with background removed[21]. IC_{90} results were determined in at least three biological replicates on separate days. The final result reflects the average of a minimum of three replicates that met quality control standards, including the result of ATCC 25922 on each plate, positive growth control $OD_{600\ nm} > 0.3$, negative growth control $OD_{600\ nm} < 0.05$, and accepting no more than one skip (defined as a break in the inhibition pattern). When one skip was observed, the IC_{90} value was consistently interpreted as the lowest concentration tested that resulted in ≥90% inhibition of growth. Fold change in IC_{90} was calculated as the ratio between the resistant mutant and its respective wild-type. The IC_{90} testing varied for two antimicrobials (according to EUCAST recommendations), where fosfomycin was tested in MHB supplemented with 25 µg mL^{-1} glucose-6-phosphate (Sigma-Aldrich) and tigecycline was tested in fresh MHB media that was prepared daily.

Dose–response curves were generated with average OD_{600} values (background subtracted) for concentrations tested during IC_{90} testing. Averages were plotted for mutants and respective wild-type strains.

MPC testing. We determined the MPC for 17 of 20 conserved collateral responses. Temocillin was excluded due to lack of supply and trimethoprim-sulfamethoxazole was excluded for trimethoprim-resistant isolates due to fundamental CR between trimethoprim and trimethoprim-sulfamethoxazole. MPC determination was based on previous work by Marcusson et al.[64]. Briefly, 10 mL overnight culture was centrifuged and the pellet re-suspended in 1 mL MHB, estimated to contain $\geq 10^{10}$ CFU (actual values were 1.4×10^{10}–7×10^{10} CFU). The inoculum was split and spread onto four large (14 cm diameter) MHA-SA agar plates for each antimicrobial concentration tested in a two-fold dilution series. The MPC was the lowest concentration with no visible growth after 48 h. Where growth/no growth was difficult to interpret, suspected growth was re-streaked on plates at the same antimicrobial concentration. Azithromycin and ertapenem were regularly inconsistent, making re-streaking essential. Resistant mutants and wild-types were tested in parallel, and results represent the average of at least two biological replicates.

Growth rate measurements. To obtain growth curves of wild-types and resistant mutants, single colonies were used to inoculate at least three biological replicates of MHB starter cultures (2 mL) that were incubated at 37 °C for 24 h shaking at 500 rpm. Each culture was diluted 1:100 in MHB (resulting in ~2×10^7 cell mL^{-1}) and 250 µL was added in triplicate to a 96-well microtiter plate. The plate was incubated overnight at 37 °C in a Versamax plate reader (Molecular Devices Corporation, California, USA) with shaking for 9.2 min between reads. OD_{600} measurements were taken every 10 min and growth rates were estimated using the GrowthRates v.2.1 software[65]. To a varying extent, the ciprofloxacin-resistant mutants of K56-12, K56-16, K56-44, and K56-68, as well as, K56-44 MEC^R, K56-68 MEC^R, and K56-70 TMP^R displayed noise in the growth curves due to clumping or non-homogeneous growth, and GrowthRates was unable to fit a line with *R*-value above the 0.98 cut-off value. Additional experiments and visual inspection of the log-transformed OD_{600} values were used to solve this issue. If GrowthRates failed to analyze the curves, a line was fitted within the log phase through at least five consecutive points that displayed log-linear growth. Growth rate (*r*) was calculated based on the slope[65]. Relative growth rates were calculated as $r_{(\text{resistant mutant})}\ r_{(\text{wild-type})}^{-1}$.

Whole genome sequencing. Genomic DNA was isolated using the GenElute Bacterial Genomic DNA kit (Sigma-Aldrich) following guidelines for Gram-positive DNA extraction. Purity and quantification was determined with Nanodrop (Thermo Scientific) and Qubit High Sensitivity DNA assay (Life Technologies), respectively. For library preparation of wild-types and resistant mutants, 1 µg of DNA was sheared on a Covaris S2 to ≈400 bp using the recommended settings (intensity: 4, duty cycle: 10%, cycles per burst: 200, treatment time: 55 s). Libraries were then prepared and indexed using the DNA Ultra II Library Preparation Kit (New England Biolabs, E7645). For library preparation of DNA from first-step ciprofloxacin mutants, 1 ng of DNA was used with the Nextera XT DNA prep kit (Illumina, San Diego), according to the producer's instructions. All libraries were quantified by Qubit High Sensitivity DNA assay and distributions and quality assessed by Bioanalyser DNA 1000 Chip (Agilent, 5067-1504) before normalizing and pooling. Illumina sequencing, NextSeq 550, and MiSeq, was used for the first-step ciprofloxacin mutants and the wild-types and resistant mutants, respectively, using paired-end reads. For NextSeq 550 a mid-output flowcell with 300 cycles was used. V2 chemistry was used for the MiSeq sequencing.

Wild-type genomes were assembled, as follows. Illumina adapters on wild-type reads were removed with Trimmomatic version 0.36[66] using standard settings, then assembled with SPAdes[67]. Contigs less than 500 bp in length or less than 2.0 coverage were removed. Wild-type genome assemblies were inspected and compared to the *E. coli* MG1655 genome (GenBank U00096.2) using QUAST[68]. Final assembled genomes of wild-type strains were annotated using the automated Prokaryotic Genome Annotation Pipeline (https://www.ncbi.nlm.nih.gov/genome/annotation_prok/).

Wild-type and mutant sequences were compared to identify putative resistance mechanisms. First, wild-type genomes were annotated with Rapid Annotation using Subsystem Technology server (RAST, version 2.0) for *E. coli*[69]. SeqMan NGen (DNASTAR, Madison, WI) was used to align raw mutant reads to the corresponding, annotated wild-type genomes, using standard settings. Reported SNPs had ≥10× coverage depth and ≥90% variant base calls. SNPs present in the wild-type assembly or in at least two mutants resistant to different antimicrobials from the same strain background were excluded. Reported SNPs, indels, and rearrangements were manually inspected and gene annotations confirmed using Gene Construction Kit (Textco Biosoftware Inc., Raleigh, NC) and NCBI BLAST searches, respectively.

Multilocus sequence typing (MLST), as well as, plasmid replicon and acquired antimicrobial resistance gene content were determined for the wild-type genomes using MLST version 1.8, PlasmidFinder version 1.3, and ResFinder version 3.0[70], respectively (http://genomicepidemiology.org/). The MLST of each wild-type strain was confirmed compared to the original reported sequence type[32] for all but two strains, K56-41 and K56-70. These strains were originally described as ST420 and ST550, but were ST73 and ST537 in our analysis, respectively (Supplementary Table 4). The wild-type strains were previously described as plasmid free, but we identified two small plasmid replicons, Col156 in K56-16 and K56-44 and Col (MP18) in K56-75 (Supplementary Table 4). Using ResFinder, we detected only one acquired genetic element, *sul*2 (linked to sulfonamide resistance) in K56-44, and two point mutations, PmrB V161G in K56-50 and K56-70 and ParE D475E in K56-78, that are linked to colistin and quinolone (ciprofloxacin) resistance, respectively (Supplementary Table 4). Though all of the wild-type strains were phenotypically pan-susceptible (Supplementary Fig. 1c), these resistance determinants could affect antimicrobial susceptibilities differentially in the presence of other mutations[71,72].

To assess genetic diversity, a phylogenic tree was generated based on the genome sequences of wild-type strains. Assembled wild-type genomes were annotated with PROKKA[73], the core gene-encoding regions were extracted and compared using ROARY[74], and a maximum-likelihood tree with 100 bootstraps

was generated using RAxML[75]. Genetic distances were calculated in R[76] using previously described methods[77].

Multivariate statistical analyses. The fold changes of mean IC_{90} values relative to the parental wild-type strain (collateral responses) were log transformed. Statistical analyses were performed on the complete data set, as well as a subset of the data excluding five antimicrobials (ciprofloxacin, mecillinam, nitrofurantoin, trimethoprim, and trimethoprim-sulfamethoxazole). To estimate and test the effects of strain background, resistance group, resistance mechanism, growth rate, and relative fitness we relied on multivariate modeling (redundancy analysis) to address the co-variation in IC_{90} across antimicrobials. A redundancy analysis is a constrained version of a principle component analysis that additionally allows for hypothesis testing. Linear constraint scores were plotted for each mutant. Response variables were overlaid with independent scaling to illustrate the direction of steepest ascent (increasing CR) from the origin for each antimicrobial. Data were inspected to check whether the assumptions underlying redundancy analysis were met. Significance testing of multivariate models and their factors (Supplementary Table 3) was done via permutation tests (1000 permutations), an approach robust to deviations from multivariate normality and variance homogeneity; $p < 0.05$ was considered significant. Analyses were done in R[76] using the Vegan work package[78].

Data availability

Whole-genome sequencing data are available at NCBI (BioProject PRJNA419689). All other relevant data are available within this article, the Supplementary Information, or from the corresponding author upon request.

Received: 23 January 2018 Accepted: 16 August 2018
Published online: 10 September 2018

References

1. Holmes, A. H. et al. Understanding the mechanisms and drivers of antimicrobial resistance. *Lancet* **387**, 176–187 (2016).
2. Cantas, L. et al. A brief multi-disciplinary review on antimicrobial resistance in medicine and its linkage to the global environmental microbiota. *Front. Microbiol.* **4**, 96 (2013).
3. Andersson, D. I. & Hughes, D. Microbiological effects of sublethal levels of antibiotics. *Nat. Rev. Microbiol.* **12**, 465–478 (2014).
4. Silver, L. L. Challenges of antibacterial discovery. *Clin. Microbiol. Rev.* **24**, 71–109 (2011).
5. Walsh, C. Where will new antibiotics come from? *Nat. Rev. Microbiol.* **1**, 65–70 (2003).
6. Fischbach, M. A. & Walsh, C. T. Antibiotics for emerging pathogens. *Science* **325**, 1089–1093 (2009).
7. Davies, J. Where have all the antibiotics gone?. *Can. J. Infect. Dis. Med. Microbiol.* **17,** 287–290 2006).
8. Infectious Diseases Society of America. The 10 x '20 initiative: pursuing a global commitment to develop 10 new antibacterial drugs by 2020. *Clin. Infect. Dis.* **50**, 1081–1083 (2010).
9. World Health Organization. *WHO Global Strategy of Containment of Antimicrobial Resistance*. WHO/CDS/CSR/DRS/2001.2 (World Health Organization: Geneva, Switzerland, 2001).
10. O'Neill J. *Tackling Drug-resistant Infections Globally: Final Report and Recommendations*. https://amr-review.org/Publications.html (2016).
11. Centers for Disease Control and Prevention (U.S.). *The Core Elements of Hospital Antibiotic Stewardship Programs*. CS273578-A (Centers for Disease Control and Prevention (U.S.): Atlanta, GA, 2014).
12. Harbarth, S. et al. Antimicrobial resistance: one world, one fight! *Antimicrob Resist Infect Control* **4**. https://doi.org/10.1186/s13756-015-0091-2 (2015).
13. *High-Level Meeting on Antimicrobial Resistance [press release]*. New York, NY, USA: OPGA/WHO/FAO/OIE, 21 Sept 2016. https://www.un.org/pga/71/2016/09/21/press-release-hl-meeting-on-antimicrobial-resistance.
14. Johnsen, P. J. et al. Factors affecting the reversal of antimicrobial-drug resistance. *Lancet Infect. Dis.* **9**, 357–364 (2009).
15. Johnsen, P. J. et al. Retrospective evidence for a biological cost of vancomycin resistance determinants in the absence of glycopeptide selective pressures. *J. Antimicrob. Chemother.* **66**, 608–610 (2011).
16. Enne, V. I., Livermore, D. M., Stephens, P. & Hall, L. M. C. Persistence of sulphonamide resistance in *Escherichia coli* in the UK despite national prescribing restriction. *Lancet* **357**, 1325–1328 (2001).
17. Sundqvist, M. et al. Little evidence for reversibility of trimethoprim resistance after a drastic reduction in trimethoprim use. *J. Antimicrob. Chemother.* **65**, 350–360 (2010).
18. Andersson, D. I. & Hughes, D. Antibiotic resistance and its cost: is it possible to reverse resistance? *Nat. Rev. Microbiol.* **8**, 260–271 (2010).
19. Baym, M., Stone, L. K. & Kishony, R. Multidrug evolutionary strategies to reverse antibiotic resistance. *Science* **351**, aad3292 (2016).
20. Szybalski, W. & Bryson, V. Genetic studies on microbial cross resistance to toxic agents. I. Cross resistance of *Escherichia coli* to fifteen antibiotics. *J. Bacteriol.* **64**, 489–499 (1952).
21. Imamovic, L. & Sommer, M. O. Use of collateral sensitivity networks to design drug cycling protocols that avoid resistance development. *Sci. Transl. Med.* **5**, 204ra132 (2013).
22. Lazar, V. et al. Bacterial evolution of antibiotic hypersensitivity. *Mol. Syst. Biol.* **9**, 700 (2013).
23. Lazar, V. et al. Genome-wide analysis captures the determinants of the antibiotic cross-resistance interaction network. *Nat. Commun.* **5**, 4352 (2014).
24. Sanders, C. C., Sanders, W. E. J., Goering, R. V. & Werner, V. Selection of multiple antibiotic resistance by quinolones, β-lactams, and aminoglycosides with special reference to cross-resistance between unrelated drug classes. *Antimicrob. Agents Chemother.* **26**, 797–801 (1984).
25. Gonzales, P. R. et al. Synergistic, collaterally sensitive beta-lactam combinations suppress resistance in MRSA. *Nat. Chem. Biol.* **11**, 855–861 (2015).
26. Macvanin, M. & Hughes, D. Hyper-susceptibility of a fusidic acid-resistant mutant of *Salmonella* to different classes of antibiotics. *FEMS Microbiol. Lett.* **247**, 215–220 (2005).
27. Barbosa, C. et al. Alternative evolutionary paths to bacterial antibiotic resistance cause distinct collateral effects. *Mol. Biol. Evol.* **34**, 2229–2244 (2017).
28. Kim, S., Lieberman, T. D. & Kishony, R. Alternating antibiotic treatments constrain evolutionary paths to multidrug resistance. *Proc. Natl Acad. Sci. USA* **111**, 14494–14499 (2014).
29. Fuentes-Hernandez, A. et al. Using a sequential regimen to eliminate bacteria at sublethal antibiotic dosages. *PLoS Biol.* **13**, e1002104 (2015).
30. Jansen, G. et al. Association between clinical antibiotic resistance and susceptibility of *Pseudomonas* in the cystic fibrosis lung. *Evol. Med. Public Health* **2016**, 182–194 (2016).
31. Imamovic, L. et al. Drug-driven phenotypic convergence supports rational treatment strategies of chronic infections. *Cell* **172**, 121–134.e114 (2018).
32. Bengtsson, S., Naseer, U., Sundsfjord, A., Kahlmeter, G. & Sundqvist, M. Sequence types and plasmid carriage of uropathogenic *Escherichia coli* devoid of phenotypically detectable resistance. *J. Antimicrob. Chemother.* **67**, 69–73 (2012).
33. Munck, C., Gumpert, H. K., Wallin, A. I., Wang, H. H. & Sommer, M. O. Prediction of resistance development against drug combinations by collateral responses to component drugs. *Sci. Transl. Med.* **6**, 262ra156 (2014).
34. Munck, C., Sommer, M. *Antibiotic Resistance: Adaptive Evolution & Dissemination of Resistance Genes*. http://orbit.dtu.dk/en/publications/antibiotic-resistance(9d3346b1-8519-4167-848d-5407bf2fcd6c).html (Department of Systems Biology, Technical University of Denmark, Denmark, 2014).
35. Kushner, B., Allen, P. D. & Crane, B. T. Frequency and demographics of gentamicin use. *Otol. Neurotol.* **37**, 190–195 (2016).
36. Karageorgopoulos, D. E., Wang, R., Yu, X. H. & Falagas, M. E. Fosfomycin: evaluation of the published evidence on the emergence of antimicrobial resistance in Gram-negative pathogens. *J. Antimicrob. Chemother.* **67**, 255–268 (2012).
37. Dijkmans, A. C. et al. Fosfomycin: pharmacological, clinical and future perspectives. *Antibiotics (Basel)* **6**. https://doi.org/10.3390/antibiotics6040024 (2017).
38. Wang, H., Dzink-Fox, J. L., Chen, M. & Levy, S. B. Genetic characterization of highly fluoroquinolone-resistant clinical *Escherichia coli* strains from China: role of *acrR* mutations. *Antimicrob. Agents Chemother.* **45**, 1515–1521 (2001).
39. Pietsch, F. et al. Ciprofloxacin selects for RNA polymerase mutations with pleiotropic antibiotic resistance effects. *J. Antimicrob. Chemother.* **72**, 75–84 (2016).
40. Kern, W. V., Oethinger, M., Jellen-Ritter, A. S. & Levy, S. B. Non-target gene mutations in the development of fluoroquinolone resistance in *Escherichia coli*. *Antimicrob. Agents Chemother.* **44**, 814–820 (2000).
41. Huseby, D. L. et al. Mutation supply and relative fitness shape the genotypes of ciprofloxacin-resistant *Escherichia coli*. *Mol. Biol. Evol.* **34**, 1029–1039 (2017).
42. Thulin, E., Sundqvist, M. & Andersson, D. I. Amdinocillin (Mecillinam) resistance mutations in clinical isolates and laboratory-selected mutants of *Escherichia coli*. *Antimicrob. Agents Chemother.* **59**, 1718–1727 (2015).
43. Gullberg, E. et al. Selection of resistant bacteria at very low antibiotic concentrations. *PLoS Pathog.* **7**, e1002158 (2011).
44. Drlica, K. & Zhao, X. Mutant selection window hypothesis updated. *Clin. Infect. Dis.* **44**, 681–688 (2007).
45. Liang, B. et al. Mutant prevention concentration-based pharmacokinetic/pharmacodynamic indices as dosing targets for suppressing the enrichment of

levofloxacin-resistant subpopulations of *Staphylococcus aureus*. *Antimicrob. Agents Chemother.* **55**, 2409–2412 (2011).
46. Nielsen, K. L. et al. Adaptation of *Escherichia coli* traversing from the faecal environment to the urinary tract. *Int. J. Med. Microbiol.* **306**, 595–603 (2016).
47. Subashchandrabose, S., Mobley, H. L. Virulence and fitness determinants of uropathogenic *Escherichia coli*. *Microbiol. Spectr.* **3**. https://doi.org/10.1128/microbiolspec.UTI-0015-2012 (2015).
48. Pal, C., Papp, B. & Lazar, V. Collateral sensitivity of antibiotic-resistant microbes. *Trends Microbiol.* **23**, 401–407 (2015).
49. Poole, K. Efflux-mediated multiresistance in Gram-negative bacteria. *Clin. Microbiol. Infect.* **10**, 12–26 (2004).
50. Elkins, C. A. & Mullis, L. B. Substrate competition studies using whole-cell accumulation assays with the major tripartite multidrug efflux pumps of *Escherichia coli*. *Antimicrob. Agents Chemother.* **51**, 923–929 (2007).
51. Nishino, K. & Yamaguchi, A. Analysis of a complete library of putative drug transporter genes in *Escherichia coli* . *J. Bacteriol.* **183**, 5803–5812 (2001).
52. Jiao, Y. J., Baym, M., Veres, A., Kishony, R. Population diversity jeopardizes the efficacy of antibiotic cycling. Preprint at htt//www.biorxiv.org/content/early/2016/10/20/082107 (2016).
53. Li, X., Mariano, N., Rahal, J. J., Urban, C. M. & Drlica, K. Quinolone-resistant *Haemophilus influenzae*: determination of mutant selection window for ciprofloxacin, garenoxacin, levofloxacin, and moxifloxacin. *Antimicrob. Agents Chemother.* **48**, 4460–4462 (2004).
54. Norwegian Directorate of Health. *Antibiotic use in Norwegian Primary Healthcare. National Guidelines, Version 1.3* http://www.antibiotikaiallmennpraksis.no (2012).
55. Gupta, K. et al. International clinical practice guidelines for the treatment of acute uncomplicated cystitis and pyelonephritis in women: a 2010 update by the Infectious Diseases Society of America and the European Society for Microbiology and Infectious Diseases. *Clin. Infect. Dis.* **52**, e103–e120 (2011).
56. Tuomanen, E., Cozens, R., Tosch, W., Zak, O. & Tomasz, A. The rate of killing of *Escherichia coli* by beta-lactam antibiotics is strictly proportional to the rate of bacterial growth. *J. Gen. Microbiol.* **132**, 1297–1304 (1986).
57. Greulich, P., Scott, M., Evans, M. R. & Allen, R. J. Growth-dependent bacterial susceptibility to ribosome-targeting antibiotics. *Mol. Syst. Biol.* **11**, 796–796 (2015).
58. Schrag, S. J., Perrot, V. & Levin, B. R. Adaptation to the fitness costs of antibiotic resistance in *Escherichia coli*. *Proc. R. Soc. Lond. B* **264**, 1287–1291 (1997).
59. Björkman, J., Nagaev, I., Berg, O. G., Hughes, D. & Andersson, D. I. Effects of environment on compensatory mutations to ameliorate costs of antibiotic resistance. *Science* **287**, 1479–11482 (2000).
60. Starikova, I. et al. A trade-off between the fitness cost of functional integrases and long-term stability of integrons. *PLoS Pathog.* **8**, e1003043 (2012).
61. Kahlmeter, G. The ECO.SENS project: a prospective, multinational, multicentre epidemiological survey of the prevalence and antimicrobial susceptibility of urinary tract pathogens—interim report. *J. Antimicrob. Chemother.* **46**(Suppl. 1), 15–22 (2000). discussion 63-15.
62. Kahlmeter, G. & Poulsen, H. O. Antimicrobial susceptibility of *Escherichia coli* from community-acquired urinary tract infections in Europe: the ECO.SENS study revisited. *Int. J. Antimicrob. Agents* **39**, 45–51 (2012).
63. The European Committee on Antimicrobial Susceptibility Testing. *Breakpoint Tables for Interpretation of MICs and Zone Diameters, Version 7.1*. http://www.eucast.org (2017).
64. Marcusson, L. L., Olofsson, S. K., Komp Lindgren, P., Cars, O. & Hughes, D. Mutant prevention concentrations of ciprofloxacin for urinary tract infection isolates of *Escherichia coli*. *J. Antimicrob. Chemother.* **55**, 938–943 (2005).
65. Hall, B. G., Acar, H., Nandipati, A. & Barlow, M. Growth rates made easy. *Mol. Biol. Evol.* **31**, 232–238 (2014).
66. Bolger, A. M., Lohse, M. & Usadel, B. Trimmomatic: a flexible trimmer for Illumina sequence data. *Bioinformatics* **30**, 2114–2120 (2014).
67. Bankevich, A. et al. SPAdes: a new genome assembly algorithm and its applications to single-cell sequencing. *J. Comput. Biol.* **19**, 455–477 (2012).
68. Gurevich, A., Saveliev, V., Vyahhi, N. & Tesler, G. QUAST: Quality assessment tool for genome assemblies. *Bioinformatics* **29**, 1072–1075 (2013).
69. Aziz, R. K. et al. The RAST server: rapid annotations using subsystems technology. *BMC Genom.* **9**, 75 (2008).
70. Zankari, E. et al. Identification of acquired antimicrobial resistance genes. *J. Antimicrob. Chemother.* **67**, 2640–2644 (2012).
71. Komp Lindgren, P., Karlsson, A. & Hughes, D. Mutation rate and evolution of fluoroquinolone resistance in *Escherichia coli* isolates from patients with urinary tract infections. *Antimicrob. Agents Chemother.* **47**, 3222–3232 (2003).
72. Moon, D. C. et al. Emergence of a new mutation and its accumulation in the topoisomerase IV gene confers high levels of resistance to fluoroquinolones in *Escherichia coli* isolates. *Int. J. Antimicrob. Agents* **35**, 76–79 (2010).
73. Seemann, T. Prokka: rapid prokaryotic genome annotation. *Bioinformatics* **30**, 2068–2069 (2014).
74. Page, A. J. et al. Roary: rapid large-scale prokaryote pan genome analysis. *Bioinformatics* **31**, 3691–3693 (2015).
75. Stamatakis, A. RAxML version 8: a tool for phylogenetic analysis and post-analysis of large phylogenies. *Bioinformatics* **30**, 1312–1313 (2014).
76. R Core Team. *R: A Language and Environment for Statistical Computing*. (R Foundation for Statistical Computing, Vienna, Austria, 2016).
77. Paradis, E., Claude, J. & Strimmer, K. APE: analyses of phylogenetics and evolution in R language. *Bioinformatics* **20**, 289–290 (2004).
78. Dixon, P. VEGAN, a package of R functions for community ecology. *J. Veg. Sci.* **14**, 927–930 (2003).

Acknowledgements

We thank Tony Brooks at UCL Genomics and Hagar Taman at UiT Genomics Support Centre Tromsø for genome sequencing, Ane L.G. Utnes for generation of nitrofurantoin-resistant mutants, Jessica N. Tran for generation of first-step ciprofloxacin mutants, Jessin Janice for phylogenetic analysis, Søren Overballe-Petersen for preliminary processing of wild-type genomes, and Maria Chiara Di Luca for analysis of the genomes for MLST and identification of plasmid replicons. Funding for this project was provided through the Northern Norway Regional Health Authority and UiT—The Arctic University of Norway (Project SFP1292-16), and JPI-EC-AMR (Project 271176/H10).

Author contributions

P.J.J. and Ø.S. conceived the project; N.L.P., E.G.A.F., J.K. and V.S. designed and performed experiments; R.P. designed and R.P. and N.L.P. performed the multivariate statistical modeling; all authors analyzed, interpreted and discussed the data; and N.L.P., E.G.A.F., A.P.R., D.E.R. and P.J.J. wrote the manuscript with contributions from the other authors.

Additional information

Supplementary Information accompanies this paper at https://doi.org/10.1038/s41467-018-06143-y.

Competing interests: The authors declare no competing interests.

Reprints and permission information is available online at http://npg.nature.com/reprintsandpermissions/

Publisher's note: Springer Nature remains neutral with regard to jurisdictional claims in published maps and institutional affiliations.

Paper II

MICROBIOLOGY

RESEARCH ARTICLE

Kloos *et al.*, *Microbiology* 2021;167:001003

DOI 10.1099/mic.0.001003

MICROBIOLOGY SOCIETY

OPEN ACCESS

Tn*1* transposition in the course of natural transformation enables horizontal antibiotic resistance spread in *Acinetobacter baylyi*

Julia Kloos, Pål J. Johnsen and Klaus Harms*

Abstract

Transposons are genetic elements that change their intracellular genomic position by transposition and are spread horizontally between bacteria when located on plasmids. It was recently discovered that transposition from fully heterologous DNA also occurs in the course of natural transformation. Here, we characterize the molecular details and constraints of this process using the replicative transposon Tn*1* and the naturally competent bacterium *Acinetobacter baylyi*. We find that chromosomal insertion of Tn*1* by transposition occurs at low but detectable frequencies and preferably around the *A. baylyi* terminus of replication. We show that Tn*1* transposition is facilitated by transient expression of the transposase and resolvase encoded by the donor DNA. RecA protein is essential for the formation of a circular, double-stranded cytoplasmic intermediate from incoming donor DNA, and RecO is beneficial but not essential in this process. Absence of the recipient RecBCD nuclease stabilizes the double-stranded intermediate. Based on these results, we suggest a mechanistic model for transposition during natural transformation.

INTRODUCTION

Horizontal gene transfer drives bacterial evolution through the acquisition of novel genetic material and accelerates the spread of adaptive traits such as antimicrobial resistance (AMR) between bacteria [1]. AMR in bacterial pathogens represents a growing public health concern [2] and there is an urgent need to increase our understanding of the basic mechanisms of AMR spread.

Conjugation, transduction and natural transformation are believed to be the main routes of intercellular gene transfer [3]. During conjugation, conjugative plasmids or conjugative transposons move into a recipient bacterium through cell-to-cell contact. Transduction includes the transfer of host DNA, mispackaged into bacteriophage particles during late infection, to a recipient cell. Natural transformation is the active uptake of free DNA from the environment and subsequent genomic integration [4]. Only bacteria that are competent for natural transformation can actively take up free DNA. Competence to undergo natural transformation was experimentally demonstrated in at least 80 bacterial species, both Gram-positive and Gram-negative [5]. The majority of the 12 global priority pathogens are naturally transformable, including those categorized as critically antibiotic-resistant: *Acinetobacter baumannii*, *Pseudomonas aeruginosa* and some *Enterobacteriaceae* [6, 7]. Natural transformation as a pathway for recruiting genetic variation, including AMR genes, was recently demonstrated between different species of the genus *Acinetobacter* [8] and different genera, for example from carbapenem-resistant *Klebsiella pneumoniae* to *A. baumannii* [9].

AMR determinants are frequently captured on mobile genetic platforms such as plasmids and transposons, and in associated mobilizable elements such as integrons, which all represent multidrug resistance-conferring units [10–12]. Transposons are widespread genetic elements in bacteria [13] and in other domains of life. They move intra- and intermolecularly between different genomic positions within a cell in a process called transposition [14]. Through transposition, transposons can be inserted into conjugative plasmids or into bacteriophages, which facilitates the mobility of non-conjugative transposons between cells [12]. Thus, transposon-embedded AMR determinants can be mobilized at multiple hierarchical genetic levels, and intermolecular movement of transposons between different plasmids or between plasmids and

Received 04 June 2020; Accepted 23 November 2020; Published 03 December 2020

Author affiliations: [1]Microbial Pharmacology and Population Biology Research Group, Department of Pharmacy, Faculty of Health Sciences, UiT The Arctic University of Norway, Tromsø, Norway.

***Correspondence:** Klaus Harms, klaus.harms@spdir.net

Keywords: *Acinetobacter baylyi*; natural transformation; Tn*1*; Tn*4401*; transposition.

Abbreviations: AMR, antimicrobial resistance; dl, detection limit; LB, Luria-Bertani; MIC, minimal inhibitory concentration; TSD, target site duplication.

One supplementary figure and four supplementary tables are available with the online version of this article.

chromosomal locations also occurs within clinical pathogens [15–18]. Therefore, the investigation of transposon mobility across different bacterial hosts could aid the understanding of AMR spread.

Stable integration of horizontally acquired mobile genetic elements into the bacterial recipient genome is crucial for long-term inheritance and is facilitated by plasmid establishment or rearrangement events between donor and recipient DNA such as homology-based recombination, site-specific recombination, or transposition [12]. A recent study demonstrated the transposition of a Tn*21*-like transposon (Tn*3*-family) of *Salmonella enterica* serovar Typhimurium 490 into the chromosome of *Acinetobacter baylyi* ADP1 in the course of natural transformation [19]. Tn*21* insertion occurred independently at different loci in several transformants, and target site duplications (TSDs) at the insertion sites strongly suggested DNA recombination by transposition [19]. Since ADP1 harbours no transposons of the Tn*3*-family [20], these results indicated that the transposase was expressed from the incoming donor DNA. The authors concluded that a cytoplasmic, linear DNA double-strand formed after uptake, allowing gene expression and movement of the structural transposon [19].

In the present study, we used the Tn*3*-like replicative transposons Tn*1* [21] and Tn*4401* [22] as donor DNA to quantify and characterize transposition during natural transformation in molecular detail. As a recipient, we employed the naturally competent soil bacterium *A. baylyi* strain ADP1 also used by Domingues *et al.* [19]. ADP1 is transformable at high frequency by DNA from any source, including PCR products, which allows the detection and quantification of rare DNA recombination events [23, 24].

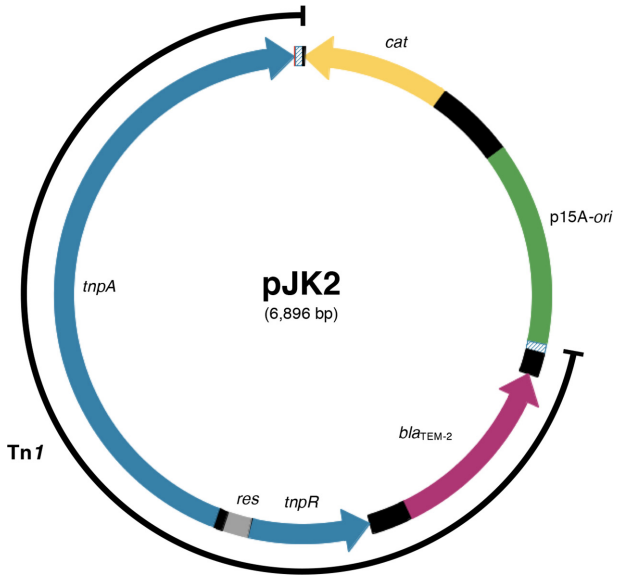

Fig. 1. Map of plasmid pJK2. The plasmid backbone contains the p15A origin of replication (green) and the *cat* gene (yellow; chloramphenicol resistance) of the *E. coli* cloning vector pACYC184. Transposon Tn*1* (4.9 kb) was cloned from plasmid RP4. In Tn*1*, *tnpA* and *tnpR* (blue) encode the transposase and resolvase, respectively. Ampicillin resistance is conferred by bla_{TEM-2} (magenta). The transposon contains a *res* site for cointegrate resolution and is flanked by two terminal 38 bp inverted repeats (dashed). Neither Tn*1* nor pACYC184 display significant sequence identity with the *A. baylyi* genome.

METHODS

Bacterial strains and growth conditions

A. baylyi ADP1 strain BD413 Rp^r (wild-type) [25] and the derivative mutants Δ*recA::tetA* (JV37) [26], Δ*dprA::aacC1* (NH29) [27], Δ*recO* (KOM82) [27] and Δ*recBCD* Δ*sbcCD* (KOM45) [28] were employed as recipient strains in natural transformation assays and have been described previously. The Δ*xerC::nptII sacB* mutant was constructed as reported previously for *A. baylyi* deletion strains [29, 30]. Briefly, DNA sequences of about 1000 bp each upstream and downstream of *xerC* (ACIAD2657) in ADP1 (GenBank CR543861) were PCR-amplified using primers xerC-up-f/xerC-up-r (upstream segment) and xerC-down-f/xerC-down-r (downstream segment; all primer sequences are listed in Table S1 available in the online version of this article). The PCR products were inserted sequentially into the plasmid vector pGT41 upstream and downstream of a *nptII sacB* selectable marker gene pair. The resulting plasmid contained a Δ*xerC::nptII sacB* allele embedded into its natural flanking regions and was used to naturally transform ADP1. The resulting XerCD-deficient transformant (kanamycin-resistant) was confirmed phenotypically and by PCR (primers xerC-up-f/xerC-down-r and xerC-ctrl/xerC-down-r; Table S1). PCR assays were carried out with high-fidelity Phusion DNA polymerase (Thermo Scientific) and standard parameters except using an additional 10% dimethylsulfoxide, or with DreamTaq DNA polymerase (Thermo Scientific).

Escherichia coli strains EC100 (Epicentre), DH5α [31] or SF8 *recA* [32] were employed as host strains for strain constructions and donor DNA preparations. Strains were grown in Luria–Bertani (LB) medium at either 30 °C (*A. baylyi*) or 37 °C (*E. coli*). For transformant selection, media were supplemented with antibiotics at the following concentrations: ampicillin, 100 mg l^{-1} (Tn*1* in pJK2, pJKH1, pJK7 and pTn*4401*); streptomycin, 40 mg l^{-1} (RSF1010); kanamycin, 10 mg l^{-1} (pKH80-PCR).

Donor DNA preparations for natural transformation experiments

Plasmid pJK2 (6896 bp; Fig. 1) was constructed as follows: transposon Tn*1* on plasmid RP4 (4951 bp; GenBank BN000925) was PCR-amplified from the left to the right border without TSDs using DNA from *E. coli* K12 J53 RP4 [German Collection of Microorganisms and Cell Cultures (DSMZ), DSM 3876] as template and primer Tn1-f+r (Table S1) as forward and reverse primer. The resulting PCR product was 5′-phosphorylated with polynucleotide kinase (Thermo Scientific) and ligated to a 1945 bp PCR product containing the p15A origin of replication and the chloramphenicol resistance gene *cat* of plasmid pACYC184 [33] (GenBank

X06403; primers cat-r and p15A-r1; Table S1) using T4 DNA ligase (Fermentas). pJKH1 (carrying Tn*1*Δ*tnpA*; 4289 bp) was derived from pJK2 by digestion with *Eco*RV and circularization of the large fragment (T4 DNA ligase). The partial deletion of *tnpA* (869 internal of 1002 codons) was confirmed by restriction analysis. To construct plasmid pJK7 (Tn*1*Δ*tnpR*; 6399 bp), we PCR-amplified pJK2 excluding *tnpR* with primers pJK2-tnpR-del-f and pJK2-tnpR-del-r (Table S1). The PCR-product was 5′-phosphorylated (polynucleotide kinase) and circularized (T4 DNA ligase), and the deletion of *tnpR* was confirmed by Sanger sequencing. The plasmids RSF1010, pKH80 and pTn*4401* have been described previously [28, 34–36]. Plasmid donor DNA was isolated using the Qiagen Plasmid Extraction kit (Qiagen) and genomic donor DNA was purified with the GenElute Bacterial Genomic DNA kit (Sigma-Aldrich).

When PCR products were employed as donor DNA, PCR reactions were performed using high-fidelity Phusion DNA polymerase. Linear donor DNA substrate pJK2-PCR (6908 bp) was obtained by inverse PCR amplification of pJK2 with primers cat-f and p15A-ori-f-c (Table S1). This PCR product carried a 12 bp overlap at the ends. Donor DNA substrate pKH80-PCR (4760 bp) was PCR-amplified with primers sbcD-up-f and sbcC-down-r (Table S1) from plasmid pKH80. This substrate carried two approximately neighbouring 1.0 kbp DNA stretches from the *A. baylyi* chromosome covering parts of ACIAD0915 and ACIAD0918, interrupted in the centre by a 2.7 kbp *nptII sacB* marker gene cassette conferring kanamycin resistance. The PCR products were purified using the Qiaquick PCR purification kit (Qiagen). When indicated, pJK2-PCR was purified by agarose gel electrophoresis (Sea Plaque, LONZA) and subsequent recovery using the Qiaquick Gel Extraction kit (Qiagen).

Natural transformation assays in liquid medium

Preparation of naturally competent cells of *A. baylyi* as well as natural transformation assays were conducted as described previously [29]. In brief, competent cell stocks were prepared by dilution of an overnight culture 1:100 into liquid LB and growth of that culture under aeration until logarithmic growth (1×10^9 cells ml^{-1} determined with a haemocytometer) was reached. The cells were chilled, centrifuged for 10 min at 5000 ***g*** and 4 °C, and concentrated 1:10 in LB media containing 20% glycerol (v/v). Finally, the cells were aliquoted and stored at −80 °C until further use.

For transformation assays, aliquoted competent cells were thawed on ice, diluted 1:40 in liquid LB to 2.5×10^8 cells ml^{-1}, and DNA was added at 100 ng ml^{-1} unless indicated otherwise. The assays were incubated under aeration for 90 min before the cells were chilled on ice, washed and resuspended in phosphate-buffered saline. Appropriate dilutions were plated on LB (recipient titre) and media containing selective antibiotics (transformant titre). LB plates were incubated for 24 h while transformant plates were incubated 48 to 72 h. Colonies were counted and transformation frequencies were calculated as transformants per recipient. If no transformant colonies were obtained, the limit of detection was calculated instead. In control experiments, recipient cells were incubated without donor DNA to identify resistant mutants arising and unselective and selective plating were performed according to the respective assay with donor DNA.

Verification of transposition events

To identify transposition events, ampicillin-resistant transformant colonies were picked and restreaked three times on selective medium. In some cases, an intermittent cultivation step on non-selective medium was carried out. Typically, isolates were investigated after the final restreak by PCR for the presence of Tn*1* (primer Tn1-f+r) and pJK2 vector backbone DNA (primers cat-r/p15A-r1), or for the presence of Tn*4401* (primers KPC-A/KPC-B) and pTn*4401* vector backbone DNA (primers cat-r/p15A-r1), respectively (Table S1). Occasionally, ampicillin-resistant mutants arose during these cultivation steps, presumably through mutations. These isolates typically displayed an aberrant colony phenotype and were distinguished by the absence of transposon and pJK2 vector DNA in PCR analyses. These procedures clearly separated so-termed transposants from transient (unstable) transformants and mutants. Divergent transformant types were found in experiments using wild-type ADP1 with pJK7 donor DNA, or strain Δ*recBCD* Δ*sbcCD* with pJK2 donor DNA (see the Results and Discussion section for details).

To verify transposants, genomic DNA was isolated from stable ampicillin-resistant isolates that were PCR-positive for Tn*1* and PCR-negative for pJK2 vector backbone, using the GenElute Bacterial Genomic DNA kit (Sigma-Aldrich). Purified DNA was used as template for Sanger DNA sequencing (BigDye 3.1 technology; Applied Biosystems) as follows: 1 µg genomic DNA was mixed with 4 µl BigDye, 2 µl BigDye buffer and 10 µM of primer (either bla-ins-f or Tn1-tnpA-ins-f; Table S1) in a volume of 20 µl. Assays were denatured for 5 min at 95 °C, followed by 99 cycles of 30 s at 95 °C, 10 s at 55 °C and 4 min at 60 °C, and subsequently analysed on an Applied Biosystems 3130*xl* Genetic Analyzer (in-house sequencing facility). BLAST was used to identify both recombinant joints of Tn*1* with the chromosome of ADP1 (GenBank CR543861.1) and to verify the TSDs (Tables S2 and S3). The transposition frequency was calculated as transposants per transformant isolates multiplied by the transformation frequency.

Characterization of target site sequences

A consensus DNA sequence logo was generated by multiple sequence alignment and visualized using WebLogo software [37] (Figs 2 and Fig. S1) The aligned regions covered the 5 bp TSD plus 45 nucleotides upstream and downstream of the duplication (Table S4). The total number and positions of this TSD consensus sequence (TTWTA) were determined for the chromosome of ADP1 using Gene Construction kit v 4.0.3 (Textco BioSoftware, Inc.). Linear regression analysis of the TSD consensus sequence distribution over the chromosome of ADP1 was performed using GraphPad v 8.4.2 (GraphPad Software; P *** <0.001, ** <0.01, * <0.05).

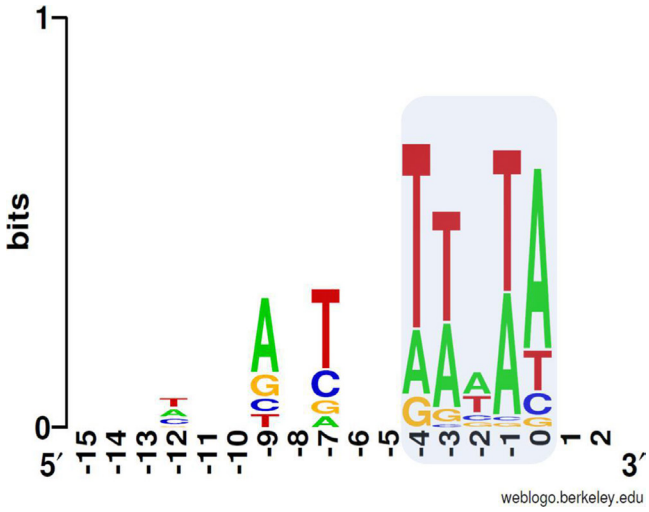

Fig. 2. Consensus DNA sequence logo for Tn*1*-insertions into the chromosome of ADP1. Blue background colour indicates the target site duplication (TSD) consensus sequence at positions −4 to 0. Additional conserved positions around the TSD are shown. The TSD sequence motif (TTWTA; W: T or A) and preference for T at position −7 are typical for this transposon family. The logo was generated using WebLogo [37].

Susceptibility testing

The minimal inhibitory concentrations (MICs) were determined using gradient diffusion strips (Liofilchem) following the manufacturer's instructions. Briefly, 0.5 McFarland solutions in 0.9% saline (w/v) were prepared from freshly grown colonies on LB and spread evenly onto Müller–Hinton agar plates with a sterile cotton swab. A gradient strip for ampicillin was applied and plates were incubated at 30 °C for 18 h. Results were read at 100% growth inhibition (n=1 per strain).

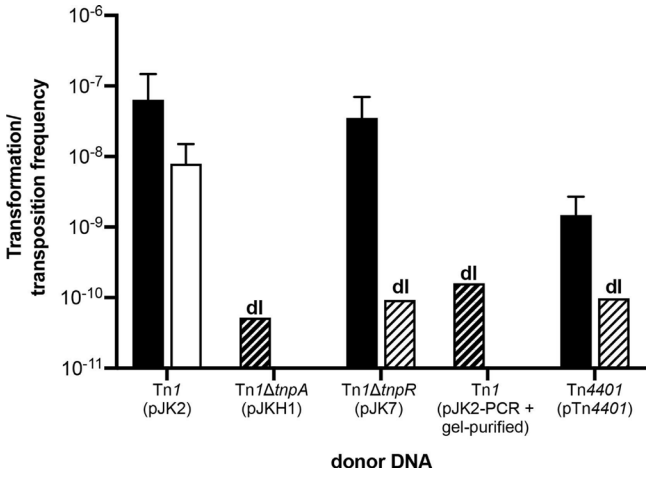

Fig. 3. Frequencies of transformation (black bars) and transposition (white bars) in *A. baylyi* wild-type using different transposon-containing donor DNA substrates: pJK2 (Tn*1*; n=3), pJKH1 (Tn*1*Δ*tnpA*; n=4), pJK7 (Tn*1*Δ*tnpR*; n=3), pJK2-PCR (agarose gel-purified; n=3) and pTn*4401* (Tn*4401*; n=9). Bars represent the mean with standard deviation. Striped bars indicate the detection limit (dl) when no transformation or transposition events were observed.

Electroporation assays

Electrocompetent cells of *A. baylyi* were prepared as published for *E. coli* [38] with modifications. Briefly, a logarithmic culture of *A. baylyi* was grown at 30 °C in LB to 2.5×10^8 cells ml^{-1}. The cells were chilled, washed twice with ice-cold distilled water, and concentrated 500 times in 10% ice-cold glycerol solution (v/v). A 40 µl aliquot was mixed with DNA (400 ng pJK2 or 200 ng RSF1010 DNA), transferred into a 2 mm gap electroporation cuvette and pulsed with 12.5 kV cm^{-1} (25 µF, 200 Ω) using a BioRad electroporator. Next, the cells were suspended in 1 ml prewarmed SOC (2% tryptone, 0.5% yeast, 10 mM NaCl, 2.5 mM KCl, 10 mM $MgCl_2$, 10 mM $MgSO_4$, 20 mM glucose) and aerated for 1 h at 30 °C. Appropriate dilutions were plated on LB (recipient titre) and LB containing antibiotics (transformants) and the plates were incubated at 30 °C for 16 to 20 h or 36 to 48 h, respectively.

RESULTS AND DISCUSSION

Natural transformation by transposon-containing DNA

We inserted the replicative transposon Tn*1* into the narrow-host-range plasmid vector pACYC184 that replicates in *Enterobacteriaceae* but not in *A. baylyi*. The resulting circular plasmid pJK2 (Fig. 1) was used as donor DNA to naturally transform *A. baylyi* ADP1 wild-type cells. Ampicillin-resistant transformant colonies were obtained at a frequency of $(6.4\pm8.4)\times10^{-8}$ per recipient cell (Fig. 3).

Analyses of resistant colonies revealed two distinguishable groups of transformants. In the first group, ampicillin resistance was stably maintained after repeated restreaking on selective medium and also after intermittent non-selective cultivation. PCR analyses showed the presence of Tn*1* but the absence of pJK2 vector backbone DNA. This result indicates that Tn*1* was chromosomally acquired by DNA uptake and transposition. In contrast, the ampicillin resistance was unstable in transformants of the second group, resulting in heterogeneous colony size and shape when restreaked. The resistance was generally lost after repeated purification on selective medium or after intermittent non-selective cultivation, and both Tn*1* and pJK2 backbone DNA could be PCR-amplified from cell material of the first, and with decreasing frequency of subsequent recultivations. This result suggests that transformants of group 2 received the pJK2 plasmid and became resistant through transient expression of bla_{TEM-2}, but lost the plasmid and resistance with further cultivation due to the inability of pJK2 to propagate stably in *A. baylyi*.

To confirm that transformants of the first group occurred by transposition of Tn*1* into the recipient chromosome, we determined the DNA sequences upstream and downstream of Tn*1* by Sanger sequencing of genomic DNA. We analysed 20 group 1 isolates with circular pJK2 DNA and an additional 8

isolates obtained with linear pJK2-derivatives (Supplemental Information: Supplemental Results). Altogether, we identified 29 transposition events of Tn*1* into the chromosome of ADP1, including one isolate with two transposons (Table S2). In all transposition transformants ('transposants'), Tn*1* was found as a chromosomal insert with a 5 bp TSD at the recombinant joints, which is a hallmark of transposase activity. The consensus sequence of the TSD is in agreement with previous reports on Tn*3*-family transposons (Fig. 2) [39, 40]. We did not identify fragments of pACYC184 vector DNA or indications of non-transposition recombination events. The MIC of ADP1 for ampicillin (2 µg ml^{-1}) was increased to >256 µg ml^{-1} in eight randomly chosen transposants (Table S2). Together, these results confirm that the transposants have acquired Tn*1* during natural transformation through transposition.

The frequency of transposants using pJK2 donor DNA was (7.9±7.1)×10^{-9} (Fig. 3). To compare this transposition frequency to extra-chromosomal plasmid establishment or to homologous recombination during natural transformation, we used circular plasmid DNA (RSF1010) or linear homologous DNA (pKH80-PCR) in transformation assays with *A. baylyi* and obtained frequencies of (5.4±1.1)×10^{-6} and (1.3±0.5)×10^{-4}, respectively. These data indicate that Tn*1* transposition in the course of natural transformation is about 680 times lower than plasmid aquisition and about 16000 times lower than homologous recombination during natural transformation. Nonetheless, the transposant frequency was higher than illegitimate recombination frequencies with fully heterologous donor DNA in *A. baylyi* [24, 41]. We conclude that transposon spread through natural transformation can occur at biologically relevant frequencies, although reports showing this process *in situ* are currently lacking. The importance of transposant formation in the environment or for AMR spread in the hospital is unknown but probably low compared with conjugation.

Chromosomal distribution of transposition events

All but one of the Tn*1* insertions occurred in nonessential genes [42] or in intergenic regions of the ADP1 chromosome (Tables S2 and S3). However, the distribution of insertions was nonrandom, and 24 of 29 transpositions clustered within a 170 kbp sector around the assumed terminus of replication (Fig. 4a) [20]. This distribution was supported by 14 additional unique Tn*1* insertions recovered from an *A. baylyi* Δ*recBCD*

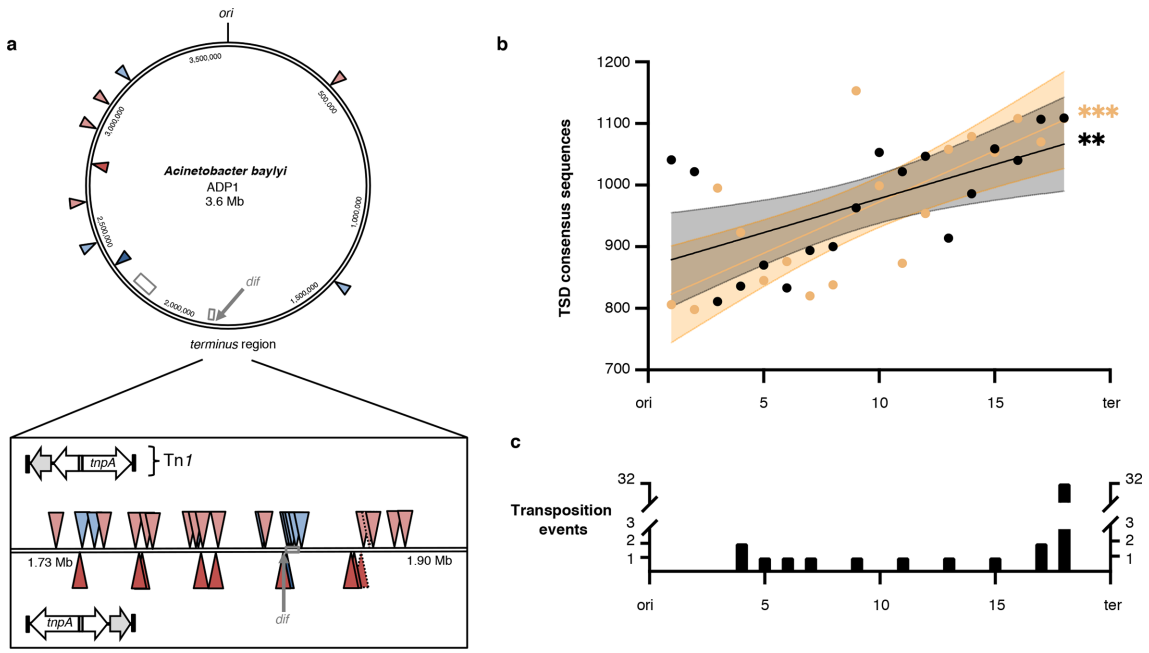

Fig. 4. Characterization of Tn*1* insertion sites. (a) Chromosome map of ADP1 with a magnified section of ~170 kbp (box) around the approximate terminus of replication (ter; G-C/G+C skew inversion site). This region contains 174 open reading frames, of which 12 are essential [42]. The two major prophage regions of ADP1 and the *dif* site for chromosome partitioning by XerCD are indicated by grey open boxes and grey arrows, respectively [20, 47]. Tn*1* insertions are marked as triangles (red, wild-type; blue, Δ*recBCD* Δ*sbcCD*). The orientation of Tn*1* is indicated by the colour intensity (light, transcriptional orientation of *tnpA* in sense; dark, *tnpA* in antisense). A dashed triangle edge specifies insertion sites in a double transposant. Thirty-four out of 43 insertions occurred around the terminus (24 in wild-type and 10 in the Δ*recBCD* Δ*sbcCD* strain). (b) Number and distribution of TSD consensus sequences across the chromosome of ADP1, which was bi-directionally grouped into 2×18 100 kb segments from origin (ori) to ter. The number of TSD consensus sequence hits per group is plotted along the ori–ter axis (black and orange, first and second replichore, respectively). For both directions, linear regression showed a significant increase in the number of hits (first replichore: P=0.0076, R^2=0.5544; second replichore: P=0.0004, R^2=0.3683; 95% confidence intervals are indicated); lowest hit number: 798 (group 2, second replichore), highest hit number: 1153 (group 9, second replichore). (c) Number of experimentally observed transposition events per region.

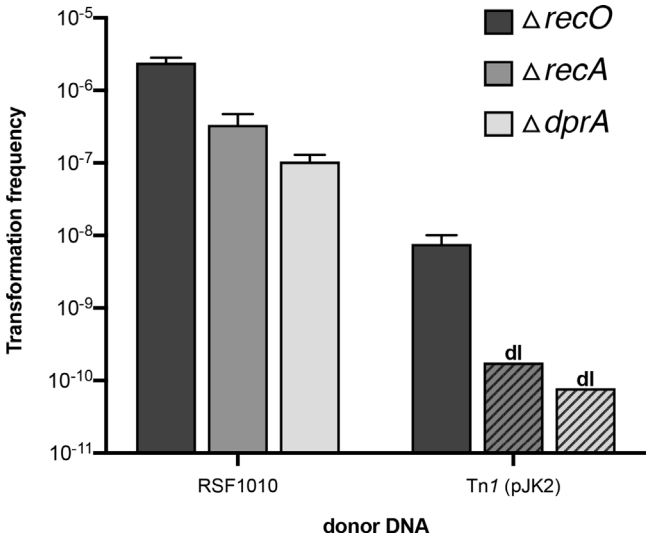

Fig. 5. Transformation frequencies of *A. baylyi* mutant strains (Δ*recO*, Δ*recA* or Δ*dprA*) by circular donor DNA substrates (RSF1010 or pJK2). Bars represent the mean with standard deviation from three to five experiments. Striped bars indicate the detection limit (dl) when no transformation or transposition events were observed.

Δ*sbcCD* strain (Supplemental Information: Supplemental Results and Fig. 4a). To further characterize the distribution bias, we determined the total number of TSD consensus sequence sites and their positions across the *A. baylyi* chromosome. The TSD consensus sequence positions (n=34863) followed a normal distribution, indicated by a small difference between the median and mean (0.16%) relative to genome size. Although the incidence of TSD consensus sequence hits increases significantly along the origin–terminus axis of replication (Fig. 4b), even the highest increase in hit counts (30%) does not explain why we observed more than 80% of the verified Tn*1* insertions in a region representing only 5% of the ADP1 chromosome (Fig. 4c).

A comparable transposon insertion bias has been observed previously, although not in the context of natural transformation. Tn*917* is a Tn*3*-like transposon in Gram-positive bacteria and preferentially inserts at the terminus in *B. subtilis* [43] and *Entercoccus faecalis* [44], but not in staphylococci [45, 46]. The bias is less strong in *B. subtilis* cells lacking functions involved in postreplicational chromosome segregation (RipX, SpoIIIE) or lacking the replication termination protein RTP [43]. In *B. subtilis*, *codV* and *ripX* encode the *dif*-directed chromosome partitioning recombinase often termed XerCD in Gram-negative bacteria [47]. We hypothesized that the absence of XerCD would alter the observed insertion bias of Tn*1* in *A. baylyi*. We naturally transformed an ADP1 Δ*xerC* mutant by pJK2 donor DNA but did not obtain any transformants (detection limit: 2.2×10^{-10}; n=3). The reason for this result is unclear. Further experimental investigation was impeded by the genetic limitations of the employed recipient strain: *A. baylyi* carries no gene homologous to *rtp* (*tus* in *E. coli*) [24], and the orthologue of *spoIIIE* (*ftsK*) is essential in *A. baylyi* [42]. Using RSF1010 as donor DNA for the *A. baylyi*Δ*xerC* strain, the transformation frequency was $(1.4\pm0.7)\times10^{-6}$ (n=3), which was only four times decreased compared to the wild-type.

Finally, we hypothesized that the distribution of Tn*1* insertions would be different using artificial transformation (electroporation). During electroporation, circular double-stranded DNA is directly delivered to the cytoplasm. However, no ampicillin-resistant isolates were obtained after electroporation of *A. baylyi* by circular pJK2 DNA (detection limit: 3.6×10^{-10}; n=3). In contrast, electroporation by RSF1010 (n=1) resulted in streptomycin-resistant transformants at a frequency of 5.6×10^{-5}, which was 10 times higher than the frequency observed with natural transformation of *A. baylyi*. The reason for the distribution bias of transposition events remains unknown.

Requirement of transposon genes for transposition

Tn*1* carries two genes involved in transposition: *tnpA* is the transposase gene, and *tnpR* encodes the resolvase for cointegrate intermediates created by TnpA. TnpR also acts as a repressor for both *tnpA* and *tnpR* [48] (Fig. 1). We hypothesized that transposition and cointegrate resolution during natural transformation were conferred by the *tnpA* and *tnpR* gene products encoded by the donor DNA and that deletion of these genes would decrease transposant frequency. We removed the *tnpA* gene from Tn*1* of pJK2, and natural transformation of *A. baylyi* by the resulting plasmid pJKH1 yielded no ampicillin-resistant transformants (detection limit: 5.2×10^{-11}; Fig. 3), confirming that *tnpA* of Tn*1* but no recipient functions act as transposase for Tn*1*.

We also used plasmid pJK7 (carrying Tn*1*Δ*tnpR*) as donor DNA for the transformation of *A. baylyi* and the transformation frequency was similar to that obtained with pJK2 [$(3.5\pm3.5)\times10^{-8}$; Fig. 3]. We PCR-screened 150 transformant isolates that were stably resistant after three consecutive streakouts and found that Tn*1* and pJK2 vector backbone was detectable in all isolates. This transformant type was not detected with pJK2 but is consistent with unresolved cointegrate intermediates. We conclude that in the absence of TnpR, the derepressed TnpA efficiently recombined Tn*1* with the recipient and formed cointegrates that remained unresolved. Recipient functions such as RecA may contribute to their eventual resolution, but, taken together, these findings indicate that the main resolvase is the TnpR encoded by the donor DNA.

Formation of double-stranded cytoplasmic intermediates

Taken together, the presented results demonstrate that *tnpA* and *tnpR* genes as well as $bla_{\text{TEM-2-}}$ in the transient transformants of group 2 described above are expressed after uptake of DNA into the cytoplasm. Moreover, our data suggest that a circular intermediate is involved in the first (cointegration) step of transposition. However, the donor DNA is transported as linear single-strands into the cytoplasm

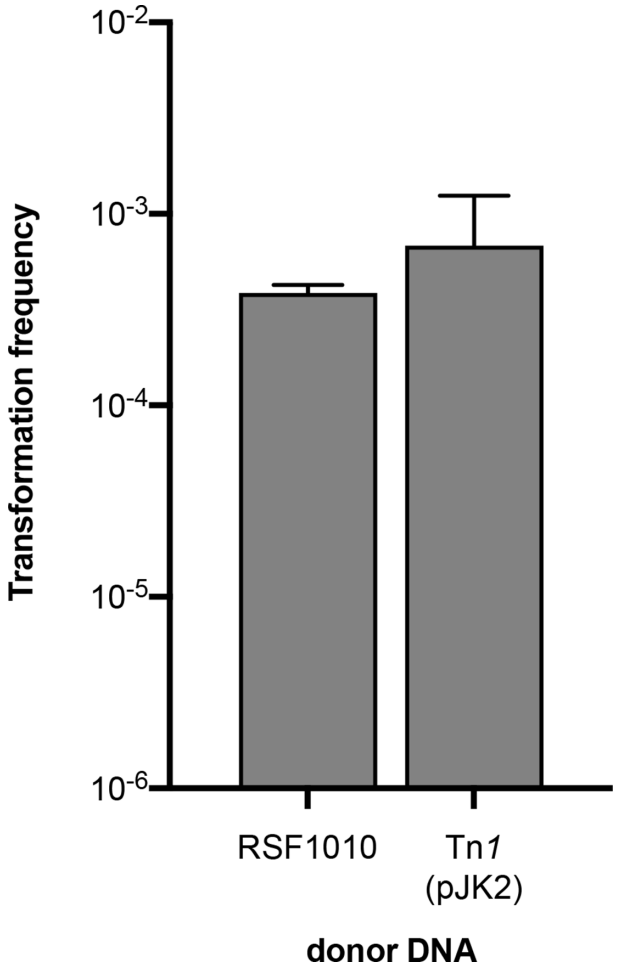

Fig. 6. Transformation frequencies of the Δ*recBCD* Δ*sbcCD* strain using plasmid DNA substrates (RSF1010 or pJK2; *n*=5). Bars represent the mean with standard deviation.

during natural transformation [49, 50]. We hypothesized that the uptake of two complementary DNA single-strands is required for double-strand formation by hybridization. The resulting linear DNA double-strands, however, would be susceptible to degradation by exonucleases such as RecBCD [51, 52-]. Subsequent circularization by annealing at overlapping ends, followed by fill-in DNA synthesis or gap repair, would protect these double-strands from exonucleolytic degradation [53].

In *B. subtilis*, *recO* is required for efficient plasmid transformation [54], which can be explained by the activity of RecO to hybridize complementary DNA single-strands [55]. To investigate the role of RecO in double-strand formation in *A. baylyi,* we transformed a Δ*recO* strain by circular pJK2 DNA. The resulting frequency of ampicillin-resistant transformants was eight times lower than in wild-type *A. baylyi* [(7.7±2.4)×10^{-9}; Fig. 5]. With RSF1010 as donor DNA, the frequency was (2.4±0.4)×10^{-6}, which was two times lower than in wild-type *A. baylyi* (Fig. 5).

Unlike *recO*, the *recA* gene is not required for plasmid transformation of *B. subtilis* [54], suggesting that RecO is sufficient to restore circular plasmids from two complementary single-strands in this organism. We tested whether this was also the case in *A. baylyi*. In a Δ*recA* mutant transformed by circular RSF1010 DNA, plasmid transformants occurred at a frequency of (3.4±1.3)×10^{-7} (Fig. 5), which was ~16 times lower than in wild-type *A. baylyi*. With pJK2 as donor DNA, no transformants were obtained (detection limit: 1.8×10^{-10}; Fig. 5). This result suggests an unexpected role of RecA in plasmid circularization in *A. baylyi*.

The DprA (DNA processing A) protein is thought to load incoming DNA single-strands with RecA protein [56]. In many naturally competent bacteria, deletion of *dprA* abolishes or severely reduces natural transformation [27, 57–60]. We investigated whether natural transformation by circular extrachromosomal DNA was affected in an *A. baylyi* Δ*dprA* mutant. Using pJK2 as donor DNA, the transformation frequencies of the Δ*dprA* strain dropped below detection limit (7.8×10^{-11}) (Fig. 5). With RSF1010, the transformation frequency was (1.4±0.2)×10^{-7} and thus approximately 50 times lower than that of the wild-type (Fig. 5). These frequencies are comparable with those using the Δ*recA* strain as recipient. The results support the assumption that DprA acts upstream of the RecA recombination pathway. They also demonstrate that plasmid transformation (RSF1010) is not abolished in the absence of DprA.

Our findings show that deficiencies of RecA, DprA and, to a lesser degree, RecO reduce transformation of circular extrachromosomal DNA in *A. baylyi*, suggesting a role of these functions in plasmid circularization. In our experiments, the non-replicative plasmid pJK2 generally yielded poorer transformation frequencies than the replicative plasmid RSF1010. We cannot exclude the possibility that some or all of the investigated genes also modulate the transposition efficiency in addition to double-strand conversion and circularization.

Next we tested whether circularization is a requirement for transposons to jump during natural transformation. We used an inverse PCR product of pJK2 as donor DNA with Tn*1* approximately in the centre (pJK2-PCR). The substrate was agarose gel-purified to eliminate all traces of contaminating template DNA (confirmed by PCR; Supplemental Information: Supplemental Results). Using this linear DNA substrate for transformation of wild-type *A. baylyi*, no ampicillin-resistant transformants were obtained (detection limit: 1.6×10^{-10}, Fig. 3), suggesting that pJK2-PCR is insufficient to produce both transient transformants and transposants, presumably due to the cytoplasmic instability of linear double-stranded intermediates.

Antagonistic activity of RecBCD

Cytoplasmic linear double-stranded DNA is target for degradation by the RecBCD exonuclease in many bacteria [52] and the absence of the nuclease may protect linear intermediates and enhance plasmid circularization. In *A. baylyi*, RecBCD is thought to destroy donor DNA following uptake into the

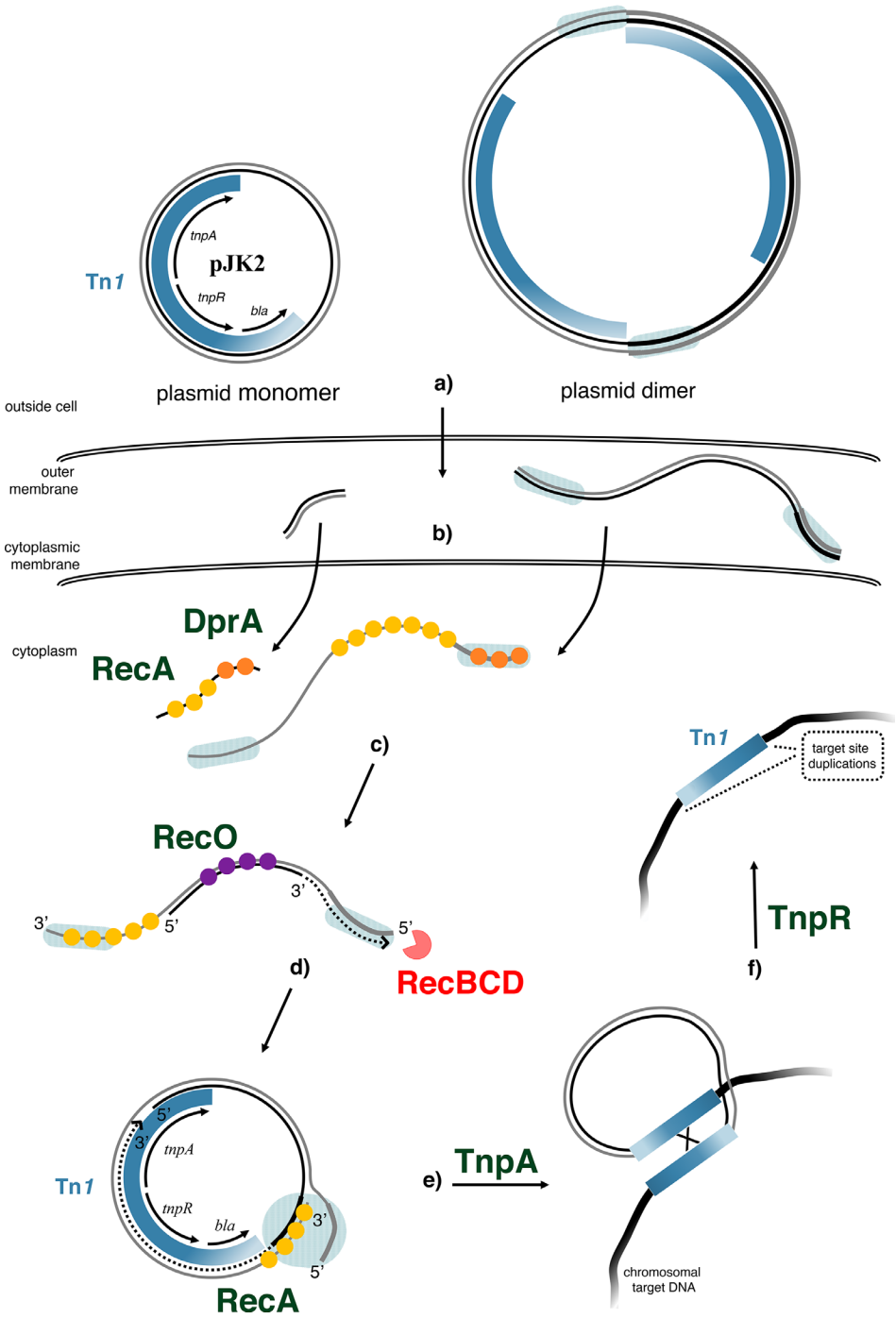

Fig. 7. Model of Tn*1* transposition during natural transformation of *A. baylyi*. Proteins with beneficial or necessary functions are represented in green, and proteins with antagonistic functions are red; exemplary sequence segments providing homology are indicated by a shaded background. (a) Circular monomeric as well as sporadic dimeric forms of plasmid DNA are available for uptake into the periplasm. (b) DNA single-strands are taken up into the cytoplasm and protected from degradation by DprA (orange). DprA also loads RecA (yellow) onto single-stranded DNA. (c) RecO (purple) is involved in the annealing of DNA single-strands [55], in initiating or improving gap repair as part of RecFOR or RecOR [63, 64], or both. The linear double-stranded molecule is susceptible to degradation by RecBCD exonuclease (red). (d) The RecA-loaded DNA 3'-single-strand end invades the double-stranded fragment at its terminal homology, and circularization of the donor plasmid is completed by DNA repair and gap synthesis. (e) From the established circularized plasmid, the genes necessary for transposition (*tnpA*, *tnpR*) are expressed, and TnpA together with a recipient DNA polymerase form a transposon–target DNA cointegrate and generate the TSD. (f) TnpR resolves the cointegrate, and the recipient chromosome contains now a copy of Tn*1*.

cytoplasm after the creation of double-stranded ends during homologous recombination [30]. However, in the context of plasmid transformation, in *B. subtilis* strains lacking AddAB, the functional equivalent of RecBCD, transformation frequencies are somewhat reduced [61]. To investigate the effect of RecBCD deficiency on plasmid transformation in *A. baylyi*, we transformed a Δ*recBCD* Δ*sbcCD* strain by RSF1010 and obtained a 70 times increased transformation frequency [$(3.9\pm0.4)\times10^{-5}$] compared with the wild-type (Fig. 6). We also transformed the Δ*recBCD* Δ*sbcCD* strain by Tn*1*-containing donor substrates. Using a gel-purified linear pJK2-PCR substrate, no transformants were obtained (detection limit: 4.9×10^{-10}; n=3), strongly suggesting that a circular intermediate is required for transposition and transformation. With circular pJK2 donor DNA the frequency of ampicillin-resistant transformants was $(6.8\times\pm5.6)\times10^{-4}$ (Fig. 6), which was four orders of magnitude higher than that of the wild-type. Analysis of 40 ampicillin-resistant isolates revealed stable resistance even after repeated recultivation. PCR analyses verified the presence of Tn*1* and pJK2 vector backbone DNA in all isolates and circular pJK2 plasmid DNA could be isolated from cell material of restreaks, indicating extrachromosomal DNA rather than cointegrates. No transposants were identified during our standard screening, but a transformational screening approach revealed 14 unique chromosomal insertions (Supplemental Information: Supplemental Results and Table S3). These results were unexpected, and we concluded that established pJK2 replicated relatively stably in *A. baylyi* in the absence of RecBCD. The parental plasmid of pJK2, pACYC184 [33], propagates as a theta replicon in *E. coli* and in other *Enterobacteriaceae* [62]. It is possible that absence of RecBCD allows rolling circle replication of pACYC184 in *A. baylyi*, as in *E. coli* RecBCD-deficient mutants [62]. In wild-type *E. coli*, the exonucleolytic activity of RecBCD is thought to degrade the nascent multimers of the rolling circle, forcing the plasmid into theta replication. In contrast, loss of RecBCD allows rolling circle replication [62].

A model for natural transformation by transposons

In this study we experimentally verify that bacteria can acquire transposons horizontally through transposition in the course of natural transformation, as observed previously for a Tn*21* transposon [19]. In control experiments, we investigated the circularization of a replicative plasmid in *A. baylyi* during transformation, which has been studied before in *B. subtilis* [54]. Our results indicate differences in plasmid transformation between the two species. In contrast to our results, absence of RecA in *B. subtilis* did not affect plasmid establishment; instead RecO protein was required for that process [54].

Based on our findings, we propose a model for plasmid transformation and transposition in *A. baylyi* (Fig. 7). We suggest that sporadic dimeric forms of plasmid DNA with redundant ends are the main substrate for cytoplasmic donor DNA circularization. To initiate circularization, a small single-strand fragment is annealed with a large dimeric complementary strand with 5′- and 3′-overhangs. DNA fill-in synthesis converts the 5′-overhang into a double-strand (using the 3′-recessed end as primer), while the 3′-overhang is charged with RecA protein. It is consistent with our findings that DprA has a RecA-loading function [56]. The resulting nucleoprotein filament can undergo homology search. When it finds the homology of the redundant double-stranded end, the result is a circular intermediate with a displaced strand, and textbook DNA repair and gap synthesis generate a circular double-strand. This model is supported by lack of transformants with linear pJK2-PCR as donor DNA, since this substrate did not contain dimeric DNA molecules. The resulting circular double-stranded intermediate is temporally protected from DNA degradation (Fig. 7). Finally, the *tnpA* and *tnpR* genes are expressed and can lead to transposition of Tn*1*.

Is circular double-stranded DNA in general a necessary requirement for transposition in the course of natural transformation? Probably not. Domingues *et al.* obtained transposants using chromosomal DNA for natural transformation of *A. baylyi* [19]. Hypothetically, such DNA can form circular intermediates at direct repeats, and transposons surrounded by direct repeats may be stabilized through DNA circularization. It is also conceivable that Chi sequences surrounding the transposon protect the double-stranded intermediate from exonucleolytic degradation [51].

To put the results of this study into broader perspective, we employed a published transposon-containing plasmid as donor DNA for transformation of ADP1. The pACYC184 derivative pTn*4401* (15.6 kbp) [35] carries the replicative transposon Tn*4401* (~10 kbp) of the Tn*3*-family that contains the carbapenemase gene bla_{KPC-2} [22]. Ampicillin-resistant transformants formed at a frequency of $(1.5\pm1.2)\times10^{-9}$ (Fig. 3), which was 40 times lower than the frequency observed with pJK2 DNA. Among 60 investigated transformants, no transposants were found (detection limit: 9.8×10^{-11}). Several explanations for the lack of transposition of Tn*4401* are conceivable: the MIC conferred by KPC-2 may be too low to detect transposants in this organism. The plasmid size possibly reduces the dimer/monomer ratio. Alternatively, the repression of *tnpA* may be tighter in Tn*4401* than in Tn*1*. Taken together, this result shows that additional constraints exist for transposition during natural transformation, and further investigations are needed.

In conclusion, we showed that transposition of Tn*1* in the course of natural transformation occurs at biologically relevant frequencies. Our results open up the possibility that transposable elements can even spread from dead cells, where fully heterologous, transposon-containing free DNA can transform naturally competent bacteria, albeit at low frequencies. Transposons play an important role in the dissemination of multi-drug resistance, and the identification of both the transferred resistance genes and the genetic context that was transferred is crucial to understand AMR spread.

Funding information
J. K. received a project stipend from The Norwegian Pharmaceutical Society. K. H. was funded by the Research Council of Norway (grant number 275672).

Acknowledgements
Plasmid pTn*4401* was a kind gift from Gaëlle Cuzon and Thierry Naas. We are grateful to João A. Gama for help with target site distribution and Kaare M. Nielsen and Sören Abel for helpful discussions.

Author contributions
K. H. conceived the project; J. K. performed the experiments; J. K. and K. H. analysed the data; J. K. and K. H. wrote the paper with input from P. J. J. and K. H.; and P. J. J. supervised the project. All authors approved the final version of the manuscript.

Conflicts of interest
The authors declare that there are no conflicts of interest.

References

1. von Wintersdorff CJ, Penders J, van Niekerk JM, Mills ND, Majumder S *et al*. Dissemination of antimicrobial resistance in microbial ecosystems through horizontal gene transfer. *Front Microbiol* 2016;7:173.
2. Cassini A, Högberg LD, Plachouras D, Quattrocchi A, Hoxha A *et al*. Attributable deaths and disability-adjusted life-years caused by infections with antibiotic-resistant bacteria in the EU and the European Economic Area in 2015: a population-level modelling analysis. *Lancet Infect Dis* 2019;19:56–66.
3. Thomas CM, Nielsen KM. Mechanisms of, and barriers to, horizontal gene transfer between bacteria. *Nat Rev Microbiol* 2005;3:711–721.
4. Lorenz MG, Wackernagel W. Bacterial gene transfer by natural genetic transformation in the environment. *Microbiol Rev* 1994;58:563–602.
5. Johnston C, Martin B, Fichant G, Polard P, Claverys J-P *et al*. Bacterial transformation: distribution, shared mechanisms and divergent control. *Nat Rev Microbiol* 2014;12:181–196.
6. Tacconelli E, Carrara E, Savoldi A, Harbarth S, Mendelson M *et al*. Discovery, research, and development of new antibiotics: the WHO priority list of antibiotic-resistant bacteria and tuberculosis. *Lancet Infect Dis* 2018;18:318–327.
7. Lerminiaux NA, Cameron ADS. Horizontal transfer of antibiotic resistance genes in clinical environments. *Can J Microbiol* 2019;65:34–44.
8. Domingues S, Rosário N, Cândido Â, Neto D, Nielsen KM *et al*. Competence for Natural Transformation Is Common among Clinical Strains of Resistant *Acinetobacter* spp. *Microorganisms* 2019;7:E30
9. Traglia GM, Place K, Dotto C, Fernandez JS, Montaña S *et al*. Interspecies DNA acquisition by a naturally competent *Acinetobacter baumannii* strain. *Int J Antimicrob Agents* 2019;53:483–490.
10. Liebert CA, Hall RM, Summers AO. Transposon Tn*21*, flagship of the floating genome. *Microbiol Mol Biol Rev* 1999;63:507–522.
11. Carattoli A. Resistance plasmid families in *Enterobacteriaceae*. *Antimicrob Agents Chemother* 2009;53:2227–2238.
12. Partridge SR, Kwong SM, Firth N, Jensen SO. Mobile genetic elements associated with antimicrobial resistance. *Clin Microbiol Rev* 2018;31:UNSP:e00088–17.
13. Tansirichaiya S, Rahman MA, Roberts AP. The transposon registry. *Mob DNA* 2019;10:40.
14. Hickman AB, Dyda F. Mechanisms of DNA transposition. *Microbiol Spectr* 2015;3:MDNA3-0034–3-2014.
15. Martínez T, Vázquez GJ, Aquino EE, Martínez I, Robledo IE *et al*. ISEcp1-mediated transposition of bla_{KPC} into the chromosome of a clinical isolate of *Acinetobacter baumannii* from Puerto Rico. *J Med Microbiol* 2014;63:1644–1648.
16. Sheppard AE, Stoesser N, Wilson DJ, Sebra R, Kasarskis A *et al*. Nested russian Doll-Like genetic mobility drives rapid dissemination of the carbapenem resistance gene bla_{KPC}. *Antimicrob Agents Chemother* 2016;60:3767–3778.
17. Brolund A, Rajer F, Giske CG, Melefors Ö, Titelman E *et al*. Dynamics of resistance plasmids in extended-spectrum-β-lactamase-producing *Enterobacteriaceae* during postinfection colonization. *Antimicrob Agents Chemother* 2019;63
18. Evans DR, Griffith MP, Sundermann AJ, Shutt KA, Saul MI *et al*. Systematic detection of horizontal gene transfer across genera among multidrug-resistant bacteria in a single Hospital. *eLife* 2020;9.
19. Domingues S, Harms K, Fricke WF, Johnsen PJ, da Silva GJ *et al*. Natural transformation facilitates transfer of transposons, integrons and gene cassettes between bacterial species. *PLoS Pathog* 2012;8:e1002837.
20. Barbe V, Vallenet D, Fonknechten N, Kreimeyer A, Oztas S *et al*. Unique features revealed by the genome sequence of *Acinetobacter* sp. ADP1, a versatile and naturally transformation competent bacterium. *Nucleic Acids Res* 2004;32:5766–5779.
21. Nicolas E, Lambin M, Dandoy D, Galloy C, Nguyen N *et al*. The Tn*3*-family of replicative transposons. *Microbiol Spectr* 2015;3.
22. Naas T, Cuzon G, Villegas M-V, Lartigue M-F, Quinn JP *et al*. Genetic structures at the origin of acquisition of the beta-lactamase bla_{KPC} gene. *Antimicrob Agents Chemother* 2008;52:1257–1263.
23. Elliott KT, Neidle EL. *Acinetobacter baylyi* ADP1: transforming the choice of model organism. *IUBMB Life* 2011;63:1075–1080.
24. Harms K, Lunnan A, Hülter N, Mourier T, Vinner L *et al*. Substitutions of short heterologous DNA segments of intragenomic or extragenomic origins produce clustered genomic polymorphisms. *Proc Natl Acad Sci U S A* 2016;113:15066–15071.
25. Nielsen KM, van Weerelt MD, Berg TN, Bones AM, Hagler AN *et al*. Natural transformation and availability of transforming DNA to *Acinetobacter calcoaceticus* in soil microcosms. *Appl Environ Microbiol* 1997;63:1945–1952.
26. Overballe-Petersen S, Harms K, Orlando LAA, Mayar JVM, Rasmussen S *et al*. Bacterial natural transformation by highly fragmented and damaged DNA. *Proc Natl Acad Sci U S A* 2013;110:19860–19865.
27. Hülter N, Sørum V, Borch-Pedersen K, Liljegren MM, Utnes ALG *et al*. Costs and benefits of natural transformation in *Acinetobacter baylyi*. *BMC Microbiol* 2017;17:34.
28. Harms K, Wackernagel W. The RecBCD and SbcCD DNases suppress homology-facilitated illegitimate recombination during natural transformation of *Acinetobacter baylyi*. *Microbiology* 2008;154:2437–2445.
29. Harms K, Schön V, Kickstein E, Wackernagel W. The RecJ DNase strongly suppresses genomic integration of short but not long foreign DNA fragments by homology-facilitated illegitimate recombination during transformation of *Acinetobacter baylyi*. *Mol Microbiol* 2007;64:691–702.
30. Kickstein E, Harms K, Wackernagel W. Deletions of recBCD or recD influence genetic transformation differently and are lethal together with a recJ deletion in *Acinetobacter baylyi*. *Microbiology* 2007;153:2259–2270.
31. Hanahan D. Studies on transformation of *Escherichia coli* with plasmids. *J Mol Biol* 1983;166:557–580.
32. Romanowski G, Lorenz MG, Wackernagel W. Use of polymerase chain reaction and electroporation of *Escherichia co*li to monitor the persistence of extracellular plasmid DNA introduced into natural soils. *Appl Environ Microbiol* 1993;59:3438–3446.
33. Chang AC, Cohen SN. Construction and characterization of amplifiable multicopy DNA cloning vehicles derived from the P15A cryptic miniplasmid. *J Bacteriol* 1978;134:1141–1156.
34. Scholz P, Haring V, Wittmann-Liebold B, Ashman K, Bagdasarian M *et al*. Complete nucleotide sequence and gene organization of the broad-host-range plasmid RSF1010. *Gene* 1989;75:271–288.
35. Cuzon G, Naas T, Nordmann P. Functional characterization of Tn*4401*, a Tn*3*-based transposon involved in bla_{KPC} gene mobilization. *Antimicrob Agents Chemother* 2011;55:5370–5373.

36. Singer JT, van Tuijl JJ, Finnerty WR. Transformation and mobilization of cloning vectors in *Acinetobacter* spp. *J Bacteriol* 1986;165:301–303.
37. Crooks GE, Hon G, Chandonia J-M, Brenner SE. Weblogo: a sequence logo generator. *Genome Res* 2004;14:1188–1190.
38. Dower WJ, Miller JF, Ragsdale CW. High efficiency transformation of *E. coli* by high voltage electroporation. *Nucleic Acids Res* 1988;16:6127–6145.
39. Seringhaus M, Kumar A, Hartigan J, Snyder M, Gerstein M *et al*. Genomic analysis of insertion behavior and target specificity of mini-Tn*7* and Tn*3* transposons in *Saccharomyces cerevisiae*. *Nucleic Acids Res* 2006;34:e57.
40. Davies CJ, Hutchison CA. Insertion site specificity of the transposon Tn*3*. *Nucleic Acids Res* 1995;23:507–514.
41. Hülter N, Wackernagel W. Double illegitimate recombination events integrate DNA segments through two different mechanisms during natural transformation of *Acinetobacter baylyi*. *Mol Microbiol* 2008;67:984–995.
42. de Berardinis V, Vallenet D, Castelli V, Besnard M, Pinet A *et al*. A complete collection of single-gene deletion mutants of *Acinetobacter baylyi* ADP1. *Mol Syst Biol* 2008;4:174.
43. Shi Q, Huguet-Tapia JC, Peters JE. Tn*917* targets the region where DNA replication terminates in *Bacillus subtilis,* highlighting a difference in chromosome processing in the firmicutes. *J Bacteriol* 2009;191:7623–7627.
44. Garsin DA, Urbach J, Huguet-Tapia JC, Peters JE, Ausubel FM *et al*. Construction of an *Enterococcus faecalis* Tn*917*-mediated-gene-disruption library offers insight into Tn*917* insertion patterns. *J Bacteriol* 2004;186:7280–7289.
45. Grueter L, Koenig O, Laufs R. Transposon mutagenesis in *Staphylococcus epidermidis* using the *Enterococcus faecalis* transposon Tn*917*. *FEMS Microbiol Lett* 1991;66:215–218.
46. Bae T, Banger AK, Wallace A, Glass EM, Aslund F *et al*. *Staphylococcus aureus* virulence genes identified by *bursa aurealis* mutagenesis and nematode killing. *Proc Natl Acad Sci U S A* 2004;101:12312–12317.
47. Castillo F, Benmohamed A, Szatmari G. Xer site specific recombination: double and single recombinase systems. *Front Microbiol* 2017;8:453.
48. Casadaban MJ, Chou J, Cohen SN. Overproduction of the Tn*3* transposition protein and its role in DNA transposition. *Cell* 1982;28:345–354.
49. Palmen R, Vosman B, Buijsman P, Breek CK, Hellingwerf KJ *et al*. Physiological characterization of natural transformation in *Acinetobacter calcoaceticus*. *J Gen Microbiol* 1993;139:295–305.
50. de Vries J, Wackernagel W. Integration of foreign DNA during natural transformation of *Acinetobacter* sp. by homology-facilitated illegitimate recombination. *Proc Natl Acad Sci U S A* 2002;99:2094–2099.
51. Dillingham MS, Kowalczykowski SC. RecBCD enzyme and the repair of double-stranded DNA breaks. *Microbiol Mol Biol Rev* 2008;72:642–671.
52. Amundsen SK, Neiman AM, Thibodeaux SM, Smith GR. Genetic dissection of the biochemical activities of RecBCD enzyme. *Genetics* 1990;126:25–40.
53. Saunders CW, Guild WR. Monomer plasmid DNA transforms *Streptococcus pneumoniae*. *Mol Gen Genet* 1981;181:57–62.
54. Kidane D, Carrasco B, Manfredi C, Rothmaier K, Ayora S *et al*. Evidence for different pathways during horizontal gene transfer in competent *Bacillus subtilis* cells. *PLoS Genet* 2009;5:e1000630.
55. Ryzhikov M, Gupta R, Glickman M, Korolev S. RecO protein initiates DNA recombination and strand annealing through two alternative DNA binding mechanisms. *J Biol Chem* 2014;289:28846–28855.
56. Mortier-Barrière I, Velten M, Dupaigne P, Mirouze N, Piétrement O *et al*. A key presynaptic role in transformation for a widespread bacterial protein: DprA conveys incoming ssDNA to RecA. *Cell* 2007;130:824–836.
57. Karudapuram S, Zhao X, Barcak GJ. DNA sequence and characterization of Haemophilus influenzae *dprA*$^+$, a gene required for chromosomal but not plasmid DNA transformation. *J Bacteriol* 1995;177:3235–3240.
58. Ando T, Israel DA, Kusugami K, Blaser MJ. HP0333, a member of the *dprA* family, is involved in natural transformation in *Helicobacter pylori*. *J Bacteriol* 1999;181:5572–5580.
59. Bergé M, Mortier-Barrière I, Martin B, Claverys J-P. Transformation of *Streptococcus pneumoniae* relies on DprA- and RecA-dependent protection of incoming DNA single strands. *Mol Microbiol* 2003;50:527–536.
60. Friedrich A, Prust C, Hartsch T, Henne A, Averhoff B *et al*. Molecular analyses of the natural transformation machinery and identification of pilus structures in the extremely thermophilic bacterium *Thermus thermophilus* strain HB27. *Appl Environ Microbiol* 2002;68:745–755.
61. Fernández S, Kobayashi Y, Ogasawara N, Alonso JC. Analysis of the *Bacillus subtilis recO* gene: RecO forms part of the RecFLOR function. *Mol Gen Genet* 1999;261:567–573.
62. Cohen A, Clark AJ. Synthesis of linear plasmid multimers in *Escherichia coli* K-12. *J Bacteriol* 1986;167:327–335.
63. Morimatsu K, Kowalczykowski SC. RecFOR proteins load RecA protein onto gapped DNA to accelerate DNA strand exchange: a universal step of recombinational repair. *Mol Cell* 2003;11:1337–1347.
64. Sakai A, Cox MM. RecFOR and RecOR as distinct RecA loading pathways. *J Biol Chem* 2009;284:3264–3272.

Edited by: J. Stülke and K. Palmer

Paper III

Article

Discoveries

Piggybacking on niche-adaptation improves the maintenance of multidrug resistance plasmids

Julia Kloos[1#] (ORCID: 0000-0002-8773-3463), João A. Gama[1#] (ORCID: 0000-0003-0967-6616), Joachim Hegstad[1,2] (ORCID: 0000-0001-9173-7195), Ørjan Samuelsen[1,3] (ORCID: 0000-0002-5525-2614), Pål J. Johnsen[1*] (ORCID: 0000-0002-6455-6433)

[1]Department of Pharmacy, Faculty of Health Sciences, UiT The Arctic University of Norway, Tromsø, Norway; [2]Department of Microbiology and Infection Control, University Hospital of North Norway, Tromsø, Norway; [3]Norwegian National Advisory Unit on Detection of Antimicrobial Resistance, Department of Microbiology and Infection Control, University Hospital of North Norway, Tromsø, Norway.

[#]These authors contributed equally to this work.

[*]Corresponding author:
UiT The Arctic University of Norway
Department of Pharmacy
Faculty of Health Sciences
9037 Tromsø
Norway
Phone: +47 47688974
e-mail: paal.johnsen@uit.no

Abstract

The persistence of plasmids in bacterial populations represents a puzzling evolutionary problem with serious clinical implications due to their role in the ongoing antibiotic resistance crisis. Recently, major advancements have been made towards resolving this "plasmid paradox" but mainly in a non-clinical context. Here we propose an additional explanation for the maintenance of multidrug resistance (MDR) plasmids in clinical *Escherichia coli* strains. After co-evolving two MDR plasmids encoding last resort carbapenem resistance with an extraintestinal pathogenic *E. coli* strain, we observed that chromosomal media adaptive mutations in the global regulatory systems CCR (Carbon Catabolite Repression) and ArcAB (Aerobic Respiration Control) pleiotropically improved the maintenance of both plasmids. Mechanistically, a net downregulation of plasmid gene expression reduced the fitness cost. Our results suggest that global chromosomal transcriptional re-wiring during bacterial niche-adaptation may facilitate plasmid maintenance.

Introduction

Plasmids are self-replicating extrachromosomal elements that often decrease bacterial fitness due to the requirement of host functions for their own replication and spread (reviewed in [Baltrus 2013; San Millan and MacLean 2017]), although beneficial (or non-costly) plasmids have been reported (Enne et al. 2004; Monarrez et al. 2019). These genetic elements play a key role in the evolution and spread of antibiotic resistance determinants in bacterial populations world-wide (Carattoli 2013; Partridge et al. 2018). This is particularly true for nosocomial pathogens in the family *Enterobacteriaceae* including *Escherichia coli* and *Klebsiella pneumoniae* where resistance determinants of high clinical relevance such as carbapenemases and extended-spectrum β-lactamases are frequently encoded on plasmids (Mathers et al. 2015; Rozwandowicz et al. 2018).

From an evolutionary perspective, persistence of plasmids in bacterial populations has for a long time been a conundrum often referred to as the "plasmid paradox" (Stewart and Levin 1977; Harrison and Brockhurst 2012). This paradox can be resolved in at least five different ways. First, maintenance can be ensured by positive selection for plasmid encoded traits (Gullberg et al. 2014; San Millan et al. 2014; Stevenson et al. 2018). But, if too beneficial, positively selected traits may be captured by the chromosome rendering the plasmid obsolete and consequently lost, as demonstrated theoretically (Bergstrom et al. 2000) and experimentally (Kottara et al. 2018). Second, mathematical models predict that high rates of horizontal plasmid transfer can counteract segregational plasmid loss and the competitive disadvantage of plasmid-carriers (Stewart and Levin 1977). *In vitro* studies report that conditions exist where conjugation frequencies are indeed extremely high (Dionisio et al. 2002; Lopatkin et al. 2017). It is however generally accepted that conjugation is a costly process (San Millan and MacLean 2017) and evolution towards increased conjugation rates does not constitute a general solution of the paradox (Turner et al. 1998; Dahlberg and Chao 2003; Porse et al. 2016). Third, transmissible plasmids under purifying selection may "escape" their host and enter less hostile environments. This has been termed cross-ecotype transfer (Bergstrom et al. 2000). Fourth, plasmid stability can evolve through improved replication control (Wein et al. 2019) and the acquisition of addiction mechanisms (Loftie-Eaton et al. 2016). Fifth, and perhaps most prominent, negative effects on host fitness can be mitigated through compensatory evolution (San Millan and MacLean 2017), and plasmids may even become beneficial (Bouma and Lenski 1988; Dionisio et al. 2005; Starikova et al. 2013; Loftie-Eaton et al. 2017). Fitness compensating mutations have been demonstrated to occur both in the presence and absence of selective agents and identified on bacterial chromosomes (San Millan et al. 2014; Harrison et al. 2015; Loftie-Eaton et al. 2017), on plasmids (De Gelder et al. 2008; Sota et al. 2010; Porse et al. 2016), or both (Dahlberg and Chao 2003; Starikova et al. 2013; Bottery et al. 2017).

The last ten years have brought significant advancements in the understanding of plasmid-host evolutionary dynamics. However, it is not clear how the different solutions to the plasmid paradox as listed above are relevant for clinical strains and plasmids since the majority of published work has

focused on emblematic laboratory strains and/or environmental bacteria. In this report we asked if and how two clinical plasmids encoding the VIM-1 and NDM-1 carbapenemases affected fitness of an *E. coli* strain isolated from a patient, before and after experimental evolution. We observed striking parallel evolution of the CCR (Carbon Catabolite Repression) and ArcAB (Aerobic Respiration Control) regulatory systems in the chromosomes of both plasmid-containing and plasmid-free populations resulting in adaptation to the experimental conditions. No apparent plasmid-specific compensatory mutations were identified across evolved populations and the plasmid sequences were largely unchanged. Yet, the initial plasmid costs were ameliorated in the co-evolved cultures. We demonstrate that fitness amelioration resulted from "piggybacking" on the clinical strains' adaptation to a new niche, suggesting a novel solution to the "plasmid paradox".

Results

Plasmid acquisition moderately reduces fitness in a clinical *E. coli* host strain. To mimic the acquisition of plasmid-mediated resistance to a last resort antibiotic, we transferred each of the two carbapenemase-producing clinical plasmids pG06-VIM-1 from *K. pneumoniae* (bla_{VIM-1} [Samuelsen et al. 2011]) and pK71-77-1-NDM from *E. coli* (bla_{NDM-1} [Samuelsen et al. 2011]) into an Extraintestinal Pathogenic *E. coli* sequence type (ST) 537 (strain ExPEC [Bengtsson et al. 2012]; Supplementary Table 1). pG06-VIM-1 is non-conjugative (Di Luca et al. 2017) while pK71-77-1-NDM is conjugative (Gama et al. 2020). Plasmid transfer resulted in strains ExPEC+VIM and ExPEC+NDM, both otherwise isogenic to strain ExPEC (Figure 1a and Supplementary Table 1).

We measured the cost of the newly introduced clinical plasmids in head-to-head competition experiments lasting ~40 generations. Acquisition of either pG06-VIM-1 or pK71-77-1-NDM affected host fitness similarly, resulting in moderate but significant costs of 5.3% and 5.5%, respectively (one-sample *t*-test, two-sided: ExPEC+VIM: $w = 0.947 \pm 0.002$, $P < 0.001$; ExPEC+NDM: $w = 0.945 \pm 0.012$, $P = 0.017$; Figure 1b and Supplementary Table 6).

Strong parallel evolution in global *E. coli* regulators occurs independently of plasmid-carriage. Four replicate lineages of the plasmid-containing strains ExPEC+VIM and ExPEC+NDM as well as the plasmid-free strain ExPEC were serially transferred for ~300 generations (over which the plasmids are stably maintained [Di Luca et al. 2017; Gama et al. 2020]). This resulted in 12 evolved populations (Pop 1-4_{VIM}, Pop 5-8_{NDM} and Pop 9-12; Figure 1c and Supplementary Table 1), that we deep sequenced to identify putative mutations mitigating the fitness costs of plasmid carriage.

At the population level, no changes were identified in the evolved plasmid sequences except in Pop 5_{NDM} harboring a deletion in the evolved pK71-77-1-NDM (Supplementary information section IIIa, Supplementary Table 3 and Supplementary Figure 1). However, all 12 evolved lineages revealed patterns of extensive parallel evolution in chromosomal genes that are directly or indirectly linked to the CCR and the ArcAB regulatory systems of *E. coli* (Figure 2a). In total, 68 different mutations were identified in genes *cpdA* (3',5'-**c**yclic adenosine monophosphate (cAMP) **p**hospho**d**iesterase), *crp* (**c**AMP **r**eceptor **p**rotein; DNA-binding transcriptional regulator), *arcA* (**a**erobic **r**espiration **c**ontrol protein; DNA-binding transcriptional regulator) and *arcB* (**a**erobic **r**espiration **c**ontrol sensor protein; histidine kinase). Evolved lineages had on average acquired eight variations in these genes ranging from three (Pop 5_{NDM}) to 18 (Pop 6_{NDM}) different mutations for individual populations (Supplementary Figure 2). Our data revealed 25, 12, 23 and eight unique mutations in *arcA* (717 bp), *arcB* (2337 bp), *cpdA* (828 bp) *and crp* (633 bp), respectively (Supplementary Figure 2). Among these unique mutations in the respective target genes, 12, one, three and three were found repeatedly across more than one evolved population. The majority of mutations in these genes were non-synonymous single nucleotide exchanges leading to amino acid substitutions (88%). Furthermore, Pop 2_{VIM} acquired mutations upstream and in the open reading

frame of *cyaA* (adenylate cyclase; cAMP synthesis). For a detailed list of mutations identified across evolved populations, including small indels, as well as mutations found in single populations, see Supplementary Table 4. Whereas *cpdA* and *arcA* were mutation targets in all 12 populations, *crp* and *arcB* were identified in ten and four populations, respectively (Figure 2a and Supplementary Figure 2). Surprisingly, the mutation profiles were not different in populations that co-evolved with any of the plasmids compared to the plasmid-free control populations, strongly suggesting that the observed mutational changes were not plasmid-specific. Genes of the CCR and ArcAB systems are indeed frequently reported as mutational targets for adaptive responses to the experimental growth conditions occurring during laboratory evolution experiments (Knoppel et al. 2018; Phaneuf et al. 2019).

Mutations in CCR and ArcAB regulatory systems pleiotropically mitigate the cost of pG06-VIM-1 and pK71-77-1-NDM carriage. Immediate acquisitions of pG06-VIM-1 and pK71-77-1-NDM reduced host fitness significantly (Figure 1b). We have previously demonstrated complete retention of the same plasmids following experimental evolution under the same antibiotic-free conditions (Di Luca et al. 2017; Gama et al. 2020). Since one of the plasmids was non-conjugative, we assumed that fitness amelioration by compensatory adaptation was the most likely route for the plasmids to persist in evolved populations. However, the sequencing data presented above revealed no apparent plasmid-specific compensatory mutations. Therefore, we hypothesized that adaptation to the growth conditions could have pleiotropic effects on the costs of plasmid carriage.

To test this hypothesis, we isolated a single clone from each evolved plasmid-carrying population (Pop 1-4_{VIM} and Pop 5-8_{NDM}) with mutations in both regulatory systems, CCR and ArcAB, since population sequencing data suggested that both systems were affected simultaneously (Figures 2a and 2b). In the selected Clones 1-4_{VIM} and Clones 5-8_{NDM}, Sanger and Illumina sequencing confirmed the presence of mutations as expected from population sequencing results and no further chromosomal or plasmid-located point mutations (Figure 1c and 2c; Supplementary information section I and IIIb, and Supplementary Table 1).

Here, we also identified large deletions in the evolved pK71-77-1-NDM for Clone 5_{NDM} and Clone 7_{NDM} (~8.8 kb and ~58.9 kb, respectively; Supplementary information section IIIb, Supplementary Table 3, Supplementary Figure 1), and susceptibility testing by disc diffusion phenotypically confirmed the deletions involving antibiotic resistance genes (Supplementary information section VI, Supplementary Table 8). The plasmid copy-number for pG06-VIM-1 and pK71-77-1-NDM before and after experimental evolution was unchanged (0.9-1.5 copies in all sequenced plasmid-carrying clones based on read coverage; Supplementary information section IIIb; Supplementary Table 5). Next, we attempted to isolate a set of spontaneous plasmid-free segregants of Clones 1-4_{VIM} and Clones 5-$8_{NDM,}$ to use in competition experiments, by screening for ampicillin-susceptible colonies. We obtained segregants for pG06-VIM-1 resulting in Clones 1-4, but not for pK71-77-1-NDM, which we confirmed by Sanger sequencing to have the niche-adaptive

mutations (Figure 1c). Illumina sequencing of Clones 2 and 3 verified that no chromosomal mutations were acquired during the curing procedure.

The costs of pG06-VIM-1-carriage in co-evolved Clones 1-4_{VIM} were assessed in head-to-head competitions with the respective plasmid-free isogenic strains (Clones 1-4) over ~40 generations. Our data show that the initial costs were significantly ameliorated to ≤ 1% in all four evolved backgrounds irrespective of the combination of chromosomal mutations in these clones (one-sample *t*-test, two-sided: Clone 1_{VIM}: 0.7% or $w = 0.993 \pm 0.002$, $P = 0.017$; Clone 2_{VIM}: 0.4% or $w = 0.996 \pm 0.001$, $P = 0.016$; Clone 3_{VIM}: 0.9% or $w = 0.991 \pm 0.0003$, $P = 0.001$ and Clone 4_{VIM}: 0.6% or $w = 0.994 \pm 0.002$, $P = 0.056$; one-way ANOVA assuming equal variances, df = 4, $P < 0.001$, followed by Dunnett's test: $P < 0.001$; Figure 3a and Supplementary Table 6). Illumina sequencing confirmed that the plasmid sequences in Clones 1-4_{VIM} were unchanged after evolution suggesting that the chromosomal mutations were responsible for the fitness mitigation. To further test this we introduced the ancestral pG06-VIM-1 into Clone 2 and Clone 3 carrying mutations in *arcA/cpdA* and *arcA/crp*, respectively, resulting in Clone 2+VIM and Clone 3+VIM (Figure 3b). Competition experiments with the isogenic, plasmid-free genetic backgrounds revealed a significant fitness increase compared to the original plasmid-host combination and an amelioration of the initial cost of harboring pG06-VIM-1 to 1.3% and 1%, respectively (one-sample *t*-test, two-sided: Clone 2+VIM: $w = 0.987 \pm 0.004$, $P = 0.026$; Clone 3+VIM: $w = 0.990 \pm 0.001$, $P = 0.002$; one-way ANOVA assuming equal variances, df = 2, $P < 0.001$, followed by Dunnett's test: $P < 0.001$; Figure 3b and Supplementary Table 6). To exclude that plasmid-specific adaptation in these pG06-VIM-1-co-evolved clones was responsible for the observed fitness amelioration, we introduced the ancestral pG06-VIM-1 into an isolated clone of Pop 12 (Clone 12+VIM; Figure 3d) and determined fitness as described above. In this background, which had evolved without a plasmid and acquired mutations in *arcA/cpdA*, the cost of pG06-VIM-1-carriage was also significantly reduced to ≤ 1% (one-sample *t*-test, two-sided: Clone 12+VIM: 0.9% or $w = 0.991 \pm 0.002$, $P = 0.009$, Figure 3d). While this was significantly different from the initial plasmid cost, it did not differ from the cost of ancestral pG06-VIM-1 in co-evolved Clones 2+VIM and 3+VIM (one-way ANOVA assuming equal variances, df = 3, $P < 0.001$, followed by Tukey's test; Supplementary Table 6).

Similarly, the initial fitness cost of 5.5% imposed by the ancestral pK71-77-1-NDM in strain ExPEC+NDM was significantly decreased in pG06-VIM-1-free segregants carrying this plasmid (one-sample *t*-test, two-sided: Clone 2+NDM: 2.4% or $w = 0.976 \pm 0.007$; $P = 0.025$; Clone 3+NDM: 2.7% or $w = 0.973 \pm 0.002$; $P = 0.002$; one-way ANOVA assuming equal variances, df = 2, $P = 0.006$, followed by Dunnett's test: $P = 0.006$ and $P = 0.010$, respectively; Figure 3c and Supplementary Table 6). Note that we did not obtain a plasmid-free background of Clones 5-8_{NDM} to test the fitness of pK71-77-1-NDM-co-evolved strains. The results from competition experiments with Clone 2+NDM and Clone 3+NDM carrying the ancestral pK71-77-1-NDM strongly suggest that the chromosomal mutations are responsible for partial fitness amelioration. We acknowledge that the

deletions in evolved plasmids of Clone 5_{NDM} and Clone 7_{NDM}, removing conjugation and resistance genes, could result in further fitness improvements as demonstrated previously (Turner et al. 2014; Porse et al. 2016).

We transformed the evolved pG06-VIM-1 from Clone 2_{VIM} into the ancestral ExPEC strain (Figure 3d) to test for adaptive changes occurring in plasmid sequences that could be undetected using short-read sequencing. The evolved pG06-VIM-1 affected the ancestral host significantly (one-sample *t*-test, two-sided: ExPEC+evVIM: 3.2% or $w = 0.968 \pm 0.005$, $P = 0.01$) being less costly than the ancestral pG06-VIM-1, but more costly in the ancestral than in an adapted background (one-way ANOVA assuming equal variances, df = 3, $P < 0.001$, followed by Tukey's test; Figure 3d and Supplementary Table 6). Some undetected plasmid mutations may reduce the cost of the evolved plasmid, however to a lesser extent than the mutations in CCR and ArcAB systems as demonstrated with Clone 12+VIM above.

Taken together, our data indicate clearly that the different mutations identified in the CCR and ArcAB regulatory systems are sufficient to improve plasmid maintenance. The usage of isogenic strains, distinguishable only by plasmid-encoded markers is however a limitation that could skew the accuracy of the fitness measurements because of plasmid loss or conjugation. Plasmid loss could lead to an over-estimation of the fitness cost, but during the ~40 generations of fitness measurement (Methods and Supplementary information section IV) all tested plasmids were stable (Supplementary Table 7) such that the effect of this parameter can be neglected. This is further corroborated by our inability to select any spontaneous pK71-77-1-NDM-free segregant. We also measured the conjugation efficiencies for pK71-77-1-NDM (12 hours) in additional experiments (Methods and Supplementary information section V), revealing small but significantly increased plasmid transfer frequencies in the adapted backgrounds (Supplementary Figure 3). This effect could lead to under-estimation of the fitness cost of pK71-77-1-NDM in evolved hosts. Nevertheless, we conclude that the mutations in the regulatory systems improve the maintenance of this plasmid, either directly reducing the fitness cost or through increased conjugative transfer.

Plasmid cost mitigation is linked specifically to the CCR system. To investigate the individual roles of the CCR and ArcAB systems on plasmid cost mitigation we measured plasmid costs in deletion mutants for *arcA, cpdA* and *crp* – the targeted loci for adaptation in our co-evolved clones. Unfortunately, genetic modifications using clinical strains are notoriously difficult and for these experiments we used deletion mutants of *E. coli* (K-12 derivatives) from the Keio collection (Baba et al. 2006). We introduced the ancestral pG06-VIM-1 into the individual deletion strains as well as the Keio parent strain (Datsenko and Wanner 2000) by electroporation, resulting in strains BW25113+VIM, BWΔ*cpdA*+VIM, BWΔ*arcA*+VIM and BWΔ*crp*+VIM (Supplementary information section I and Supplementary Table 1). We measured fitness of plasmid-carrying strains relative to their plasmid-free counterparts in head-to-head competitions as described above. As a general

observation, pG06-VIM-1 was less costly in BW25113 than in the clinical isolate (one-sample *t*-test, two-sided: 2.3% or $w = 0.977 \pm 0.005$, $P = 0.016$; Figure 4a and Supplementary Table 6). While deletion of *arcA* and *crp* had no significant effect on the fitness burden imposed by pG06-VIM-1 compared to BW25113+VIM, we measured a significant fitness improvement of the pG06-VIM-1-carrying Δ*cpdA* mutant (one-way ANOVA not assuming equal variances, df = 3, $P = 0.004$ followed by Dunnett's test: BWΔ*arcA*+VIM, $P = 0.993$; BWΔ*crp*+VIM, $P = 0.051$; BWΔ*cpdA*+VIM, $P = 0.001$; Figure 4a and Supplementary Table 6) and a reduction of plasmid cost to 0.4% (one-sample *t*-test, two-sided: BWΔ*arcA*+VIM: 2.2% or $w = 0.978 \pm 0.007$, $P = 0.007$; BWΔ*crp*+VIM: no cost or $w = 1.006 \pm 0.020$, $P = 0.534$; BWΔ*cpdA*+VIM: $w = 0.996 \pm 0.002$, $P = 0.034$; Figure 4a and Supplementary Table 6). These data strongly suggest that beyond the known effect on adaptation to growth conditions, *cpdA* mutations identified in our study pleiotropically mitigated plasmid costs. We could however not obtain the same level of consistency across biological replicates in competitions using the Δ*crp* mutant even though CpdA and CRP are tightly linked in the CCR regulatory system (Imamura et al. 1996; Matange 2015). Based on the observation that pG06-VIM-1 no longer imposes a cost in the Δ*crp* mutant, as confirmed by the one-sample *t*-test, we argue that *crp* is also involved in fitness mitigation despite the relatively high variance that renders the Dunnett's test (borderline) not significant.

In *E. coli*, the phosphodiesterase CpdA affects intracellular levels of cAMP by specifically hydrolyzing this signaling molecule (Imamura et al. 1996). To investigate the effect of the most frequently observed mutation in *cpdA* (*cpdA*.Δ3.bp488-490; Supplementary Table 4) on protein function, we measured intracellular cAMP concentrations in ancestral and evolved strains with and without pG06-VIM-1. The levels of intracellular cAMP increased significantly by 49% between ancestral and evolved strains (ExPEC and ExPEC+VIM: 2.6 to 4.3 pmol mL^{-1}, mean = 3.7 ± 0.72 pmol mL^{-1}; Clone 2 and Clone 2_{VIM}: 5.7 to 11.6 pmol mL^{-1}, mean = 7.2 ± 2.2 pmol mL^{-1}; two-way ANOVA with interactions: df = 3, $P = 0.005$ [assuming equal variances] and $P = 0.001$ [adjusted for unequal variances]; Figure 4b), but were unaffected by plasmid presence (two-way ANOVA with interactions: df = 3, $P = 0.53$ [assuming equal variances] and $P = 0.40$ [adjusted for unequal variances]). These data are consistent with the previously observed CpdA deficiency of an identical *E. coli* mutant resulting in an approximate doubling of intracellular cAMP (Chib and Seshasayee 2018). Similarly, protein function analysis of evolved population data indicates that the majority of mutations in *cpdA* lead to the loss of CpdA function (Supplementary information section VII and Supplementary Table 9).

Mutations in CCR and ArcAB regulatory systems lead to general adaptation to the growth conditions. The gene products of *cyaA, cpdA*, *crp*, *arcA*, *arcB* can be associated with transcription in *E. coli* involving the global regulators CRP and ArcA (Martínez-Antonio and Collado-Vides 2003).

cAMP is an important second messenger that binds to CRP (Frendorf et al. 2019) and the complex activates cAMP-dependent regulation of carbon source utilization via the CCR system (Imamura et al. 1996; Matange 2015). Intracellular levels of cAMP in *E. coli* are controlled by CyA (synthesis) and CpdA (degradation) (Imamura et al. 1996). Proteins ArcA and ArcB compose the ArcAB two-component regulatory system involved in respiratory and energy metabolism of *E. coli* (Iuchi and Lin 1988; Iuchi et al. 1989). Mutations in CCR- and ArcAB-associated proteins may lead to growth optimization in varying environments due to adaptation in downstream transcriptional regulatory networks (Saxer et al. 2014; Frendorf et al. 2019; Phaneuf et al. 2019).

To verify that the mutations identified in the two regulatory systems increase fitness in the given *in vitro* environment, we assessed the fitness of pG06-VIM-1-containing and -free, evolved and ancestral strains by measuring exponential growth rates. Plasmid pG06-VIM-1 in Clones 1-4_{VIM} displayed no mutations after experimental evolution and this approach allowed us to directly measure the effects of the chromosomal mutations on general fitness. Growth rates of evolved strains were increased by 7-17% across all comparisons independent of presence or absence of the plasmid (one-sample *t*-test, one-sided: Clone 1: $w = 1.11 \pm 0.02$; $P = 0.022$; Clone 2: $w = 1.17 \pm 0.03$; $P = 0.019$; Clone 3: $w = 1.13 \pm 0.02$; $P = 0.009$; Clone 4: $w = 1.14 \pm 0.02$; $P = 0.007$; Clone 1_{VIM}: $w = 1.07 \pm 0.02$; $P = 0.023$; Clone 2_{VIM}: $w = 1.13 \pm 0.06$; $P = 0.072$; Clone 3_{VIM}: $w = 1.17 \pm 0.05$; $P = 0.040$; Clone 4_{VIM}: $w = 1.16 \pm 0.04$; $P = 0.026$; Figure 5a and b). Despite lower resolution than competition experiments, these data show that the identified mutations increase fitness under the given growth conditions and independent of plasmid carriage. They provide further support for the plasmid cost mitigating role of the observed chromosomal mutations.

Transcriptional alterations contribute to reduced plasmid costs. CRP and ArcA represent two of seven global transcription factors in *E. coli* and directly or indirectly control the expression of several hundred genes (Liu and De Wulf 2004; Shimada et al. 2011). Changes in gene expression may lead to a reduced burden of plasmid carriage as demonstrated previously (Harrison et al. 2015; San Millan et al. 2015; Kawano et al. 2020). We sought to elucidate both the origin of the initial pG06-VIM-1 cost and its amelioration due to mutations in CCR and ArcAB associated genes and performed RNA-Seq. Six replicate samples of plasmid-free strains ExPEC, Clone 2 and Clone 3, and plasmid-carrying strains ExPEC+VIM, Clone 2+VIM, Clone 3+VIM were sequenced resulting in on average 25 million paired-end reads per sample (Supplementary Table 10). Comparing the two ancestral strains ExPEC and ExPEC+VIM revealed differential expression of seven chromosomal genes immediately upon plasmid acquisition, of which only the one encoding a putative selenium delivery protein displayed a fold-change (2.36) beyond a 2-fold threshold (Figure 6a and Supplementary Table 11). Similarly, plasmid pCAR1 also significantly changes the expression of only a limited set of chromosomal genes in *Pseudomonas putida*, but with a stronger effect (>40 fold) on only one gene designated *parI*

(Miyakoshi et al. 2007). The lack of substantial evidence for altered chromosomal gene expression in our work suggests that the costly plasmid acquisition may not severely disrupt transcriptional regulation (Buckner et al. 2018) or specific cellular pathways e.g. SOS response (San Millan et al. 2015). Instead, the cost can derive from the usage of building blocks or molecular machinery for plasmid replication (*e.g.* nucleotides), but most likely those required for expression and post-translational events, such as amino acids, ribosomes, chaperones and acetyl/succinyl modification (San Millan et al. 2018; Vasileva et al. 2018 and reviewed in Baltrus 2013).

Given that the CCR and ArcAB systems are involved in global gene regulation it is not surprising that mutations in evolved Clone 2 and 3 lead to considerable changes in chromosomal gene expression when compared to the ancestral ExPEC strain. Indeed, hundreds of genes are differently up and downregulated independently of pG06-VIM-1 presence (Figure 6c; Supplementary Table 11). Despite some differences among the four evolved clones, enrichment (Supplementary Table 12) and over-representation (Supplementary Table 13) analyses of protein-encoding genes show common trends; cell motility via cilia/flagella (and other processes that require cell component organization, such as the expression of adhesion factors) tends to be downregulated (Supplementary Figure 5), while there is upregulation of diverse metabolic processes that target macromolecule biosynthesis (e.g. amino acids) and ribosome assembly which are, directly or indirectly, connected to translation and gene expression (Supplementary Figure 4).

After evolution, only 16 chromosomal genes of Clone 3 were affected by pG06-VIM-1 acquisition, of which one gene encoding a phage tail protein, exhibited overexpression > 2-fold (Figure 6a; Supplementary Table 11). In Clone 2 we found upregulation of four chromosomal genes while 116 were downregulated (Figure 6a; Supplementary Table 11). Analyzing the 115 downregulated protein-encoding genes revealed an over-representation of biological processes involved in tRNA metabolism and nucleotide biosynthesis (Supplementary Table 13; Supplementary Figure 6), while the remaining gene encodes a tRNA. Furthermore, the comparison Clone 2+VIM vs ExPEC+VIM revealed that 52 (or 65%) of the strain's tRNA-encoding genes are downregulated (Figure 6c; Supplementary Table 11) which is indicative of altered translation processes. Therefore, at least in Clone 2 the low cost of pG06-VIM-1 can be attributable to interference in translation, which is in agreement with other reports showing that low plasmid costs are associated with gene expression (McNally et al. 2016; Buckner et al. 2018).

Interestingly, overall expression of pG06-VIM-1 genes decreased in evolved hosts, such that in Clone 2+VIM 12 plasmid genes are downregulated and four upregulated, while in Clone 3+VIM seven plasmid genes are downregulated but only one is upregulated (Figure 6b; Supplementary Table 11). Although transcriptional changes in these genes never exceed a 2-fold threshold, the net fold-change is negative (-13.08 for Clone 2+VIM and -9.01 for Clone 3+VIM; Supplementary Table 17). Plasmid RNA represents 2.33 ± 0.11% of the total transcripts for ExPEC+VIM, but a significantly lower proportion for evolved strains (one-way ANOVA assuming equal variances, df = 2, $P = 0.001$,

followed by Dunnett's test: $P < 0.001$ and $P = 0.03$), respectively 2.08 ± 0.08% for Clone 2+VIM and 2.18 ± 0.11% Clone 2+VIM (Supplementary Figure 7). Taken together, these data suggest that net downregulation of plasmid genes after evolution offer a plausible explanation for the reduced fitness costs, while in other works such reduction is explained by down-regulation of highly specific plasmid genes (San Millan et al. 2015). Although the differences in the proportions of plasmid transcripts among hosts are small, they can lead to significant fitness effects if the synthesized proteins require chaperones (Ma et al. 2018) and post-translational modification (Vasileva et al. 2018). Thus, reshaping gene expression at a global level through the identified mutations in the CCR and ArcAB systems affects plasmid transcription levels. This represents a novel solution to the plasmid paradox where adaptation to a new niche (growth medium in this case) pleiotropically mediates plasmid cost reductions.

Discussion

In this report we asked if and how plasmid-host coevolution would mitigate the fitness costs of two clinically highly relevant MDR plasmids newly acquired by a plasmid-free ExPEC isolate. Our data show that the moderate initial costs of both carbapenemase-encoding plasmids were significantly alleviated during laboratory evolution. Curiously, the main causes for amelioration were not plasmid-specific compensatory mutations as reported in several recent studies (San Millan et al. 2014; Harrison et al. 2015; Loftie-Eaton et al. 2016; Loftie-Eaton et al. 2017), although deletions of costly plasmid regions (Turner et al. 2014; Porse et al. 2016) and undetected plasmid mutations could also have played a role. Instead, after ~300 generations we identified strong parallel evolution in chromosomal genes only, independent of plasmid carriage. The mutational target genes represented two global regulatory systems involved in *E. coli* carbon catabolite repression (CCR) and aerobic respiration (ArcAB). Moreover, the mutations in these transcriptional regulators improved the maintenance of two unrelated plasmids strongly suggesting that the ExPEC host became generally more permissive towards plasmid acquisition, and in the future it would be interesting to test the effect on additional plasmid types. The pleiotropic effects on plasmid cost amelioration appears to be mainly due to mutations affecting the CCR regulatory system, as demonstrated by fitness results using *cpdA* and *crp* deletion mutants. Mechanistically, RNA-seq analyses revealed a net transcriptional relief on plasmid genes as a collateral cost-mitigating effect of environmental adaptation by global regulatory changes.

Other studies have also reported that mutations in regulatory systems improved plasmid-host relationships. In a seminal study, mutations in the *gacA/gacS* two-component regulatory system reduced the cost of the mega plasmid pQBR103 by decreasing plasmid transcriptional demand in *Pseudomonas fluorescens* (Harrison et al. 2015). These mutations were specifically ameliorating the cost of the plasmid since they did not appear in the plasmid-free evolved lineages (true compensatory mutations) (Harrison et al. 2015). This is categorically different from our findings since we observed that adaptation in the CCR and ArcAB regulatory systems was not specific to plasmid-carrying populations. Two other reports frequently identified mutations in regulatory systems across multiple plasmid-carrying evolving populations that improved plasmid maintenance (Loftie-Eaton et al. 2016; Stalder et al. 2017). However, the absence of evolved plasmid-free lineages in these studies preclude direct comparisons with the results presented here.

On a broader perspective, our results warrant further research on plasmid-evolutionary dynamics in different *E. coli* lineages and sub-lineages to better understand why some of them appear to be more prone to acquire and maintain MDR plasmids (Mathers et al. 2015; McNally et al. 2016). Available data support that plasmids of clinical origins rarely reduce fitness of clinical host strains (Sandegren et al. 2012; Schaufler et al. 2016; Di Luca et al. 2017; Buckner et al. 2018; Gama et al. 2020; Ma et al. 2020) to the extent often seen in the pioneering studies of plasmid-host compensatory evolution (Lenski et al. 1994; Sota et al. 2010; San Millan et al. 2014; Harrison et al. 2015). It is also

clear that this alone cannot explain how successful clone-plasmid associations emerge. From population genomic analyses McNally and co-workers demonstrated an association between mutations in regulatory regions of the high-risk *E. coli* ST131 subclade C and the accessory genome, including MDR plasmids. In their interpretation, this finding represented evidence of compensatory evolution towards MDR plasmid acquisition. However, taken together with a recent report showing that ExPEC ST131 has adapted to separate ecological niches at the sub-clade level, our results provide an alternative explanation (McNally et al. 2019).

Based on data presented here, it can be hypothesized that regulatory changes could also in part represent niche-adaptations that coincidentally facilitate MDR plasmid acquisition and maintenance. Moreover, chromosomal antibiotic-resistance mutations, which can be viewed as a form of niche-adaptation, display epistatic interactions affecting plasmid fitness cost (Silva et al 2011) as well as stability (Sota and Top 2008). Therefore, different types of mutations causing environmental adaptation can collaterally increase the permissiveness to plasmids. However, we acknowledge that the pleiotropic effects on plasmid costs reported here may be specific to a single environment, as others have reported that both fitness costs (Knoppel et al. 2018; San Millan et al. 2018; Hubbard et al. 2019) and compensatory evolution (Hall et al. 2020) are highly media-dependent. Consequently, the specific mutations reported here may be media-dependent, but the processes targeted (*i.e.* global gene regulation) are widely reported across different media, strains, and plasmids supporting the generality of our findings.

Our study is not without limitations. We specifically dissected the causes of plasmid fitness cost amelioration for the non-conjugative pG06-VIM-1, but not in detail for pK71-77-1-NDM. Maintenance of the latter improved due to mutations in CCR/ArcAB regulons, but the contribution of each system remains unclear. Due to our experimental approaches, we could not precisely identify whether the chromosomal mutations affected fitness directly, or indirectly due to observations that conjugative transfer increased in the evolved clones. To that end, ArcA has been shown to impact conjugative transfer of other plasmid types (Strohmaier et al. 1998; Serna et al. 2010). However, we cannot exclude the possibility that the small increase in pK71-77-1-NDM conjugation is an artifact resulting from different growth rates, since adapted donors display faster growth than unevolved donor and recipient strains. The effects of CCR/ArcAB mutations on the different parameters for pK71-77-1-NDM maintenance (fitness costs, stability and conjugation) need further exploration. Also, the role of large plasmid deletions represents a subject for future research.

In this report, we propose “piggybacking” on niche-adaptation as a novel, not mutually exclusive, solution for the “plasmid paradox”. Our approaches also underscore the importance of using clinically relevant strains and plasmids to investigate the evolutionary dynamics of plasmid-mediated antibiotic resistance. This knowledge can be used jointly with data from molecular epidemiology to better predict future emergence of successful combinations of clones, sub-lineages and antibiotic resistance determinants.

Methods

Bacterial hosts, plasmids and culture conditions. Strains, plasmids and primers used in this study are listed in Supplementary Tables 1 and 2. The ancestral plasmid-free strain ExPEC was chosen as it represents a clinically relevant *E. coli* isolate (originating from urinary tract infection) while being plasmid-naïve. It belongs to sequence type 537, as tested by multi-locus sequence typing, and phenotypically susceptible to 24 antibiotics tested by disc diffusion (Bengtsson et al. 2012; Kahlmeter and Poulsen 2012) (Supplementary Table 1). The lack of detected replicons and antibiotic resistance genes make this strain an ideal clinical model to study the behavior MDR plasmids. Plasmids pG06-VIM-1 and pK71-77-1-NDM originated from a *K. pneumoniae* wound infection isolate (Samuelsen et al. 2011) and an uropathogenic *E. coli* (Samuelsen et al. 2011) and were introduced into ExPEC by electroporation or conjugation, respectively. Strains were grown at 37°C under aeration in Miller Difco Luria-Bertani liquid broth (LB; Becton, Dickinson and Co.) or on LB agar (LBA) containing additional Select agar (15 g L^{-1}, Sigma-Aldrich). For selection of plasmid-carrying strains, media were supplemented with ampicillin (100 mg L^{-1}; Sigma-Aldrich). See Supplementary information section I for more details on strains constructed in this study.

Experimental evolution. Single colonies of strains ExPEC, ExPEC+VIM and ExPEC+NDM were used to initiate four independent lineages each. The 12 lineages were evolved in 1 mL of antibiotic-free LB medium using 2 mL-deep-96-well plates in checkered pattern (VWR International) and incubated at 37°C with 700 rpm constant shaking (Microplate Shaker TiMix 5, Edmund Bühler). In total, 48 transfers with estimated 6.6 generations between two transfers (~300 generations) were performed involving a 1:100 dilution of stationary-phase cultures into fresh LB every 12 hours (~10^7 cells transferred). Endpoint populations (Pop 1-4_{VIM}, Pop 5-8_{NDM} and Pop 9-12) and one representative clone per plasmid-carrying evolved population (Clones 1-4_{VIM} and Clones 5-8_{NDM}) were stored at -80°C (Supplementary information section I and Supplementary Table I).

Whole-genome sequencing. See Supplementary information section II for details on long-read sequencing and assembly of a closed reference genome of strain ExPEC (GenBank accession CP053079). For Illumina whole-genome sequencing, genomic DNA of ancestral strains ExPEC, ExPEC+VIM, ExPEC+NDM, eight evolved clones (Clones 1-4_{VIM}, Clones 5-8_{NDM}) and 12 evolved mixed populations (Pop 1-4_{VIM}, Pop 5-8_{NDM}, Pop 9-12) (Figure 1) was isolated using the GenElute Bacterial Genomic DNA Kit (Sigma-Aldrich). DNA-purity and -quantity was assessed using a NanoDrop ND-1000 spectrophotometer (Thermo Scientific). Short-read sequencing library preparation and sequencing was performed following manufacturers' instructions at the Genomic Support Centre Tromsø, UiT The Arctic University of Norway. The Nextera XT DNA Library preparation kit (Illumina) was used with an input of 1 ng genomic DNA and dual indexes. Samples were sequenced on a NextSeq 550 instrument (Illumina) with 300 cycles (2 × 150 bp paired-end

reads), and a NextSeq 500/550 mid-output flow cell was used for clonal samples. One entire high-output flow cell was explicitly used for the population samples aiming at deep coverage. We ran Trim Galore v0.5.0 with default settings to remove adapter sequences (CTGTCTCTTATA) and low-quality bases, and SPAdes v3.13.0 with read error correction (Bankevich et al. 2012; Krueger 2012). Trimmed and error corrected short-reads were controlled for adapters and quality score using FastQC v0.11.4 (Andrews 2010). The raw sequence reads (long and short) of 24 libraries are available from the NCBI Sequence Read Archive (SRA, BioProject accession PRJNA630076).

Short-read sequence analysis. We used the breseq computational pipeline v0.33.0 and v0.35.0 for prediction of mutations from clonal and population short-read sequencing data (Deatherage and Barrick 2014). Preprocessed reads (see above) of all evolved populations were mapped against the reference genome of strain ExPEC (GenBank accession CP053079), and against plasmid sequences of pG06-VIM-1 (Pop 1-4$_{VIM}$; GenBank accession KU665641 [Di Luca et al. 2017]) or pK71-77-1-NDM (Pop 5-8 $_{NDM}$; GenBank accession CP040884 [Gama et al. 2020]) when appropriate. Breseq was run with default settings except for specifications when analyzing clonal sequencing data ('consensus-mode'; 'frequency-cutoff 0.9'; 'minimum-variant-coverage 10'; 'consensus-minimum-total-coverage 10') or population sequencing data ('polymorphism-mode'; 'frequency-cutoff 0.01'; 'minimum-variant-coverage 10'; 'minimum-total-coverage 100'; 'base quality score 20'). We focused on the identification of *de novo* single nucleotide substitutions, deletions, insertions and small indels by manually evaluating the predicted mutations from the breseq outputs (Supplementary information section IIIb). The use of short-read sequencing data bears an inherent limitation regarding the interpretation of chromosomal inversions, rearrangements and mutations in repeat regions due to misaligned reads, and these mutations were thus omitted from further analysis. Repeats were confirmed using 'tandem repeat finder' v4.09 (Benson 1999) or by manually searching the reference genome for multiple alignment options. For population sequencing analysis, we report genetic changes as low as 1% mutation frequency considering that the mutated locus reached ≥ 10% mutation frequency at least in one of the evolved populations. Artemis v16.0.0 (http://sanger-pathogens.github.io/Artemis/), Gene Construction Kit v4.0.3 (Textco Biosoftware Inc.) and the Integrative Genomics Viewer v2.6.0 (http://software.broadinstitute.org/software/igv/) were used to support manual inspection of sequencing data.

Competitive fitness and plasmid stability. The relative competitive fitness (w) of plasmid-carrying clones was determined in pairwise serial competition experiments (~40 generations) with the isogenic plasmid-free strain, as described before (Starikova et al. 2013), with minor modifications. Briefly, pre-adapted cultures of each competitor were adjusted to the same OD_{600}, mixed in a 1:1 ratio, and used to initiate 1 mL batch cultures at a density of ~10^7 CFU (= T_0), in antibiotic-free LB and 2 mL-deep-96-well plates in checkered pattern (VWR International). Plates were incubated at 37°C with

700 rpm shaking (Microplate Shaker TiMix 5, Edmund Bühler), and the cultures were diluted 1:100 into fresh LB every 12 hours (= $T_{12\text{-}72}$). To determine the CFU of each competitor, cultures were diluted in 0.9% saline (m/v) and plated selectively on LBA-ampicillin ($CFU_{plasmid\text{-}carrying}$) and non-selectively on LBA (CFU_{total}) at T_0 and every following timepoint. The selection coefficient was calculated as $s = 0.5 \times b/\ln(1/d)$ with b (= slope) obtained from regressing the natural logarithm of the ratio ($CFU_{plasmid\text{-}carrying}/CFU_{plasmid\text{-}free}$) over timepoints, and d as the dilution factor at each transfer (here 1:100) (Levin et al. 2000). It was multiplied by 0.5 to account for two transfers per day (to obtain s per day). Relative fitness was calculated as $w = 1+s$, where the fitness of the plasmid-free strain equals 1 (Supplementary Table 6). To determine spontaneous plasmid loss during competition experiments we proceeded similarly with pre-adapted cultures of plasmid-carrying strains as described above. Briefly, the density at T_0 was $\sim 5 \times 10^6$ CFU mL^{-1} and cultures were transferred, diluted and plated selectively and non-selectively, as described above. The slope obtained by regressing the frequency of the plasmid-carrying population ($CFU_{plasmid\text{-}carrying}/CFU_{total}$) over timepoints was calculated (Supplementary Table 7). For determination of relative competitive fitness and spontaneous plasmid loss, results were obtained from at least three biological replicates, initiated on separate days, with three technical replicates each.

Exponential growth rates. As a proxy for fitness changes due to acquired mutations in evolved clones with and without the plasmid, the exponential growth rates of separately growing strains were determined. Briefly, overnight cultures in 1 mL LB were started from a single colony grown on LBA, diluted 1:100 in LB, and 250 µl were aliquoted into a 96-well-microtiter plate (Thermo Scientific). Absorbance at OD_{600} nm was measured in a BioTek EPOCH2 microtiter spectrophotometer (BioTek Instruments), every 10 minutes, and with linear shaking. Growth rates (r) were determined using GrowthRates v3.0 (Hall et al. 2014). Fitness of the evolved strain was calculated as relative growth rate = $r_{evolved\ strain}/r_{ancestral\ strain}$. Results were obtained from three biological replicates including five technical replicates all displaying a correlation coefficient $R \geq 0.97$.

Intracellular cyclic adenosine monophosphate (cAMP) concentration. Intracellular cAMP was quantified using the Cyclic AMP Select ELISA Kit (Cayman Chemical) following manufacturers' instructions. For this purpose, overnight cultures were started from single colonies into 2 mL LB, diluted 1:100 into fresh LB and incubated until mid-exponential growth phase (between 5.3-6.7 $\times 10^8$ CFU mL^{-1}). Five mL of each culture were spun down at 4°C, 4000 rpm for 10 min (Eppendorf Centrifuge 5810), supernatant was removed, and the pellet was subsequently washed three times in ice-cold 0.9% saline (m/v). Cells were resuspended in 250 µl of 0.1 M HCl to stop endogenous phosphodiesterase activity and the suspensions were boiled for 5 minutes. After centrifugation at 4°C, 4000 rpm for 10 min (Eppendorf Centrifuge 5810) an aliquot of the supernatant was diluted 1:2 (ExPEC, ExPEC+VIM) or 1:8 (Clone 2_{VIM}, Clone 2) in ELISA buffer followed by a subsequent 1:2

dilution step for all samples. The cAMP standard was reconstituted in 0.1 M HCl but thereafter diluted into ELISA buffer. Samples were applied in two dilutions, each in three biological and three technical replicates on the same ELISA plate. The standard was applied once and in two technical replicates on the same plate. The plate was incubated in the dark for 18 hours at 4°C and thereafter developed under slow orbital shaking and dark conditions. Absorbance was measured at 410 nm periodically in a BioTek EPOCH2 microtiter spectrophotometer (BioTek Instruments). Final reads were taken at $B_{0\text{-average}} = 0.7$ and data was analyzed using the spreadsheet available at https://www.caymanchem.com/analysisTools/elisa (R^2 standard curve = 0.96).

Total RNA isolation. For transcriptome analysis, overnight cultures were initiated from single colonies into 2 mL LB, diluted 1:100 into fresh LB, and incubated until mid-exponential growth phase (OD_{600} 0.5-0.6; average $2.2\pm0.9 \times 10^8$ CFU mL^{-1}). Total RNA was isolated in six biological replicates per strain from 0.5 mL of culture using the RNeasy Protect Bacteria Mini kit (Qiagen) on six consecutive days. RNA-quality and -quantity were assessed with Nanodrop ND-1000 spectrophotometer (Thermo Scientific). Contaminating genomic DNA (gDNA) was digested following rigorous DNAse I treatment of the Ambion DNA-free DNase kit (Thermo Scientific). Briefly, 50 µl assays of maximum 10 µg RNA were treated in two consecutive incubation steps at 37°C for 30 minutes and addition of 5 µl DNase I enzyme before each step. RNA-quality and -quantity were again assessed as described above and the absence of gDNA was tested by PCR amplification (40 cycles) of the *adk* housekeeping gene (Supplementary Table 2). The RNA integrity numbers (RIN) were obtained via the Agilent RNA 6000 Nano kit and the Agilent 2100 Bioanalyzer system (Agilent Technologies 2100), and all samples reached RIN > 9 (Supplementary Table 10). Depletion of ribosomal RNA from 1 µg total RNA per sample with the QIAseq FastSelect RNA Removal kit and library preparation using the Truseq Stranded mRNA library kit were performed at Qiagen (Genomic Service Hilden, Germany). The Norwegian Sequencing Centre (NSC) (http://www.sequencing.uio.no) performed sequencing of the library on 1/2×SP Novaseq flow cell with 300 cycles (2 × 150 bp paired-end reads). The raw sequence reads of 36 libraries are available from NCBI SRA (BioProject accession PRJNA630076).

RNA-Seq analysis. NSC performed initial filtering of raw reads including adapter trimming and removal of low-quality reads using BBMap v34.56 (therein BBDuk) (Bushnell 2014). NSC mapped clean and adapter removed reads against the merged version of the ExPEC chromosome and the pG06-VIM-1 sequence using Hisat2 v2.1.0 (Kim et al. 2019) and generated count tables using FeatureCounts v1.4.6-p1 (Liao et al. 2014), resulting in an average sample alignment of 65% (Supplementary Table 10). Count tables were used as input for the Differential Expression analysis (data normalization and statistical tests) performed in R version 4.0.2 (R Core Team 2018) using the

default script for SARTools version 1.7.3 (Varet et al. 2016) with default settings and strain ExPEC as reference.

PANTHER Generic Mappings of chromosomal genes were generated using the PANTHER HMM Scoring tool with the PANTHER HMM library Version 15.0 (Ashburner et al. 2000; Huaiyu Mi et al. 2019; H. Mi et al. 2019; The Gene Ontology Consortium 2019; Supplementary Table 16) and functional classification of the PANTHER accessions was retrieved from the website (Supplementary Table 15). Tabular lists containing the gene ID, PANTHER accession and fold change for all differentially expressed chromosomal genes were uploaded as PANTHER Generic Mappings to http://pantherdb.org/ and ran for enrichment of PANTHER GO-Slim Biological Processes with FDR (false discovery rate) correction. Enrichment analysis (Supplementary Table 12) was performed for each of the comparisons in Supplementary Table 11, except ExPEC+VIM vs ExPEC. For the over-representation analyses, subsets of the same lists (up and downregulated genes only) were uploaded separately to http://pantherdb.org/. Over-representation analyses (Supplementary Table 13) was performed against the PANTHER Generic Mapping of all chromosomal protein-encoding genes (Supplementary Table 14), with Fisher exact test and FDR correction. All GO terms displaying significant enrichment or over-representation were compiled in three subsets (up and downregulated processes independent of plasmid presence, and downregulated processes due to plasmid presence) and used to generate Supplementary Figures 4-6, respectively, in Visualize (Day-Richter et al. 2007) available at http://amigo.geneontology.org/visualize?mode = client_amigo.

Statistical analyses. Statistical analyses were performed in R version 4.0.2 (R Core Team 2018). Samples were verified for normality with Shapiro-Wilk test and/or graphical visualization. Homogeneity of variances was tested with Levene's test (from package car [Fox and Weisberg 2019]) and/or graphical visualization. One-sample or two-sample comparisons were performed with Student t-tests. Packages sandwich (Zeileis 2004), car (Fox and Weisberg 2019) and multcomp (Hothorn et al. 2008) were required for ANOVA and multiple comparisons, respectively. Graphs in Figures 1, 3, 4, 5 and 6 were produced with packages ggplot2 (Kassambara 2020), patchwork (Pedersen 2020), ggthemes (Arnold 2019), and RColorBrewer (Neuwirth 2014). Significance levels are indicated as: *P*-value * < 0.05; ** < 0.01; *** < 0.001. Packages openxlsx (Schauberger and Walker 2019) and writexl (Ooms 2020) were used to read/write xlsx files. Packages data.table (Dowle and Srinivasan 2019) and jsonlite (Ooms 2014) were required to generate Supplementary Tables 11-16.

Acknowledgements

We thank Francois Pierre Alexandre Cléon for technical assistance, and Prof. Ruth H. Paulssen and Hagar Taman at UiT Genomics Support Centre Tromsø for valuable discussions about sequencing approaches and service regarding Illumina sequencing. The PacBio and RNA sequencing services were provided by the Norwegian Sequencing Centre (www.sequencing.uio.no), a national

technology platform hosted by the University of Oslo and supported by the "Functional Genomics" and "Infrastructure" programs of the Research Council of Norway and the South-Eastern Regional Health Authorities. We thank Teodora Ribarska and Arvind Sundaram at NSC for excellent correspondence and bioinformatic advice. We thank three anonymous reviewers for constructive criticism and suggestions that improved the manuscript. This work was supported by the Northern Norway Regional Health Authority (grant number SFP1168-14), and a joint grant from Northern Norway Regional Health Authority and UiT The Arctic University of Norway (project A23270).

Author contributions

P.J.J. and Ø.S. conceived the project; J.K., J.G. and P.J.J designed and J.K. and J.G. performed wet-lab experiments; J.H. performed reference genome assembly and provided bioinformatic support; J.K., J.G. and J.H. analyzed the data; all authors interpreted and discussed the data; J.K., J.G. and P.J.J. wrote the manuscript; all authors reviewed the manuscript and approved the final version.

Competing interest

The authors declare no competing interests.

Data availability

The genome of reference strain ExPEC is available at GenBank (accession CP053079) and raw DNA- and RNA-sequencing data are accessible at NCBI SRA (BioProject accession PRJNA630076). All other relevant data are available within this article, the Supplementary Information files, or from the corresponding author upon request.

References

Andrews S. 2010. FASTQC. A quality control tool for high throughput sequence data. doi:avalable at http://www.bioinformatics.babraham.ac.uk/projects/fastqc

Arnold JB. 2019. ggthemes: Extra Themes, Scales and Geoms for "ggplot2". *R Package Version 4.2.0*(accessed May 13, 2019). doi:available at https://CRAN.R-project.org/

Ashburner M, Ball CA, Blake JA, Botstein D, Butler H, Cherry JM, Davis AP, Dolinski K, Dwight SS, Eppig JT et al. 2000. Gene ontology: tool for the unification of biology. The Gene Ontology Consortium. *Nature genetics, 25*(1), 25-29. doi:10.1038/75556

Baba T, Ara T, Hasegawa M, Takai Y, Okumura Y, Baba M, Datsenko KA, Tomita M, Wanner BL, Mori H. 2006. Construction of Escherichia coli K-12 in-frame, single-gene knockout mutants: the Keio collection. *Mol Syst Biol, 2*, 2006 0008. doi:10.1038/msb4100050

Baltrus DA. 2013. Exploring the costs of horizontal gene transfer. *Trends Ecol Evol, 28*(8), 489-495. doi:10.1016/j.tree.2013.04.002

Bankevich A, Nurk S, Antipov D, Gurevich AA, Dvorkin M, Kulikov AS, Lesin VM, Nikolenko SI, Pham S, Prjibelski AD et al. 2012. SPAdes: a new genome assembly algorithm and its applications to single-cell sequencing. *J Comput Biol, 19*(5), 455-477. doi:10.1089/cmb.2012.0021

Bengtsson S, Naseer U, Sundsfjord A, Kahlmeter G, Sundqvist M. 2012. Sequence types and plasmid carriage of uropathogenic Escherichia coli devoid of phenotypically detectable resistance. *J Antimicrob Chemother, 67*(1), 69-73. doi:10.1093/jac/dkr421

Benson G. 1999. Tandem repeats finder: a program to analyze DNA sequences. *Nucleic Acids Res, 27*(2), 573-580. doi:10.1093/nar/27.2.573

Bergstrom CT, Lipsitch M, Levin BR. 2000. Natural selection, infectious transfer and the existence conditions for bacterial plasmids. *Genetics, 155*(4), 1505-1519. Retrieved from https://www.ncbi.nlm.nih.gov/pubmed/10924453

Bottery MJ, Wood AJ, Brockhurst MA. 2017. Adaptive modulation of antibiotic resistance through intragenomic coevolution. *Nat Ecol Evol, 1*(9), 1364-1369. doi:10.1038/s41559-017-0242-3

Bouma JE, Lenski RE. 1988. Evolution of a Bacteria-Plasmid Association. *Nature, 335*(6188), 351-352. doi:10.1038/335351a0

Buckner MMC, Saw HTH, Osagie RN, McNally A, Ricci V, Wand ME, Woodford N, Ivens A, Webber MA, Piddock LJV. 2018. Clinically Relevant Plasmid-Host Interactions Indicate that Transcriptional and Not Genomic Modifications Ameliorate Fitness Costs of Klebsiella pneumoniae Carbapenemase-Carrying Plasmids. *mBio, 9*(2). doi:10.1128/mBio.02303-17

Bushnell B. (2014, 2014-03-17). *BBMap: A Fast, Accurate, Splice-Aware Aligner*, United States.

Carattoli A. 2013. Plasmids and the spread of resistance. *Int J Med Microbiol, 303*(6-7), 298-304. doi:10.1016/j.ijmm.2013.02.001

Chib S, Seshasayee AS. 2018. Modulation of rpoS fitness by loss of cpdA activity during stationary-phase in Escherichia coli. doi:10.1101/460451

Dahlberg C, Chao L. 2003. Amelioration of the cost of conjugative plasmid carriage in Eschericha coli K12. *Genetics, 165*(4), 1641-1649. Retrieved from https://www.ncbi.nlm.nih.gov/pubmed/14704155

Datsenko KA, Wanner BL. 2000. One-step inactivation of chromosomal genes in Escherichia coli K-12 using PCR products. *Proc Natl Acad Sci U S A, 97*(12), 6640-6645. doi:10.1073/pnas.120163297

Day-Richter J, Harris MA, Haendel M, The Gene Ontology OBOEWG, Lewis S. 2007. OBO-Edit—an ontology editor for biologists. *Bioinformatics, 23*(16), 2198-2200. doi:10.1093/bioinformatics/btm112

De Gelder L, Williams JJ, Ponciano JM, Sota M, Top EM. 2008. Adaptive plasmid evolution results in host-range expansion of a broad-host-range plasmid. *Genetics, 178*(4), 2179-2190. doi:10.1534/genetics.107.084475

Deatherage DE, Barrick JE. 2014. Identification of mutations in laboratory-evolved microbes from next-generation sequencing data using breseq. *Methods Mol Biol, 1151*, 165-188. doi:10.1007/978-1-4939-0554-6_12

Di Luca MC, Sorum V, Starikova I, Kloos J, Hulter N, Naseer U, Johnsen PJ, Samuelsen O. 2017. Low biological cost of carbapenemase-encoding plasmids following transfer from Klebsiella

pneumoniae to Escherichia coli. *J Antimicrob Chemother, 72*(1), 85-89. doi:10.1093/jac/dkw350

Dionisio F, Matic I, Radman M, Rodrigues OR, Taddei F. 2002. Plasmids spread very fast in heterogeneous bacterial communities. *Genetics, 162*(4), 1525-1532. Retrieved from <Go to ISI>://WOS:000180502300004

Dionisio F, Conceicao IC, Marques AC, Fernandes L, Gordo I. 2005. The evolution of a conjugative plasmid and its ability to increase bacterial fitness. *Biol Lett, 1*(2), 250-252. doi:10.1098/rsbl.2004.0275

Dowle M, Srinivasan A. 2019. data.table: Extension of `data.frame`. *R package version 1.12.8*. doi:available at https://CRAN.R-project.org/package=data.table

Enne VI, Bennett PM, Livermore DM, Hall LM. 2004. Enhancement of host fitness by the sul2-coding plasmid p9123 in the absence of selective pressure. *J Antimicrob Chemother, 53*(6), 958-963. doi:10.1093/jac/dkh217

Fox J, S. W. 2019. An R Companion to Applied Regression. *Sage, Thousand Oaks CA*(Third edition). doi:available at https://socialsciences.mcmaster.ca/jfox/Books/Companion/

Frendorf PO, Lauritsen I, Sekowska A, Danchin A, Norholm MHH. 2019. Mutations in the Global Transcription Factor CRP/CAP: Insights from Experimental Evolution and Deep Sequencing. *Comput Struct Biotechnol J, 17*, 730-736. doi:10.1016/j.csbj.2019.05.009

Gama JA, Kloos J, Johnsen PJ, Samuelsen O. 2020. Host dependent maintenance of a blaNDM-1-encoding plasmid in clinical Escherichia coli isolates. *Sci Rep, 10*(1), 9332. doi:10.1038/s41598-020-66239-8

Gullberg E, Albrecht LM, Karlsson C, Sandegren L, Andersson DI. 2014. Selection of a multidrug resistance plasmid by sublethal levels of antibiotics and heavy metals. *mBio, 5*(5), e01918-01914. doi:10.1128/mBio.01918-14

Hall BG, Acar H, Nandipati A, Barlow M. 2014. Growth rates made easy. *Mol Biol Evol, 31*(1), 232-238. doi:10.1093/molbev/mst187

Hall JPJ, Wright RCT, Guymer D, Harrison E, Brockhurst MA. 2020. Extremely fast amelioration of plasmid fitness costs by multiple functionally diverse pathways. *Microbiology, 166*(1), 56-62. doi:10.1099/mic.0.000862

Harrison E, Brockhurst MA. 2012. Plasmid-mediated horizontal gene transfer is a coevolutionary process. *Trends Microbiol, 20*(6), 262-267. doi:10.1016/j.tim.2012.04.003

Harrison E, Guymer D, Spiers AJ, Paterson S, Brockhurst MA. 2015. Parallel compensatory evolution stabilizes plasmids across the parasitism-mutualism continuum. *Curr Biol, 25*(15), 2034-2039. doi:10.1016/j.cub.2015.06.024

Hothorn T, Bretz F, Westfall P. 2008. Simultaneous inference in general parametric models. *Biom J, 50*(3), 346-363. doi:10.1002/bimj.200810425

Hubbard ATM, Jafari NV, Feasey N, Rohn JL, Roberts AP. 2019. Effect of Environment on the Evolutionary Trajectories and Growth Characteristics of Antibiotic-Resistant Escherichia coli Mutants. *Front Microbiol, 10*, 2001. doi:10.3389/fmicb.2019.02001

Imamura R, Yamanaka K, Ogura T, Hiraga S, Fujita N, Ishihama A, Niki H. 1996. Identification of the cpdA gene encoding cyclic 3',5'-adenosine monophosphate phosphodiesterase in Escherichia coli. *J Biol Chem, 271*(41), 25423-25429. doi:10.1074/jbc.271.41.25423

Iuchi S, Cameron DC, Lin ECC. 1989. A second global regulator gene (arcB) mediating repression of enzymes in aerobic pathways of Escherichia coli. *J Bacteriol, 171*(2), 868-873. doi:10.1128/jb.171.2.868-873.1989

Iuchi S, Lin EC. 1988. arcA (dye), a global regulatory gene in Escherichia coli mediating repression of enzymes in aerobic pathways. *Proceedings of the National Academy of Sciences, 85*(6), 1888. doi:10.1073/pnas.85.6.1888

Kahlmeter G, Poulsen HO. 2012. Antimicrobial susceptibility of Escherichia coli from community-acquired urinary tract infections in Europe: the ECO.SENS study revisited. *Int J Antimicrob Agents, 39*(1), 45-51. doi:10.1016/j.ijantimicag.2011.09.013

Kassambara A. 2020. ggpubr: 'ggplot2' Based Publication Ready Plots. *R package Version 0.4.0, accessed June, 27, 2020*. doi:available at https://CRAN.R-project.org/package=ggpubr

Kawano H, Suzuki-Minakuchi C, Sugiyama D, Watanabe N, Takahashi Y, Okada K, Nojiri H. 2020. A Novel Small RNA on the Pseudomonas putida KT2440 Chromosome Is Involved in the

Fitness Cost Imposed by IncP-1 Plasmid RP4. *Front Microbiol, 11*, 1328. doi:10.3389/fmicb.2020.01328

Kim D, Paggi JM, Park C, Bennett C, Salzberg SL. 2019. Graph-based genome alignment and genotyping with HISAT2 and HISAT-genotype. *Nature Biotechnology, 37*(8), 907-915. doi:10.1038/s41587-019-0201-4

Knoppel A, Knopp M, Albrecht LM, Lundin E, Lustig U, Nasvall J, Andersson DI. 2018. Genetic Adaptation to Growth Under Laboratory Conditions in Escherichia coli and Salmonella enterica. *Front Microbiol, 9*, 756. doi:10.3389/fmicb.2018.00756

Kottara A, Hall JPJ, Harrison E, Brockhurst MA. 2018. Variable plasmid fitness effects and mobile genetic element dynamics across Pseudomonas species. *FEMS Microbiol Ecol, 94*(1). doi:10.1093/femsec/fix172

Krueger F. 2012. Trim galore. A wrapper tool around Cutadapt and FastQC to consistently apply quality and adapter trimming to FastQ files. doi:available at https://github.com/FelixKrueger/TrimGalore

Lenski RE, Simpson SC, Nguyen TT. 1994. Genetic analysis of a plasmid-encoded, host genotype-specific enhancement of bacterial fitness. *J Bacteriol, 176*(11), 3140-3147. doi:10.1128/jb.176.11.3140-3147.1994

Levin BR, Perrot V, Walker N. 2000. Compensatory mutations, antibiotic resistance and the population genetics of adaptive evolution in bacteria. *Genetics, 154*(3), 985-997. Retrieved from https://www.ncbi.nlm.nih.gov/pubmed/10757748

Liao Y, Smyth GK, Shi W. 2014. featureCounts: an efficient general purpose program for assigning sequence reads to genomic features. *Bioinformatics, 30*(7), 923-930. doi:10.1093/bioinformatics/btt656

Liu X, De Wulf P. 2004. Probing the ArcA-P modulon of Escherichia coli by whole genome transcriptional analysis and sequence recognition profiling. *J Biol Chem, 279*(13), 12588-12597. doi:10.1074/jbc.M313454200

Loftie-Eaton W, Bashford K, Quinn H, Dong K, Millstein J, Hunter S, Thomason MK, Merrikh H, Ponciano JM, Top EM. 2017. Compensatory mutations improve general permissiveness to antibiotic resistance plasmids. *Nat Ecol Evol, 1*(9), 1354-1363. doi:10.1038/s41559-017-0243-2

Loftie-Eaton W, Yano H, Burleigh S, Simmons RS, Hughes JM, Rogers LM, Hunter SS, Settles ML, Forney LJ, Ponciano JM et al. 2016. Evolutionary Paths That Expand Plasmid Host-Range: Implications for Spread of Antibiotic Resistance. *Mol Biol Evol, 33*(4), 885-897. doi:10.1093/molbev/msv339

Lopatkin AJ, Meredith HR, Srimani JK, Pfeiffer C, Durrett R, You L. 2017. Persistence and reversal of plasmid-mediated antibiotic resistance. *Nat Commun, 8*(1), 1689. doi:10.1038/s41467-017-01532-1

Ma K, Feng Y, Zong Z. 2018. Fitness cost of a mcr-1-carrying IncHI2 plasmid. *PLoS One, 13*(12), e0209706. doi:10.1371/journal.pone.0209706

Ma T, Fu J, Xie N, Ma S, Lei L, Zhai W, Shen Y, Sun C, Wang S, Shen Z et al. 2020. Fitness Cost of blaNDM-5-Carrying p3R-IncX3 Plasmids in Wild-Type NDM-Free Enterobacteriaceae. *Microorganisms, 8*(3). doi:10.3390/microorganisms8030377

Martínez-Antonio A, Collado-Vides J. 2003. Identifying global regulators in transcriptional regulatory networks in bacteria. *Curr Opin Microbiol, 6*(5), 482-489. doi:10.1016/j.mib.2003.09.002

Matange N. 2015. Revisiting bacterial cyclic nucleotide phosphodiesterases: cyclic AMP hydrolysis and beyond. *FEMS Microbiology Letters, 362*(22). doi:10.1093/femsle/fnv183

Mathers AJ, Peirano G, Pitout JD. 2015. The role of epidemic resistance plasmids and international high-risk clones in the spread of multidrug-resistant Enterobacteriaceae. *Clin Microbiol Rev, 28*(3), 565-591. doi:10.1128/CMR.00116-14

McNally A, Kallonen T, Connor C, Abudahab K, Aanensen DM, Horner C, Peacock SJ, Parkhill J, Croucher NJ, Corander J. 2019. Diversification of Colonization Factors in a Multidrug-Resistant Escherichia coli Lineage Evolving under Negative Frequency-Dependent Selection. *mBio, 10*(2). doi:10.1128/mBio.00644-19

McNally A, Oren Y, Kelly D, Pascoe B, Dunn S, Sreecharan T, Vehkala M, Valimaki N, Prentice MB, Ashour A et al. 2016. Combined Analysis of Variation in Core, Accessory and Regulatory

Genome Regions Provides a Super-Resolution View into the Evolution of Bacterial Populations. *PLoS Genet, 12*(9), e1006280. doi:10.1371/journal.pgen.1006280

Mi H, Muruganujan A, Ebert D, Huang X, Thomas PD. 2019. PANTHER version 14: more genomes, a new PANTHER GO-slim and improvements in enrichment analysis tools. *Nucleic Acids Res, 47*(D1), D419-D426. doi:10.1093/nar/gky1038

Mi H, Muruganujan A, Huang X, Ebert D, Mills C, Guo X, Thomas PD. 2019. Protocol Update for large-scale genome and gene function analysis with the PANTHER classification system (v.14.0). *Nat Protoc, 14*(3), 703-721. doi:10.1038/s41596-019-0128-8

Miyakoshi M, Shintani M, Terabayashi T, Kai S, Yamane H, Nojiri H. 2007. Transcriptome analysis of Pseudomonas putida KT2440 harboring the completely sequenced IncP-7 plasmid pCAR1. *J Bacteriol, 189*(19), 6849-6860. doi:10.1128/JB.00684-07

Monarrez R, Braun M, Coburn-Flynn O, Botelho J, Odetoyin BW, Otero-Vera JI, Quartey NKE, Peixe L, Aboderin AO, Okeke IN. 2019. A large self-transmissible resistance plasmid from Nigeria contains genes that ameliorate a carrying cost. *Sci Rep, 9*(1), 19624. doi:10.1038/s41598-019-56064-z

Neuwirth E. 2014. RColorBrewer: ColorBrewer Palettes. *R package version 1.1-2*. doi:available at https://CRAN.R-project.org/package=RColorBrewer

Ooms J. 2014. The jsonlite Package: A Practical and Consistent Mapping Between JSON Data and R Objects. doi:available at https://arxiv.org/abs/1403.2805

Ooms J. 2020. writexl: Export Data Frames to Excel 'xlsx' Format. *R package version 1.3*. doi:available at https://CRAN.R-project.org/package=writexl

Partridge SR, Kwong SM, Firth N, Jensen SO. 2018. Mobile Genetic Elements Associated with Antimicrobial Resistance. *Clin Microbiol Rev, 31*(4). doi:UNSP e00088-1710.1128/CMR.00088-17

Pedersen TL. 2020. patchwork: The Composer of Plots. (accessed June 22, 2020). doi:available at https://patchwork.data-imaginist.com

Phaneuf PV, Gosting D, Palsson BO, Feist AM. 2019. ALEdb 1.0: a database of mutations from adaptive laboratory evolution experimentation. *Nucleic Acids Res, 47*(D1), D1164-D1171. doi:10.1093/nar/gky983

Porse A, Schonning K, Munck C, Sommer MO. 2016. Survival and Evolution of a Large Multidrug Resistance Plasmid in New Clinical Bacterial Hosts. *Mol Biol Evol, 33*(11), 2860-2873. doi:10.1093/molbev/msw163

R Core Team, R: A language and environment for statistical computing. R Foundation for Statistical Computing, Vienna, Austria. . 2018. doi:available online at https://www.R-project.org/

Rozwandowicz M, Brouwer MSM, Fischer J, Wagenaar JA, Gonzalez-Zorn B, Guerra B, Mevius DJ, Hordijk J. 2018. Plasmids carrying antimicrobial resistance genes in Enterobacteriaceae. *J Antimicrob Chemother, 73*(5), 1121-1137. doi:10.1093/jac/dkx488

Samuelsen O, Thilesen CM, Heggelund L, Vada AN, Kummel A, Sundsfjord A. 2011. Identification of NDM-1-producing Enterobacteriaceae in Norway. *J Antimicrob Chemother, 66*(3), 670-672. doi:10.1093/jac/dkq483

Samuelsen O, Toleman MA, Hasseltvedt V, Fuursted K, Leegaard TM, Walsh TR, Sundsfjord A, Giske CG. 2011. Molecular characterization of VIM-producing Klebsiella pneumoniae from Scandinavia reveals genetic relatedness with international clonal complexes encoding transferable multidrug resistance. *Clin Microbiol Infect, 17*(12), 1811-1816. doi:10.1111/j.1469-0691.2011.03532.x

San Millan A, Pena-Miller R, Toll-Riera M, Halbert ZV, McLean AR, Cooper BS, MacLean RC. 2014. Positive selection and compensatory adaptation interact to stabilize non-transmissible plasmids. *Nat Commun, 5*, 5208. doi:10.1038/ncomms6208

San Millan A, Toll-Riera M, Qi Q, MacLean RC. 2015. Interactions between horizontally acquired genes create a fitness cost in Pseudomonas aeruginosa. *Nat Commun, 6*, 6845. doi:10.1038/ncomms7845

San Millan A, MacLean RC. 2017. Fitness Costs of Plasmids: a Limit to Plasmid Transmission. *Microbiol Spectr, 5*(5). doi:10.1128/microbiolspec.MTBP-0016-2017

San Millan A, Toll-Riera M, Qi Q, Betts A, Hopkinson RJ, McCullagh J, MacLean RC. 2018. Integrative analysis of fitness and metabolic effects of plasmids in Pseudomonas aeruginosa PAO1. *ISME J, 12*(12), 3014-3024. doi:10.1038/s41396-018-0224-8

Sandegren L, Linkevicius M, Lytsy B, Melhus A, Andersson DI. 2012. Transfer of an Escherichia coli ST131 multiresistance cassette has created a Klebsiella pneumoniae-specific plasmid associated with a major nosocomial outbreak. *J Antimicrob Chemother, 67*(1), 74-83. doi:10.1093/jac/dkr405

Saxer G, Krepps MD, Merkley ED, Ansong C, Deatherage Kaiser BL, Valovska MT, Ristic N, Yeh PT, Prakash VP, Leiser OP et al. 2014. Mutations in global regulators lead to metabolic selection during adaptation to complex environments. *PLoS Genet, 10*(12), e1004872. doi:10.1371/journal.pgen.1004872

Schauberger P, Walker A. 2019. openxlsx: Read, Write and Edit xlsx Files. *R Package Version 4.1.3*(accessed May 06, 2020). doi:available at https://CRAN.R-project.org/package=openxlsx

Schaufler K, Semmler T, Pickard DJ, de Toro M, de la Cruz F, Wieler LH, Ewers C, Guenther S. 2016. Carriage of Extended-Spectrum Beta-Lactamase-Plasmids Does Not Reduce Fitness but Enhances Virulence in Some Strains of Pandemic E. coli Lineages. *Front Microbiol, 7*, 336. doi:10.3389/fmicb.2016.00336

Serna A, Espinosa E, Camacho EM, Casadesus J. 2010. Regulation of bacterial conjugation in microaerobiosis by host-encoded functions ArcAB and sdhABCD. *Genetics, 184*(4), 947-958. doi:10.1534/genetics.109.109918

Shimada T, Fujita N, Yamamoto K, Ishihama A. 2011. Novel roles of cAMP receptor protein (CRP) in regulation of transport and metabolism of carbon sources. *PLoS One, 6*(6), e20081. doi:10.1371/journal.pone.0020081

Silva RF, Mendonca SC, Carvalho LM, Reis AM, Gordo I, Trindade S, Dionisio F. 2011. Pervasive sign epistasis between conjugative plasmids and drug-resistance chromosomal mutations. *PLoS Genet, 7*(7), e1002181. doi:10.1371/journal.pgen.1002181

Sota M, Top EM. 2008. Host-specific factors determine the persistence of IncP-1 plasmids. *World Journal of Microbiology and Biotechnology, 24*(9), 1951-1954. doi:10.1007/s11274-008-9653-2

Sota M, Yano H, Hughes JM, Daughdrill GW, Abdo Z, Forney LJ, Top EM. 2010. Shifts in the host range of a promiscuous plasmid through parallel evolution of its replication initiation protein. *ISME J, 4*(12), 1568-1580. doi:10.1038/ismej.2010.72

Stalder T, Rogers LM, Renfrow C, Yano H, Smith Z, Top EM. 2017. Emerging patterns of plasmid-host coevolution that stabilize antibiotic resistance. *Sci Rep, 7*(1), 4853. doi:10.1038/s41598-017-04662-0

Starikova I, Al-Haroni M, Werner G, Roberts AP, Sorum V, Nielsen KM, Johnsen PJ. 2013. Fitness costs of various mobile genetic elements in Enterococcus faecium and Enterococcus faecalis. *J Antimicrob Chemother, 68*(12), 2755-2765. doi:10.1093/jac/dkt270

Stevenson C, Hall JPJ, Brockhurst MA, Harrison E. 2018. Plasmid stability is enhanced by higher-frequency pulses of positive selection. *Proc Biol Sci, 285*(1870). doi:10.1098/rspb.2017.2497

Stewart FM, Levin BR. 1977. The Population Biology of Bacterial Plasmids: A PRIORI Conditions for the Existence of Conjugationally Transmitted Factors. *Genetics, 87*(2), 209-228. Retrieved from https://www.ncbi.nlm.nih.gov/pubmed/17248761

Strohmaier H, Noiges R, Kotschan S, Sawers G, Hogenauer G, Zechner EL, Koraimann G. 1998. Signal transduction and bacterial conjugation: characterization of the role of ArcA in regulating conjugative transfer of the resistance plasmid R1. *J Mol Biol, 277*(2), 309-316. doi:10.1006/jmbi.1997.1598

The Gene Ontology Consortium. 2019. The Gene Ontology Resource: 20 years and still GOing strong. *Nucleic Acids Res, 47*(D1), D330-D338. doi:10.1093/nar/gky1055

Turner PE, Cooper VS, Lenski RE. 1998. Tradeoff between horizontal and vertical modes of transmission in bacterial plasmids. *Evolution, 52*(2), 315-329. doi:DOI 10.1111/j.1558-5646.1998.tb01634.x

Turner PE, Williams ES, Okeke C, Cooper VS, Duffy S, Wertz JE. 2014. Antibiotic resistance correlates with transmission in plasmid evolution. *Evolution, 68*(12), 3368-3380. doi:10.1111/evo.12537

Varet H, Brillet-Guéguen L, Coppée J-Y, Dillies M-A. 2016. SARTools: A DESeq2- and EdgeR-Based R Pipeline for Comprehensive Differential Analysis of RNA-Seq Data. *PLoS One, 11*(6), e0157022. doi:10.1371/journal.pone.0157022

Vasileva D, Suzuki-Minakuchi C, Kosono S, Yoshida M, Okada K, Nojiri H. 2018. Proteome and acylome analyses of the functional interaction network between the carbazole-degradative plasmid pCAR1 and host Pseudomonas putida KT2440. *Environmental Microbiology Reports, 10*(3), 299-309. doi:10.1111/1758-2229.12639

Wein T, Hülter NF, Mizrahi I, Dagan T. 2019. Emergence of plasmid stability under non-selective conditions maintains antibiotic resistance. *Nature Communications, 10*(1), 2595. doi:10.1038/s41467-019-10600-7

Zeileis A. 2004. Econometric Computing with HC and HAC Covariance Matrix Estimators. *Journal of Statistical Software, 1*(10). Retrieved from https://www.jstatsoft.org/v011/i10. http://dx.doi.org/10.18637/jss.v011.i10

Figures

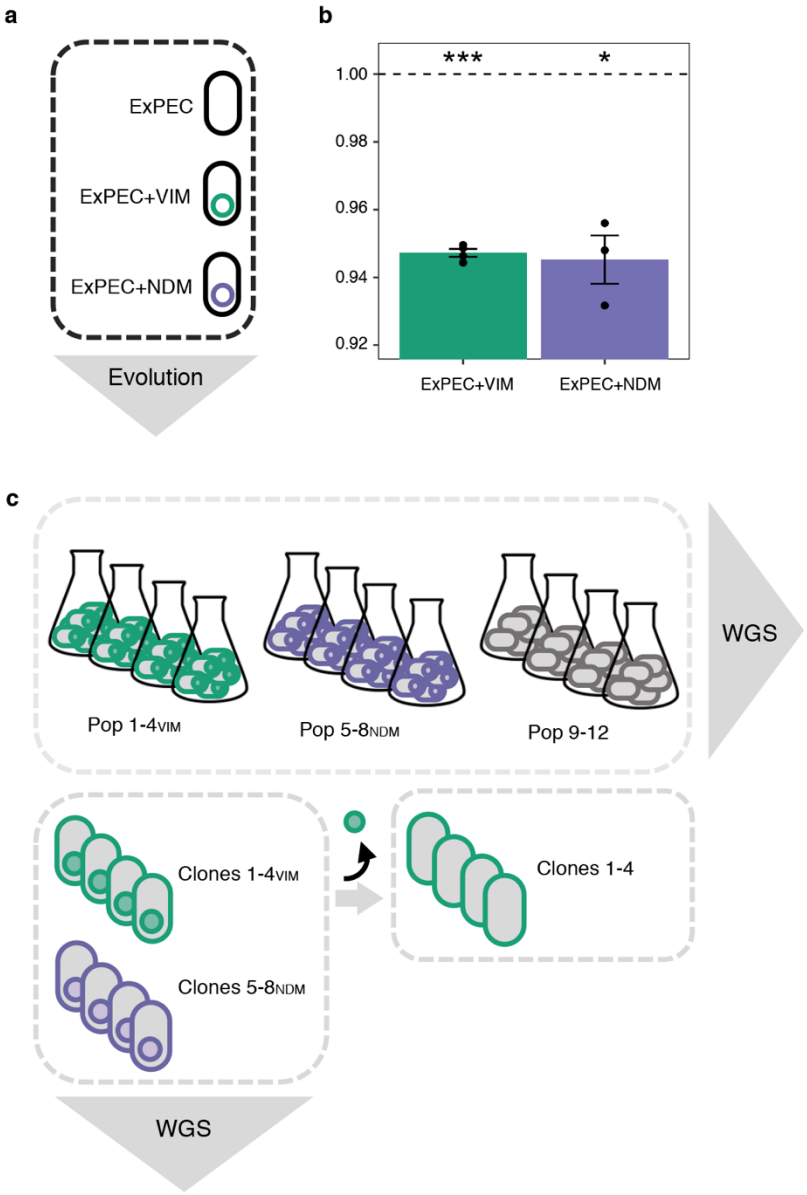

Fig. 1 Fitness effect of plasmid acquisition and experimental procedures. a An ExPEC strain (black) acquired each of the two MDR plasmids pG06-VIM-1 (green; 53 kB; IncR [Di Luca et al. 2017]) and pK71-77-1-NDM (purple; 145 kB; IncC [Gama et al. 2020]) of clinical origin encoding the carbapenemases VIM-1 and NDM-1, respectively. **b** Initial fitness costs of newly transferred plasmids in strains ExPEC+VIM and ExPEC+NDM (n = 4 and 3, respectively). Significant plasmid costs are indicated by asterisks (*P* = * < 0.05, ** < 0.01, *** < 0.001; one-sample *t*-test, two-sided). Error bars indicate ± s.e.m. **c** Experimental evolution in absence of selective pressure (~300 generations) resulted in plasmid-carrying (Pop 1-4$_{VIM}$ and Pop 5-8$_{NDM}$) and plasmid-free (Pop 9-12) populations which were subjected to whole-genome sequencing (WGS). Representative clones per plasmid-carrying evolved population (Clones 1-4$_{VIM}$ and Clones 5-8$_{NDM}$) were sequenced and segregants without evolved pG06-VIM-1 (filled green circle) were generated for subsequent competition experiments (Clones 1-4).

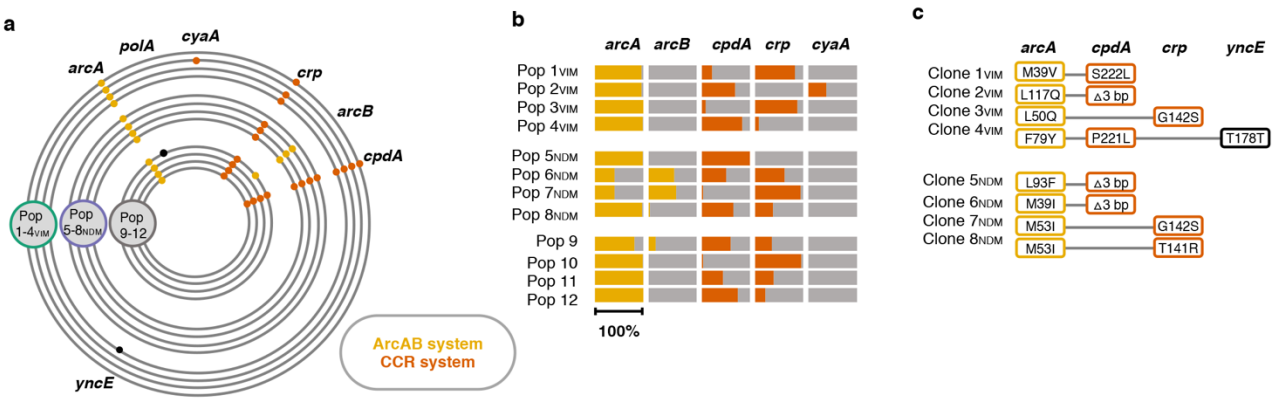

Fig. 2 Identified mutations in the ArcAB (Aerobic Respiration Control) and CCR (Carbon Catabolite Repression) regulatory systems. a Chromosomal mutations after ~300 generations of experimental evolution. Plasmid-carrying (Pop 1-4VIM = green; Pop 5-8NDM = purple) and plasmid-free (Pop 9-12 = grey) populations had acquired chromosomal mutations in genes associated to the ArcAB (yellow) and CCR (orange) regulatory system. Black indicates otherwise mutated genes in single evolved populations. No point mutations were identified in plasmid sequences. See also Supplementary information section IIIa and Supplementary Table 4. **b** Total frequency of all mutations targeting the same gene within single evolved populations for genes linked to ArcAB and CCR regulatory systems (entire bar length = 100%). **c** Chromosomal mutations identified in co-evolved, plasmid-carrying, whole-genome sequenced Clones 1-4VIM and Clones 5-8NDM; 'Δ3 bp' in cpdA = cpdA.Δ3.bp488-490.

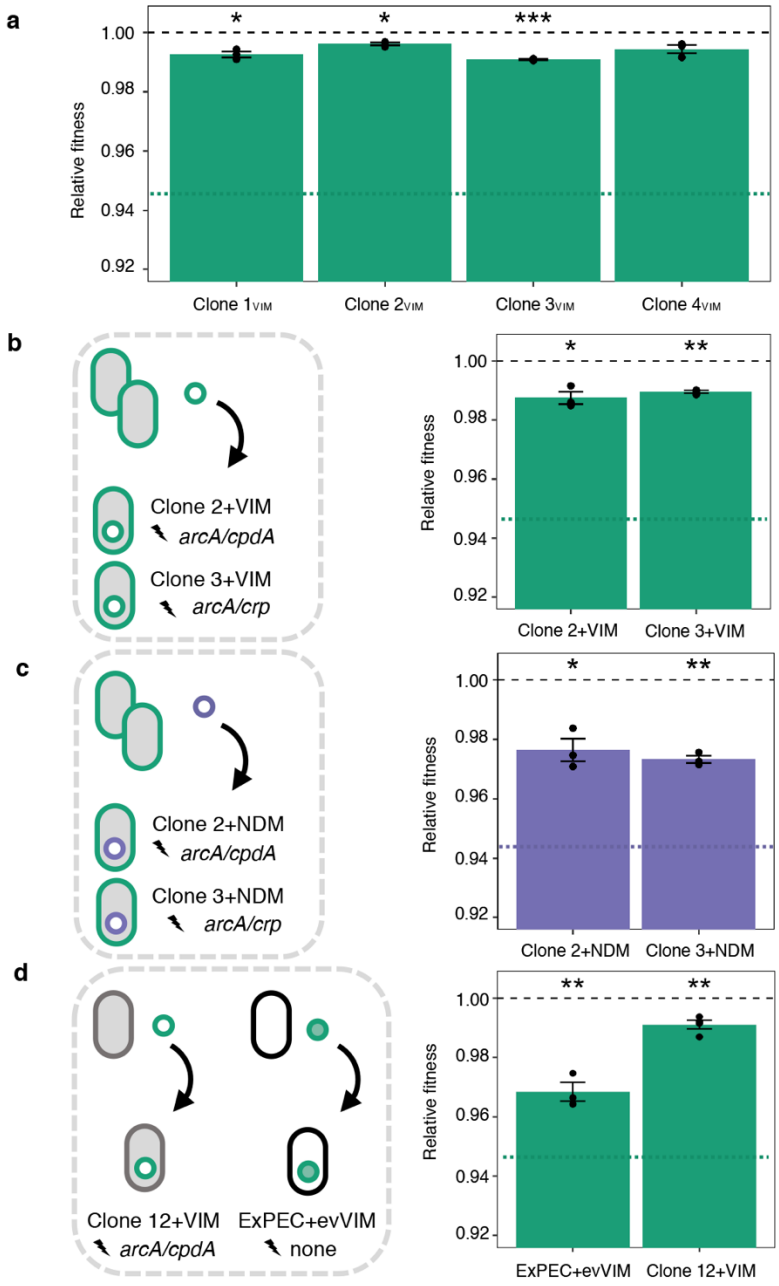

Fig. 3 Fitness costs of evolved and ancestral plasmids in adapted backgrounds. a Relative fitness of co-evolved pG06-VIM-1-carrying clones (n = 3). Fitness of the ancestral strain ExPEC+VIM is indicated by a dotted green line. **b** Fitness cost of ancestral pG06-VIM-1 re-introduced into co-evolved Clone 2 and Clone 3. Fitness of ancestral strain ExPEC+VIM is indicated by a dotted green line. **c** Fitness cost of ancestral pK71-77-1-NDM introduced into co-evolved Clone 2 and Clone 3 (n = 3). Fitness of the ancestral strain ExPEC+NDM is indicated by a dotted purple line. **d** Fitness cost of ancestral pG06-VIM-1 introduced into evolved Clone 12, and of evolved pG06-VIM-1 isolated from co-evolved Clone2$_{VIM}$ introduced into ancestral strain ExPEC (n = 3-4). Significant plasmid costs are indicated by asterisks (P = * < 0.05, ** < 0.01, *** < 0.001; one-sample t-test, two-sided). Error bars indicate ± s.e.m.

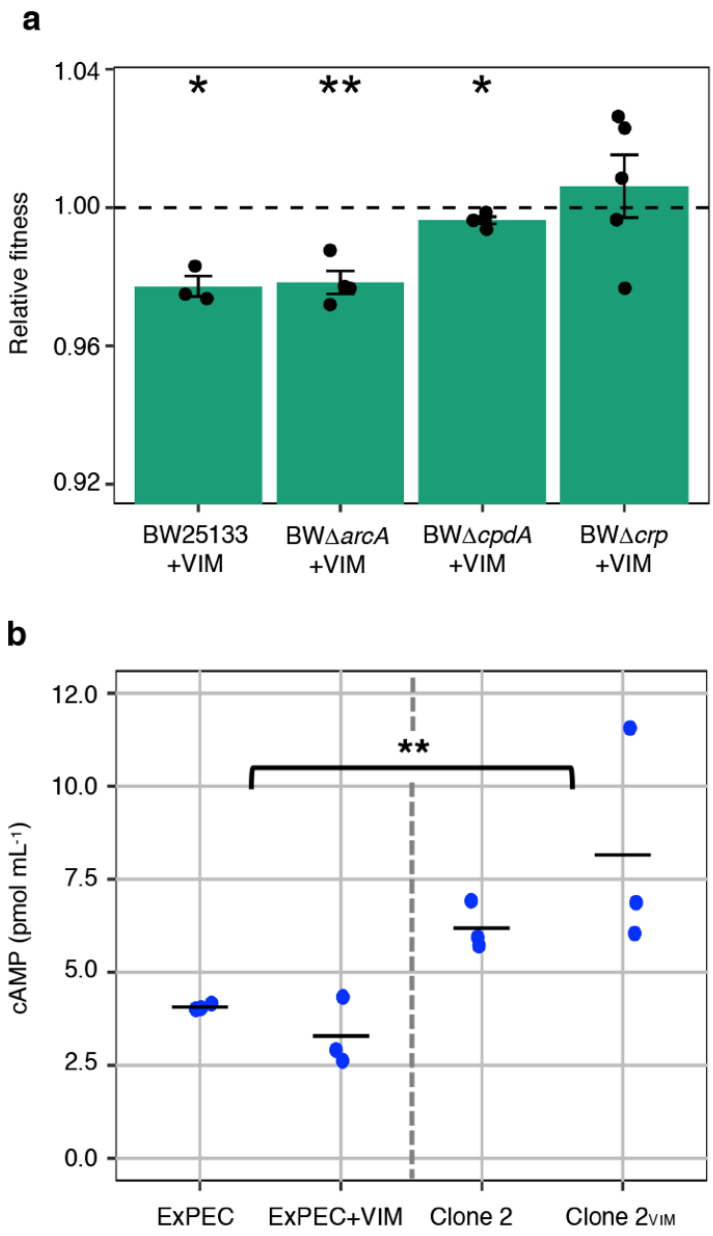

Fig. 4 Effect of CCR and ArcAB systems mutations on plasmid cost and intracellular cAMP concentration. a Relative fitness of pG06-VIM-1 in parent strain BW25133 and deletion strains (n = 3-5). Significant plasmid costs are indicated by asterisks (P = * < 0.05, ** < 0.01, *** < 0.001; one-sample t-test, two-sided). Error bars indicate ± s.e.m. **b** Intracellular cAMP concentrations of ancestral strains (ExPEC and ExPEC+VIM; n = 6; left) and evolved strains (Clone 2 and Clone 2_{VIM} carrying mutation *cpdA*.Δ3.bp488-490; n = 6; right) (two-way ANOVA; P = ** < 0.01; df = 3).

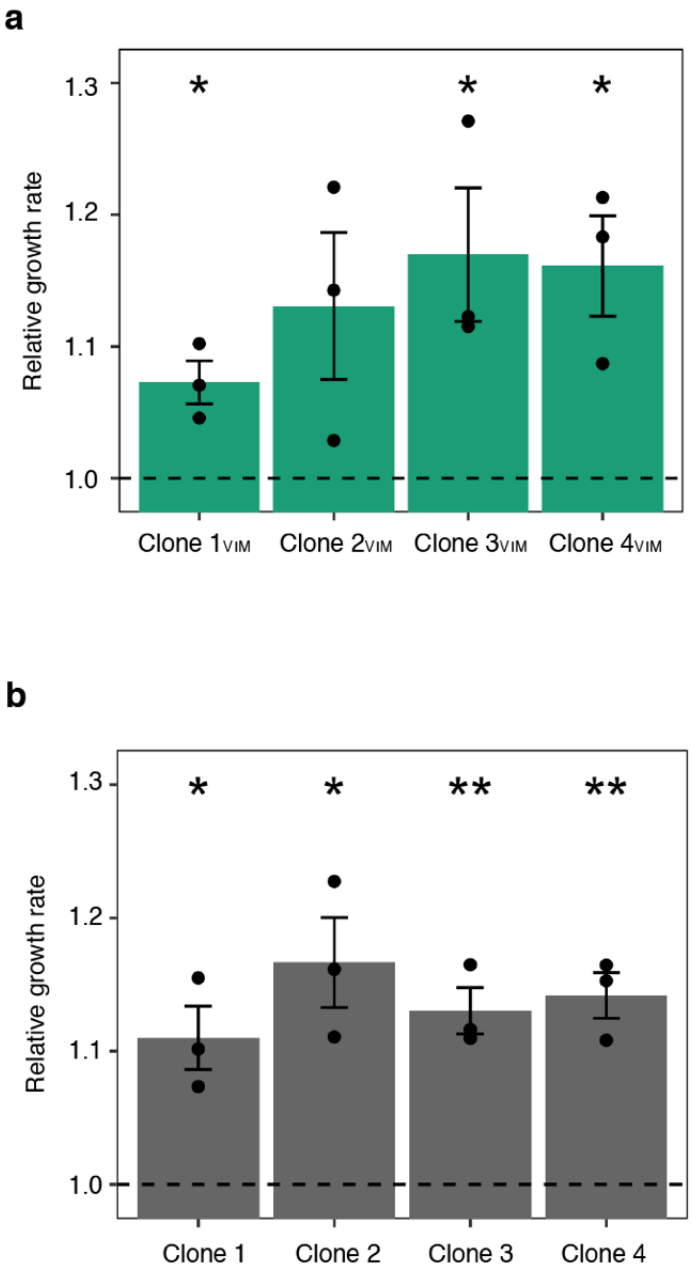

Fig. 5 Fitness-improved adapted backgrounds. Exponential growth rates of **a** co-evolved pG06-VIM-1-carrying strains relatively to strain ExPEC+VIM and (each comparison n = 3) **b** co-evolved pG06-VIM-1 segregants relatively to ancestral strain ExPEC (each comparison n = 3). Significant fitness changes are indicated by asterisks (*P* = * < 0.05, ** < 0.01, *** < 0.001; one-sample *t*-test, one-sided). Error bars indicate ± s.e.m.

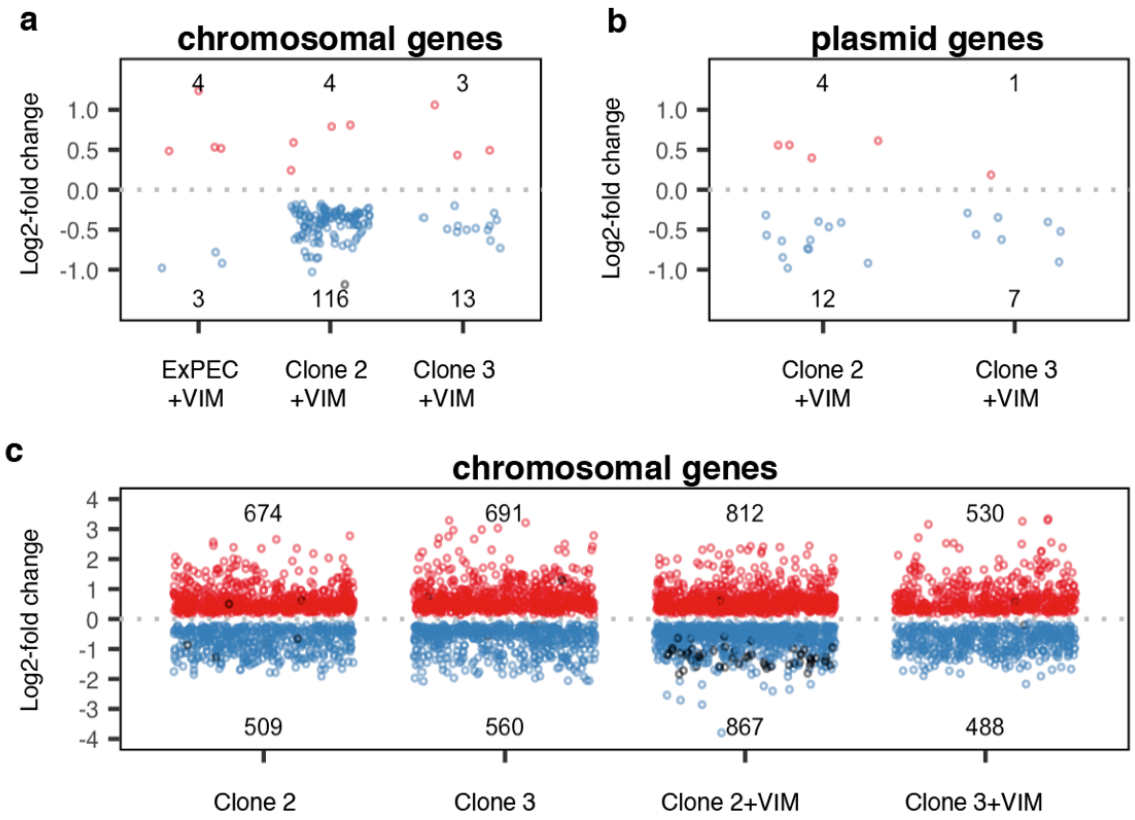

Fig. 6 Differential expression analysis. Number of up and downregulated genes (Log_2-fold change) on **a** chromosomes of ancestral strain ExPEC+VIM, evolved Clone 2+VIM and Clone 3+VIM upon acquisition of native pG06-VIM-1 (compared to respective plasmid-free strain) **b** evolved pG06-VIM-1 of Clone 2+VIM and 3+VIM due to adaptive chromosomal mutations (compared to ancestral ExPEC+VIM) **c** chromosomes of evolved pG06-VIM-1-free/-carrying Clone 2 and Clone 3 due to adaptive chromosomal mutations (compared to ExPEC and ExPEC+VIM, respectively). Circles: up (red) and downregulated (blue) protein-encoding genes; differently regulated RNA-encoding genes (black).